6-1-2013

Biochemistry of 1, 2-Dehydro-N-Acetyldopamine Derivatives

Adal T. Abebe
University of Massachusetts Boston

BIOCHEMISTRY OF 1, 2-DEHYDRO-N-ACETYLDOPAMINE DERIVATIVES

A Dissertation Presented

by

ADAL T. ABEBE

Submitted to the Office of Graduate Studies,
University of Massachusetts Boston,
in partial fulfillment of the requirements for the degree of

DOCTOR OF PHILOSOPHY

June 2013

Molecular, Cellular and Organismal Biology Program

BIOCHEMISTRY OF 1, 2-DEHYDRO-N-ACETYLDOPAMINE DERIVATIVES

A Dissertation Presented

by

ADAL T. ABEBE

Approved as to style and content by:

_____
Manickam Sugumaran, Professor
Chairperson of Committee

_____
Steven Ackerman, Associate Professor
Member

_____
Jason Evans, Associate Professor
Member

_____
William Robinson, Professor
Member

_____
Alexey Veraksa, Associate Professor
Member

_____
Linda Huang, Program Director
Biology Graduate Program

_____
Richard Kesseli, Chairperson
Biology Department

ABSTRACT

BIOCHEMISTRY OF 1,2-DEHYDRO-N-ACETYLDOPAMINE DERIVATIVES

June 2013

Adal T Abebe, B.S., Addis Ababa University, Addis Ababa, Ethiopia
M.S., University of Massachusetts Boston
Ph.D., University of Massachusetts Boston

Directed by Professor Manickam Sugumaran

Dehydrodopa/dopamine derivatives form an important group of biomolecules participating in sclerotization of all arthropod cuticles, gluing and cementing mussels and related organisms to solid surfaces, and defense reactions of countless marine and invertebrate organisms. Yet very little information is available on the biochemistry of these highly reactive and unstable molecules. To understand their physiological role, I conducted a thorough biochemical study on three representative compounds that cover the entire plethora of dehydrodopa/dopamine derivatives. Employing diode array UV-visible spectroscopy, HPLC, liquid chromatography-mass spectrometry, and electrospray ionization tandem mass spectrometry, I investigated the oxidation chemistry of 1,2-dehydro-N-acetyldopamine (dehydro NADA), 1,2-dehydro-N-acetyldopa and 1,2-dehydro-N-acetyldopa methyl ester. Tyrosinase converted dehydro NADA to a reactive

quinone methide that formed oligomeric products with the parent compound. The sister enzyme laccase, produced semiquinone radicals that exhibited a novel coupling reaction producing just dimers. Nonenzymatic oxidation of dehydro NADA also produced semiquinone radicals that formed oligomeric products. Moreover, nonenzymatic oxidation resulted in the production of superoxide anions that could function in defense reactions. The nonenzymatic oxidation studies on dehydro NADA at mild alkaline conditions revealed the mechanisms of defense reactions and tunic formation in a vast array of tunicates. Oxidative transformations of 1,2-dehydro-N-acetyldopa indicated a new route for the biosynthesis of a vast array of bioactive marine molecules possessing dihydroxycoumarin skeleton. In addition, it revealed new transformations of coumarins to oligomeric products *via* highly reactive quinone methide intermediates. Biochemical studies on 1,2-dehydro-N-acetyldopa methyl ester revealed a new Diels Alder type condensation of its quinone with the parent compound. This reaction shed light on the mode of gluing of mussels and other bivalves to solid surfaces as well as the hardening reactions occurring in their periostracum. I also examined the oxidation chemistry of dehydro NADA with a model nucleophile, N-acetylcysteine and discovered yet another new addition reaction of dehydro NADA that has tremendous biological significance. Finally, I investigated the mechanism of dehydro NADA binding to insect cuticle using labeled compounds and established that they could uniquely produce ketocatecholic compound, arterenone upon hydrolysis. The biochemical significances of all these new reactions are discussed in the dissertation.

ACKNOWLEDGEMENTS

Completing my Ph.D. degree is probably the most challenging activity of my life. The best and worst moments of my journey have been shared with many people. It has been a great privilege to spend several years in the department of Biology at the University of Massachusetts Boston, and its members will always remain dear to me.

Foremost, I will like to express my sincere gratitude to my advisor professor Manickam Sugumaran for the continuous support of my Ph.D. study and research, for his patience, motivation, enthusiasm, and immense knowledge. His guidance helped me in all the time of research and writing of this thesis. I could not have asked for better role model and mentor for my study.

Special thanks to my thesis committee, Associate Professor Jason Evans, without his help in mass spectrometer study I could have not completed my research. Thanks also to Associate Professor Alexey Veraksa for helpful discussion and suggestion. I will also like to thank Associate Professor Steven Ackerman and Professor William Robinson for their support and guidance.

I will also like to thank Zheng Dong and Qun Kung for their help in mass spectrometer analysis and friendship. I wish to thank my wife Tiruwork Abebe, whose love and encouragement allowed me finish this journey. My mom Kebebush and my siblings their love provided me inspiration and was my driving force. Finally to my friends in Boston, Washington D.C, Ethiopian and other parts of the world, they were source of laughter and joy.

TABLE OF CONTENTS

CHAPTER Page

CHAPTER Page

LIST OF TABLES

CHAPTER 4

CHAPTER 6

LIST OF FIGURES

CHAPTER 3

CHAPTER 4

CHAPTER 6

CHAPTER 7

LISTS OF ABBREVIATIONS

APCI = Atmospheric Pressure Chemical Ionization

CID = Collision Induced Decomposition

DeNAcDopa methyl ester = 1,2-dehydro-N-acetyldopa methyl ester

Dehydro NADA = 1,2-dehydro-N-acetyldopamine

DTT = Dithiothreitol

ESI/MS-MS= Electrospray ionization/ tandem mass spectrometry

gm = gram

IR = infrared

kV = kilovolt

LC-MS = liquid chromatography-mass spectrometry

min = minute

M. pt = melting point

mM = millimolar

M = molar

mg = milligram

ml = milliliters

mm = millimeter

m/z = mass to charge ratio

NAcDeDopa = 1, 2-dehydro-N-acetyldopa

NAcCys = N-acetyl cysteine

NAcHis = N-acetyl histidine

NADA = N-acetyldopamine

NBAD = N-β-alanyl dopamine

NMR = nuclear magnetic resonance

N= normality

nm = nanometer

QMIA = Quinone methide imine amide

RP-HPLC-MS = reversed phase high performance liquid chromatography mass spectrometry

rpm = revolution per minute

sec = second.

UV-Vis = ultraviolet-visible

µA = microampere

µg = microgram

µl = microliter

^{o}C = degree celsius

CHAPTER 1

INTRODUCTION

1.1 Dehydrodopa in insect cuticle sclerotization, in small molecules and peptides

A variety of metabolic transformations convert the aromatic amino acid, tyrosine into biologically important products such as dopa, dopamine, epinephrine, N-acyldopamines, homogentistic acid, cinnamate derivatives, thyroxine, etc. In addition, peptidyl tyrosine also undergoes a variety of post-translational modifications and generates a plethora of compounds that have crucial roles in several biological processes. The focus of this dissertation is on a particular group of compounds possessing dehydrodopamine (or dehydrodopa) units. Dehydrodopamine units are biosynthesized both from free tyrosine and peptidyl tyrosine compounds. In the last two decades, a vast variety of compounds possessing this unit have been identified from a diverse array of organisms (Sugumaran and Robinson, 2010). However, their biosynthesis and reactivity has remained largely unraveled due to their extreme instability and high reactivity. Our laboratory has been investigating the molecular mechanisms associated with the metabolic transformations of these novel compounds for over three decades. The simplest compound in this group is 1,2-dehydro-N-acyldopamine. The acyl group can be either acetyl group or β-alanyl group. Both 1,2-dehydro-N-acetyldopamine (Dehydro NADA)

and 1,2-dehydro-N-β-alanyldopamine (Dehydro NBAD) are produced in practically all insects for the construction and hardening of their exoskeleton. These two compounds are mainly responsible for protecting soft-bodied insects. Therefore, the biochemistry of these compounds will be discussed first.

Insects and other arthropods, have a tough exoskeleton protecting them from the environment, enemies and dehydration. The exoskeleton also serves additional roles such as providing an anchorage point for the attachment of muscle and other tissues, allowing gaseous exchange as well as some waste deposition. But this comes with a major drawback. The hard cuticle (= exoskeleton) does not permit the continuous growth of the organism. Insects and arthropods have managed to overcome this difficulty by shedding their old cuticle periodically and making a new, larger one to accommodate growth. Freshly made cuticle is soft and transparent and it soon becomes hard and sometimes colored by a set of reactions collectively known as sclerotization. During sclerotization, cuticular sclerotizing enzymes oxidize catecholamine derivatives and the resultant quinonoid products form adducts and crosslinks that are necessary to harden and protect the cuticle.

Simple ortho-benzoquinone arising from the oxidation of protocatechuic acid was the first sclerotizing agent to be identified in any insect system. Working with cockroach ootheca Pryor (1940) found that the interaction of phenoloxidase and protocatechuic acid lead to the hardening of ootheca. Phenoloxidases were known to oxidize catechols to ortho-benzoquinones at that time. This coupled with the fact that quinones have the

tendency to react with the nucleophilic groups present on protein side chains lead to the quinone tanning proposal (Pryor 1940). Thus, quinones act as glue in binding and making the ootheca proteins hard to protect the egg cases of cockroaches. Subsequently this proposal was extended to the insect cuticle. With the discovery of universal sclerotizing precursor, N-acetyldopamine (NADA) by Karlson and Sekaris (1962), the quinone tanning hypothesis gained wide acceptance and found its way into textbooks of entomology. According to the quinone tanning hypothesis, cuticular phenoloxidase oxidizes NADA (and related catecholamine derivatives that serve as the precursors of sclerotizing agents) to their oxidation products, quinones, during the onset of sclerotization. Quinones react with the cuticular protein and chitin polymer generating adducts and crosslinks (Figure 1.1).

However, concrete proof for the operation of quinone tanning was not obtained until the 1980's. Using radioactive studies, our laboratory first provided evidence for the presence of catecholamine-amino acid adducts in the acid hydrolyzates of the sclerotized cuticle (Sugumaran and Lipke, 1982). Subsequently our laboratory was also successful in demonstrating protein polymerization reactions during the interaction of commercially available phenoloxidase with test proteins (Sugumaran et al., 1987).

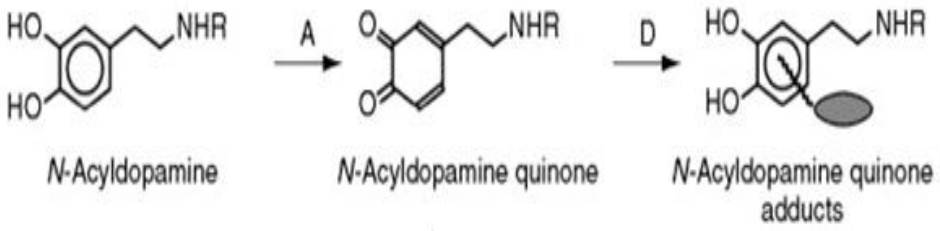

Figure 1.1: Mechanism of quinone tanning. Phenoloxidases, both ortho-diphenoloxidases and laccases (A), oxidize sclerotizing precursors, such as NADA and NBAD (designated as N-acyldopamine), to their quinones. Quinones react with cuticular nucleophiles forming adducts by non-enzymatic reactions (D).

Operation of a different mode of sclerotization came to light soon after Andersen's group discovered arterenone and ketocatechol (Figure 1.2). In 1970, Andersen and his group isolated and characterized arterenone and ketocatechol from the cuticular hydrolyzates and proposed that the side chain of catecholamine derivatives such as NADA are somehow involved in crosslinking process.

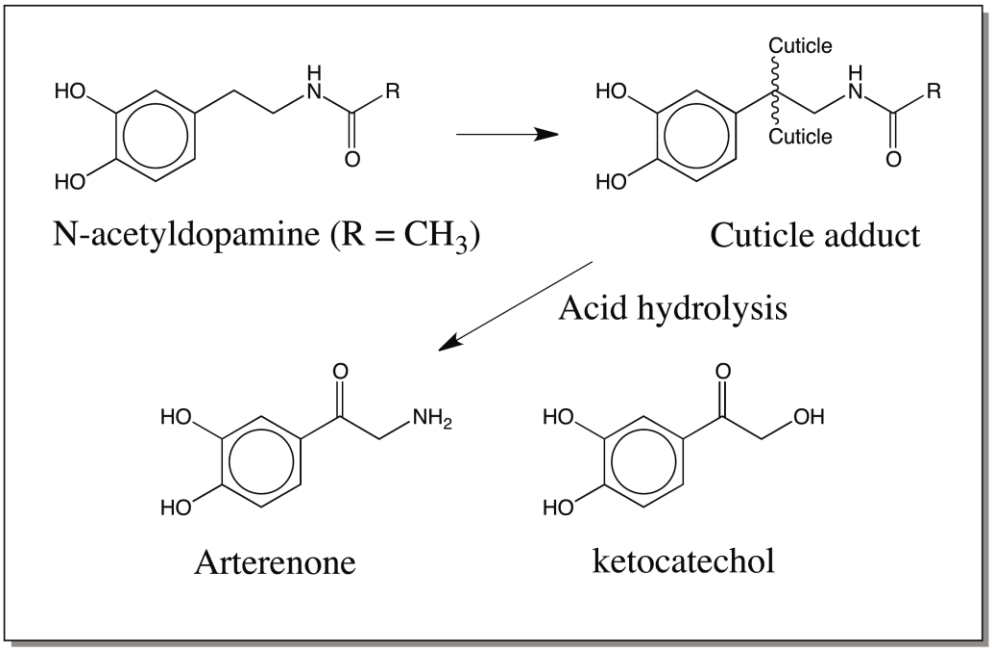

Figure 1.2: Proposed mechanism for the formation of arterenone and ketocatechol in insect cuticle. NADA and related catecholamine derivatives are somehow activated at the β-carbon atom of the side chain and used to make cuticle adducts through their side chain. Acid hydrolysis of these adduct will produce arterenone and ketocatechol.

However the reactive species responsible for this kind of side chain participation as well as the mechanisms of the crosslinking reactions were not identified at that time. Based on the presence of a carbonyl group at the β-position of arterenone, initially the β-carbon atom was proposed to participate in the crosslinking process and the process was named as β-sclerotization. In support of this proposal, Andersen's group also claimed that incubation of cuticle with side chain labeled NADA resulted in the release of tritium from the β-position of labeled NADA and not from α-position labeled NADA. In 1980s however a number of benzodioxan derivatives of NADA were isolated from the cuticle of

insects. These compounds indicated the participation of the side chain of catecholamine in the crosslinking process. Subsequently, a new dehydro derivative of NADA was isolated from the lightly sclerotized cuticle of locusts by mild alkali hydrolysis and identified to be 1,2-dehydro-N-acetyldopamine (dehydro NADA) (Andersen and Roepstorff, 1980). These authors suggested that the quinone of this compound is somehow using both its side chain carbon atoms for crosslinking reactions. Therefore, β-sclerotization was renamed as α,β-sclerotization (Figure 1.3).

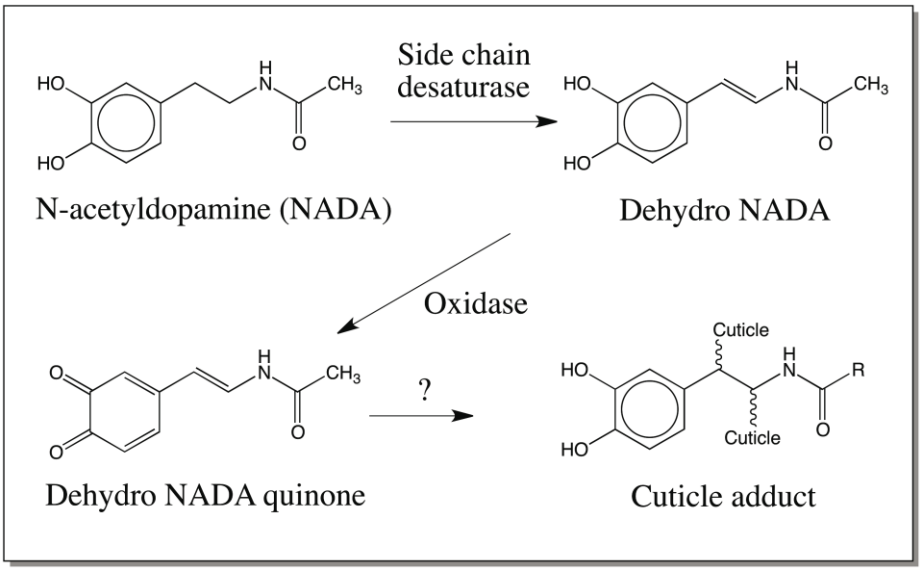

Figure 1.3: The proposed mechanism for α,β-sclerotization. The isolation and characterization of dehydro NADA from locust cuticle called for the presence of cuticular "NADA desaturase" which converts NADA to dehydro NADA. The phenoloxidase generated quinone of the dehydro compound is believed to be the reactive intermediate responsible for cross-linking of proteins through its side chain carbon..

They also proposed the existence of a side chain desaturase that specifically converted NADA to dehydro NADA in insect cuticle. These authors, however did not explain why the quinone of dehydro NADA would exhibit side chain reactivity while all known quinones exhibit only ring reactivity. Also the mode of extraction of this compound (by mild alkaline extraction) casted doubts about the natural occurrence of dehydro NADA in cuticle. Finally this proposal also contradicted their tritium release studies.

Our group, after examining these fit falls, proposed an alternate theory whereby two-electron oxidation of catechols with methylene side chains at the 4-position would generate a quinone methide, an isomer of 4-alkyl quinones (Sugumaran and Lipke, 1983). Quinone methides have the tendency to undergo an addition reaction at the 1,6 position resulting in the regeneration of the catecholic group with nucleophiles attached to the methylene side chain. Accordingly, this process was named quinone methide sclerotization. Our proposal accounted for the side chain reactivity of the catecholamine sclerotizing agent as well as the liberation of dehydro NADA (Figure-1.4). A quinone mehtide adduct in cuticle would easily account for the generation of dehydro NADA by a β-elimination reaction during alkaline treatment. However, Andersen's group also isolated trace amounts of dehydro NADA as a naturally occurring compound from the insect cuticle (Andersen and Roepstroff, 1982). Our group initially argued that dehydro NADA could be formed in trace amounts by a nonenzymatic reaction of enzymatically generated NADA quinone methide. In any case, the search for the enzyme producing dehydro NADA as well as quinone methide was seriously pursued in several laboratories to prove the operation these two mechanisms.

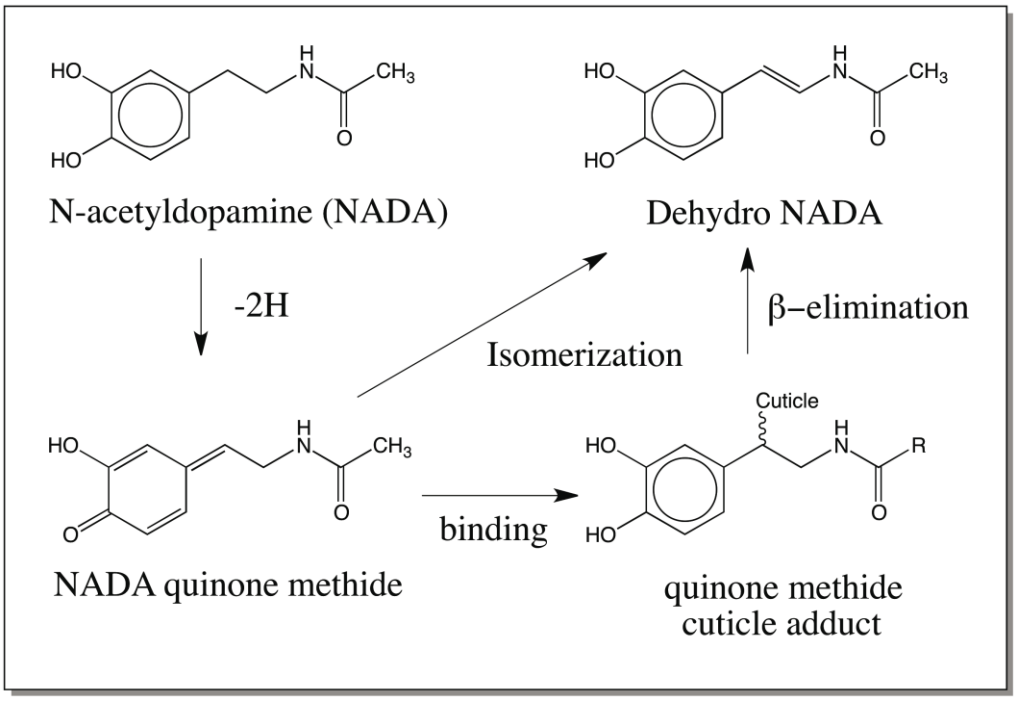

Figure 1.4: Quinone methide sclerotization. N-acyldopamines are converted to quinone methide intermediate by two electron oxidation, which react nonenzymatically with available nucleophile using side chain carbon atom. Quinone methide also undergoes isomerization to dehydro NADA accounting for most of the observed reactions.

Our laboratory finally succeeded in isolating not only the enzyme responsible for NADA quinone methide production in cuticle, but also the enzymes associated with dehydro NADA production. Contrary to the initial proposal, NADA quinone was not directly produced by a two-electron oxidation of catecholamine sclerotizing precursor, but by the combined action of two enzymes. Phenoloxidase converted the catecholamine derivatives to their quinones as usual. But a new enzyme called quinone isomerase converted the resultant 4-alkyl quinones to *para*-quinone methides and provided them for

quinone methide sclerotization. Additionally, yet another enzyme was discovered from this laboratory that generated dehydro NADA from NADA quinone methide by another isomerization reaction. Thus, dehydro NADA is biosynthesized by the combined action of three enzymes, phenoloxidase, quinone isomerase and quinone methide isomerase rather than a specific action of a side chain desaturase (Figure-1.5).

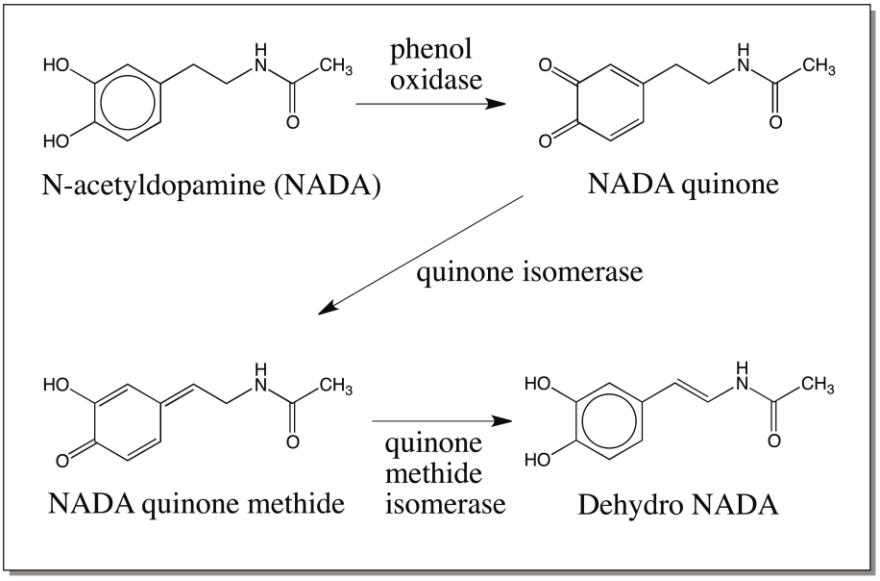

Figure 1.5: Biosynthesis of dehydro NADA. Dehydro NADA is not biosynthesized by the direct side chain desaturation of NADA by a NADA desaturase, but by the combined action of three enzymes. Phenoloxidases convert NADA to its quinone, which is isomerized by quinone isomerase. Quinone methide isomerase converts NADA quinone methide to dehydro NADA.

Discovery of quinone isomerase and quinone methide isomerase accounted for all the observations made on lightly sclerotized cuticle. The reactivity of dehydro NADA through its side chain however remained unsolved for some time. To explore all possible reactivities of dehydro NADA, we needed synthetic dehydro NADA. To this goal, several attempts were made to synthesize dehydro NADA in large scale. Initially dehydro NADA was synthesized using a multi step synthesis, but subsequently a simpler synthetic strategy was devised and large-scale synthesis of dehydro NADA was accomplished from norepinephrine (Dali and Sugumaran, 1988). Norepinephrine was first converted to tetraacetyl norepinephrine by acetylation and then deacylated under mild alkaline conditions to generate dehydro NADA in excellent yield. With the unlimited availability of dehydro NADA, examination of its oxidation chemistry became easier, despite the fact dehydro NADA is very unstable and often difficult to handle in solutions.

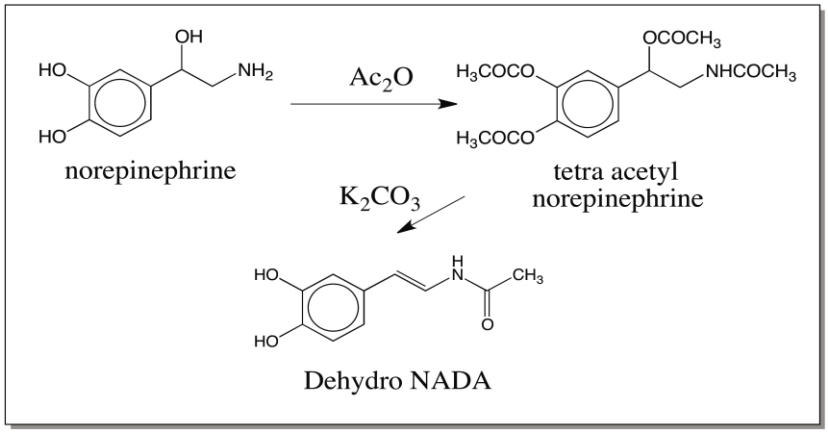

Figure 1.6: Chemical synthesis of dehydro NADA. Dehydro NADA was synthesized from commercially available norepinephrine via tetraacetyl norepinephrine by a simple β-elimination reaction.

Availability of dehydro NADA in large amounts helped us to study all of its reactivities. Oxidation of dehydro NADA by mushroom tyrosinase readily generated the two electron oxidation product (Sugumaran et al., 1987). The product exhibited a broad absorbance maximum centered around 480 nm, nearly 60 nm higher than that expected for a typical *o*-quinone. This observation was puzzling initially, but extensive subsequent work lead to the confirmation that this quinonoid species is not an *o*-quinone but a *p*-quinone methide. Based on physicochemical evidence and quantum chemical calculations this compound was conclusively identified as the quinone methide imine amide (QMIA) (Sugumaran, 2000; Sugumaran et al., 1992). The normal *o*-quinone product turned out to be less stable and could only be visualized under acidic conditions. Since quinone to quinone methide tautomerization is a base catalyzed reaction (Sugumaran 2000), the quinone rapidly isomerized to the QMIA, as soon as the pH was raised to even neutral conditions. Thus, the only product that could be observed during the oxidation of dehydro NADA by tyrosinase at physiological pH is its QMIA derivative (Figure 1.7).

The QMIA thus formed is not stable and readily undergoes reaction with the parent dehydro NADA, forming benzodioxan type adducts. The quinone methide nucleus will add on to the phenolic group first and the modified Schiff's base will subsequently undergo ring closure as shown in Figure 1.8, producing a benzodioxan type dimer. Since such nonenzymatic additions are non-stereoselective, one would get all possible isomeric products. Accordingly Tada et al., 2002 have isolated and separated all possible isomers

of dehydro NADA dimers from the cuticular exuvia of *Cicada* as naturally occurring compounds.

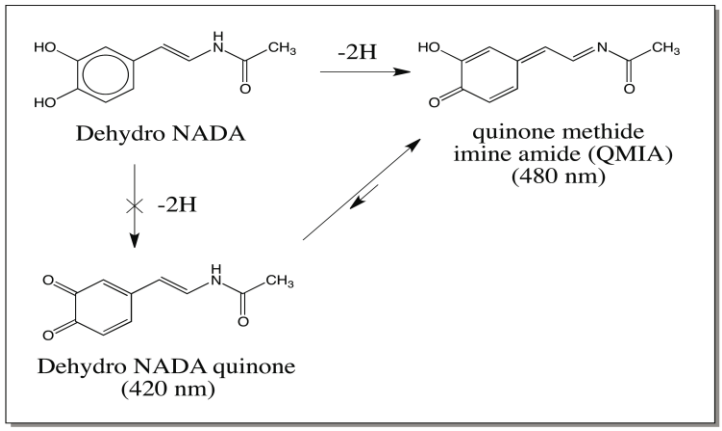

Figure 1.7: Oxidation of dehydro NADA. Oxidation of dehydro NADA produces a novel quinone methide instead of the normally expected quinone.

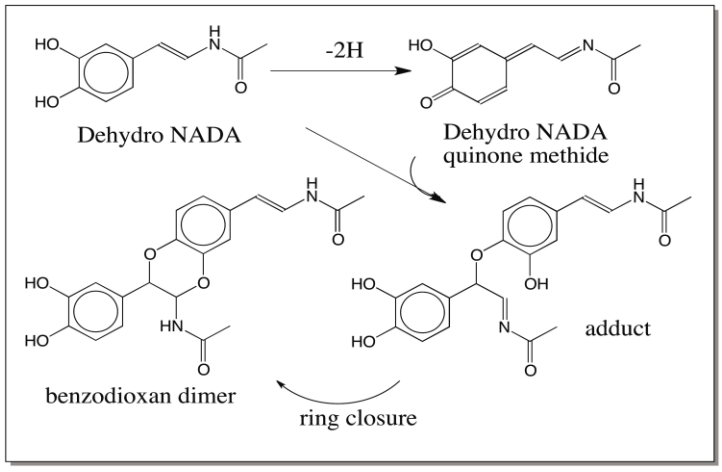

Figure 1.8: Mechanism for oxidative dimerization of dehydro NADA. Oxidation of dehydro NADA produces the QMIA which reacts with the parent compound generating benzodioxan dimers.

The dimerization reaction was not unique to dehydro NADA. Not only dehydro NADA reacts with QMIA, but also a number of catechols such as NADA, 1,2-dihydroxybenzene etc., react with QMIA producing benzodioxan type dimers. Since these reactions involve the side chain addition, a similar addition of cuticular nucleophiles can also be envisaged and the result would be binding of dehydro NADA to the cuticle through both its side chain as shown in Figure 1.9. Thus the benzodioxan type adduct formation explains the participation of both side chain carbon atoms in crosslinking process.

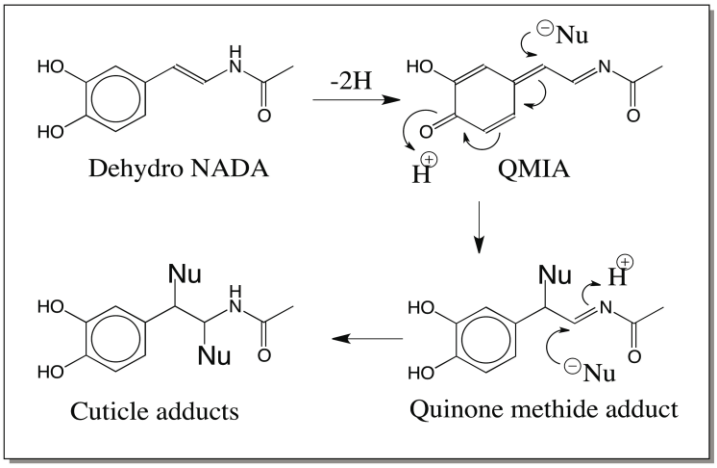

Figure 1.9: The oxidation product of dehydro NADA, could add on to cuticular nucleophiles also forming quinone methide adducts and crosslinks as shown in this figure.

Our laboratory also established that N-β-alanyldopamine (NBAD) could also be converted by the same set of enzymes used for the conversion of NADA to dehydro NADA to dehydro NBAD. These four compounds - NADA, dehydro NADA, NBAD and

dehydro NBAD -appear to be the major sclerotizing precursors used by most if not all species of insects. Based on our studies we have proposed a unified mechanism for sclerotization of insects that is depicted in Figure 1.10.

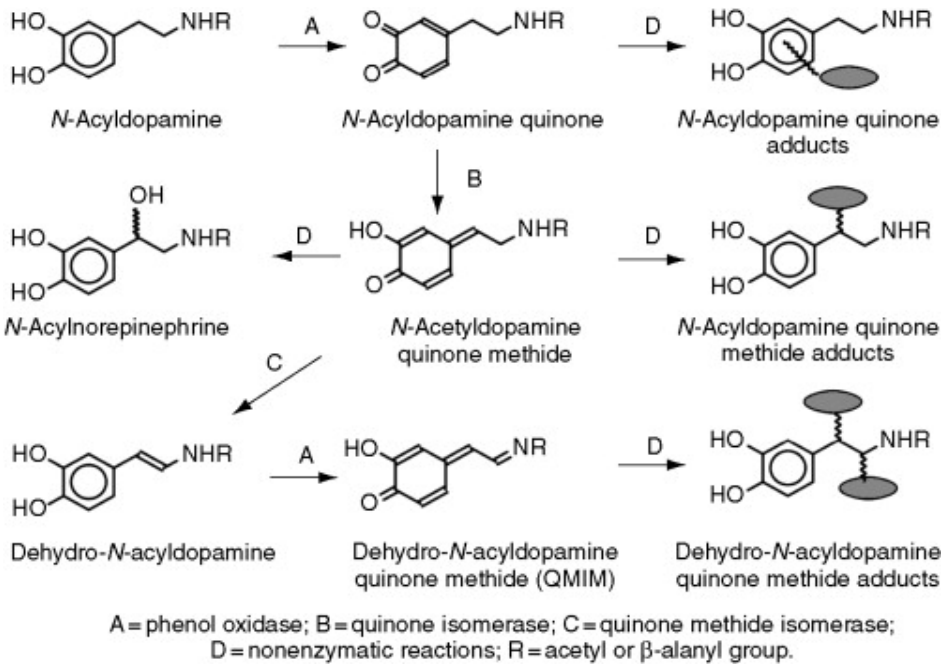

Figure 1.10: Unified Mechanism for Sclerotization of insect cuticle. Phenoloxidase generated quinones react with proteins and chitin forming adducts (called quinone tanning). Quinones also serve as substrates for quinone isomerase generating quinone methides that react with proteins and chitin (Quinone methide sclerotization). Quinone methides are converted by quinone methide isomerase to dehydro-N-acyldopamine, which is further oxidized by phenoloxidases producing quinone methide imine amide that will generate adducts and crosslinks (quinone methide sclerotization) (Sugumaran, 1998).

According to the unified mechanism for sclerotization depicted in Figure 1. 10, during sclerotization NADA and NBAD, the two most common sclerotizing precursors are oxidized to their corresponding quinones by phenoloxidases. Quinone reacts with protein and chitin through a Michael 1,4-addition reaction forming adducts that account for quinone tanning. Quinones are also acted upon by quinone isomerase generating quinone methides. Quinone methides will undergo a Michael 1,6-reaction generating quinone methide adducts (quinone methide sclerotization). Some of the quinone methides serve as substrate for quinone methide isomerase generating dehydro N-acyldopamine derivatives. Dehydro N-acyldopamines are oxidized by cuticular phenoloxidases to a reactive QMIA that forms adducts and crosslinks through its side chain with nucleophilic groups of proteins and chitins, thereby accounting for another mode of quinone methide sclerotization reactions.

Sclerotization reactions are not limited to insects alone. Other arthropods as well as marine organisms also use similar pathways, several of which are yet to be unraveled. Several marine organisms belonging to the phylum Mollusca attach to the substratum through sclerotization reactions. One system that has been well characterized is the hardening of the mussel byssal threads. The mussel byssus is strong threads which are made in succession, one at a time, throughout the life time of the organism, serve as holdfast to keep the mussel securely tethered to a hard substratum in wet environment. Mussels settle on a substratum and the glands from their foot secret polyphenolic proteins that are rich in tyrosine and dopa and a phenoloxidase. The interaction of polyphenolic

protein and the phenoloxidase leads to cementing and the mussels permanently adhere to the substratum (Waite 1990; Rubin et al., 2010). Dopyl proteins seem to be undergoing oxidation and bonding to achieve this cementing. Much like the conversion of NADA to dehydro NADA, dopyl proteins may also undergo conversion to dehydrodopyl derivatives and further oxidized to form crosslinks. The notable exception is the lack of quinone isomerase and quinone methide isomerase. Peptidyl derivatives such as N-acetyldopa esters upon phenoloxidase action readily undergo oxidative transformation to dehydro dopyl compounds via quinone and quinone methide (Figure 1. 11). Thus, only for the production of quinones, enzyme action is needed in this case. The rest of the reactions, viz., quinone isomerization to quinone methide and the conversion of quinone methide to dehydro dopyl compound occur through nonenzymatic reactions. Use of dopyl proteins rather than soluble small catechols such as NADA has another advantage for marine organisms. Since the hardening takes place at the water rich interphase, use of a small molecule may be subjected to dilution and loss while the sticky protein may remain at the site where it is needed and function both as a structural protein and as a sclerotizing compound. Based on the unified mechanism for sclerotization of insect cuticle, one can also propose a parallel mechanism for cementing reactions occurring in mussels as depicted in Figure 1.12 (Sugumaran, 2010). The same reactions are also likely used for the hardening of periostracum in mollusks (Waite, 1990; Sugumaran, 2010; Rubin et al., 2010).

The possible occurrence of dopyl proteins and their participation in cuticular hardening even in insects is a matter of speculation only at this time as various studies have indicated this possibility but concrete evidence is yet to come although the presence of dopa containing protein in the cuticle of *Manduca sexta* has been demonstrated (Okot-Kotber et al., 1994).

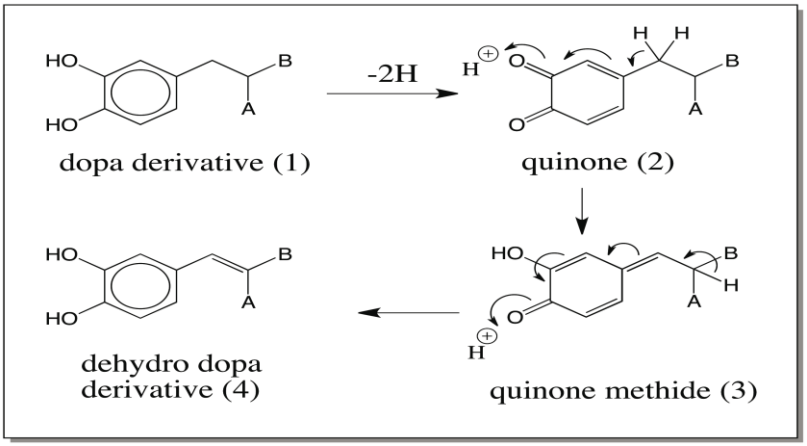

Figure 1.11 Oxidative transformations of dopyl derivatives. Dihydrocaffeic acid derivatives (compound 1; A = H; B = $CONHCH_3$ or $COOCH_3$) upon oxidation produces the corresponding quinone (2) that isomerizes to quinone methide (3) rapidly and nonenzymatically. Quinone methide undergoes subsequent isomerization yielding caffeic acid derivatives (Compound 4; A = H; B = $CONHCH_3$ or $COOCH_3$). If dopa is decarboxylated and the amino group is protected (compound 1 N-acetyldopamine A = H; B = $NHCOCH_3$) the quinone generated from this compound is incapable of undergoing spontaneous conversion to quinone methide but needs the enzyme quinone isomerase. The resultant quinone methide (3) again needs another isomerase - quinone methide

isomerase, to generate dehydro N-acetyldopamine (Compound 4; A = H; B = $NHCOCH_3$). Both amino and carboxyl protected dopa derivatives such as N-acyldopa esters (Compound 5; A = $COOCH_3$; B = NHCOCH3 or $NHCOC_2H_5$) do not need the assistance of any isomerases to generate dehydrodopa derivatives.

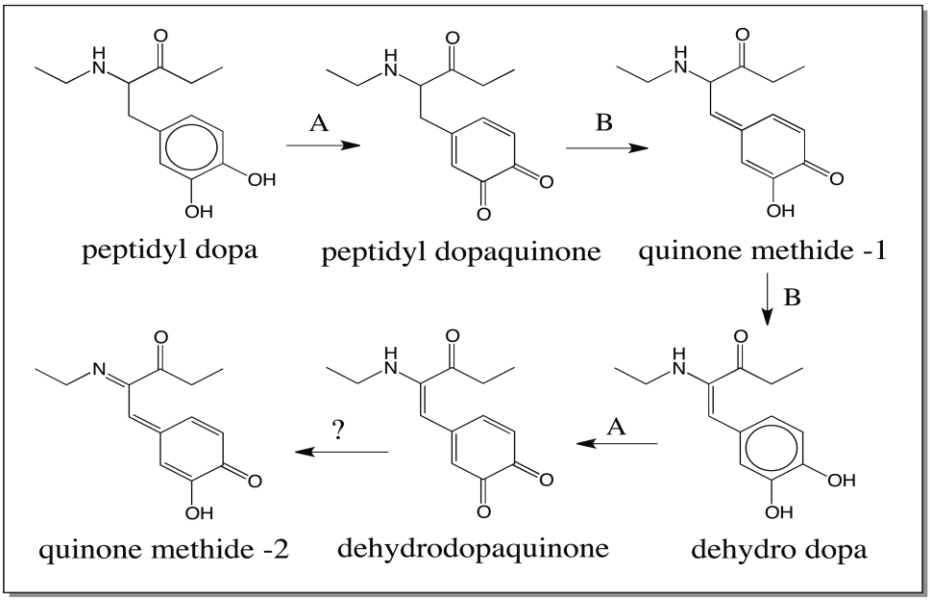

Figure 1.12: Proposed mechanism for the oxidative transformation of dopyl peptides. Peptidyl dopas are oxidized by phenoloxidases (A) to their corresponding quinones that can participate in quinone tanning reactions. Quinone also undergoes nonenzymatic isomerization to quinone methide and participates in quinone methide sclerotization. Quinone methide is also isomerized to a dehydrodopa derivative, again by a nonenzymatic reaction. Oxidation of the dehydrodopas will produce quinones and quinone methides that can also participate in additional crosslinking (A = phenoloxidase; B = nonenzymatic reactions).

The use of the dehydrodopa/dehydrodopamine group is not unique for sclerotization alone. A number of marine organisms seem to generate these compounds for a variety of purposes. The ocean covers over 70% of the Earth's surface and contains an incredible diversity of life with diverse species of plants, animals, and microorganisms. It can provide myriad compounds that can potentially serve as pharmaceuticals, nutritional supplements, cosmetics and material chemicals. Many pharmacologically important substances have been isolated with unique antitumor, antimicrobial and anti-inflammatory properties from marine organisms. A well-known example, azidothymidine or AZT, the first anti retroviral medicine approved for treating HIV/AIDS, is obtained from the sponge *Cryptotethya*. Despite the dramatic potentials shown by marine compounds, relatively few studies have been conducted on the marine organisms. A cursory survey of marine compounds containing the dehydro dopyl unit was recently published (Sugumaran and Robinson, 2010). The survey clearly indicated the diverse potentials of marine dehydro dopyl compounds. Among the promising candidates are lamellarins, which are a group of about 70 condensed polycyclic aromatic compounds possessing dehydrodopa units. Lamellarins were first isolated from the prosobranch mollusk of the genus *Lamellaria* (Andersen et al., 1985). They were later extracted and identified from various species of ascidians and sponges collected from diverse areas (Urban et al., 1995). Following the discovery of the potent anti-proliferative and pro-apoptotic activities of lamellarins their biological activities have been extensively studied. Some lamellarins are found to be potent inhibitor of topoisomerase I (Facompre

et al., 2003). They also function as multi-drug resistance reversal drugs (Vanhuyse et al., 2005). Furthermore some are found to inhibit HIV-1 integrase (Menna et al., 2011). The majority of the lamellarins possess either Type 1a or 1b structure shown in Figure 1. 13. In addition to lamellarins, ningalin A and ningalin B, whose structures are also shown in the same figure, possess a coumarin ring structure. Ningalins, as well as their derivatives, exhibit marked cytotoxicity against several cancer cell lines. They also exhibit significant multi-drug resistance reversal activity at non-cytotoxic concentrations. It is important to stress that 6, 7-dihydroxycoumarin units found in these compounds have dehydrodopa units embedded in them (Figure 1.13).

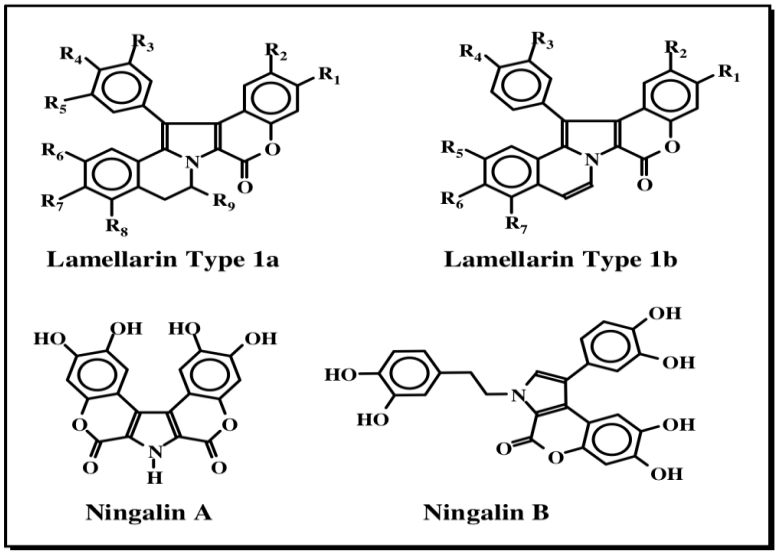

Figure 1.13: Structure of lamellarins and ningalins. Structures of marine natural products possessing 6,7-dihydroxycoumarin unit (R_1 and R_2 substituent in lamellarins are often either hydroxyl groups or its ester derivatives). Note the presence of dehydro dopa units in all these compounds.

The other group of dehydrodopa containing compounds is the low molecular weight oligopeptides isolated from tunicates, called tunichromes. The structure of these compounds along with other dehydro dopa containing compounds are shown in Figure 1.14 and in Table 1.1. The biological role of tunichromes and related marine dehydrodopyl compounds remains largely speculative, although various researchers have proposed different possible functions over the years (Taylor et al., 1997a; Sugumaran and Robinson, 2010; Cai et al., 2008). Like other marine invertebrates, such as sponges and bivalves, tunicates are filter feeders. They could potentially accumulate high concentrations of marine viruses and bacteria in their system by this process. For successful survival the hosts must have potent antiviral and antibacterial compounds to combat any opportunistically infecting microorganisms. Tunichromes could play a crucial role in defense reactions, as they seem to possess suitable reactivity. They are extremely unstable and rapidly undergo oxidation producing harmful quinonoid compounds and free radicals that may be useful to kill invaders (Cai et al., 2008). Some of the tunichromes seem to possess antibiotic properties (Cai et al., 2008; Tincu et al., 2003). In spite of such a crucial role only limited research has been carried out on the biochemistry of dehydrodopa and its derivatives. Instability, unusual reactivity, and difficulty in making these novel biological molecules severely hampered the advancement of knowledge of dehydrodopas. Because of their importance, I examined the oxidation chemistry of dehydro NADA and related compounds in detail and present the results in this dissertation thesis.

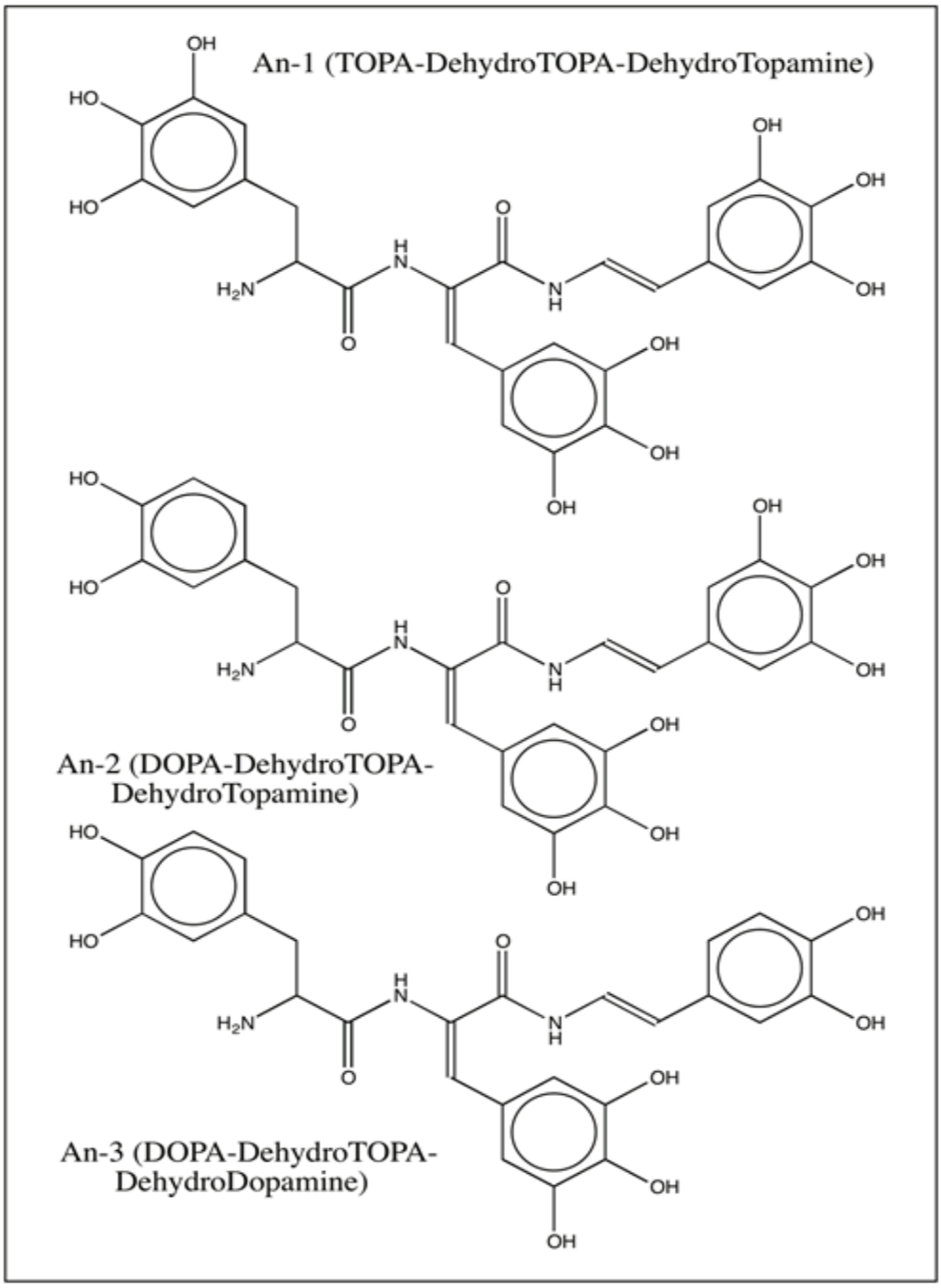

Figure 1.14: Structure of tunichrome An-1, An-2 and An-3.

Table 1.1: Naturally occurring marine compounds possessing one or more dehydro dopamine units

No.	Compound	Structure
1.	Tunichrome An-1	Topa-DeTopa-DeTopamine
2.	Tunichrome An-2	Dopa-DeTopa-DeTopamine
3.	Tunichrome An-3	Dopa-DeTopa-DeDopamine
4.	Tunichrome Pm-1	Topa-Topa-DeTopamine
5.	Tunichrome Pm-2	Dopa-Topa-DeTopamine
6.	Tunichrome Pm-3	Dopa-Topa-DeDopamine
7.	Tunichrome Mm-1	Gly-DeDopa-DeDopamine
8.	Tunichrome Mm-2	Leu-DeDopa-DeDopamine
9.	Tunichrome Sp-1	Dopa-Dopa-Gly-Pro-DeDopamine
10.	Plicatamide	Phe-Phe-His-Leu-His-Phe-His-DeDopamine
11.	Morulin Pm	Polypeptide with 6BrTrp and DeDopamine
12.	Clionamide1	6-BrTrp-DeTopamine
13.	Celenamide A	Leu-DeTopa-6-BrTrp-DeDopamine
14.	Celenamide B	Val-DeTopa-6-BrTrp-DeDopamine
15.	Celenamide C	Leu-DeTopa-6-BrTrp-DeTyramine
16.	Celenamide D	Leu-DeTopa-DeTopa-DeDopamine
17.	Celenamide E	DeTopa-6-BrTrp-DeDopamine
18.	Lamellarins	Polycyclic compounds with deDopamine
19.	Ningalins A-D	Polycyclic compound with deDopamine
20.	Purpurone	Polycyclic compound with deDopamine
21.	Stroniamides A-D	Polycyclic compound with deDopamine

1.2 Research objectives: Insects and other arthropods serve as vectors to transmit a variety of diseases such as malaria, West Nile virus, Eastern Equine Encephalitis, yellow fever, and dengue fever. Insect vector-borne diseases infect nearly half of the world's population. A variety of insecticides have been used to eradicate/control harmful insect populations. Unfortunately, an excessive and continuous use of pesticides has induced the development and spread of resistance, which presents the major obstacle in controlling arthropod born diseases. Moreover, many pesticides used are also persistent and highly toxic not only to insects but also to other animals including humans. As a result vector-borne diseases continue to incur tremendous health and economic burdens especially in developing and underdeveloped countries. A rational approach to overcome resistance and minimize threats posed to public health is targeting a molecular process which is unique and extremely vital for insect development and survival, but is absent in human and other vertebrate animals. Cuticular sclerotization has been recognized as one such biological process. But to develop insecticides based solely on this process, it is essential to understand the biochemistry and molecular biology of this process. The core objective of the present research is to understand the biochemistry of cuticle hardening. To this end, studies were designed to elucidate the unique reactivities of dehydrodopa containing compounds. Because of the complexity of the reaction and multiplicity and instability of products coupled with the lack of appropriate separation and characterization techniques, simple model compounds synthesized in our lab are used for the study. The model compound 1,2-dehydro-N-acetyldopamine (dehydro NADA) is used to study the biochemistry of cuticle sclerotization. The second objective focuses on the biosynthesis

and metabolic fate of bioactive natural compounds isolated from diverse marine organisms. These compounds have a wide range of different biological activities which are of pharmacological importance to humans. Their reactivity is investigated using a model compound, 1,2-dehydro-N-acetyldopa (DeNAcDopa). The third objective is to understand modifications of peptidyl dopa which seem critical and associated with a number of biological processes such as biological glue and cement formation using a model compound 1,2-dehydro-N-acetyldopa methyl ester (DeNAcDopa methyl ester). Better understanding of this transformation will establish the ground work to develop new kinds of biocompatible building materials and develop medical adhesives.

The results of oxidative transformation of dehydro NADA by tyrosinase and laccase are separately presented in Chapter 2 and 3 respectively. The nonenzymatic oxidative transformation of dehydro NADA is presented in Chapter 4. The results of enzymatic oxidation of DeNAcDopa and DeNAcDopa methyl ester are presented in Chapter 5 and 6 respectively. The reactivity of dehydro NADA with external nucleophiles, and its incorporation into insect cuticle and fate during hydrolysis are presented in Chapter 7 and 8 respectively.

CHAPTER 2

TYROSINASE CATALYZED OXIDATION OF 1, 2-DEHYDRO-N-ACETYLDOPAMINE

2.1 Chapter summary

Dehydrodopas are a group of important catecholamine derivatives synthesized from the amino acid tyrosine and peptidyl bound tyrosine residues, by a myriad of organisms for use in a diverse array of biological processes. The first well established process where dehydrodopa plays a crucial role is sclerotization of insect cuticle. During sclerotization, crosslinking occurs as a result of oxidative and nucleophilic reactions between highly reactive sclerotizing agents derived from catechols and nucleophilic side chain groups of protein and chitin. Dehydro NADA is a novel catecholamine compound that was first isolated from the sclerotized cuticle of locusts and proposed to be a reactive intermediate participating in the hardening and sclerotization of insect cuticle (Andersen and Roepstroff, 1981, 1982; Andersen et al., 1980). Oxidation of dehydro NADA by tyrosinase produces a transient QMIA intermediate which shows an absorbance maximum at about 485 nm and exhibits a Michael 1,6-addition reaction, and the Schiff's base can undergo simple addition. The net result is the reactivity of the side chain to produce adducts and/or crosslinks through the two side chain carbon atoms leaving the

ring carbon intact. If no external nucleophiles are present, the two phenolic hydroxyl groups of dehydro NADA add to QMIA, forming the dimers (Sugumaran et al., 1988). Reexamination of oxidation of dehydro NADA by tyrosinase not only generated dimers as reported earlier, but also generated significant amounts of oligomers as a result of dimer addition onto another molecule of QMIA. This supports the idea that a similar reaction with cuticular nucleophiles can generate QMIA adducts in the cuticle.

2.2 Introduction

Dehydro NADA is a novel catecholamine compound that was first isolated from the sclerotized cuticle of locusts and proposed to be a reactive intermediate participating in the hardening and sclerotization of insect cuticle (Andersen and Roepstroff, 1981, 1982; Andersen et al., 1980). The same group also proposed that dehydro NADA is synthesized from NADA by a specific NADA desaturase (Andersen and Roepstroff, 1982; Andersen et al., 1996). However, a specific desaturase causing the transformation of NADA to dehydro NADA has not been isolated and characterized from any insect cuticle so far. Available experimental evidence also did not support the presence of such a desaturase in insect cuticle. However, biosynthetic studies revealed that the dehydrogenation of NADA is achieved by the combined action of three enzymes, viz., phenoloxidase, quinone isomerase and quinone methide isomerase (Saul and Sugumaran 1988, 1989 a-c, 1990a & b, 1992b; Ricketts and Sugumaran, 1994). Occurrence of this reaction has been shown in a number of insects including *Sarcophaga bullata*, *Drosophila melanogaster*, *Manduca*

sexta, and *Calliphora vicina,* thus accounting for the generation of this reaction. Dehydro NADA is biosynthesized from the amino acid tyrosine sequentially and the process involves hydroxylation of tyrosine to dopa by phenoloxidase. Upon oxidative transformation to its quinone DOPA rapidly undergoes intramolecular cyclization because of the unprotected nucleophilic amine group and this limits its potential as a cross-linking precursor. Insects overcome this problem by first decarboxylating dopa to dopamine by dopadecarboxylase, acylation of dopamine by N-acetyl transferase/ N-beta alanyl transferase to form N-acetyldopamine in epidermis and finally transporting N-acetyldopamine to cuticle where phenoloxidases oxidize it to quinone followed by tautomerization to quinone methide by quinone isomerase and rearranged to N-acyl dehydrodopamine by quinone methide isomerase. In dehydrodopa, the nucleophilic nitrogen is deactivatd by the adjacent carbonyl group through resonance. The consequence of which is the loss of the amino group's nucleophilicity. This allows the side chains and the quinonoid nucleus to participate in external reactions (Saul and Sugumaran 1988, 1989 a-c, 1990a &b, 1992b; Ricketts and Sugumaran 1994). Furthermore, using cuticular enzymes consisting of phenoloxidase, quinone isomerase, and quinone methide isomerase, the generation of another dehydrodopamine derivative, 1,2-dehydro-N-β-alanyldopamine, was also demonstrated from its saturated analog, N-β-alanyldopamine (Ricketts and Sugumaran, 1994).

In the absence of external nucleophiles, oxidation of dehydro NADA produces a transient intermediate possessing a visible absorbance maximum at 485 nm before

generating stable dimeric end products (Sugumaran 1998; Sugumaran et al., 1987a, 1988, 1990, 1992a). Theoretically three possible reaction intermediates viz., dehydro NADA quinone, dehydro NADA semiquinone, and dehydro NADA quinone methide, can lead to the production of dimeric products. Pulse radiolysis, electron spin resonance, and time resolved UV-Visible spectral studies of the dehydro NADA oxidation reaction mixtures led to the identification of quinone methide imine amide (QMIA) as the transient reactive intermediate under the conditions employed for phenoloxidase reaction (Sugumaran, 1998; Sugumaran et al., 1987a; 1988, 1992a). Thus dehydro NADA possesses unique reactivity in that it produces a reactive QMIA as the primary two-electron oxidation product at neutral pH values which subsequently undergoes a rapid addition reaction with the starting material generating dimeric products. Both the quinone methide nucleus and the imine amide part in the molecule act as electrophiles to form adducts with nucleophilic centers. In the cuticular environment, such reactions are expected to generate adducts with cuticular nucleophiles resulting in the production of various combinations of protein, chitin and dehydro NADA adducts and cross-links that are necessary for stabilization and hardening of the cuticle (Sugumaran, 1998).

During sclerotization, dehydro NADA is oxidized by cuticular phenoloxidase to a reactive QMIA that forms adducts and crosslinks through its side chain with nucleophilic groups of proteins and chitins, thereby accounting for sclerotization reactions. Tyrosinase (tyrosine: 3, 4-dihydroxy phenylalanine: oxygen oxidoreductase, EC.1.14.8.1) catalyzes both the ortho hydroxylation of monophenols (monophenolase activity) and the two

electron oxidation of *ortho* diphenol to *ortho* quinones (diphenolase activity) and have been suggested to be responsible for catalyzing the oxidation of sclerotizing agents to a highly reactive intermediate during sclerotization (Sugumaran, 1987). In insects tyrosinase catalyzes both hydroxylation of monophenols to *ortho*-diphenols and oxidation of *ortho* diphenols to *ortho* quinones; they will not oxidize *para* diphenols, and are inhibited by phenylthiourea. The study of *Tribolium casteneum* genome has demonstrated the presence of two genes for tyrosinase, *TcTyr1* and *TcTyr2* (Arakane et al., 2005). Tyrosinases occur both in hemocytes and cuticle. The hemolymphal tyrosinases are produced without N-terminal signal peptide, indicating that they are released to the hemolymph via rupture of the cells (Kanost and Gorman, 2008). Because products of the enzymatic reaction phenoloxidase are potentially cytotoxic, phenoloxidase is present in hemocyte and hemolymph as an inactive proenzyme and activated by limited proteolysis, where the N-terminal region of the peptide chain is removed, making the active center of the enzyme accessible for the substrate. In vitro activation of the proenzyme is also obtained by treatment with deteregents. The activation of tyrosinase in the cuticle probably occurs via limited proteolysis by proteases. Inaddition to sclerotization catechol oxidation by tyrosinase is also important in other process such as wound healing and immune response in insects. When cuticle is damaged or infected by microorganisms the proenzyme becomes activated and produces reactive intermediates which destroy the invaders.

Andersen and Roepstroff, 1982 have isolated a number of benzodioxan derivative from sclerotized cuticle of *L. migratoria* and proposed that dehydro NADA could be oxidized by cuticular enzymes to the benzodioxan type dimer through corresponding quinone. However, later work (Sugumaran et al., 1987a) by fast scanning of the reaction mixture demonstrated tyrosinase catalyzed the dimerization of dehydro NADA through quinone methide. A closer look at the ultraviolet spectral changes associated with tyrosinase catalyzed oxidation of dehydro NADA shows the consumption of more than half of the starting material at the end of the reaction. This indicates the production of not only dimers, as thought earlier, but also oligomers. The kinetics and mechanism of oxidative transformation of dehydro NADA catalyzed by tyrosinase purified from *Sarcophaga bullata* and commercial tyrosinase was therefore reexamined using UV-Vis spectroscopy, RP-HPLC and high performance liquid chromatography-tandem mass spectrometry. Oxidation by tyrosinase (both commercial and purified) not only generated dimers as reported earlier, but also generated significant amounts of oligomers.

2.3 Materials and methods

Dehydro NADA was synthesized from norepinephrine following the published protocol (Dali and Sugumaran, 1988) (Figure 1.6). Briefly, a mixture of (±) norepinephrine hydrochloride (25 g, 0.12 mol), acetic anhydride (150 ml) and triethylamine (25 ml) was stirred under nitrogen at 100 ºC for 1 hr. The cooled mixture was poured onto ice and extracted with 700 ml of ethyl acetate. The organic extract was washed with water, followed by brine and dried over anhydrous $MgSO_4$. Removal of solvent gave tetraacetylnorepinephrine which was recrystallized from hexane to give 40 g (97%) of white solid, mp. 104-105 ºC:Rf (A) : 0.46. ^{1} H-NMR ($CDCl_3$): δ 1.85 (s, 3H, CH_3), 2.00 (s, 3H, CH_3), 2.15 (s, 3H, CH_3), 2.33 (s, 3H, CH_3), 3.30-3.70 (m, 2H, CH_2), 5.60-6.00 (m, 1H, CH), 6.80-7.40 ppm (m, 4H, ArH and NH). IR (nujol):3250 (NH), 1805 (CO), 1780 (CO), 1730 (CO), 1630 (NH), 1370 (CH_3) cm^{-1}, MS: m/e 337 (M^+). A mixture of tetraacetylnorepinephrine (2.0 g, 6 mmol) and anhydrous potassium carbonate (2.0 g) in dimethyl sulfoxide (15 mL) was heated under nitrogen at 110 ºC for 2 hr. The reaction mixture was then poured onto water and extracted with 350 ml of ethyl acetate. The organic solution was washed with brine solution and dried over anhydrous $MgSO_4$. Solvent removal on a rotary evaporator gave 1.4 g of an oily product. Crystallization from 0.2 N acetic acid produced 0.64 g (55%) of pure dehydro NADA, mp. 197-198 ºC, as white crystals. The NMR, IR, UV, and MS were identical as reported earlier. It was further purified by Biogel P-2 column chromatography and used. Mushroom tyrosinase, and laccase were purchased from Sigma Chemical Co., St. Louis Mo. HPLC grade

methanol and ammonium formate (99%) were purchased from Acros, Morris Plains NJ. HPLC-grade water used to prepare the ammonium acetate buffer and HPLC mobile phase was obtained from a Milli-Q® synthesis A10 water purification system from Millipore, Milford, MA. All other chemicals were of analytical grade purchased from Fisher and/or VWR.

Tyrosinase from the larvae of *Sarcophaga bullata* was isolated as follows. Larvae of *S. bullata* were obtained from Carolina Biological Supplies Co., NC and maintained on dog food diet at 27 ºC with a 16 hr photoperiod. All operations were carried out 0-5 °C. Wandering stage larvae (3rd instar) were collected and cleaned with ice cold water and homogenized in a Waring blender for 1-2 min in homogenizing buffer (1% sodium tetra borate containing 0.1% ascorbic acid) with three changes. The homogenate was filtered through a 0.2 μm sieve and washed extensively with running cold water. The translucent cuticle thus obtained was extracted overnight (12 hr) at 4 °C with the homogenizing buffer. The extract was filtered through double layers of cheese-cloth and subjected to 60% ammonium sulfate treatment at 4 ºC. The precipitated proteins were collected by centrifugation at 10,000 x *g* for 10 min. The pellet was dissolved in 50 mM sodium phosphate buffer pH 6.0, dialyzed against the same buffer and subjected to size exclusion chromatography on a Sephacryl S-200 column (115 x 2.0 mm) using 50 mM sodium phosphate pH 6.0 at a flow rate of 0.5 ml/min. Fractions exhibiting tyrosinase activity were pooled, concentrated, and used.

Assay of tyrosinase activities. All spectrophotometric assays were carried out using a Beckman DU-7500 spectrophotometer. Tyrosinase activity in the purified fractions was assayed using a 1 ml reaction mixture containing 2 mM dopamine in 50 mM sodium phosphate, pH 6.0. After adding the enzyme (usually 10-15 μg) the increase in absorbance at 475 nm due to dopamine quinone formation at room temperature was monitored.

RP- HPLC Parameters : A low-flow Shimadzu (Kyoto, Japan) HPLC system, which included a SCL-10A vp controller, two LC-10AD vp pumps, a SIL-10AD vp auto injector, and a C_{18} BetaBasic column (100 mm x 1 mm, 3 mm size) from ThermoElectron Corporation Sunnyvale, CA was used to separate the oligomers of dehydro NADA. The HPLC was operated at a flow rate of 35 μl/min under gradient elution conditions. The gradient consisted of mobile phase A [H_2O, 10 mM formic acid] and B [methanol, 10 mM formic acid]. The binary gradient was linear from 0%-50% B in 40 min. Injection volume was 5 μl.

Mass Spectrometer Parameters: A ThermoFinnigan LCQ Advantage ion trap mass spectrometer (Sunnyvale, CA) was used to detect and characterize dehydro NADA oligomers. The connection from the HPLC column to the electrospray source was made through a 1/16″ stainless steel zero-dead volume union and a 30 cm long, 50 μm ID, 185 μm OD, segment of fused silica capillary. The end of the fused silica capillary was fed into the electrospray interface through a metal sheath. The tip of the capillary was carefully cut to provide a uniformly shaped tip. The tip of the capillary was positioned so

that it was at the edge of the metal sheath. Prior to the start of the experiment, the instrument was tuned using a standard peptide solution. The operating parameters of the ion trap mass spectrometer were as follows; capillary temperature (280 °C), spray voltage (4.00 kV), sheath gas (30 cm^3/min). Collision-induced decomposition (CID) was performed at a relative collision energy of 28, an isolation mass window of 2.5 amu, and a default activation Q and activation time of 0.250 and 30.000 ms, respectively. The CID experiment was designed to obtain the product spectra of a specific parent oligomer by programming the mass spectrometric method to perform CID for the appropriate m/z ratio during the time window that corresponded to elution time of the oligomer.

2.4 Results

Earlier from this laboratory it was shown that tyrosinase-catalyzed oxidation of dehydro NADA results in the rapid formation of a novel quinone methide imine amide (QMIA) as the initial two electron oxidation product (Sugumaran et al., 1992a). It was also shown that the QMIA thus formed reacts with the parent compound generating dimeric products as shown in Figure 1.8 (Sugumaran et al., 1987a; 1988, 1990, 1992a). At that time the product analysis was done on a low resolution RP-HPLC and low resolution NMR which gave poor resolution of products and proton signals respectively. Although it supported the generation of a conclusion that dimeric products are generated during the oxidation of dehydro NADA, the UV spectral analysis indicated further transformation of dimers. Figure 2.1 for instance shows the spectral changes associated with oxidation of dehydro NADA by tyrosinase. As is evident, the reduction in UV spectra keeps on proceeding and did not stop at half the original absorbance value of dehydro NADA. This indicated that dehydro NADA polymerization does not stop at dimer level but is proceeding further to other oligomers also.

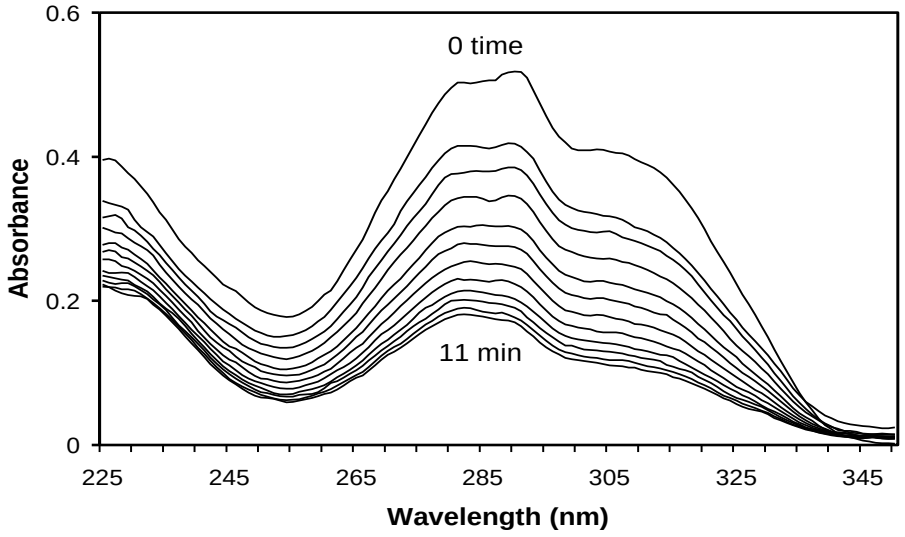

Figure 2.1: Ultraviolet spectral changes associated with tyrosinase-catalyzed oxidation of dehydro NADA. A reaction mixture (1 ml) containing 50 μmoles of dehydro NADA in 50 mM sodium phosphate, pH 6.0 and 10 μg of tyrosinase was incubated at room temperature and the spectral changes associated with oxidation of dehydro NADA was monitored at 1 min interval. The reaction was initiated by the addition of substrate.

To evaluate this proposal, I conducted a detailed analysis of the dehydro NADA - tyrosinase reaction. As pointed out earlier, the reaction accompanied the rapid production of QMIA as witnessed by the intermediate absorbance increase at 485 nm in Figure 2.2. The QMIA rapidly degraded as shown in Figure 2.2. Note that absorbance change at 400 nm as an indication of quinone production is not as drastic as observed for QMIA production and its further transformation. This observation is consistent with the

mechanism described in Sugumaran (2000) where tyrosinase oxidation of dehydro NADA form QMIA followed by its coupling with dehydro NADA.

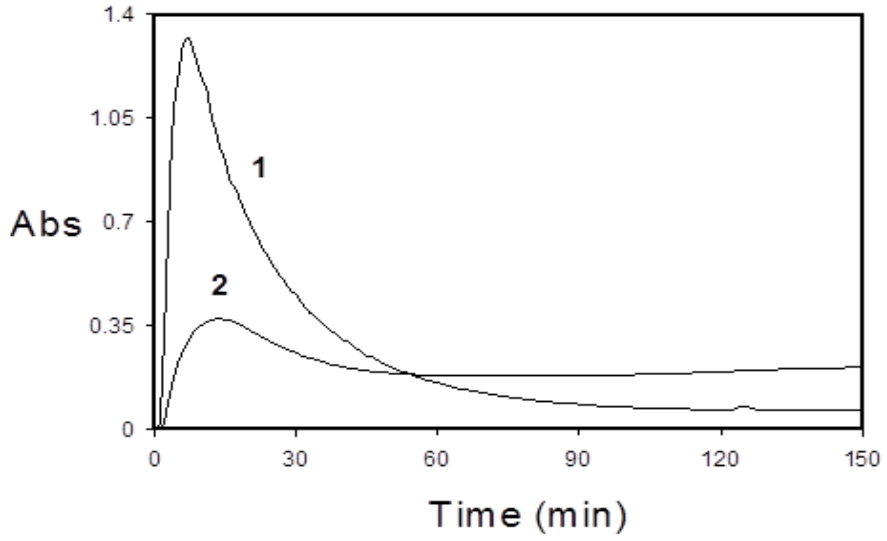

Figure 2.2: Assessing the QMIA production during tyrosinase catalyzed oxidation of dehydro NADA. A reaction mixture (1 ml) containing 50 μmoles of dehydro NADA in 50 mM sodium phosphate buffer, pH 6.0 and tyrosinase (10 μg) was incubated at room temperature and the production of quinone methide imine amide (or quinone) was assessed by monitoring their absorbance maxima at indicated wavelengths.

1. Tyrosinase-catalyzed reaction monitored at 485 nm is due to QMIA formation.

2. Tyrosinase-catalyzed reaction monitored at 400 nm is due to potential quinone formation.

In order to assess the products formed, HPLC studies were conducted on the tyrosinase - dehydro NADA reaction. HPLC analysis of the reaction mixtures containing dehydro NADA and tyrosinase are presented in Figure 2.3. Incubation of dehydro NADA with tyrosinase produced not only dimers (8 min peak) but also other oligomers such as trimers (eluting at about 11 min; Figure 2.3).

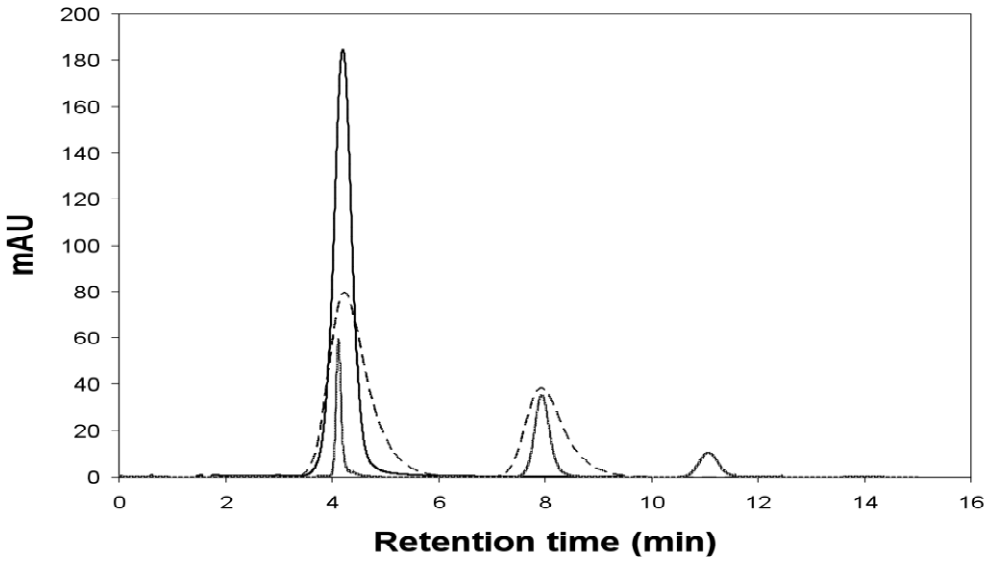

Figure 2.3: RP-HPLC analysis of dehydro NADA-tyrosinase reaction. A reaction mixture (1 ml) containing 50 µmoles of dehydro NADA, 10 µg tyrosinase in 50 mM sodium phosphate, pH 6.0 was incubated at room temperature, an aliquot of the reaction mixture (5 µl) was subjected to HPLC analysis on Agilent 1100 HPLC series, C_{18} cartridge (Agilent Technologies, Santa Clara, CA) using isocratic elution with 50 mM citrate buffer pH 3.0 containing 7% acetonitrile at a flow rate of 0.6 ml/min. The solid line represents the zero min (control) reaction; the broken line represents the 10 min and the dotted line represents 20 min reaction.

To further support the occurrences of the oligomerization reaction, reaction products were further analyzed by RP-HPLC/ESI/MS-MS. The base peak chromatogram depicted in Figure 2.4 shows the products of dehydro NADA oxidation catalyzed by tyrosinase as analyzed by RP-HPLC/ESI/MS-MS. These data correspond to a reaction time of 1 hr. The mass spectra associated with the initial two peaks at 13.66 min and 14.15 min are indicative of isomers of dehydro NADA dimers. The mass spectra associated with the next set of peaks at 15.46 min and 16.61 min indicate that these peaks are due to trimers of dehydro NADA. The mass spectra associated with the chromatographic peaks between 17.76 min and 19.90 min are due to tetramers of dehydro NADA. The multiple peaks for each of the oligomers arise because of the formation of different stereo isomeric addition products. For example, nonenzymatic coupling of dehydro NADA quinone methide to dehydro NADA can give rise to at least four different isomeric products, all of which has been identified as naturally occurring compounds in the cuticle of insects (Tada et al., 2002). Upon further reaction with dehydro NADA quinone methide these isomeric dimers produce an array of isomeric trimers. These non-stereospecific chemical additions naturally result in the production of broad oligomeric peaks in the chromatogram. As a result, there is a significant degree of co-elution between dimer and trimer species, as well as, between trimer and tetramer species.

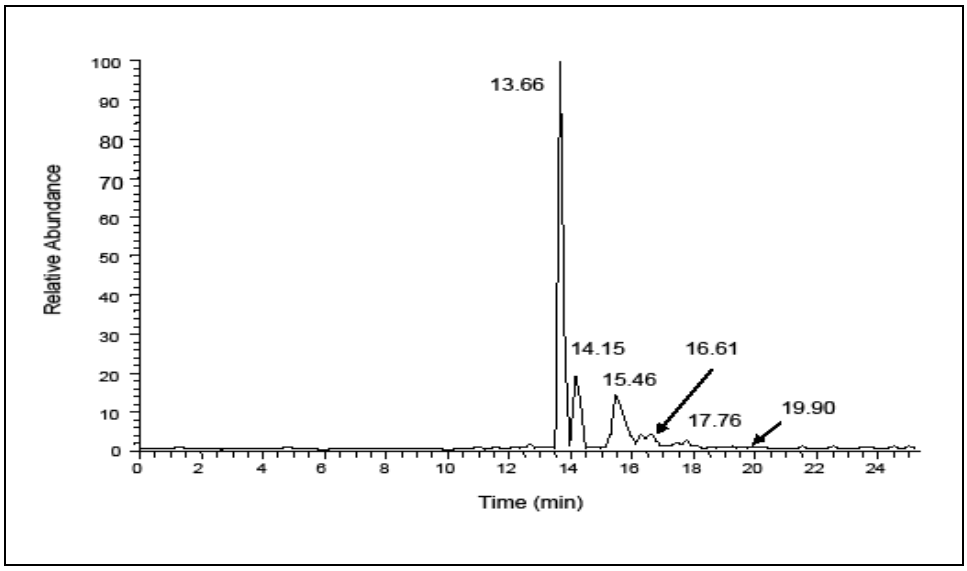

Figure 2.4: The Base Peak Chromatogram from the RP-HPLC/ESI/MS-MS analysis of dehydro NADA/tyrosinase reaction mixture. The marked retention times indicate the location of the polymeric species identified. The first two chromatographic peaks between 13.66 and 14.15 min are identified as isomers of the dimeric product. The peaks between 15-17 min are identified as isomers of the trimeric product. The peaks between 17.5-21 min are identified as isomers of the tetrameric product.

The average ESI-mass spectrum from 13.66 to 14.15 min peaks (from Figure 2.4) is shown in Figure 2.5. It exhibits major ions at m/z 385, 769 and 1153. The ion at m/z 385 corresponds to the protonated dimer of dehydro NADA, $[D+H]^+$, the m/z 769 ion represents its proton-bound dimeric ion, $[2D+H]^+$, and the m/z 1153 ion represents its proton-bound trimeric ion, $[3D+H]^+$. The $[2D+H]^+$ and $[3D+H]^+$ are formed in the gas-

phase during electrospray ionization. The CID mass spectrum of the m/z 769 ion shows a dominant product ion at m/z 385, supporting its assignment as a proton-bound dimer formed in the gas-phase. The CID spectrum of the m/z 385 ion (Figure 2.5 inset) shows an abundant product ion at m/z 192. This corresponds to the protonated quinone methide imine amide ion, which is a logical decomposition product of the protonated dimer. The intense product ion at m/z 326 corresponds to the loss of NH_2COCH_3. Other major product ions include m/z 284 (loss of 101), and m/z 267 (loss of 118).

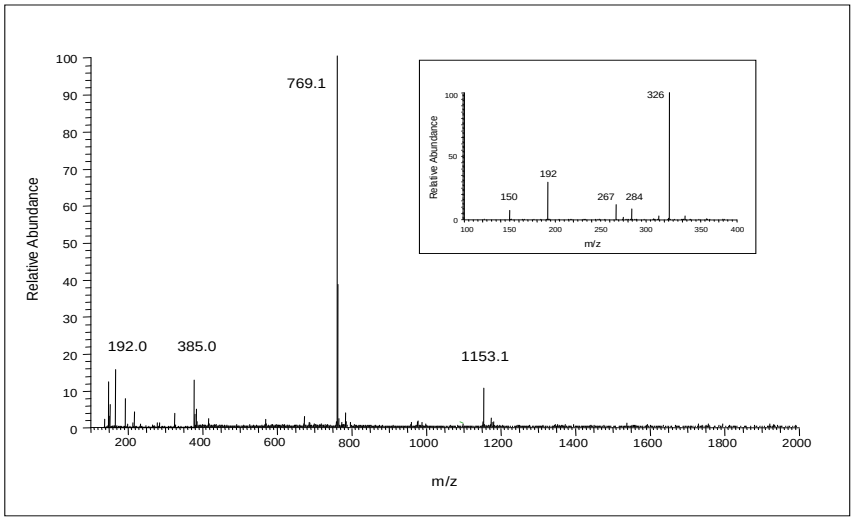

Figure 2.5: The average electrospray mass spectrum of dimeric product of dehydro NADA. The m/z 385 ion corresponds to the protonated dimer ion. The m/z 769 ion corresponds to the proton-bound dimer of the dimeric product and is formed in the gas-phase during electrospray ionization. Inset: The average CID mass spectrum of the m/z 385 parent ion.

The average ESI mass spectrum from 15.46 to 16.61 min (from Figure 2.4) is shown in Figure 2.6. It shows dominant ions at m/z 576 and m/z 1151. These peaks are ascribed to the protonated trimer, $[T+H]^+$, and its corresponding proton-bound dimeric ion, $[2T+H]^+$ respectively. Again, the latter is formed in the gas-phase during electrospray ionization. Accordingly, the CID spectrum of the m/z 1151 ion shows a dominant peak at m/z 576, supporting its assignment as a proton-bound dimer of the trimer. The CID spectrum of the m/z 576 parent ion (Figure 2.6 inset) shows dominant product ions at m/z 385, 383 and m/z 192, corresponding to the loss of the monomeric and dimeric moieties respectively. This confirms the assignment of the m/z 576 ion as the protonated trimer of dehydro NADA. The m/z 517-product ion corresponds to the loss of NH_2COCH_3 from the parent ion. The major product ions include m/z 517 (loss of 59), m/z 458 (loss of 101), m/z 385 (loss of 118), m/z 383 (loss of 193), m/z 326 (loss of 250), m/z 324 (loss of 252), m/z 282 (loss of 294), and m/z 191 (loss of 384).

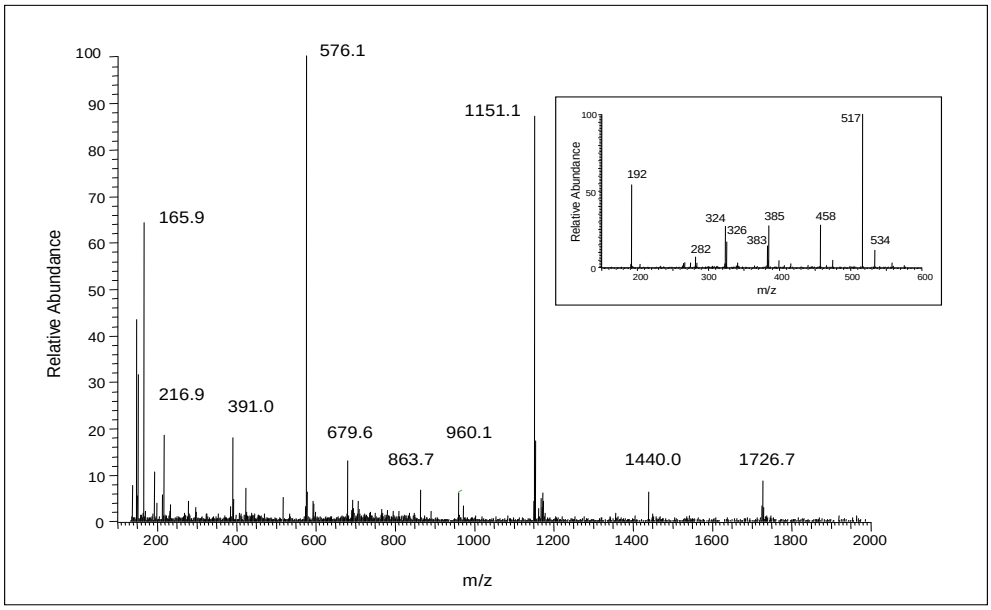

Figure 2.6: The average electrospray mass spectrum of trimeric product of dehydro NADA.The m/z 576 ion corresponds to the protonated trimer ion. Inset: The average CID mass spectrum of the m/z 576 parent ion.

The average mass spectrum from 17.76 to 19.90 min peaks (from Figure 2.4) is shown in Figure 2.7. It contains a dominant ion at m/z 767 which corresponds to protonated tetramer, $[Tet+H]^{+\cdot}$ The CID spectra of the m/z 767 parent ion (Figure 2.7 inset) shows dominant product ions at m/z 576 and 574 and m/z 385 and 383, corresponding to the loss of the monomer and dimer moieties, respectively. These

product ions provide strong evidence that the m/z 767 parent ion corresponds to the protonated tetrameric product of dehydro NADA. The m/z 708-product ion corresponds to the loss of NH_2COCH_3 group. The major product ions include m/z 708 (loss of 59), m/z 576 (loss of 191), m/z 574 (loss of 193), m/z 517 (loss of 250), m/z 385 (loss of 382), m/z 383 (loss of 384), m/z 324 (loss of 443), and m/z 282 (loss of 485).

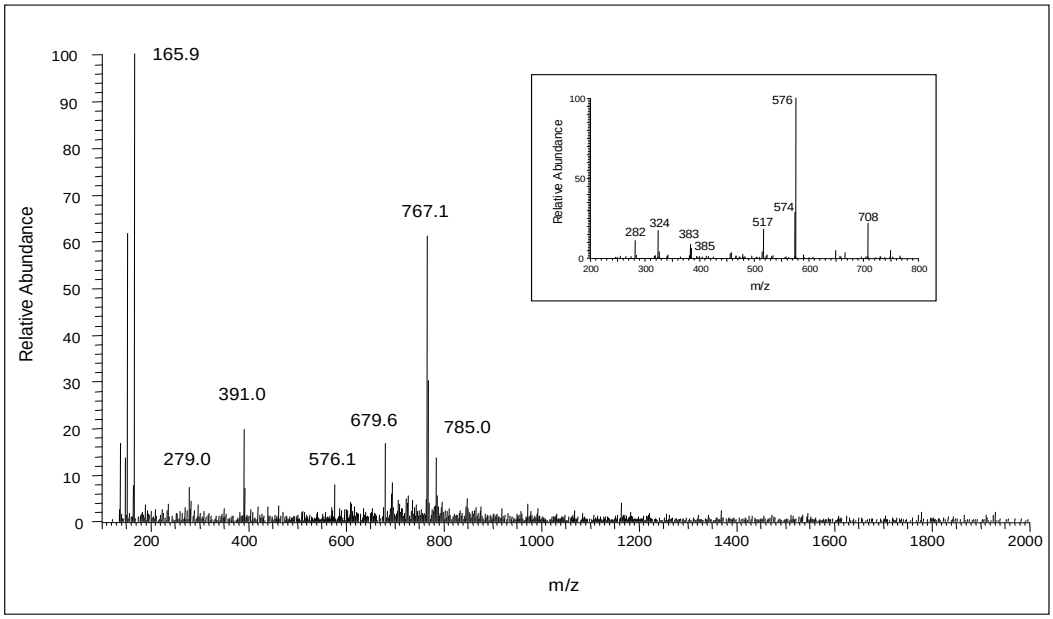

Figure 2.7: The average electrospray mass spectrum of tetrameric product of dehydro NADA. The m/z 767 ion corresponds to the protonated tetrameric ion. Inset: The average CID mass spectrum of the m/z 767 parent ion.

Inspection of the product ions in the CID spectra illustrated in the inserts of Figures 2.5-2.7 show similarities that provide convincing evidence for the presence of the oligomeric series. Figure 2.8 illustrates the key dissociation pathways for the protonated dimer, trimer and tetramer species. The m/z 192, m/z 385 and m/z 576 are major product ions in the CID spectra of the $[M+H]^+$ parent ions of the dimer, trimer and tetramer, respectively, that correspond to the loss of a monomeric moiety. In addition, the loss of NH_2COCH_3 is a dominant pathway for each of the species. The dimer, trimer, and tetramer species contain two, three, and four NH_2COCH_3 groups, respectively. The scheme shown in Figure 2.8 suggests that it is the terminal NH_2COCH_3 group that is lost. However, the group that is lost probably depends upon which site is protonated and it is likely that electrospray ionization results in some combination of species protonated at each of these cites. The m/z 192 product ion does not appear in the CID spectrum of the protonated tetramer because the lower mass range in an ion trap mass spectrometer is limited to 1/3 the mass-to-charge ratio of the parent mass.

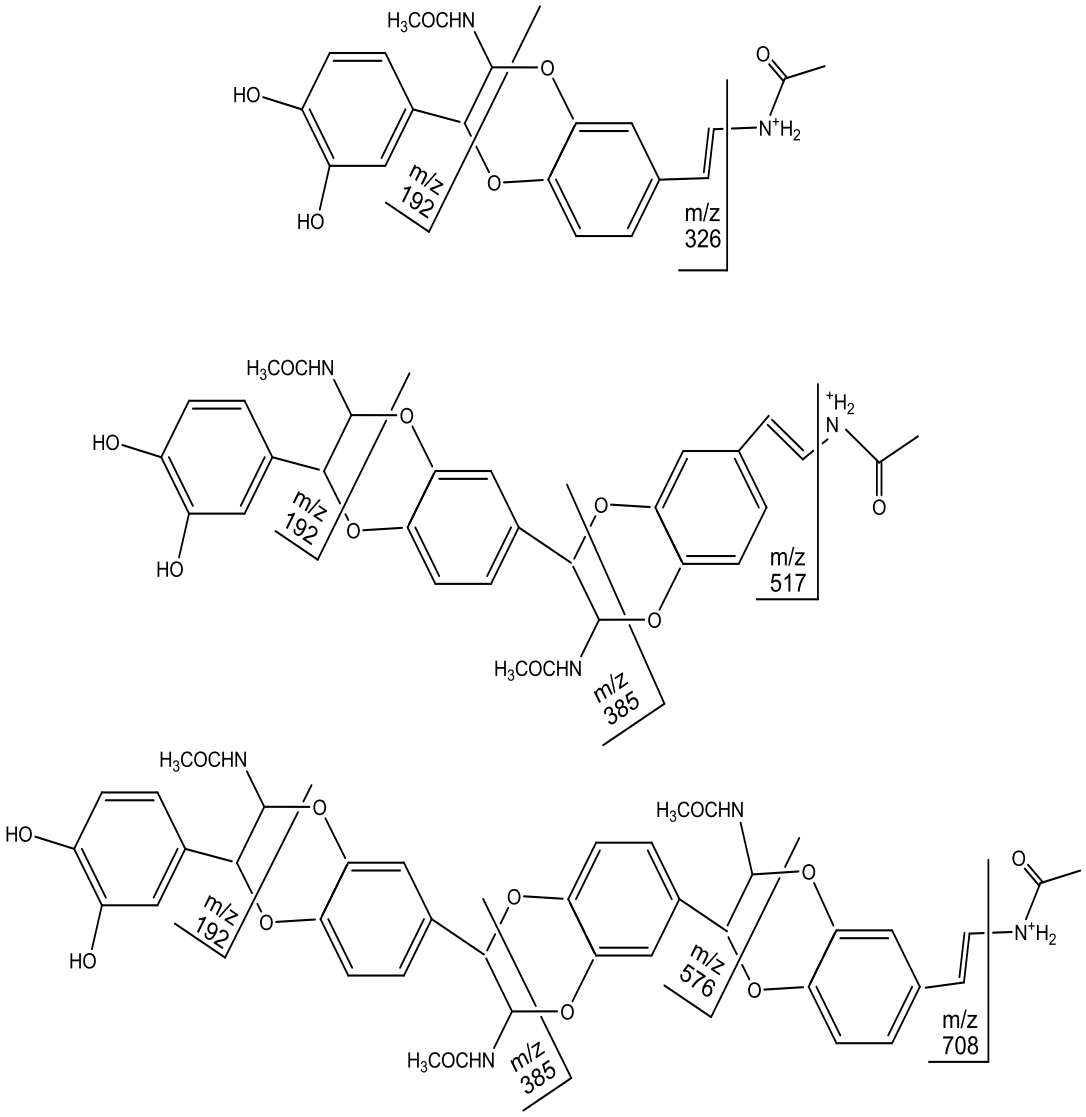

Figure 2.8: Analogous dissociation pathways for the protonated dimer (top), trimer (middle) and tetramer (bottom) species. The m/z 192, m/z 385 and m/z 576 are major product ions in the CID spectra of the [M+H] $^{+}$ *parent ions of the dimer, trimer and tetramer, respectively. The m/z 192 product ion does not appear in the CID spectrum of the protonated tetramer because the lower mass range in an ion trap mass spectrometer is limited to 1/3 the mass-to-charge ratio of the parent mass.*

Using the average mass spectrum from 13-22 min peaks and assuming these oligomeric species have similar ESI/MS sensitivities, it is estimated that the reaction products consist of 73 % dimers, 22 % trimers, and 5 % tetramers. These results correspond to a two hr incubation. Results at longer reaction times (> 24 hr) were very similar, indicating that the polymerization reaction does not continue to form higher oligomers. In the estimation of the relative abundances of the reaction products the intensities of all of the ions containing these species were used as follows:

Relative abundance of dimer = $I_{385}([D+H]^+) + 2I_{769}([2D+H]^+) + I_{960}([D+H+Tri]^+) + 3I_{1153}([3D+H]^+$

Relative abundance of trimer = $I_{576}([Tri+H]^+) + 2I_{1151}([2Tri+H]^+) + I_{960}([D+H+Tri]^+) + I_{1342}([Tri+H+Tet]^+$

Relative abundance of tetramer = $I_{767}([Tet+H]^+) + 2I_{1533}([2Tet+H]^+) + I_{1342}([Tri+H+Tet]^+$

The mixed proton-bound dimeric species at m/z 960 and m/z 1342 were of relatively low abundance. Formation of these ions occurred as a result of co-elution between dimer and trimer species, as well as, between trimer and tetramer species.

The reaction is not confined to only mushroom tyrosinase. Even insect phenoloxidase, isolated from *Sarcophaga bullata*, catalyzed this oligomerization reaction. The base peak chromatogram obtained using the insect cuticle tyrosinase was similar to the base peak chromatogram obtained using the commercial tyrosinase. Figure 2.9 shows the average mass spectrum obtained across the chromatographic peaks of dimers, trimers and tetramers for dehydro NADA incubated with the insect phenoloxidase for 2 hr. This data shows the presence of sodiated species that were not nearly as dominant in the data shown in Figures 2.5-2.7. It is likely that the reaction is contaminated to some degree with sodium ion as insect tyrosinase was purified using sodium phosphate buffer. Nevertheless, the sodiated peaks could be used for estimation of the relative abundances of the dimer, trimer and tetramer species, as described above for the commercial tyrosinase data. The analysis of the insect phenoloxidase data suggests that the reaction products consist of 66 % dimer, 28 % trimer and 6 % tetramer, which is very similar to the results obtained with the commercial tyrosinase.

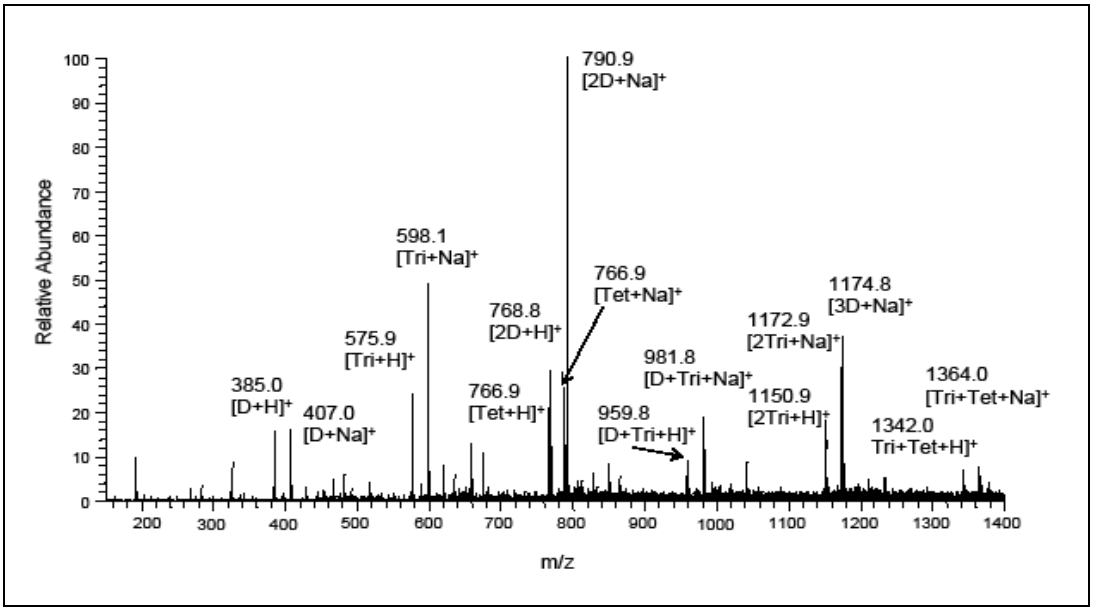

Figure 2.9: The average mass spectrum obtained across the chromatographic peaks of dimers, trimers and tetramers for dehydro NADA incubated with insect phenoloxidase. The reaction conditions are as outlined in materials and methods. The relative intensities of the annotated peaks were used to estimate the relative abundances of the dimer, trimer and tetramer species using the same approach outlined in the text for the commercial tyrosinase data.

The base peak chromatogram of insect tyrosinase reaction given in Figure 2.10 clearly shows the presence of not only dimers, but also trimers and to certain extent tetramers. Thus the results presented in this chapter support not only dimerization of dehydro NADA by tyrosinase action but also the production of other oligomers such as trimer and tetramer.

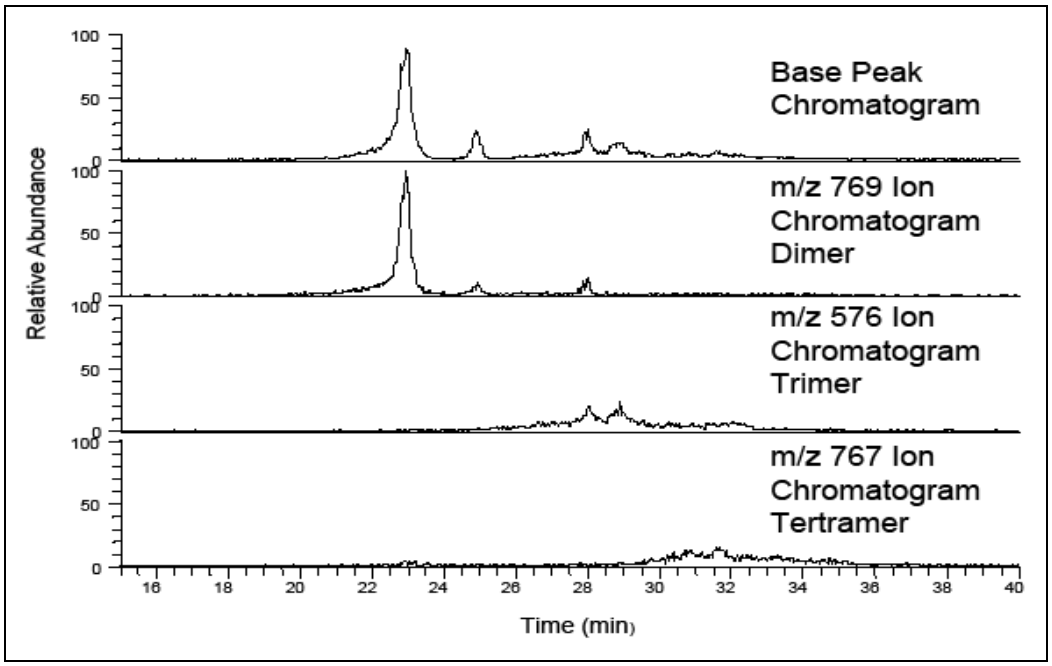

Figure 2.10: The Base Peak Chromatogram and ion chromatograms corresponding to the dimer, trimer and tetramer products obtained from the RP-HPLC/ESI/MS-MS analysis of dehydro NADA/insect tyrosinase reaction. The ion chromatograms of the m/z 769, m/z 576 and m/z 767 correspond to the dimer, trimer and tetramer products. Detailed structural analysis of these ions is described in the text and Figures 2.5, 2.6, and 2.7.

2.5. Discussion

Earlier it was reported that the tyrosinase-catalyzed oxidation of dehydro NADA produces dimeric products (Sugumaran et al., 1987a, 1988, 1990, 1992a; Sugumaran 1998, 2000). The evidence for this proposal was based on the ultraviolet spectral data and low-resolution NMR spectra. It was contended that the reaction was probably arrested after dimer formation. Dehydro NADA dimers have also been isolated from the cuticle of *Cicada* as naturally occurring compounds and shown to be a mixture of four isomeric compounds (Tada et al., 2002). Close examination of the reactivity of QMIA reveals that formations of additional oligomeric products are possible. For instance, the reaction of QMIA with the free catecholic group of the benzodioxan dimer will result in the production of a trimeric compound (Figure 2.11). Similar additions to trimer will produce tetramer and the process can thus go on. However, this possibility has never been examined. Reversed-phase liquid chromatography electrospray mass spectrometry (RP-HPLC/ESI/MS-MS) offered a unique way to look at such polymerization reactions, and reexamination of the oxidation chemistry of dehydro NADA using RP-HPLC/ESI/MS-MS confirmed tyrosinase-catalyzed oxidation of dehydro NADA produces dimeric, trimeric and tetrameric products in the reaction mixture.

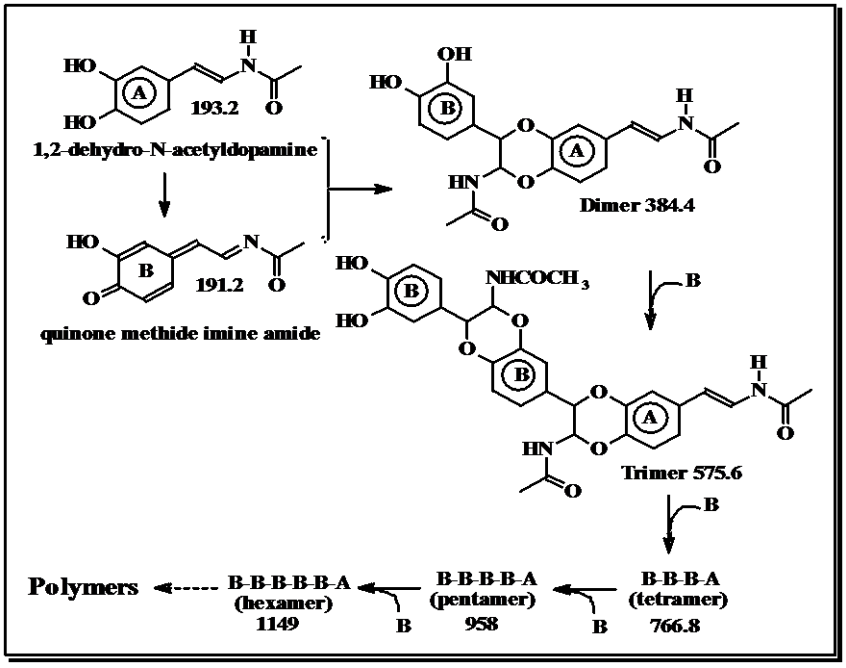

Figure 2.11: Proposed mechanism for oligomerization of dehydro NADA by tyrosinase. Tyrosinase-catalyzed oxidation of dehydro NADA produces the QMIA which reacts with the parent molecule (in the absence of any other nucleophiles) generating the benzodioxan dimer (addition of two OH groups to the two reactive groups quinone methide and the imine amide). Since the dimer has two free OH groups similar to the parent catechol, when enough dimers are produced in the reaction mixture, QMIA can add on to the dimer also, producing trimeric and other polymeric products as indicated in the figure. The numbers in the figure indicate the molecular weight of each oligomer.

Tyrosinase is widely distributed in the cuticle, hemolymph, and other tissues of insects (Brunet, 1980). Catechol oxidase activity is typically found in flexible larval cuticles where its function may be associated more with wound healing than with

sclerotization (Andersen, 1985; Barett, 1987). Tyrosinases have also been isolated from pharate pupal integument of *Manduca sexta* undergoing cuticle sclerotization, so its role in oxidation of N-acylcatecholamines and in sclerotization has not been ruled out (Morgan et al., 1990; Aso et al., 1984; Gorman et al., 2010). Insect tyrosinase will also oxidize dehydro NADA and produces QMIA as transient intermediate which will form oligomers due to the addition of two phenolic hydroxyl groups to the reactive sites on QMIA. Both the quinone methide nucleus and the imine amide part in the molecule act as electrophiles to form adducts with nucleophilic center. In the cuticular environment, such reactions are expected to generate adducts with cuticular nucleophiles resulting in the production of various combinations of protein, chitin and dehydro NADA adducts and crosslinks that are necessary for stabilization and hardening of the cuticle apart from producing dimers and other oligomers.

2.6 Conclusion

Results presented in this chapter confirms the earlier published work on dimerization of dehydro NADA via QMIA (Sugumaran et al., 1992a). In addition, it reveals the production of trimeric and other oligomeric products that has not been shown before. Since QMIA has the tendency to react with ortho-diphenols, it will keep on adding to monomer producing dimer, and then will add on to trimmers built in the reaction. Continuation of this reaction therefore produces trimmers, tetramers and other oligomers. The results of this new reaction have been published already (Abebe et al., 2010).

CHAPTER 3

LACCASE CATALYZED OXIDATION OF 1, 2-DEHYDRO-N-ACETYLDOPAMINE

3.1 Chapter summary

In insects during sclerotization crosslinking occurs as a result of oxidative and nucleophilic reactions between highly reactive sclerotizing agents derived from catechols and nucleophilic side chain group of protein and chitin. Laccases are multicopper oxidases that have been recently shown to play a crucial role in cuticular sclerotization (Arakane et al., 2005). Therefore I undertook a study on the oxidation of dehydro NADA with laccase in hope of learning the detailed mechanism of its oxidation. Preliminary studies indicated that the course of oxidation of dehydro NADA differs drastically from that of tyrosinase and produced neither the quinone nor QMIA. Since laccases are known to generate primarily semiquinones as the initial products, lack of accumulation of two electron oxidation products indicated that laccase reaction is primarily occuring via free radical coupling mechanism. Consistent with this proposal, laccase catalyzed oxidation of dehydro NADA, resulted in the production of largely dimeric products, and failed to produce any significant amount of oligomeric materials. Thus laccases seems to use a radical coupling mechanism for the dimerization reaction. In insect cuticle, such reactions are likely to occur and cause free radical coupling reaction.

3.2 Introduction

Laccase (benzenediol: oxidoreductases; EC 1.10.3.2) are blue, multicopper oxidases, widely distributed in nature, and catalyze the oxidation of an array of aromatic substrates concomitantly with the reduction of molecular oxygen to water (Rosenzweig and Sazinsky, 2006). In addition to mono-and polyphenols, laccases have been found to be capable of oxidizing various aromatic compounds, such as substituted phenols, diamines, aromatic amines and thiols (Flurkey, 2003). Syringaldazine (4-hydroxy-3, 5-dimthoxybenzaldehyde azine), for example, is a synthetic substrate often used to demonstrate the presence of laccases (Claus, 2003). Laccases exhibit no monophenol hydroxylase activity. O*rtho*-diphenoloxidases possess this activity to a varying degree. Laccases are also known to oxidize both *para*-, and *ortho*-diphenols while *ortho*-diphenols are specific to their substrates. Interestingly laccases produce semiquinone as primary product (Nakumara, 1960). But the extremely reactive semiquinones (2 molecules) undergo reverse dismutation generating one molecule of parent diphenol and a molecule of quinone. This is in sharp contrast to tyrosinase or *ortho*-diphenoloxidase reaction where two electron oxidation product is the primary product. Irrespective of the course, the net reactions in both cases are the same that these two enzymes produce dimers as the products. Laccases are inhibited by azides and fluorides, but not phenythiourea while the latter is a potent inhibitor of *ortho*- diphenoloxidase.

Recently, Arakane et al (2005), using RNA interference demonstrated that cuticular laccase 2 is the primary enzyme responsible for sclerotization of cuticle in *Tribolium*

castanaeum. RNA interference inhibition of laccase 1 gene product as well as *ortho* diphenoloxidases in the same organism had no influence on the process. Other workers also showed involvement of laccase 2 in sclerotization of cuticle in the bettle species *Monochamus alteranus* (Niu et al., 2008), in the mosquito *Culex pipens* (Pan et al., 2009), in *Manduca sexta* (Dittmer et al., 2009) and *B.mori* (Yatsu and Asano, 2009). These results clearly indicate the participation of laccase 2 in sclerotization reaction. In the light of these findings, it became obvious that the oxidation of dehydro NADA by laccase should be examined.

Therefore, I undertook a study on the kinetics and mechanism of oxidation of dehydro NADA by laccase purified from *Manduca sexta* and commercial laccase. I employed UV-Vis spectroscopy, RP-HPLC, and high performance liquid chromatography - tandem mass spectrometry to study the course of the reaction. Interestingly, oxidation by laccase failed to produce any detectable quinone or quinone methide as the primary two-electron oxidation product. Since laccases are known to generate primarily semiquinones as the initial products, lack of accumulation of two-electron oxidation products indicated that laccase produced semiquinones are primarily undergoing radical coupling generating dimer and not the quinone by dismutation. Consistent with this proposal, laccase-catalyzed oxidation of dehydro NADA, resulted in the production of largely dimeric products and failed to produce any significant amount of oligomeric materials.

3.3 Materials and methods

Dehydro NADA was synthesized as outlined in Chapter 2, section 2.3. Cuticular laccase was isolated from the pharate cuticle of *Manduca sexta* using the protocol developed by Thomas et al., (1989) with the following modifications. *Manduca sexta* eggs were obtained from a commercial supplier (Carolina Biological Supply Company, Burlington, North Carolina) and reared on *Manduca* diet at 30 ºC with 16 hr photoperiod. Integuments (50 mg) from pharate pupae collected at 4 ºC after the epidermis and fat body removed using glass/ metal spatula were homogenized in 0.1 M Tris-HCl buffer containing 1.0 M sodium chloride and 50 mM ascorbic acid, pH 7.8. It was digested with trypsin (3 mg) at 37 ºC for 2 h in 0.1 M sodium phosphate buffer pH 7.0 containing 50 mM ascorbic acid and the digest was passed through cheesecloth. The filtrate was treated with solid ammonium sulfate and brought to 40% saturation. After centrifugation at 15,000 rpm for 15 min at 4 ºC, the pellet was dissolved in 20 mM sodium phosphate pH 6.0, dialyzed against the same buffer and subjected to size exclusion chromatography on Sephacryl S-200 column (115 x 2.0 mm) using 20 mM sodium phosphate pH 6.0 at a flow rate of 0.5 ml/min. Fractions exhibiting laccase activity were pooled, concentrated and used in biochemical studies.

Assay of Laccase activities. All spectrometric assays were carried out using Beckman DU-7500 spectrophotometer. The purified laccase activity was assayed using dopamine and syringaldazine as the chromogenic substrates separately. A 1.0 ml reaction mixture containing either 3 mM syringaldazine (prepared in 95% ethanol) or 3 mM dopamine in

50 mM sodium phosphate, pH 6.0 was incubated at room temperature and the increase in absorbance (475 nm for dopamine and 525 nm for syringaldazine) was monitored after adding 30 µl aliquot of enzyme. All other techniques used such as RP-HPLC, RP-HPLC/ESI/MS-MS are outlined in chapter 2 materials and methods.

3.4 Results

Laccase also rapidly oxidized dehydro NADA as indicated by the fast UV spectral changes shown in Figure 3.1A. The UV spectral changes exhibited a marked reduction in UV spectrum of dehydro NADA peak. Comparison of laccase reaction with tyrosinase reaction (shown in Figure 3.1B) clearly revealed that these two spectral changes are different and indicated a different course of reaction for these two enzymes.

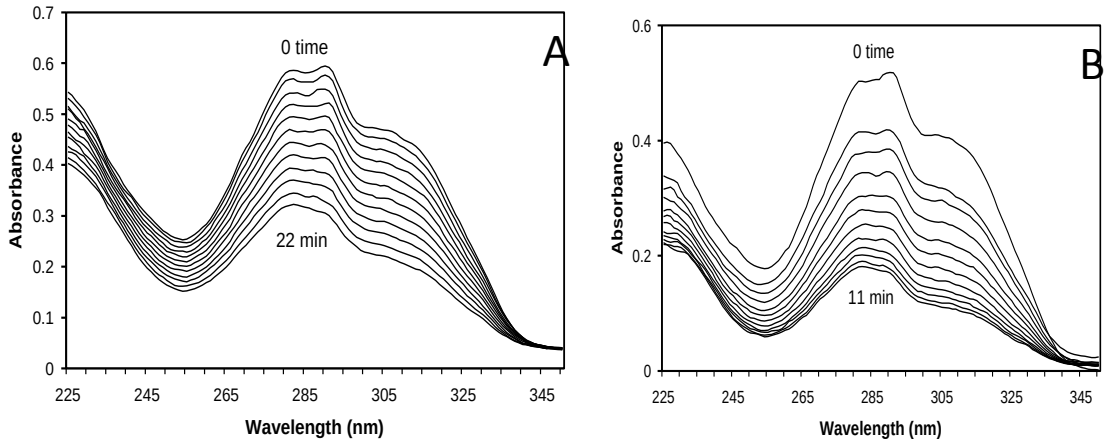

Figure 3.1: Ultraviolet spectral changes associated with laccase-mediated oxidation of dehydro NADA (A). A reaction mixture (1 ml) containing 50 μmoles of dehydro NADA in 50 mM sodium phosphate, pH 6.0 and 10 μg of laccase was incubated at room temperature and the spectral changes associated with oxidation of dehydro NADA was monitored at 2 min intervals. The reaction was initiated by the addition of substrate. For comparison tyrosinase-mediated oxidation of dehydro NADA is shown in B (for conditions see Figure 2.2).

As stated in the earlier chapter, tyrosinase catalyzed oxidation of dehydro NADA resulted in the transient accumulation and rapid decomposition of its two electron oxidation product QMIA as shown in Figure 3.2. The laccase catalyzed reaction is in sharp contrast, neither produced the transient QMIA nor the quinones as absorbance changes at either 485 nm (due to QMIA formation) or 400 nm (due to quinone formation) remained at nearly undetectable range. Furthermore laccase mediated oxidation of dehydro NADA exhibited a linear decay with respect to time (Figure 3.3, lanes 1 to 4), compared to an exponential decay for tyrosinase-dehydro NADA reaction (Figure 3.3, lines 5 to 8). This again indicates a different route for the oxidative transformation of dehydro NADA by laccase and tyrosinase. Since lacasses are well known to produce free radicals as the primary oxidation products (Nakumara, 1960), it is conceivable that the observed decay of dehydro NADA could be due to a slow production of free radicals followed by a fast coupling reaction. In accordance with the well-established laccase chemistry, one would expect the oxidation of dehydro NADA leading to the production of radical dismutation yielding two electron oxidized quinonoid product and the parent catechol. But again evidence for quinonoid production (Figure 3.2) did not support the dismutation.

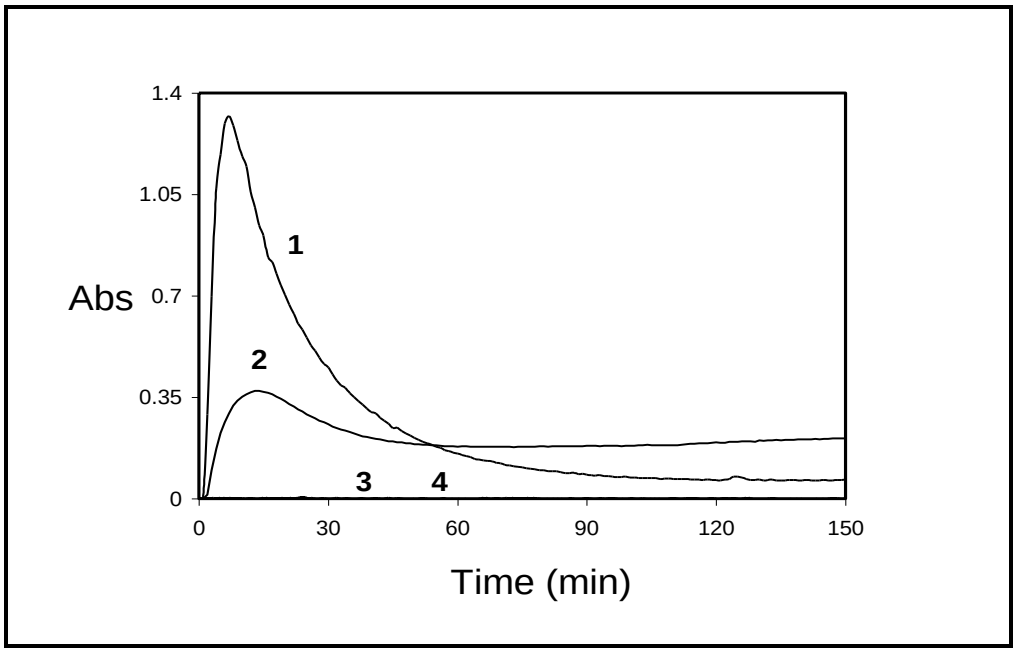

Figure 3.2: Assessing the quinone methide imine amide production during laccase catalyzed oxidation of dehydro NADA. A reaction mixture (1 ml) containing 50 μmoles of dehydro NADA in 50 mM sodium phosphate buffer, pH 6.0 and indicated enzyme (10 μg) was incubated at room temperature and the production of quinone methide imine amide (or quinone) was assessed by monitoring their absorbance maxima at indicated wavelengths. For comparison tyrosinase catalyzed oxidation of dehydro NADA are given in lines 1 and 2.

Line 1- Tyrosinase catalyzed reaction monitored at 485 nm due QMIA formation, line 2 tyrosinase catalyzed reaction monitored at 400 nm due to potential quinone formation, line 3- laccase catalyzed reaction monitored at 485 nm due QMIA formation and line 4- laccase catalyzed reaction monitored at 400 nm due quinone formation.

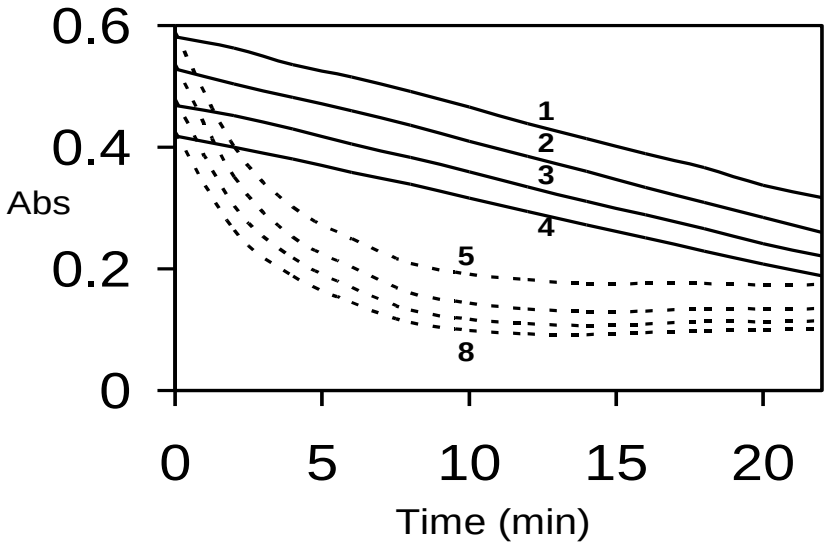

Figure 3.3: Kinetics of oxidation of dehydro NADA by laccase (solid lines). For comparison the results of tyrosinase oxidation of dehydro NADA are shown in broken lines. A reaction mixture (1 ml) containing 25 μmoles of dehydro NADA in 50 mM sodium phosphate, pH 6.0 and 10 μg of laccase was incubated at room temperature. The absorbance changes associated with oxidation of dehydro NADA was monitored continuously for 20 min 1 and 5 at 285 nm; 2 and 6 at 295 nm; 3 and 7at 305 nm and 4 and 8 at 315 nm. For comparison tyrosinase results are presented (broken lines).

Most likely radical coupling rather than radical dismutation must be accompanying the laccase reaction. If this is true, laccase catalyzed oxidation also lead to dimer formation similar to tyrosinase reaction albeit employing a different route. To further investigate the reaction course, RP-HPLC studies were conducted on laccase catalyzed

oxidation of dehydro NADA. The RP-HPLC analysis of this reaction is shown in Figure 3.4. As outlined earlier tyrosinase generated dimer and trimeric products, while laccase produced only the dimer.

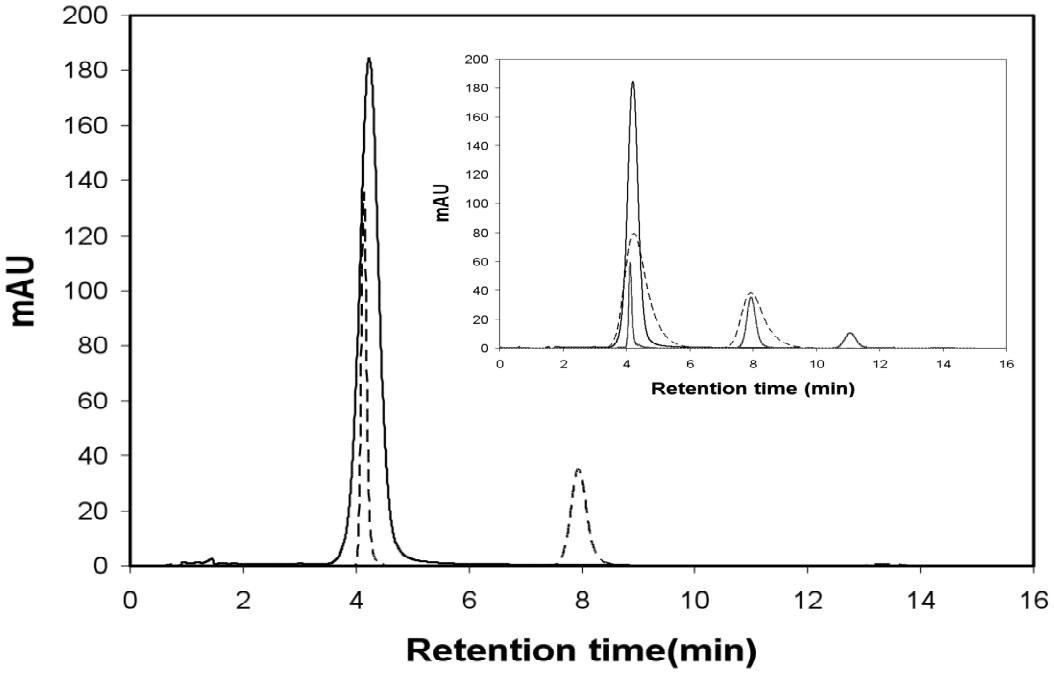

Figure 3.4: HPLC analysis of dehydro NADA-laccase reaction. The same reaction conditions are used as in Figure 2.3 except tyrosinase is replace by laccase. Inset: RP-HPLC analysis of tyrosinase-dehydro NADA reaction. Note the presence of dimer and trimer in tyrosinase-dehydro NADA reaction and the presence of only dimer in laccse reaction.

To further confirm the course of reaction catalyzed by laccase RP-HPLC/ESI/MS-MS studies were carried out. The average ESI-mass spectrum for dimer is shown in Figure 3.5. It exhibited major ions at m/z 385, 769 and 1153. The ion at m/z 385 corresponds to the protonated dimer of dehydro NADA, $[D+H]^+$, the m/z 769 ion represents its proton-bound dimeric ion [2D+H] + and the m/z 1153 ion represent its proton bound trimeric ion, $[3D+H]^+$. The $[2D+H]^+$ and $[3D+H]^+$ are formed in the gas-phase during electrospray ionization.

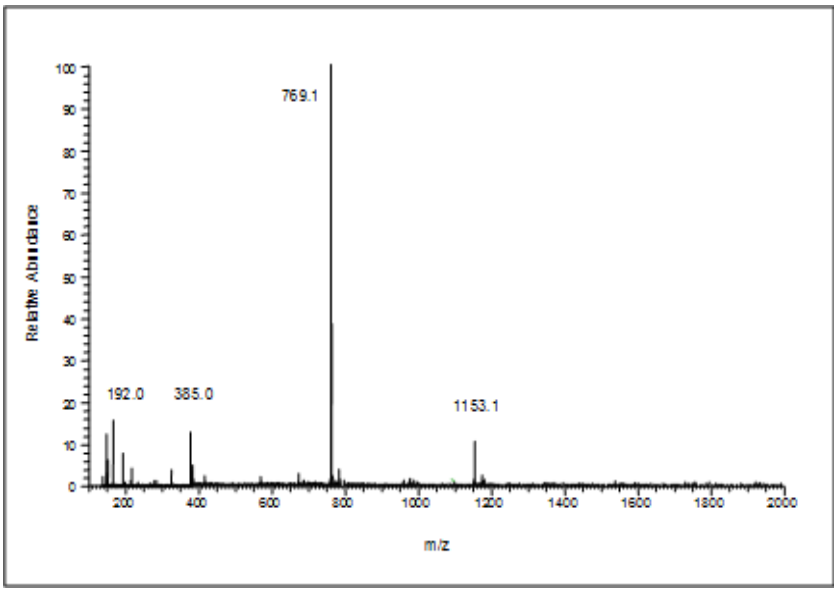

Figure 3.5: The average electrospray mass spectrum of dimeric product of dehydro NADA. The m/z 385 ion corresponds to the protonated dimer ion. The m/z 769 ion corresponds to the proton-bound dimer of the dimeric product and is formed in the gas phase during electrospray ionization. The average CID mass spectrum of the m/z 385 parent ion is similar to Figure 2.5 inset.

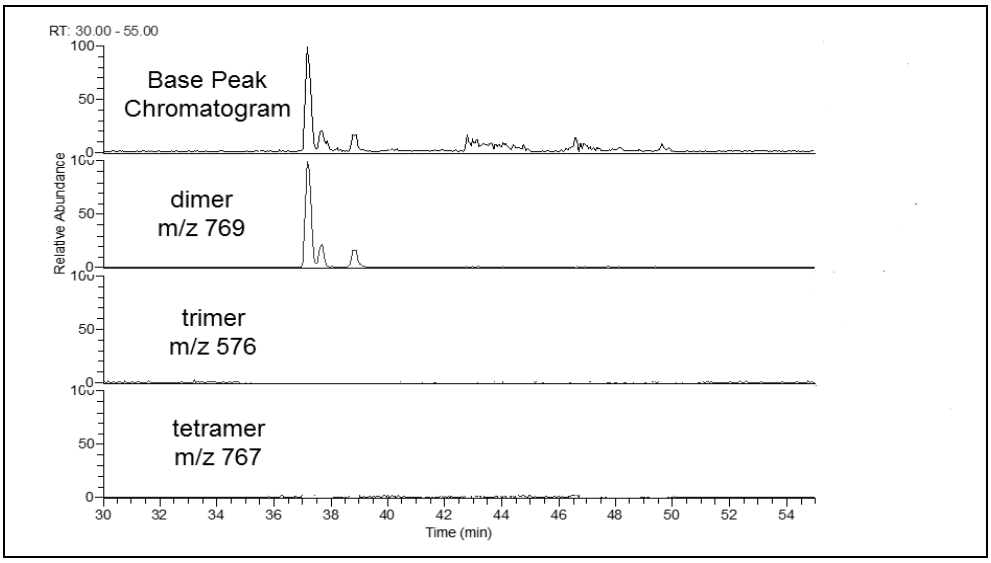

Figure 3.6: The Base Peak Chromatogram and ion chromatograms corresponding to the dimer, trimer and tetramer products obtained from the RP-HPLC/ESI/MS-MS analysis of the reaction mixture containing dehydro NADA-commercial laccase reaction. The ion chromatograms of the m/z 769 correspond to the dimer products. Detailed structural analysis of this ion is described in the previous chapter text and Figure 2.5. Essentially, reaction of dehydro NADA with commercial laccase forms only the dimeric products.

The base peak chromatogram depicted in Figure 3.6 shows the products of dehydro NADA oxidation catalyzed by laccase as analyzed by RP-HPLC/ESI/MS-MS. The mass spectra associated with the peaks between 37-40 min corresponded to the isomers of dehydro NADA dimers. They appear to make up nearly 100 % of the products. That the reaction is not limited to commercial laccase and that even insect cuticular laccase could also perform such a reaction is illustrated in Figure 3.7.

Incubation of *Manduca* cuticular laccase with dehydro NADA generated the base peak chromatogram depicted in Figure 3.7. The dimeric products accounted for almost 100 % of the products. Thus the laccase-catalyzed reaction of dehydro NADA seem to differ significantly from that of the tyrosinase-catalyzed reaction.

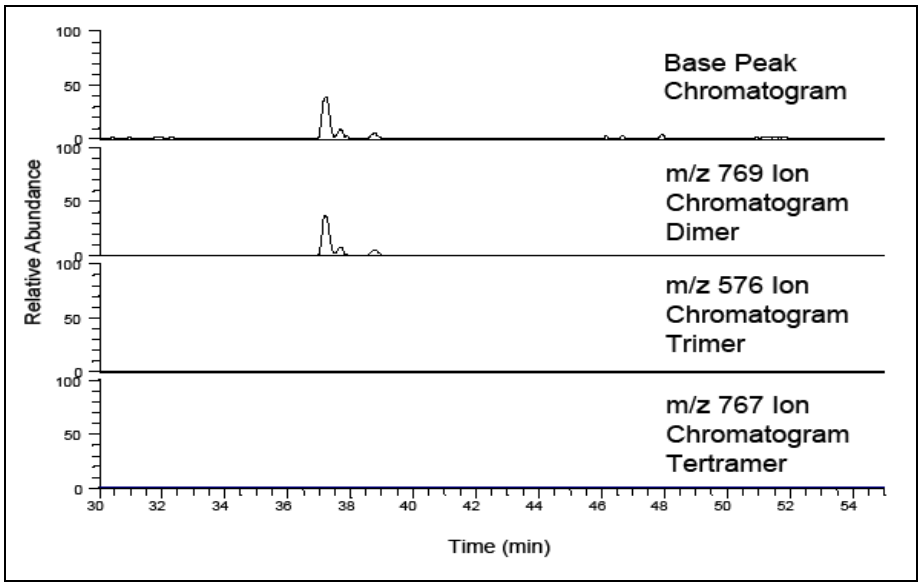

Figure 3.7: The base peak chromatogram and ion chromatogram corresponding to the dimer, trimer and tertameric products obtained from the RP-HPLC-\ESI\MS-MS analysis of dehydro NADA- Manduca sexta laccase reaction. The ion chromatograms of the m/z 769, m/z 576 and m/z 767 correspond to the dimer, trimer and tetramer products. Detailed structural analysis of the m/z 769 ion is described in the text associated with Figure 2.5. Essentially, reaction of dehyro NADA with cuticle laccase forms only the dimeric product.

3.5 Discussion

Laccases have been detected in the cuticles of several species of insects and their developmental activity profile correlates with the main period of sclerotization (Andersen, 1985; Barett and Andersen, 1981). Using RNA interference (Arakane et al., 2005; Suderman et al., 2006; Niu et al., 2008) demonstrated laccase is a key enzyme associated with sclerotization. For these reasons I examined laccase catalyzed oxidation of dehydro NADA. Laccases are known to generate free radicals as the primary oxidation products (Nakamura, 1960). Since semiquinone radicals undergo rapid dismutation generating the parent catechol and the quinonoid two-electron oxidation product, it is expected that laccase-catalyzed oxidation will also produce the same quinonoid product as observed with tyrosinase reaction viz., QMIA as the first observable oxidation product. During pulse radiolytic studies, evidence was obtained for the occurrence of such a radical dismutation that generated QMIA (Sugumaran et al., 1992a). Therefore, it was suspected that the course of laccase-catalyzed oxidative transformation of dehydro NADA would be essentially identical to that of previously reported for tyrosinase reaction. On the other hand, results presented in this section indicate that the course and mechanism of transformation of dehydro NADA are quite different for laccase and tyrosinase, although ultimately both reactions generate the same dehydro NADA dimeric products. First, the spectral changes observed during laccase–catalyzed oxidation of dehydro NADA is quite different from that of tyrosinase-catalyzed reaction (Figures 3.1 and 2.1). Second, the kinetic studies at the early phase of the reaction discounted the

production of QMIA (or its corresponding quinone product) as the first observable two-electron oxidation product for laccase reaction (Figure 3.2 and 2.2). Third the kinetics of decay of dehydro NADA is different for the two enzymes (Figure 3.3).

Finally, laccase produced consistently only dimeric products (Figures 3.4, 3.5 and 3.6) while tyrosinase generated apart from dimers significant amount of higher oligomers (Figures 2.3, 2.4, 2.9 and 2.10). Thus, the course of oxidation of dehydro NADA by these two enzymes seem to differ markedly. This finding is quite surprising and unexpected because the laccase-generated semiquinones normally dismutate and form the quinonoid product and the parent catechol (Nakamura 1960). Since quinonoid product formation is not witnessed during the oxidation of dehydro NADA by laccase, it is conceivable that the semiquinones are undergoing entirely a different reaction under the experimental conditions. A cursory glance at the canonical structures of the semiquinone indicates that radical coupling rather than radical dismutation is likely to occur during the reaction (Figure 3.8). Such a coupling eventually gives rise to the same dimeric products as those observed during tyrosinase-catalyzed oxidation. Examination of the reaction mixture by LC-MS-MS confirmed the production of only dimers in the case of laccase. Thus dehydro NADA is oxidized by laccase to its free radical product first. The two isomeric forms of the radical exhibit coupling rather than dismutation allowing the generation of a quinone methide adduct. Further ring closure generates the benzodioxan dehydro NADA dimers as shown in Figure 3.8.

Since free radical coupling rapidly removes the free radicals from undergoing any further transformation, one gets only dimeric products in this case. However, as pointed out in Figure 2.11 QMIA formed in tyrosinase case not only adds to monomeric dehydro NADA, but also to oligomers accumulated in the reaction mixture producing trimmers, tetramers and other oligomers.

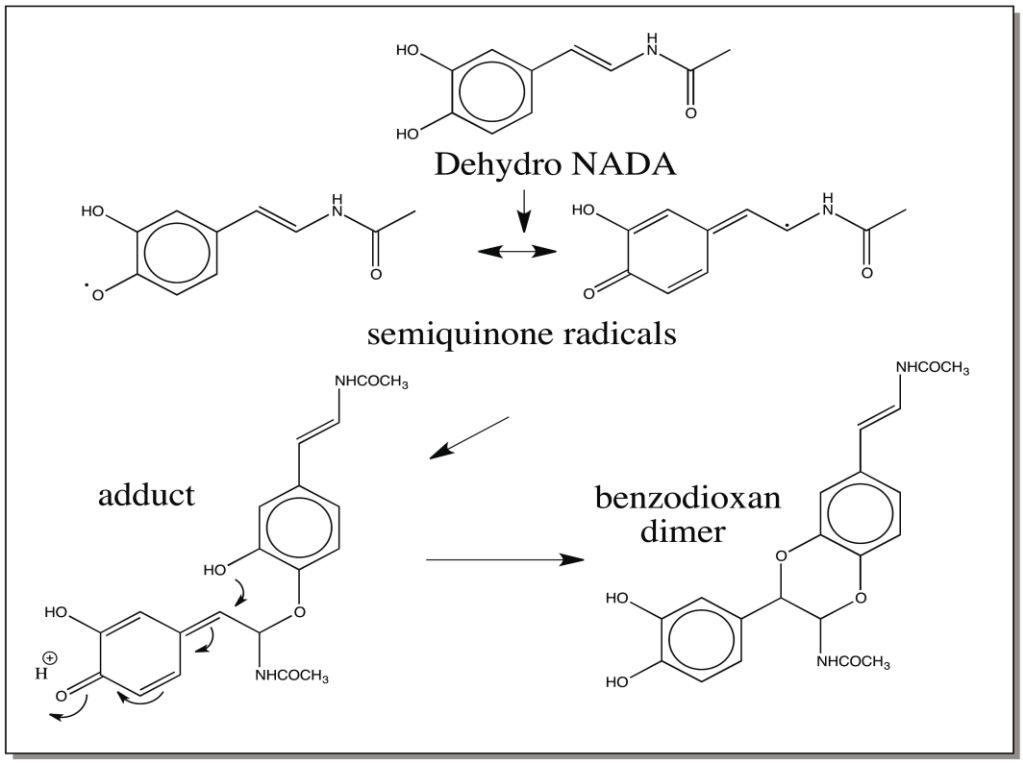

Figure 3.8: The proposed mechanism for the formation of dehydro NADA dimers by free radical coupling.

3.6 Conclusion

Benzodioxan dimer formation from dehydro NADA can occur by three different routes. The first route involves the transient formation of the two-electron oxidation product, QMIA and its subsequent addition to dehydro NADA. This route is predominantly used for the production of benzodioxan dimers and trimers by tyrosinase as shown in Figure 2.11. Quinone methide nucleus will undergo a Michael-1, 6-addtion to one of the phenolic groups of dehydro NADA and the modified Schiff's base will add to the other phenolic group resulting in ring closure and generation of dimer. As the concentration of dimers builds up in the reaction mixture, they too could add on to QMIA producing trimers. Similar addition will account for the eventual polymerization observed in the case of tyrosinase reaction. This mechanism is certainly not possible for laccase reaction due to several reasons. First, the two-electron oxidation product QMIA could not be detected even during the initial phase of the reaction either as a stable intermediate or as transient intermediate. Second, the time course of oxidation of dehydro NADA by laccase significantly differed from that of tyrosinase reactions. Third, unlike tyrosinase reaction, which produced dimers, trimers and other oligomers, laccase reaction produced only dimeric products further supporting the operation of a different route. Examination of the mechanism of operation of laccases indicates that these enzymes produce quinone products by a different route from tyrosinases from catechols. Tyrosinases oxidize catechols by a two-electron oxidation and generate the corresponding quinone (Sugumaran, 2010). On the other hand, laccases primarily produce one electron oxidation

product - semiquinones. However, semiquinones being extremely unstable and transient in nature readily undergo dismutation to quinone and the parent catechol. This reaction was witnessed during pulse radiolysis of dehydro NADA (Sugumaran et al., 1992a). Thus in spite of the mechanical differences, both tyrosinases and laccases produce the same quinonoid product. Therefore, absence of either the quinone or the quinone methide during the oxidation of laccase is quite surprising. This leaves radical coupling as a predominant mechanism for the further transformation of dehydro NADA semiquinones. As shown in Figure 3.8 if the radicals couple and form an adduct, they will also produce the same dimeric product as observed with tyrosinase catalyzed oxidation of dehydro NADA. Notably, radical coupling effectively removes the reactive intermediate thereby preventing its further reaction, as a result only dimeric products are formed in the case of laccase.

Finally, a third possible route for benzodioxan production is possible theoretically. This route calls for the production of conventional two-electron oxidation product – quinone -and its subsequent addition to dehydro NADA by a Diels Alder type reaction. Diels Alder addition can occur by two different mechanisms - one by a retro Diels Alder mechanism and other by an ionic Diels Alder mechanism. Under biological conditions an ionic cycloaddition is most likely to occur. Such an ionic cyclo [4+2] addition has been demonstrated to occur between enamines and quinones (Omote et al., 1988). But the operation of this route seems to be unlikely in the present case, due to the absence of observable quinonoid product during laccase-catalyzed oxidation. Since neither the

quinone nor the QMIA are generated as the initial observable two-electron oxidation product, it is likely that the semiquinones generated by the laccase are undergoing direct free radical coupling rather than exhibiting free radical dismutation reaction. During peroxidase catalyzed oxidation of dehydro NADA also facile production of dimer formation was also observed (Hasson and Sugumaran, 1987). Peroxidases also produce semiquinone as the primary products. Semiquinones possessing related structures have been shown to undergo radical coupling to generate similar benzodioxan dimeric products (Merlini et al., 1980). Thus free radical coupling mechanism seems to be the primary route for dimer production by laccase. This opens up a new possibility for sclerotization reactions, viz., free radical coupling as the fourth mechanism. During lignin biosynthesis, it has been shown that laccases produce free radicals from monolignols such as coniferyl alcohol and provide for free radical coupling (Sterjiades et al., 1996). A similar process can occur with sclerotization by the participation of dehydro NADA semiquinones as the fourth type of sclerotizing agent.

CHAPTER 4

NON ENZYMATIC OXIDATION OF 1,2-DEHYDRO-N-ACETYLDOPAMINE

4.1 Chapter summary

In the previous chapters enzymatic oxidations of dehydro NADA were delineated. Dehydro NADA also undergoes nonenzymatic oxidation, a property that might be useful for sclerotization. During larval puparial transformation in *S. bullata* the pH of the cuticle changes abnormally to alkaline side due to the release of ammonia. This condition would favor certainly the nonenzymatic oxidative transformation of dehydro NADA. Moreover in marine organisms, as has been pointed out earlier, a plethora of dehydrodopyl compounds are biosynthesized and used for a variety of biological processes. One such group being tunichromes produced by a number of tunicates. Tunichromes are small oligopeptides possessing one or more dehydrodopa units prevalent in the blood cells of tunicates. Tunichromes have been implicated in many physiological processes for example metal binding, wound repair, and/or tunic formation and some have been shown to possess antibacterial properties. In order to elucidate the biochemical role of these compounds, oxidation studies were conducted with tunichromes isolated from *Ascidia nigra* in parallel with its model catecholic compound dehydro NADA. Exposure of these catecholamine derivatives to even mild alkaline conditions such as pH 7.5 - 8.0 caused

rapid nonenzymatic oxidation indicating instability of these compounds. High performance liquid chromatography as well as liquid chromatography mass spectrometry indicated the production of dimeric and other oligomeric products in the reaction mixture. Visible spectral studies associated with the oxidation of tunichrome by tyrosinase failed to provide evidence for the accumulation of conventional quinonoid products. Fast reaction studies, however, indicated the transient formation and further decomposition of quinonoid intermediate(s). Ultraviolet spectral changes suggested the probable formation of dimeric and oligomeric tunichrome products in the reaction mixture. Attempts to monitor the polymerization reaction of tunichrome isolated from *Ascidia nigra* by liquid chromatography mass spectrometry were unsuccessful due to the sticky nature of the products. Essentially the same results were observed regardless of whether the tunichrome reaction was carried out in seawater (pH ~ 8.0) or in sodium phosphate buffer, pH 8.0, even in the absence of tyrosinase. These nonenzymatic oxidation reactions of dehydro NADA and related tunichromes seem to proceed through free radical intermediates. Based on my studies, a possible role for oxidative transformation of tunichrome in defense reaction, tunic formation and/or wound healing is presented.

4.2 Introduction

Tunicates (ascidians, sea squirts, Phylum Chordata, Class Ascdiacea) are sessile, marine filter feeders. Several species of tunicates contain a group of low molecular weight dehydrodopa containing oligopeptides named ‘tunichrome’ (Smith et al., 1991;

Taylor et al., 1997a); found primarily in the morula cells of their blood (Oltz et al., 1989). The first members of this group, tunichromes, An-1, An-2 and An-3, were obtained from whole blood cell lysates of the phlebobranch, *Ascidia nigra* (Macara et al., 1979a, b; Bruening et al., 1985, 1986; Lee et al., 1988) and all three were identified as tripeptides of modified tyrosines. Tunichrome An-1 is made up of topa (3, 4, 5-trihydroxyphenyl-alanine), dehydrotopa and dehydrotopamine. Tunichrome An-2 contains dopa, dehydrotopa and dehydrotopamine, while tunichrome An-3 possesses dopa, dehydrotopa and dehydrodopamine (Figure 1.14). Subsequently, tunichromes Mm-1 and Mm-2 were isolated from the stolidobranch *Molgula manhattensis* (Bruening et al., 1986, Oltz et al., 1988; 1989). Tunichromes Mm-1 and Mm-2 are very similar to tunichrome An-3 with glycine (Mm-1) and leucine (Mm-2), respectively, substituted for the N-terminal dopa unit (Kustin et al., 1990). Another group of tunichromes was isolated and characterized from the phlebobranch, *Phallusia mammilata*, (Bayer et al., 1992), which differ in their structure from that of the An tunichromes in that the central dehydrotopa units are replaced with saturated topa units (Table 1.1). The morula cells of *Phallusia mammilata* also possessed an oligopeptide containing 6-bromotryptophan and dehydrodopamine called morulin (Taylor et al., 1997b). A modified pentapeptide tunichrome (Sp-1) was identified from the hemocytes of the stolidobranch ascidian *Styela plicata,* whose structure is elucidated to be dopa-dopa-Gly-Pro-dehydrodopamine (Tincu and Taylor. 2002). From this same organism an octapeptide called plicatamide was isolated and its structure was established to be Phe-Phe-His-Leu-His-Phe-His-DehydroDopamine (Tincu et al., 2000, 2003). So far tunichromes have been isolated or characterized from eleven

species of tunicates (Macara et al., 1979a, Bruening et al., 1986, Oltz et al., 1988, Bayer et al., 1992, Parry et al., 1992, Robinson et al., 1996, Taylor et al., 1995, 1997a). Common to all tunichromes is the presence of dehydrodopa/topa and/or dehydrodopamine/topamine units. Surprisingly, these dehydrodopyl and dehydrotopyl units are also found in a number of other marine compounds such as clionamide, celenamides, purpurone, storniamides, ningalins and lamellarins (Table 1.1) (Sugumaran and Robinson, 2010).

The biological role of tunichromes and related marine dehydro dopyl compounds remains largely speculative, although various researchers have repeatedly proposed different possible functions over the years. Since tunicates that possess tunichromes also accumulate large amounts of specific trace metals (i.e. either vanadium or iron), and since catechol and pyrogallol groups are effective metal chelators, it was initially proposed, that tunichromes are involved in metal reduction and/ or accumulation (Macara et al., 1979a). However, this hypothesis lost favor once it was discovered that tunichromes are predominately located in morula cells and the vast majority of the highly reduced form of vanadium is present in the signet ring cells (Oltz et al., 1989). Since tunichrome can reduce V (V) to V (IV) and Fe (III) to Fe (II), they could still play a role in metal accumulation/metabolism (Smith et al., 1995). Another hypothesis attributes a defensive role to tunichromes. For example, the octapeptide plicatamide, isolated from the blood cells of *Styela plicata* possesses broad-spectrum antibacterial activity (Tincu et al., 2000, 2003). From this laboratory, it has been reported that the tunichrome An mixture isolated

from *Ascidia nigra* possesses antibacterial activity (Cai et al., 2008). But the general role of tunichromes in a defense mechanism remains largely unexplored, although phenoloxidase, an enzyme that will readily oxidize tunichrome, has been shown to be part of the defense mechanism and allorecognition in tunicates (Ballarin 2008, 2012; Cammarata and Parrinello, 2009; Iwanaga and Lee, 2005). Finally, tunichromes have been proposed as key components of both tunic formation and tunic wound healing, two functions that utilize the same underlying biochemical mechanisms. In this regard, it is important to point out that monomeric units found in tunichromes (dehydrodopamines) are the very same compounds that are involved in the sclerotization and hardening of insect cuticle (Andersen, 2010; Sugumaran, 1998; 2010).

The extreme instability and high reactivity of tunichromes is examined in this chapter to gain knowledge on their biological function. I examined the nonenzymatic oxidation chemistry of a model compound dehydro NADA, whose structure is present in practically all tunichromes, I also studied the enzymatic and nonenzymatic oxidation of tunichrome isolated from *Ascidia nigra* in order to shed light on the biological role of tunichromes. The results of these studies are summarized in this chapter.

4.3 Materials and methods

Pyrogallol, mushroom tyrosinase, sodium periodate, sodium borate, acetic anhydride, superoxide dismutase (SOD), cytochrome c, and general laboratory chemicals were obtained from Sigma Chemical Co., St. Louis. MO. All other chemicals were acquired from Fisher Scientific Co., and/or VWR Scientific Co, NJ. HPLC grade solvents and ammonium formate were purchased from Acros, Morris Plains, NJ. HPLC grade water was purified using a Milli-Q A-10 water purification system from Millipore, Milford, MA. Dehydro NADA was synthesized as outlined in an earlier paper (Dali and Sugumaran, 1988). The tunichrome An mixture from tunicate *Ascidia nigra* was isolated by the modified procedure (Cai et al., 2008) based on a method developed by Taylor et al., (1995). Briefly, hemocyte cells from *Ascidia nigra* were isolated by collecting the blood after cutting the tunic of the ventral base of the body and centrifuging for 20 min at 800 x *g* in a refrigerated centrifuge. Blood cells were extracted with 5% acetic acid containing 8 M urea and 0.1 M EDTA. This extract was subjected to chromatography on a Sep-Pak C_{18} cartridge (6 ml, 1 g) and eluted with 60 % aqueous acetonitrile containing 0.09% trifluoroacetic acid after a 20 ml 0.1 % aqueous trifluoroacetic acid wash. The eluent was lyophilized and a concentrated solution of the sample compounds was subjected to reversed phase thin layer chromatography using 50 % acetonitrile containing 0.09 % trifluoroacetic acid. The tunichrome band was visualized by its pumpkin color (Rf value = 0.37). It was eluted with 60 % aqueous acetonitrile containing 0.09 % trifluoroacetic acid, concentrated and used for all the biochemical studies.

Oxidation studies were conducted on model compounds and tunichrome An mixtures as follows. A typical reaction mixture contained 0.1—0.5 mM of substrate (pyrogallol or dehydro NADA, or tunichrome An mixture), appropriate amounts of tyrosinase, and 0.1 mM of sodium phosphate buffer or other specified buffers at different pH values. Reactions were conducted in 1 ml spectrophotometric cuvettes (10 mm path length) and the progress was monitored by following the UV and visible absorbance changes that occurred during the course of the reaction using a Beckman DU-7500 spectrophotometer. For non-enzymatic oxidations, reactions were conducted at specific alkaline pH values without the use of enzyme.

RP-HPLC analysis: A reaction mixture (1 ml) containing 0.2 mM dehydro NADA in 50 mM Tris-HCl buffer, pH 8.5 was incubated at room temperature and at indicated time interval, an aliquot (5 μl) of the reaction mixture was subjected to RP-HPLC analysis using isocratic elution with 50 mM acetic acid containing 0.2 mM sodium octyl sulfonate in 20% methanol at a flow rate of 0.6 ml/min on a C_{18} cartridge column (Agilent Technologies, 5 μm, 4.6 x 150 mm). The instrument was equipped with a diode array spectrophotometer to detect the UV spectrum of the eluting compounds.

Superoxide production: Superoxide production during the oxidation of dehydro NADA was monitored using a 1 ml reaction mixture containing 0.1 mM of dehydro NADA and 0.1 mM cytochrome c in 50 mM sodium phosphate buffer, pH 7.5. The reduction of cytochrome c, which is indicative of superoxide production (Koppenol et al., 1976), was continuously monitored at 550 nm. Different amounts of superoxide dismutase (18 or 180

units) were added to this reaction mixture to confirm the production of superoxide anions. Typically inclusion of superoxide dismutase inhibited the cytochrome c reduction and the increase in absorbance at 550 nm (Koppenol et al., 1976). The stoichiometry of complex formation between dehydro NADA and ferrous or ferric iron was determined by monitoring the absorbance at 650 nm (due to the complex) of different fixed molar ratios of dehydro NADA and iron. A typical inverted v shaped graph is obtained. From the graph, the mole ratio of dehydro NADA to iron in the complex is determined.

Liquid chromatography - Mass Spectrometry: A sufficient amount of tunichrome oxidation products were obtained by reacting 29.5 µg tunichrome with 10 µg mushroom tyrosinase in 1 ml of 50 mM ammonium acetate buffer (pH 6.0) at room temperature for 20 to 60 min. At the end of this incubation, 10 µl of the reaction mixture was withdrawn from the tube and the reaction was arrested by the addition of 90 µl methanol containing 2% acetic acid. It was subjected to Liquid Chromatography –Mass Spectrometry (LC-MS) analysis. A low-flow rate Shimadzu (Kyoto, Japan) HPLC system fitted with a 10 cm x 1 mm ID, 3 µm particle size, C_{18} Betabasic column from Thermo Electron Corporation (Sunnyvale, CA) was used to separate tunichrome oxidation products. The HPLC was operated at a flow rate of 35 µl/min using a linear gradient of 0 – 50% B in 40 min (mobile phase A = 10 mM formic acid in water; B = 10 mM formic acid in methanol). The HPLC was coupled to a Thermo Finnigan LCQ Advantage ion trap mass spectrometer (Sunnyvale, CA) to detect the products. The operating conditions of the mass spectrophotometer were: Capillary temperature 280˚C; spray voltage 4.00 kV; and

sheath gas 30 cm^3/min. Collision induced decomposition (CID) was performed at a relative collision energy of 28, an isolation mass window of 2.5 amu, and a default activation Q and activation time of 0.025 and 30 msec respectively.

Direct Injection Electrospray Ion Trap Mass Spectrometry: The mixture of tunichrome A1, A2 and A3 was analyzed *via* direct injection electrospray ion trap mass spectrometry. The operating parameters of the mass spectrometer were as described in the previous section. A 500 µl syringe was used to inject the sample into the instrument at a rate of 10 ml/min. An attempt was also made to analyze the oxidation products of tunichrome mixture using the same conditions.

4.4 Results

Oxidation studies with the model compound, Dehydro NADA: As early as 1988, our laboratory reported that deydro NADA is unstable in mild alkaline conditions (Sugumaran et al., 1988). However, the mechanism of nonenzymatic oxidation was not investigated in depth. Since this reaction is extremely important for understanding the reactivity's of tunichrome, a comprehensive study of nonenzymatic oxidation of dehydro NADA was undertaken. Figure 4.1 shows the ultraviolet absorbance changes accompanying the nonenzymatic oxidation of dehydro NADA. As is evident, dehydro NADA is converted into a compound(s) exhibiting a similar absorbance spectrum as that of the starting material upon exposure to mild alkaline conditions such as pH 8.5. Interestingly this nonenzymatic oxidation can be totally prevented, if the reaction is conducted in sodium borate buffer at the same pH instead of Tris-HCl buffer. Since borate complexes with catechols at alkaline pH this observation indicates that catecholic groups are involved in the oxidation (Sugumaran and Lipke, 1982).

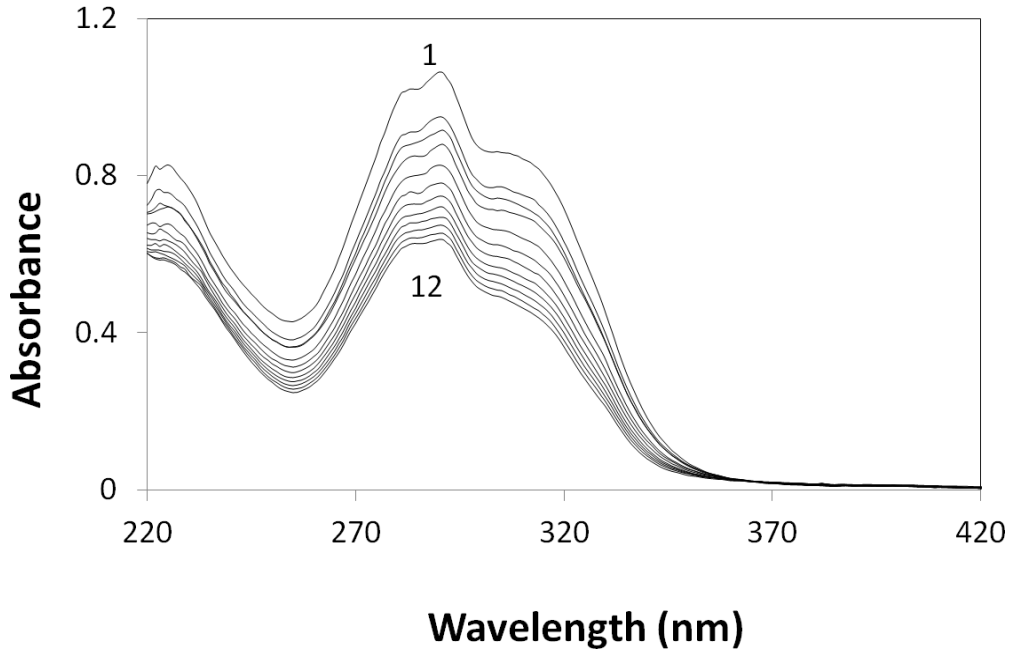

Figure 4.1: Ultraviolet spectral analysis of the nonenzymatic oxidation of dehydro NADA. A reaction mixture containing 0.2 mM of dehydro NADA in 50 mM Tris-HCl buffer, pH 8.5 was incubated at room temperature and the ultraviolet spectral changes associated with the reaction was continuously monitored at 2 min intervals. Scan 1 is zero time reaction; scan 12 is 22 min reaction.

It was reported earlier that such nonenzymatic oxidation of dehydro NADA leads to dimeric product formation (Sugumaran et al., 1988). In order to reassess the oxidation chemistry, reversed phase high performance liquid chromatography (RP-HPLC) was conducted on the nonenzymatic oxidation reaction. RP-HPLC analysis of a typical nonenzymatic reaction is shown in Figure 4.2. As indicated in the figure, incubation of dehydro NADA at mild alkaline conditions (pH 8.5) generated a number of

products. The ultraviolet absorbance spectra of these compounds remarkably resembled each other and resembled the starting material except for the disappearance of the shoulder at 330 nm indicating that they are closely related, and are most likely oligomeric products.

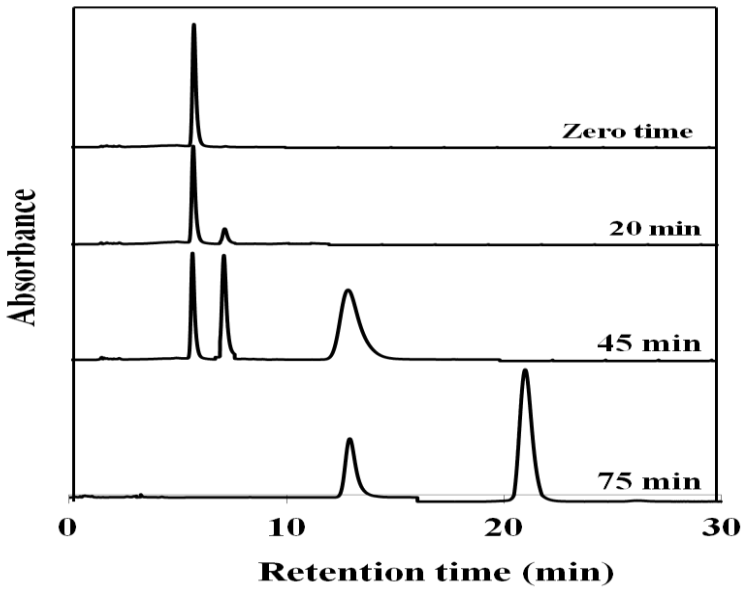

Figure 4.2: Reversed phase high performance liquid chromatography of the nonenzymatic oxidation of dehydro NADA. The reaction conditions are the same as outlined for Figure 4.1. At indicated time intervals of the reaction, aliquot of the reaction mixture (5 µl) was subjected to RP-HPLC analysis. The 5.7 min peak observed at zero time is due to dehydro NADA. The 20 min reaction has additional peak at 7.1 min which was due to dimeric products, the 12.7 min peak predominant in 45 min reaction is due to trimeric products and the 20.9 min peak from 75 min reaction is due to tetrameric products of dehydro NADA.

To confirm this contention, LC-MS analysis was conducted. The base peak chromatogram depicted in Figure 4.3 shows the products of nonenzymatic oxidation of dehydro NADA generated during a long-term incubation of the reaction (60 min) as analyzed by RP-HPLC/ESI/MS-MS. The mass spectra associated with the initial peaks at 29.5, 31.9 and 35.9 min show a parent ion at m/z 384.9, which represents the dimer of dehydro NADA plus a proton. The mass spectra associated with the next set of peaks at about 36.0 to 41.7 min indicate that these peaks are due to trimers of dehydro NADA. The mass spectra associated with the chromatographic peaks between 42.0 min and 44.0 min are identified as the tetramers of dehydro NADA.

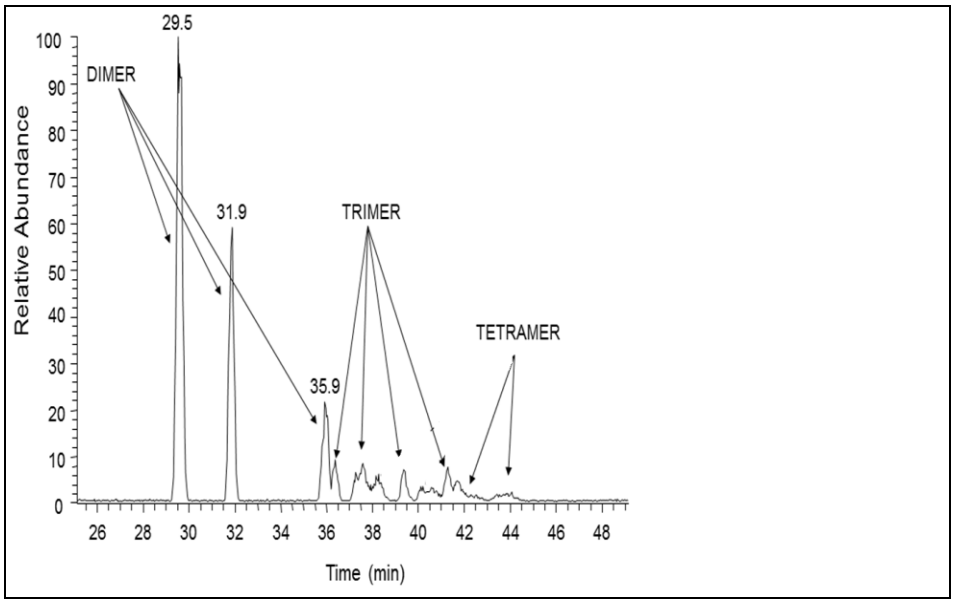

Figure 4.3: The Base Peak Chromatogram (m/z 150-2000) from the RP-HPLC/ESI/MS-MS analysis of dehydro NADA nonenzymatic reaction mixture. The reaction conditions are the same as that employed for Figure 4.2 with the exception of using ammonium acetate buffer pH 7.8 instead of Tris HCl buffer. The reaction was carried for 60 min. The marked retention times indicate the location of the polymeric species identified. The chromatographic peaks at 29.5 min, 31.9 and 35.9 are identified as isomers of the dimeric product. The subsequent peaks are due to trimers and tetramers.

The average ESI-mass spectrum of the 29.5 min peak is shown in the top frame of Figure 4.4. It exhibits major ions at m/z 385 and m/z 769. The ion at m/z 385 corresponds to the protonated dimer of dehydro NADA, $[D+H]^+$, and the m/z 769 ion represents its proton-bound dimeric ion, $[2D+H]^+$, and the weak ion at m/z 791 corresponds to the sodium bound dimeric ion, $[2D+Na]^+$ and the m/z 1174 ion represents

its sodium-bound dimeric ion, $[3D+Na]^+$. Similar spectra were obtained for the 31.9 and 35.9 min peaks. The dimeric and trimeric ions are formed routinely in the gas-phase during electrospray ionization, especially when the product concentration is high in the mixture.

The average ESI mass spectrum of the 37.5 min (from Figure 4.3) is shown in the second panel of Figure 4.4. It shows dominant ions at m/z 576 and m/z 1151, which are ascribed to the protonated trimer, $[T+H]^+$, and its corresponding proton-bound dimeric ion, $[2T+H]^+$ respectively. The weak ion at m/z 599 corresponds to the sodium bound trimeric ion, $[T+Na]^+$. Again, the latter is formed in the gas-phase ion complexation. Accordingly, the CID spectrum of the m/z 1151 ion shows a dominant peak at m/z 576, supporting its assignment as a proton-bound dimer of the trimer. A similar spectral pattern was obtained for the other three trimer peaks also.

The average mass spectrum of the 43.8 min peak (from Figure 4.3) is shown in the bottom panel of Figure 4.4. It contains a dominant ion at m/z 767 and an ion of weaker intensity at m/z 789. The m/z 767 ion corresponds to the protonated tetramer, $[Tet+H]^+$, and the weak ion at m/z 789 corresponds to the sodium bound tetramer ion, $[Tet+Na]^+$. Similar spectra were obtained for the other tetrameric peaks also (data not shown).

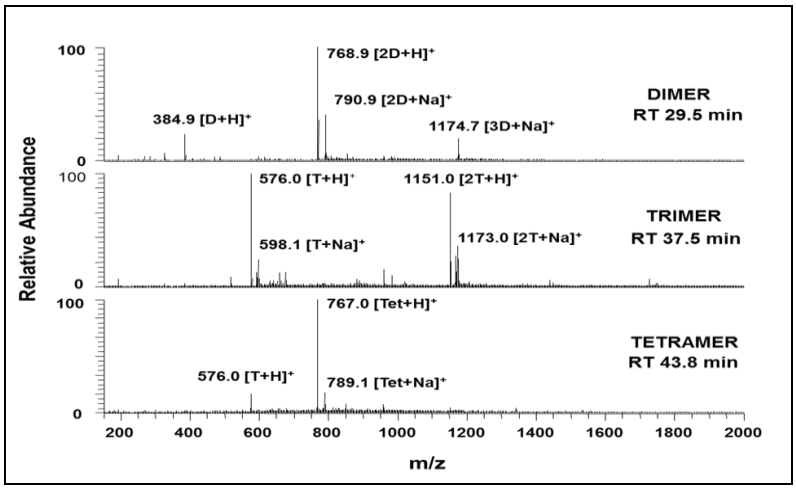

Figure 4.4: Mass spectral characteristics of selected product ions from Figure 4.3. Top frame - the mass spectrum of the dimeric product eluting at 29.5 min. Middle frame - the mass spectrum of the trimeric product eluting at 37.5 min. Bottom frame - the mass spectrum of the tetrameric product eluting at 43.8 min.

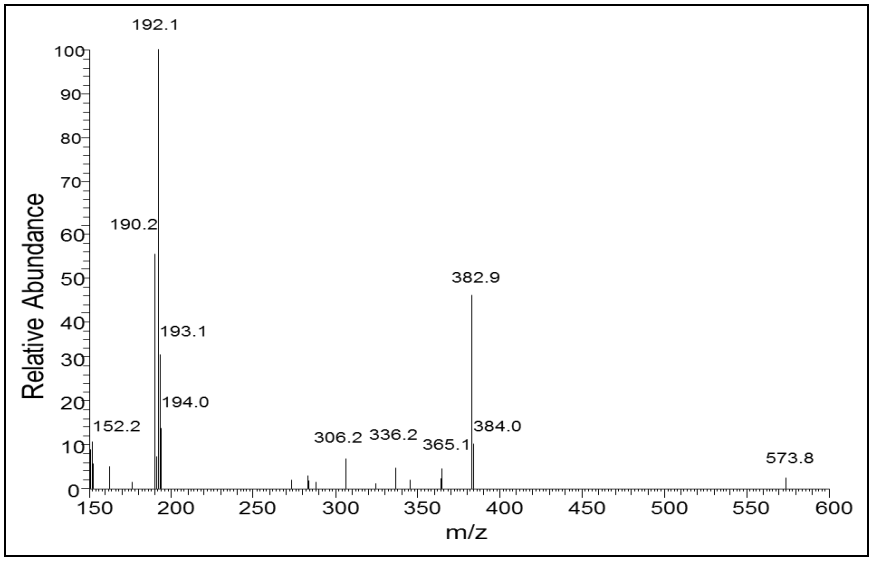

Figure 4.5: The average CID mass spectrum of the m/z 385 parent ion corresponding to the dimeric species with retention time of 29.5 min.

The CID spectrum of the m/z 385 ion (Figure 4.5) shows abundant product ion at m/z 192, corresponding to the protonated quinone methide ion, which is a logical decomposition product of the protonated dimeric species.

The average ESI mass spectrum from 36 to 41.7 min (from Figure 4.3) is shown in the middle panel of Figure 4.4. It shows dominant ions at m/z 576 and it corresponds to the protonated trimer, $[T+H]^+$. The CID spectrum of the m/z 576 ion shown in Figure 4.6 shows dominant product ions at m/z 385 and m/z 192, corresponding to the loss of the monomeric and dimeric moieties, respectively. This confirms the assignment of the m/z 576 ion as the protonated trimeric species of dehydro NADA. The m/z 517 product ion corresponds to the loss of NH_2COCH_3 from the parent ion. Other major and unidentified product ions include m/z 458 (loss of 101) and m/z 324 (loss of 252).

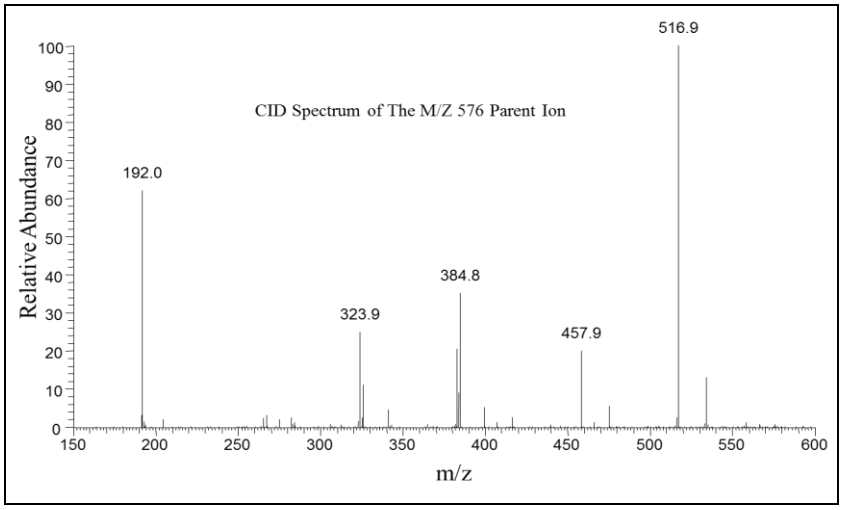

Figure 4.6: The CID spectrum of the m/z 576 parent ion which corresponds to the protonated trimeric species that eluted between 36.0 and 41.7 min.

The average mass spectrum from 42 to 44 min peaks (from Figure 4.3) is shown in the bottom panel of Figure 4.4. It contains a dominant ion at m/z 767 and it corresponds to the protonated tetramer, $[Tet+H]^+$. The CID spectra of the m/z 767 parent ion in Figure 4.7 shows dominant product ions at m/z 576/574 and m/z 383, corresponding to the loss of the monomer and dimer moieties, respectively.

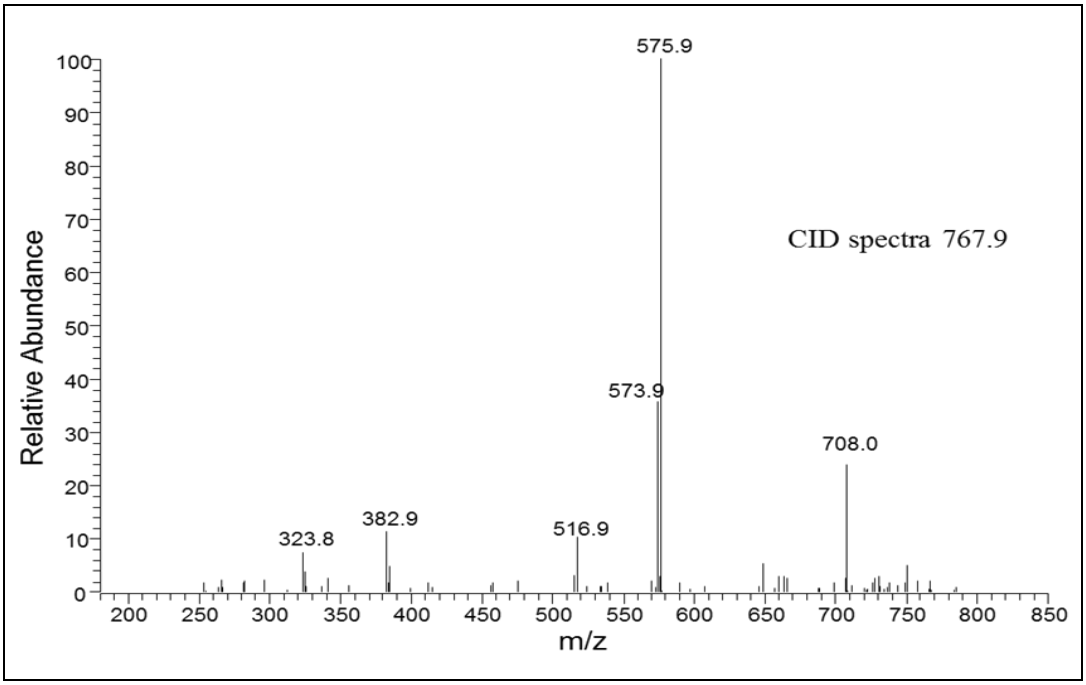

Figure 4.7: The average CID spectrum of the m/z 768 parent ion, which corresponds to the protonated tetrameric species that eluted between 42 and 44 min.

These product ions provide strong evidence that the m/z 767 parent ion corresponds to the protonated tetrameric product of dehydro NADA. The m/z 708 product ion

corresponds to the loss of NH_2COCH_3 group. The major product ions include m/z 708 (loss of 59), m/z 576 (loss of 191), m/z 574 (loss of 193), m/z 517 (loss of 250), m/z 383 (loss of 384) and m/z 324 (loss of 443). Careful inspection of the product ions in the CID spectra illustrated from Figures 4.5 to 4.7 show similarities that provide convincing evidence for the presence of the oligomeric products. For instance, $[M-192]^+$ product ion, corresponding to the loss of a monomeric moiety, is present in the CID spectra of the $[M+H]^+$ parent ion of the dimer, trimer and tetramer.

Using the average mass spectrum from 29 to 44 minutes and assuming these oligiomeric species have similar ESI/MS sensitivities, it is estimated that the reaction product consists of 74 % dimers, 23 % trimers, and 3 % tetramers. For this calculation the sum of the relative intensities of the ions at m/z 385,769, 791 and 1175 were used to estimate the relative abundance of the dimers, the sum of the relative intensities of the ions at m/z 576, 598, 1151 and 1173 were used to estimate the relative abundance of the trimers, and the sum of the relative intensities of the ions at m/z 767,789 and 1533 were used to estimate the relative abundance of the tetramers. The relative intensities of the proton bound dimer and trimer peaks were multiplied by two and three respectively prior to the summation to take into account the presence of multiple polymers in these species. For example, the relative intensity of 385*2 (the relative intensity of 767) +2 (the relative intensity of 791) +3 (the relative intensity of 1175).

Free radical participation: The oligomerization of dehydro NADA at alkaline pH should proceed *via* a free radical coupling reaction. For this reaction to occur, dehydro NADA must be oxidized to a semiquinone at alkaline pH, during this process naturally molecular oxygen should be reduced to superoxide anion. Superoxide anion formation has been documented during the reaction of different catechols such as 5, 6-dihydroxyindole with oxygen at alkaline pH (Novellino et al., 1999). One way of characterizing superoxide anion production is by measuring cytochrome c reduction which results in the increase in absorbance at 550 nm (Koppenol et al., 1976). Superoxide dismutase, which destroys the superoxide anion radical that is formed in the reaction, typically inhibits this increase in absorbance (Koppenol et al., 1976). As shown in Figure 4.8, nonenzymatic oxidation of dehydro NADA at pH 7.5 in the presence of cytochrome c resulted in the rapid reduction of cytochrome c. This reduction as is seen from the figure is strongly inhibited by increasing amounts of superoxide dismutase to the reaction mixture thus confirming the production of superoxide anions. More alkaline conditions (pH 8.0) caused faster reduction of cytochrome c and this reduction was again inhibited by superoxide dismutase .

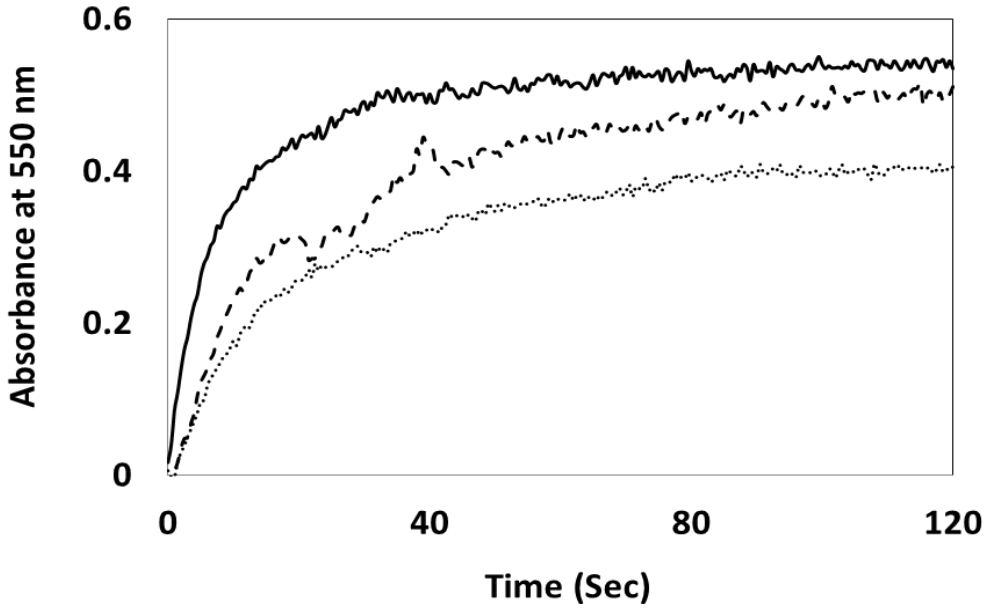

Figure 4.8: Evidence for superoxide anion production during nonenzymatic oxidation of dehydro NADA. A reaction mixture containing 0.1 mM of dehydro NADA and 0.1 mM cytochrome c in 50 mM sodium phosphate buffer pH 7.5 was mixed and the reduction of cytochrome c was continuously monitored at 550 nm. Solid line - no superoxide dismutase. Broken line - 12 µg (18 units) superoxide dismutase and dotted line - 120 µg (180 units) of superoxide dismutase.

Metal complexation: The ability of dehydro NADA to complex/react with transition state metal ions was examined using the spectral changes associated with the interaction of dehydro NADA and iron. Incubation of various fixed mole ratios of ferrous sulfate and dehydro NADA resulted in the production of different complexes in the reaction mixture with different absorbance maximum. By plotting the absorbance values against molar ratios (Figure 4.9A), one can find out the ratio of dehydro NADA to ferrous iron in the complex. From the figure, it can be deduced that a complex of three dehydro NADA to one atom of ferrous iron is formed under the conditions employed. This finding is consistent with the typical octahedral complex that is usually formed by ferrous ion during its interaction with catechols (Figure 4.9B). Interestingly such a complex formation is not readily observed with ferric iron (more of a smooth curve rather than an inverted v graph) because ferric iron cause the oxidation of dehydro NADA and interfered with a specific complex production. As a consequence spectral changes did not show a clear peak as observed for the ferrous dehydro NADA interaction, rather it produced an ill-defined smooth curve as shown in Figure 4.9A.

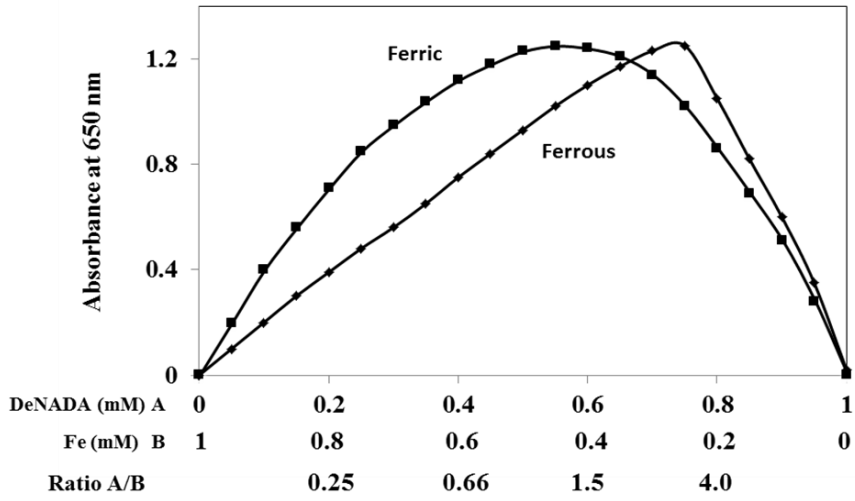

Figure 4.9A: Complex formation between dehydro NADA and iron. A 1 ml reaction mixture containing different concentrations of dehydro NADA (ranging from 0 – 1.0 mM) and either ferric sulfate or ferrous sulfate (ranging from 1 mM to 0 mM) in 50 mM sodium phosphate buffer pH 6.0 was incubated at room temperature for 2 min and the absorbance at 650 nm was recorded.

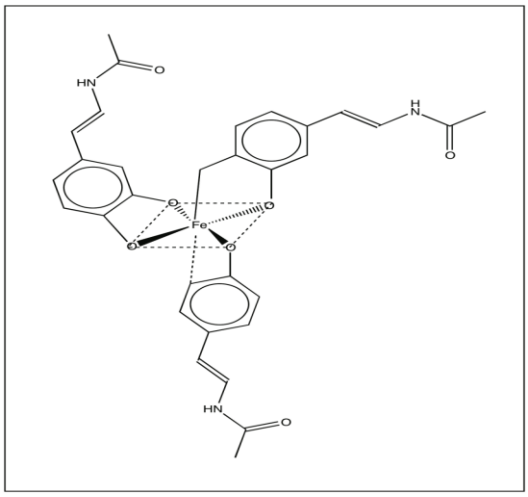

Figure 4.9B: Possible structure of the 3:1 complex formed between dehydro NADA and ferrous iron.

Tyrosinase catalyzed oxidation of tunichromes: Mushroom tyrosinase is a nonspecific phenoloxidase known to attack a number of catechols converting them to quinonoid products. It even acts on peptidyl dopa producing peptidyl dopaquinones (Burzio and Waite, 2001). Tunichrome An's are tripeptides containing topa, dehydrotopa and dehydrotopamine, or dopa, dehydrotopa and dehydrodopamine. Since all of them possess one or more pyrogallol moieties, we first checked to see if tyrosinase would act on simple pyrogallol. Oxidation of catecholic compounds usually generates quinonoid products that exhibit absorbance maximum at 400 – 480 nm range. Therefore, such oxidations can be conveniently monitored using visible spectral changes. As expected, tyrosinase readily oxidized pyrogallol generating the hydroxy-*o*-benzoquinone product, which exhibits absorbance at about 420 nm (Figure 4.10). This product is reasonably stable and accumulates in the reaction mixture. We therefore expected that the oxidation of tunichrome would also produce quinonoid product(s) that can be easily monitored by visible spectroscopy.

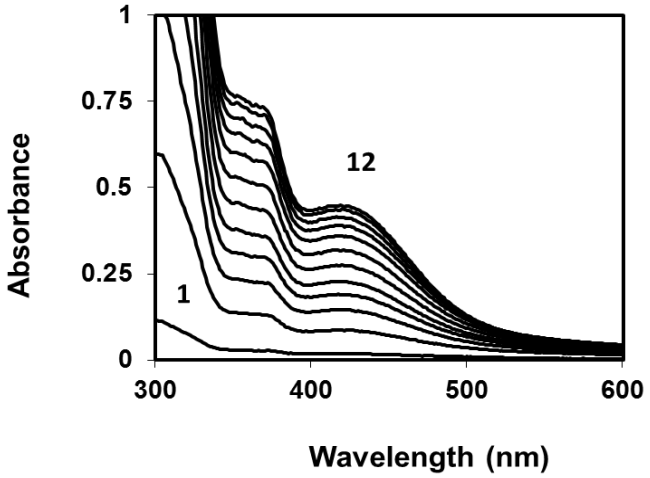

Figure 4.10: Visible spectral changes accompanying the oxidation of pyrogallol by mushroom tyrosinase. A reaction mixture containing 0.2 mM pyrogallol, 10 µg mushroom tyrosinase in 950 µl of 50 mM sodium phosphate buffer pH 6.0 was incubated at room temperature and the spectral changes accompanying the enzymatic oxidation was monitored at 20 sec intervals. Scan 1is zero time reaction; scan 12 is 220 sec reaction.

The ultraviolet and visible spectral changes accompanying the tyrosinase-catalyzed oxidation of tunichrome were however different from that of pyrogallol. First of all, there were no visible spectral changes during the entire time course of the reaction. Accordingly the reaction mixture remained nearly colorless throughout the time course of oxidation of tunichrome. Yet rapid spectral changes accompanied the oxidation in the

ultraviolet region of the spectrum (Figure 4.11). The 334 nm absorbance peak of tunichrome rapidly decreased during the oxidation and abruptly stopped at about half its original absorbance level. This phenomenon is similar to the finding demonstrated for the oxidation of dehydro NADA. For comparison, the tyrosinase catalyzed oxidation of dehydro NADA is presented in Figure 4.12. Note the close resemblance in the spectral changes occurring in the case of both these compounds. As outlined in chapter two tyrosinase-catalyzed oxidation of dehydro NADA leads to the production of dimeric and oligomeric benzodioxan type adducts in the reaction mixture (Abebe et al., 2010). Hence, I hypothesized that a similar dimerization reaction would also occur during the oxidation of tunichromes. Unfortunately, the high aromatic content and reactivity of the tunichromes resulted in failure to chromatograph tunichrome oxidation products under a variety of HPLC conditions. Electrospray mass spectrometry, however, offers a promising means to monitor oligomer formation, with the advantages of selective detection of the three tunichrome species based on their molecular masses and the requirement of a small amount of sample. Unfortunately, although we were able to obtain electrospray mass spectra of unoxidized tunichrome An-1, An-2 and An 3, we were unable to characterize the oxidation products of tunichromes most likely due to the stickiness of the oxidation products and the limited mass range of the ion trap mass spectrometer employed in the present study. Again The LC-MS analysis of the dehydro NADA oxidation products showed that abundant gas-phase dimer complexes of the dimeric oxidation products are formed in the electrospray process. If similar dimer

complexes of the dimeric oxidation products of the tunichromes form, these ions would be beyond the mass range of our instrument (2000 m/z).

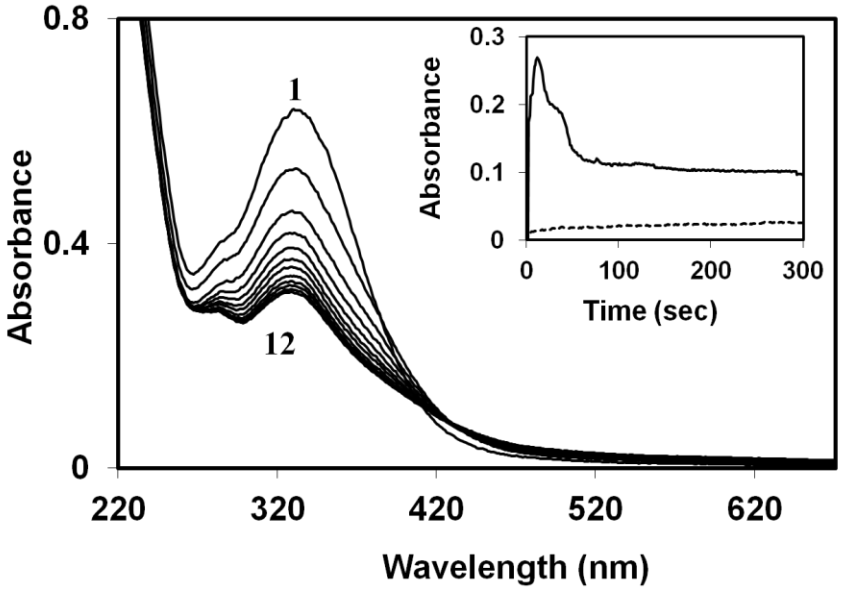

Figure 4.11: Visible spectral changes associated with oxidation of tunichrome by mushroom tyrosinase at pH 6.0. A reaction mixture containing 20 µg of tunichrome and 10 µg of mushroom tyrosinase in 950 ml of 50 mM sodium phosphate buffer, pH 6.0, was incubated at room temperature and the spectral changes associated with the enzymatic oxidation were monitored at 5 min intervals (scan 1: 0 time reaction; scan 12: 55 min reaction).

Inset: *Time course of oxidation of tunichrome monitored at 400 nm and 485 nm. Reaction conditions are as outlined above. Solid line - quinone production monitored at 400 nm; broken line - quinone methide production monitored at 485 nm.*

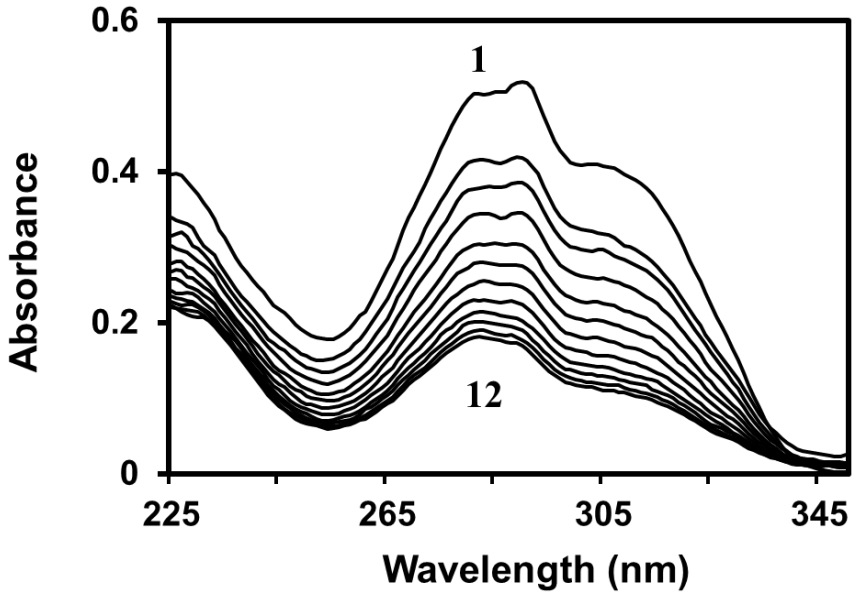

Figure 4.12: Visible spectral changes associated with the oxidation of dehydro NADA by mushroom tyrosinase. A reaction mixture containing 50 µmoles dehydro NADA and 10 µg mushroom tyrosinase in 1 ml of 50 mM sodium phosphate buffer, pH 6.0 was incubated at room temperature and the spectral changes associated with the enzymatic oxidation were monitored at 1 min intervals (scan 1: zero time reaction; scan 12: 11 min reaction).

Non-enzymatic oxidation of tunichromes: Presence of di- and tri-hydroxy groups on multiple aromatic rings could introduce high reactivity and susceptibility to aerial oxidation especially under mild alkaline conditions that are comparable to seawater (pH ~ 8.0). However, a systematic study on the oxidative mechanism of tunichromes under alkaline conditions has not been reported so far. In order to understand the fate of

tunichrome at alkaline conditions, I examined its stability at pH 8.0. As shown in Figure 4.13, exposure of tunichrome to seawater caused dramatic changes in its spectral properties. These spectral changes are remarkably similar to those observed for the tyrosinase-catalyzed oxidation of tunichrome at pH 6.0 (Figure 4.11)

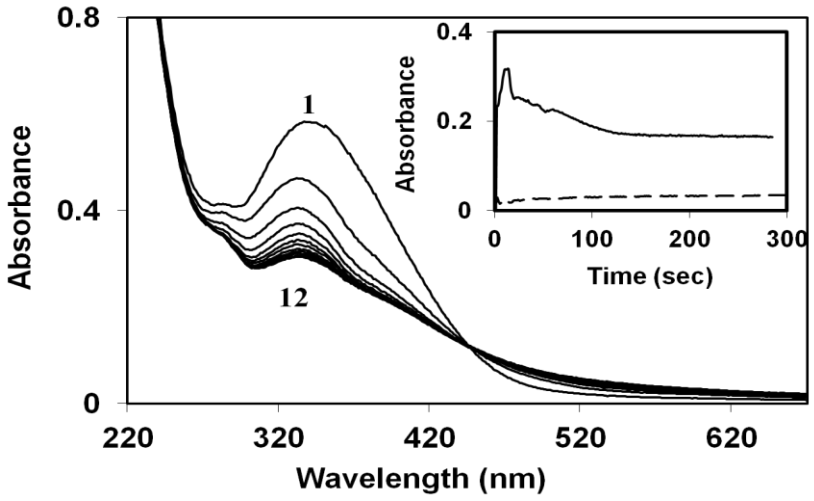

Figure 4.13: Visible spectral changes associated with the nonenzymatic oxidation of tunichrome in seawater. A reaction mixture containing 20 µg of tunichrome in 960 ml of seawater pH 8.0; salinity 32 psu, was incubated at room temperature and the spectral changes associated with the non-enzymatic oxidation were monitored at 2 min intervals. Scan 1: 0 time reaction; scan 12: 22 min reaction.

Inset: *Time course of oxidation of tunichrome in seawater monitored at 400 nm and 485 nm. The reaction conditions are the same as outlined above. Solid line - quinone production monitored at 400 nm; broken line - quinone methide production monitored at 485 nm.*

Since seawater is not a defined chemical medium, one might argue that trace metal ions present in the seawater could be causing this non-enzymatic oxidation. To rule out this possibility and to show definitively that pH plays a crucial role in the oxidation process, two experiments were conducted. The first one examined the stability of tunichrome in sodium borate buffer at pH 8.0. Borates, as mentioned earlier, forms chelate with catecholic groups under mild alkaline conditions and prevent them from undergoing aerial oxidation (Sugumaran and Lipke, 1982). Hence, at pH 8 in borate buffer, tunichrome should remain stable without exhibiting any non-enzymatic oxidation. Accordingly, when tunichrome was placed in sodium borate, its UV spectrum remained unaltered for more than an hour indicating that it is quite stable at pH 8.0 in borate. On the other hand, when tunichrome was exposed to sodium phosphate buffer at pH 8.0, it readily exhibited the same rapid spectral changes as observed in the case of seawater. Therefore, the instability of tunichrome in seawater can be ascribed to the aerial oxidation occurring during alkaline condition. Thus, the nonenzymatic oxidation seems to be occurring even without the participation of any metal ions at alkaline pH values. As demonstrated in the case of dehydro NADA, such a nonenzymatic oxidation must proceed through free radical production and superoxide anion generation. To test the production of superoxide anion, we conducted the nonenzymatic oxidation in presence of cytochrome c. As shown in Figure 4.14 the nonenzymatic oxidation of tunichrome accompanied the reduction of cytochrome c and this reduction was inhibited by increased amounts of superoxide dismutase. Thus, it can be concluded that the instability of tunichrome is due to the dehydro NADA skeleton and the reaction products obtained for

the nonenzymatic oxidation of dehydro NADA – viz., oligomerization compounds and superoxide anion production – should be applicable to tunichrome oxidation.

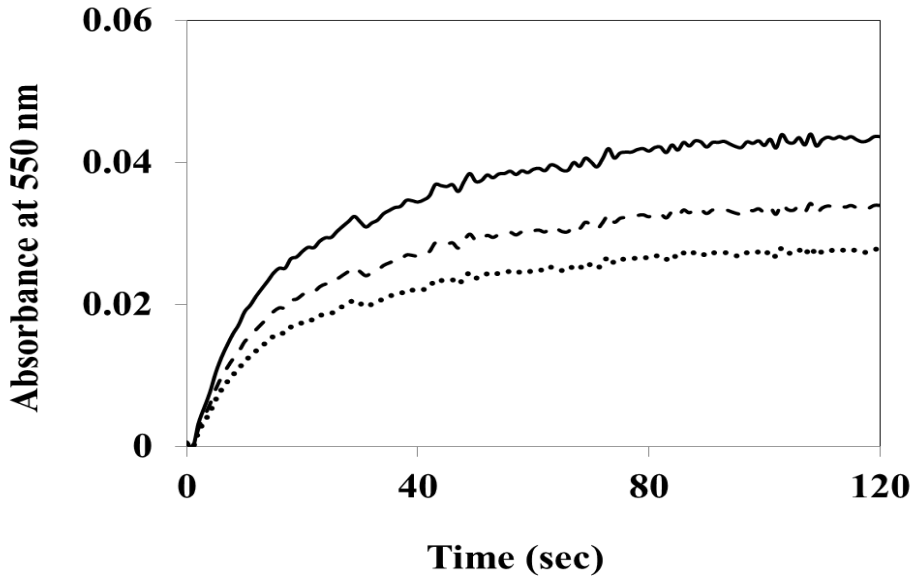

Figure 4.14: Evidence for superoxide anion production during nonenzymatic oxidation of tunichrome. A reaction mixture containing 0.01 mM of tunichrome and 0.01 mM cytochrome c in 50 mM sodium phosphate buffer pH 7.5 was mixed and the reduction of cytochrome c was monitored continuously at 550 nm. Solid line had no superoxide dismutase. Broken line had 12 µg (18 units) of superoxide dismutase and dotted line had of 120 µg (180 units) of superoxide dismutase.

4.5 Discussion

The non-enzymatic oxidation of dehydro NADA was conducted for two main reasons. First, it is formed as a key intermediate during sclerotization of insect cuticle (Sugumaran, 1998). The pH of *S.bullata* larva cuticle changes from neutral to basic while the animal undergoes larval puparial transformation. This could trigger nonenzymatic oxidation of dehydro NADA and ensure further progression of sclerotization reactions. This may be essential because, the reactive metabolites formed during sclerotization such as quinones and quinone methides are extremely deleterious to biological molecules as they react instantaneously with every nucleophile. Such a reaction with enzyme generating these transient intermediates will result in the inactivation of these essential enzymes and perhaps premature arrest of sclerotization. The availability of nonenzymatic reactions offers an additional advantage for the organism to complete the sclerotization reactions even in the absence of enzymes. The second reason is to understand the role of tunichrome in the tunicate biochemistry. Since the discovery of tunichrome An mixture in 1979 (Macara et al., 1979 a,b), their extreme instability has been documented by many researchers (Bruening et al., 1985, 1986; Oltz et al., 1988, 1989; Bayer et al., 1992; Nette et al., 2000: Tincu and Taylor 2002). Subsequently derivatization methods have been developed to protect the phenolic groups while isolating and characterizing tunichromes, thereby preventing them from undergoing facile oxidation (Oltz et al., 1988; Kim et al., 1990). Derivatization with acetyl groups prevented the oxidation of labile catecholic and pyrogallol moieties present in tunichromes. Of late, an elegant method developed by Taylor et al. (1995) using acid urea and high performance thin layer chromatography

separations have aided the successful isolation of tunichromes without derivatization. Yet their extreme instability and sensitivity to aerial oxidation has severely hampered the assessment of the biological and physiological role of these compounds. The An tunichrome mixture for example frequently adheres to gels and other column materials used for biological purifications (Bayer et al., 1992; Lee et al., 2001). They even bind to glass, as evidenced by the yellow coloration of glass walls that resists solubilization. Thus all experiments conducted to characterize the oxidation products of tunichromes by RP-HPLC/UV-Vis and electrospray mass spectrometry were unsuccessful. Nevertheless, both enzymatic oxidation studies with mushroom tyrosinase and nonenzymatic oxidation studies under mild alkaline conditions reveal that tunichromes are perhaps undergoing oxidative conversion to dimers and other oligomers. Tyrosinase catalyzed oxidation will generate the corresponding two-electron oxidation product that will undergo further reaction. In the case of dehydro NADA, tyrosinase catalyzed oxidation generates the two electron oxidation product QMIA with an absorbance maximum at 485 nm (Sugumaran et al., 1992). However, transient kinetic study seems to indicate the production of only the conventional quinone product as shown in the inset of Figure 4.11. Nonenzymatic oxidation may proceed through free radical production and subsequent polymerization. More direct evidence for the mechanism of nonenzymatic oxidation comes from the study of the model compound dehydro NADA, whose structure is embedded in most tunichromes and may be the most likely group attributing high instability to tunichromes.

At slightly alkaline pH range, nonenzymatic oxidation of dehydro NADA generated a reactive compound which is most likely the one electron oxidation product, dehydro NADA semiquinone (Figure 4.15). Molecular oxygen simultaneously undergoes reduction to superoxide anion, which was detected through the reduction of cytochrome c. This reduction of cytochrome c is inhibited by inclusion of superoxide dismutase in the reaction mixture further confirming the production of superoxide anions. Such production of free radicals and superoxide anion has been documented during the oxidation of related catecholamine derivative, 5, 6-dihydroxyindole also (Novellino et al., 1999). Since quinone to semiquinone methide isomerization is a base catalyzed reaction (Bolton et al., 1996; Sugumaran 2000) and the reaction conditions are alkaline, it is expected that QMIA would be the most predominant oxidation species present under these conditions. The QMIA seem to react with the parent dehydro NADA generating dimers and other oligomers as shown in Figure 4.15. However, such direct evidence could not be obtained in the case of tunichromes, although ultraviolet and visible spectral studies seem to indicate the occurrence of an oligomerization reaction. Even direct injection into the electrospray mass spectrometer (circumventing the liquid chromatography columns), did not give any indication of polymerization, although the “disappearance” of tunichrome was readily witnessed. Nevertheless studies described in this section clearly support the notion that dehydro NADA, one of the key structural units that is present in tunichromes, is mostly responsible for the extreme reactivity of tunichromes.

Based on these reactions one can propose a possible role for tunichromes that is depicted in Figure 4.16. When tunic is damaged by a wound or pathogen entry, morula cells containing tunichrome and phenoloxidases migrate to the damaged site to aid in the repair of the wound and/or defend against the parasites. This coupled with the fact that the pH of sea water is slightly alkaline, will trigger nonenzymatic oxidation of tunichrome and superoxide anion production. While superoxide anion could be used to defend and kill the parasite by free radical reactions through reactive oxygen species, polymerization of oxidized tunichromes can also attack the parasites and kill them. Thus tunichromes might play a crucial role in defense and wound repair reactions of tunicates; all possible by the unusual reactivity of dehydro NADA units.

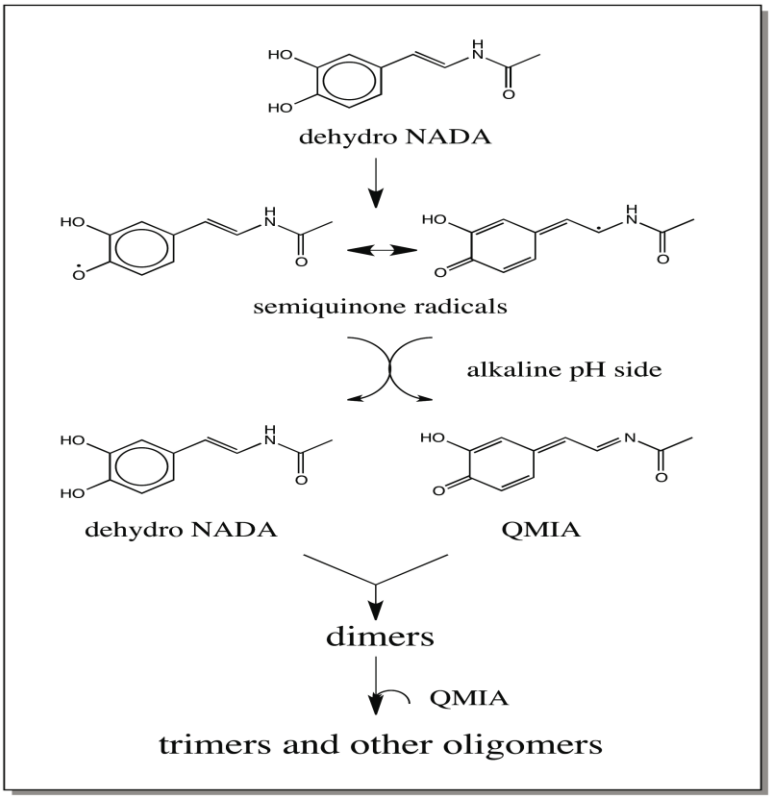

Figure 4.15: Proposed mechanism for the oligomerization of dehydro NADA via free radical coupling. Nonenzymatic oxidation of dehydro NADA produces the corresponding semiquinone free radical and superoxide anions. The QMIA coupling to the parent dehydro NADA generate an adduct that will undergo ring closure to produce the benzodioxan type dimer. Since these reactions are nonenzymatic in nature, they generate all possible streoisomeric products accounting for the multiplicity of product ions observed in the mass spectrometer. Dimers will add on to the QMIA causing trimers and other oligomers.

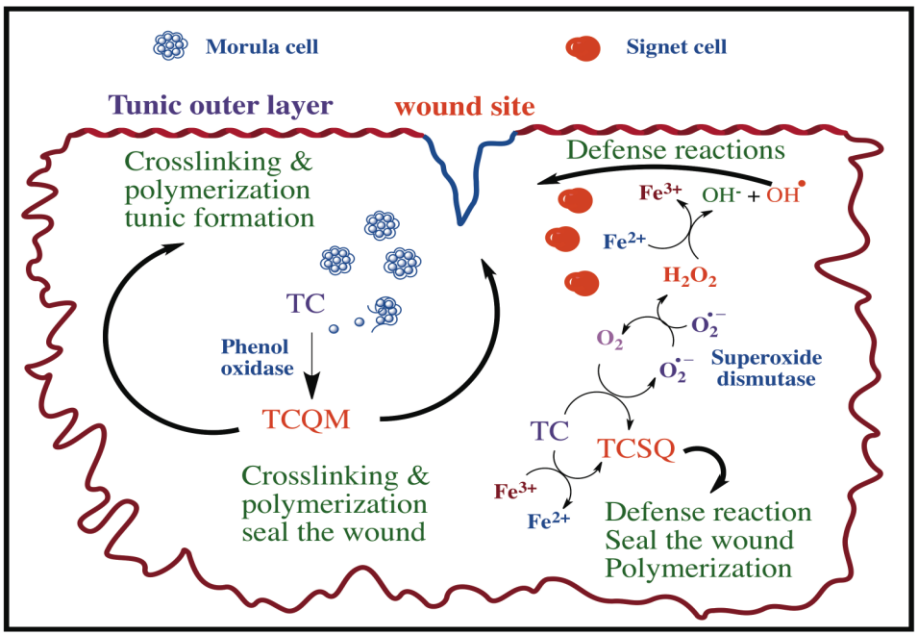

Figure 4.16: Proposed mechanism for the biological role of tunichrome. Morula cells containing tunichrome (TC) and phenoloxidase (PO) are routinely transported to the tunic by circulating blood. When tunichromes and phenoloxidase come in contact, they participate in tunic crosslinking via quinonoid products of tunichrome (TCQ). The same reaction will also occur rapidly at a wound site to seal the wound. During the defense reaction, an invading parasite can be kept at check also by this reaction. Exposure to mild alkaline pH of the sea water at wound site will initiate nonenzymatic oxidation of tunichromes and generate toxic quinonoid free radicals (TSCQ) and reactive oxygen species that can offer additional defense benefits to the ascidian. The Haber-Weiss type reaction shown in the Figure for ferrous ion is also applicable to vanadium through V (III) to V (IV) conversion and V (IV) to V (V) conversion (Sugumaran and Robinson, 2012).

4.6 Conclusion

Based on the results presented in this chapter one can propose the scheme of reactions shown in Figure 4.16 to account for the physiological role of tunichromes. Tunichrome containing morula cells travel to the tunic and may participate in tunic hardening, wound healing and antimicrobial defense. Since phenoloxidase is also present in the morula cells (apparently as an active form rather than the inactive proenzyme form, Ballarin, 2012), interaction of tunichromes with this enzyme, will produce its two electron oxidation product. The quinonoid product formed during the oxidation can directly react with the nucleophilic side chains of the proteins and the tunic biopolymers such as cellulose resulting in adduct and crosslink formation. The ability of tunichrome An mixture as well as dehydro NADA to cause protein polymerization has been demonstrated (Cai et al., 2008). Such incorporation of tunichromes into the tunic allows its strengthening and hardening, thus protecting the soft-bodied tunicates. This reaction is similar to the well-established biochemical mechanism for the sclerotization insect cuticle (Andersen, 2010; Sugumaran 1988; 2010). Direct relevance to the current study is the fact that dehydro NADA and dehydro NBAD are two important compounds that participate in exoskeletal hardening of insects. These two molecules along with their saturated counter parts are oxidized by cuticular phenoloxidases and the resultant quinone and quinone methide reactive intermediates add onto the nucleophilic sites on structural protein and the chitin polymer generating protein-protein, protein-chitin and chitin-chitin adducts and crosslinks that make the insect cuticle hard and tough. Therefore, a similar reaction with tunichrome is highly likely to occur (Cai et al., 2008). Interestingly, the

sclerotization process in insects requires three enzymes (phenoloxidase, quinone isomerase and quinone methide isomerase) working consecutively, whereas the tunic crosslinking process in tunicates only requires phenoloxidase. Preliminary studies revealed that covalent bound catechol derivatives are abundant in the tunic of a number of tunicate species. This is possible only if tunichromes and/or similar molecules are incorporated into the tunic.

The same mechanism should also be useful in sealing a wound. During tunic formation and/or the wound healing processes, tunichromes are brought in contact with seawater (pH ~8.0). At this juncture, exposure to oxygen and mild alkaline pH will cause the rapid production of free radicals from tunichromes and subsequent reduction of molecular oxygen to superoxide anions (Figure 4.16). Similar to the quinonoid products, the free radicals will also couple with the structural proteins and cellulose like carbohydrate polymer present in the tunic forming protein-protein, protein-cellulose and cellulose-cellulose adducts thus accounting for the wound sealing/healing reaction and tunic repair/formation. Free radicals also undergo coupling to generate dimeric tunichrome products and/or other polymeric condensation products, which might provide additional benefits to the organism. The superoxide anions formed during the reaction will react with metal ions released by blood cells (such as either ferrous iron or vanadium (III) present in the signet ring cells) forming even more reactive hydroxyl radicals (Kehrer, 2000) that may be recruited for killing microorganisms at the wound site, thus providing an important avenue for defense reactions (Figure 4.16). In addition, the

tunichrome radicals themselves could cause free radical damage to the foreign organism this providing a powerful defense mechanism for the tunicates. Moreover, during a microbial infection, phenoloxidase present in the morula cells along with tunichromes, could come together and generate quinonoid products at the site of infection. The role of phenoloxidase and its reaction products in the defense mechanism of invertebrate animals has been well documented (Cerenius and Söderhäll, 2004; Sugumaran, 2002; Iwanaga and Lee, 2005). Ascidians seem to be no exception to this generalization (Ballarin, 2008; 2012; Cammarata and Parrinello, 2009; Cammarata et al., 1996). Phenoloxidase activity has been identified in the cytotoxic cells in different ascidians and seems to play crucial role in defense reaction as well as allorecognition (Arizza et al., 1995; Ballarin et al., 1998; Hata et al., 1998, Jackson et al., 1993). The phenoloxidase-generated quinones would form aggregates with the blood cells and a foreign object, aiding their eventual encapsulation and killing. In support of a defense role, some of the tunichromes have been shown to possess antibiotic activity and this property could be useful in defending the invading microorganisms that breach the hard cuticle and gain access through the weak spots in tunic. (Tincu et al., 2003; Cai et al., 2008). Thus the reactivities of tunichromes - both enzymatic and nonenzymatic – may play a very critical role in the physiology and biochemistry of tunicates. All these are possible by the presence of dehydro NADA units in tunicates. Plus, the unique properties of tunichromes likely lead to their multifunctional role in tunicate physiology – tunic formation, would repair and antibacterial defense.

CHAPTER 5

ENZYMATIC OXIDATION OF 1, 2-DEHYDRO-N-ACETYL DOPA

5.1 Chapter summary

Lamellarins are a group of bioactive marine natural compounds possessing the 6,7-dihydroxycoumarin moiety. Although they seem to be synthesized from dehydro dopa derivatives, practically nothing is known on the biosynthesis and metabolic fate these compounds. The metabolic fate of these compounds was investigated using a simple synthetic model dehydro compound, 1,2-dehydro-N-acetyldopa (NAcDeDopa). Oxidation of NAcDeDopa by tyrosinase or sodium periodate resulted in the generation of quinone methide which seems to undergo rapid intramolecular ring closure generating a coumarin type product, 3-aminoacetylesculetin. Interestingly, 3-aminoacetylesculetin thus formed also suffered further oxidation and eventual polymerization producing not only dimeric and trimeric compounds but also oligomeric products. The identities of these products were established by liquid chromatography-mass spectrometry. The significance of this reaction to a number of marine natural products such as Ningalin and Lamellarin are presented in this paper.

5.2 Introduction

Marine organisms constitute a relatively untapped source of novel drugs of great biotechnological and pharmaceutical application potential. Among the promising candidates which have attracted researcher's attention due to their structural originality and complex mechanism of action are lamellarins. The lamellarins form a group of more than seventy highly condensed Dopa and Topa derived pyrrole marine alkaloids that have been isolated from diverse marine organisms, mainly ascidians and sponges (Fan et al., 2008). The first four, lamellarins A-D were isolated and characterized from the prosobranch mollusc, *Lamellaria* sp. (Faulkner et al., 1985) and four more compounds were later extracted and identified (E-H) from the ascidian didemnid ascidian *Didemnum chartaceum* (Andersen et al., 1985; Lindquist, et al., 1988). Since then, as many as seventy different, yet structurally closely related, polycyclic aromatic condensed compounds have been isolated from a number of marine organisms. A wide range of different biological activities are reported for this family of alkaloids, including, antibiotic, antitumor, antioxidant, DNA topoisomerase I inhibition (Facompe et al., 2003) and multi drug resistance reversal activities (Quesada et al., 1996). A few members of this family revealed HIV integrase inhibition activity (Reddy et al., 1999), human aldose reductase inhibition, cell division inhibition, immunomodulatory activity, and feeding deterrent activity. However, the most common and remarkable property of the lamellarins is their capacity to inhibit the proliferation of cancer cells. The majority are considerably cytotoxic with lethal dose values in the nanomolar or micromolar range (Fan et al., 2008; Ishibashi et al., 2002). The majority of the lamellarins possess either Type 1a or 1b

structure shown in Figure 1.13. In spite of the vast literature available on the isolation, characterization and biological activities of these interesting metabolites, practically nothing is known about the biosynthetic aspects and metabolic fate of these compounds. A close examination of their structure indicates that bulk of lamellarins possesses a dehydrodopamine unit and that most if not all lamellarins seem to possess a 6, 7-dihydroxycoumarin skeleton. Pyrrole-derived alkaloids related to lamellarins include ningalins which are condensed aromatic system that appear derived from the condensation of two to five DOPA precusors. The structures of ningalin A and ningalin B isolated from *Didemnum* sp. are also shown in Figure 1.13. Like lamellarins, ningalins also possess coumarin ring structure (Kang et al., 1997). Ningalins, as well as their derivatives, exhibit marked cytotoxicity against several cancer cell lines. They also exhibit significant multi drug resistance reversal activity at non-cytotoxic concentrations (Fan et al., 2008).

Coumarins are of widespread occurrence in the plant kingdom as secondary metabolites. Their exact role in plants is unclear. However, they are thought to play a key role in plant defense due to the induction of their biosynthesis following various stress events. Moreover they also seem to possess antimicrobial and antioxidant activities (Kai et al., 2008). They are usually biosynthesized from *p*-coumaryl coenzyme A and/or feruloyl Coenzyme A via phenylpropanoid pathway (Vogt., 2010). For example, 7-hydroxy-6-methoxycoumarin (scopoletin) is biosynthesized from feruloyl CoA by the formation of 6'-hydroxyferuloyl CoA and subsequent isomerization and lactonization to

produce scopoletin with the release of Coenzyme A (Figure 5.1). The Coenzyme A seems to be necessary for the activation of the carboxyl group and preparing it for lactonization reaction (Vogt, 2010; Kai et al., 2008). An alternate route involving the intramolecular cyclization of dopa derived metabolites *via* quinone formation is possible because a large number of marine organisms are known to possess dehydrodopyl and dehydrotyrosyl compounds (Sugumaran and Robinson, 2010) and their oxidation could lead to coumarin production. For example 3, 4-dihydroxyphenylpropionic acid, the simplest precursor for coumarin production, exhibits a spontaneous intramolecular cyclization reaction upon oxidation to its corresponding quinone generating dihydroesculetin (Sugumaran et al., 1989). Therefore, such a reaction is quite likely to occur in the marine environment as well (Figure 5.2). In order to assess the production of dihydroxycoumarin skeleton through oxidative cyclization of dehydrodopa units and to shed more light on the general biosynthetic and metabolic fate of dihydroxycoumarins related to lamellarins, biochemical studies were conducted on the model compound, 1, 2-dehydro-N-acetyldopa (NAcDeDopa). The results indeed confirm that tyrosinase could readily generate dihydroxycoumarin ring structure *via* oxidative cyclization of the dehydro dopa units. Interestingly the resultant dihydroxycoumarin also undergoes additional oxidative polymerization producing a series of olgomeric products arising from the coupling of reactive quinone methide imine amide (QMIA) derivative with the parent compound.

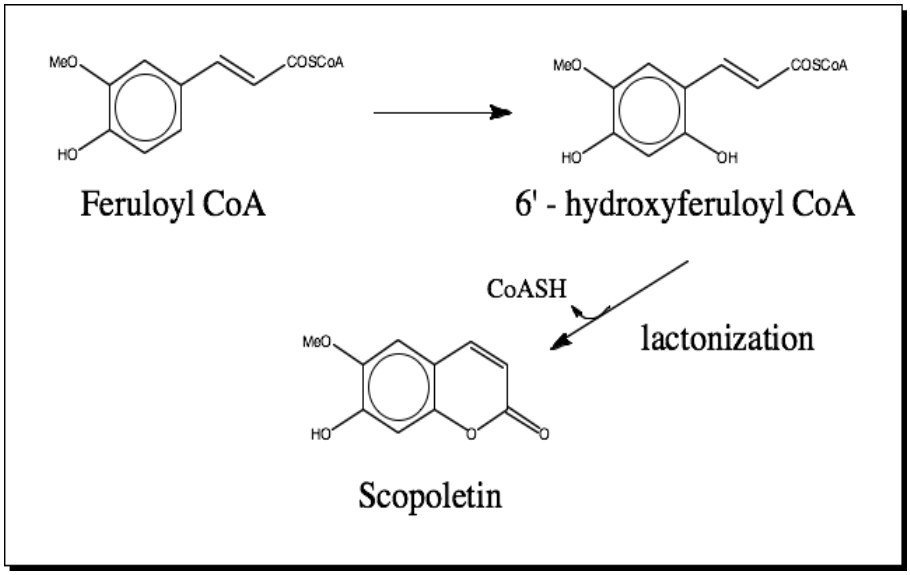

Figure 5.1: Synthesis of scopoletin from feruloyl CoA.

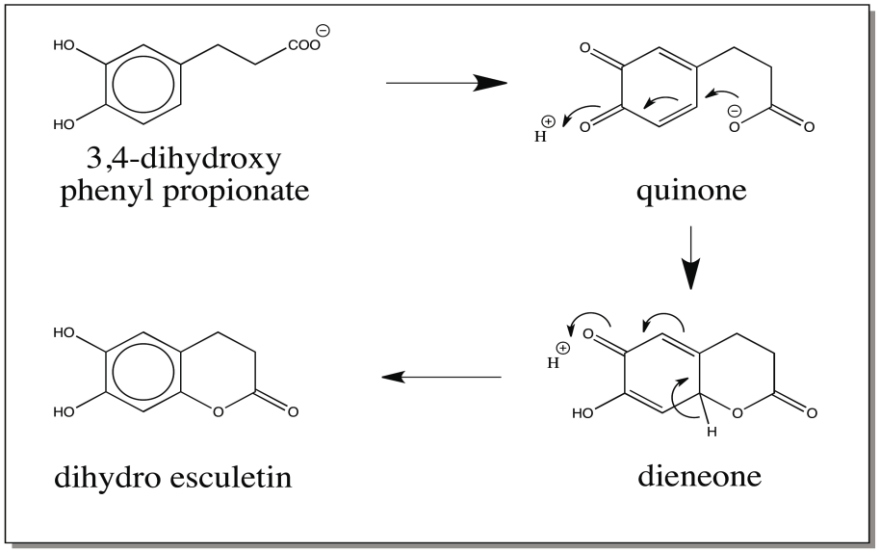

Figure 5.2: Synthesis of dihydroesculetin.

5.3 Materials and methods

Mushroom tyrosinase, sodium periodate and general laboratory chemicals were obtained from Sigma Chemical Co., St. Louis. MO. All other chemicals were acquired from Fisher Scientific Co and/or VWR Scientific Co, NJ. HPLC grade solvents and ammonium formate were purchased from Acros, Morris Plains, NJ. HPLC grade water was purified using a Milli-Q A-10 water purification system (Millipore, Milford, MA). NAcDeDopa was synthesized by Strecker synthesis and hydrolysis of the resultant cyclic ester (Dong et al., 2009). Briefly, a mixture of 3, 4-dihydroxybenzaldehyde (69.06 gm), N-acetyl glycine (58.55 gm), sodium acetate (42 gm) and 160 ml of acetic anhydride was stirred at 110 °C for 2 hr and cooled at room temperature. The contents were then poured on ice and left at 5°C for overnight. The yellow crystals precipitated were collected and re-crystallized from ethanol water mixture (1:1) to obtain pure (*Z*)-2-acetamido-3-(3',4'-diacetylphenyl) acrylic acid in 70 % yield. M.pt. 181 °C. Hydrolysis of this compound was achieved by suspending 3.21 gm of the compound in 40 ml of 5% sodium bicarbonate solution and stirring for 24 hr. Acidification of the solution to pH 5 with HCl and work up gave the required NAcDeDopa in 72% yield. M.pt. 217-218 °C.

Oxidation studies: Oxidation studies were conducted on NAcDeDopa as follows. A typical reaction mixture containing 0.1 mM of NAcDeDopa and appropriate amounts of mushroom tyrosinase in 50 mM of sodium phosphate buffer (at specified pH values) was incubated at room temperature and progress of the reaction was monitored using UV-Vis spectrophotometer. The reaction conditions for individual experiments are described

under the legends to the figures that follow. The reactions were conducted in 1 ml cuvettes (10 mm path length).

RP-HPLC analysis of NAcDeDopa: A reaction mixture (1 ml) containing 0.1 mM NAcDeDopa and 5 µg mushroom tyrosinase in 50 mM sodium phosphate pH 6.0 was incubated at room temperature. An aliquot of the reaction mixture (5 µl) was subjected to HPLC analysis on Agilent 1100 HPLC series, C_{18} cartridge (Agilent Technologies, Santa Clara, CA) using isocratic elution with 35% methanol and 65% MilliQ water containing 0.1% TFA at a flow rate of 0.5 ml/min. The ultraviolet absorbance spectra of the eluents were monitored using a diode array spectrophotometer.

Liquid Chromatography –Mass spectrometry (LC-MS) studies: A reaction mixture containing 0.1 mM NAcDeDopa and 5 µg mushroom tyrosinase in 1 ml of ammonium acetate buffer pH 6.0 was incubated at room temperature. 10 µl was withdrawn from the reaction and the reaction was arrested by the addition 90 µl of methanol containing 2% acetic acid and subsequently subjected to analysis by reversed-phase high performance liquid chromatography electrospray tandem mass spectrometry (RP-HPLC/ESI/MS-MS).

RP-HPLC conditions for Mass spectrophotometer: A low-flow rate Shimadzu (Kyoto, Japan) HPLC system fitted with a 10 cm x 1 mm ID, 3 µm particle size, C_{18} Betabasic column from ThermoElectron Corporation (Sunnyvale, CA) was used to separate the products. The HPLC was operated at a flow rate of 35 µl/min using a linear gradient of 0 – 50% B in 40 min consisting of the mobile phase A = 10 mM formic acid in water and B

= 10 mM formic acid in methanol. Flow from the column was directly fed into the source of RP-HPLC/ESI/MS-MS.

Mass spectrometric operating conditions: A Thermo Finnigan LCQ Advantage electrospray ion trap mass spectrometer (Sunnyvale, CA) was used to detect and characterize the products. The operating conditions of the ion trap mass spectrometer are: Capillary temperature 280˚C; Spray voltage 4.00 kV; and sheath gas 30 cm^3/min. Collision induced decomposition (CID) was performed at a relative collision energy of 28, an isolation mass window of 2.5 amu, and a default activation Q and activation time of 0.025 and 30 msec respectively.

5.4 Results

Oxidation of *o*-diphenols by tyrosinase, in general, results in the generation of corresponding *o*-quinonoid products that typically exhibit absorbance maximum at about 400 nm. But surprisingly in spite of rapid oxidation witnessed by the drastic spectral changes occurring in the ultraviolet spectral region, the reaction mixture containing NAcDeDopa and tyrosinase remained relatively colorless. Accordingly there was no visible absorbance maximum at the 400 – 450 nm region that is typically observed during tyrosinase-catalyzed oxidation of catechols (Figure 5.3).

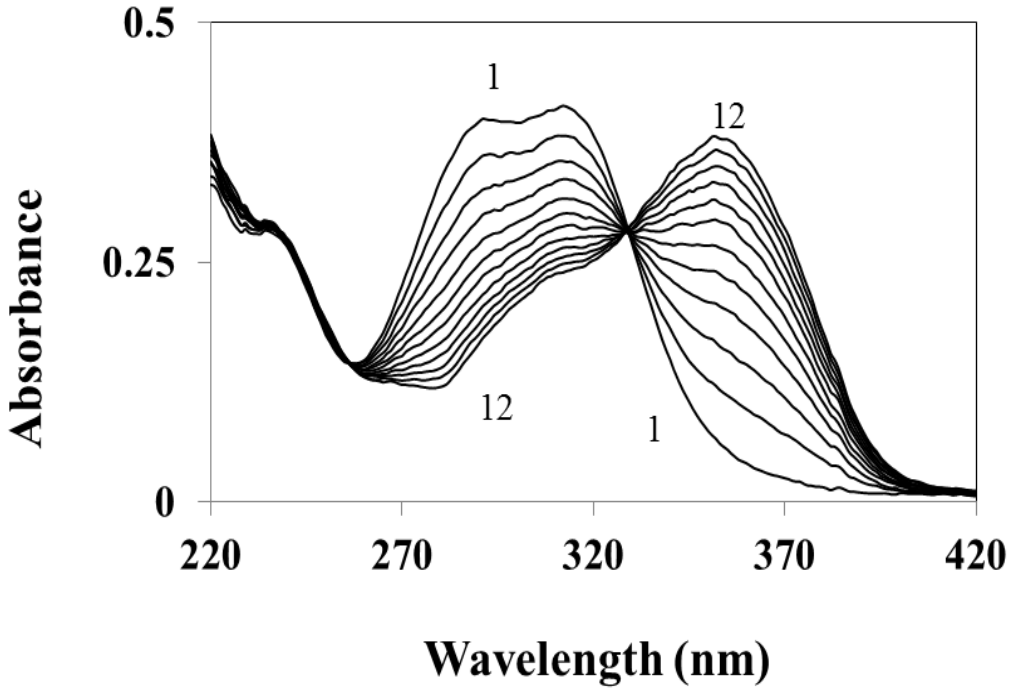

Figure 5.3: Ultraviolet spectral changes associated with the oxidation NAcDeDopa by mushroom tyrosinase at pH 6.0. A reaction mixture containing 0.1 mM NAcDeDopa and 5 µg mushroom tyrosinase in 50 mM sodium phosphate buffer pH 6.0 was incubated at room temperature and the spectral changes accompanying the enzymatic oxidation was monitored at 30 sec intervals (scan 1: 0 time reaction; scan 12; 330 sec reaction). Note the absence of absorbance maximum at 400 nm due to quinone.

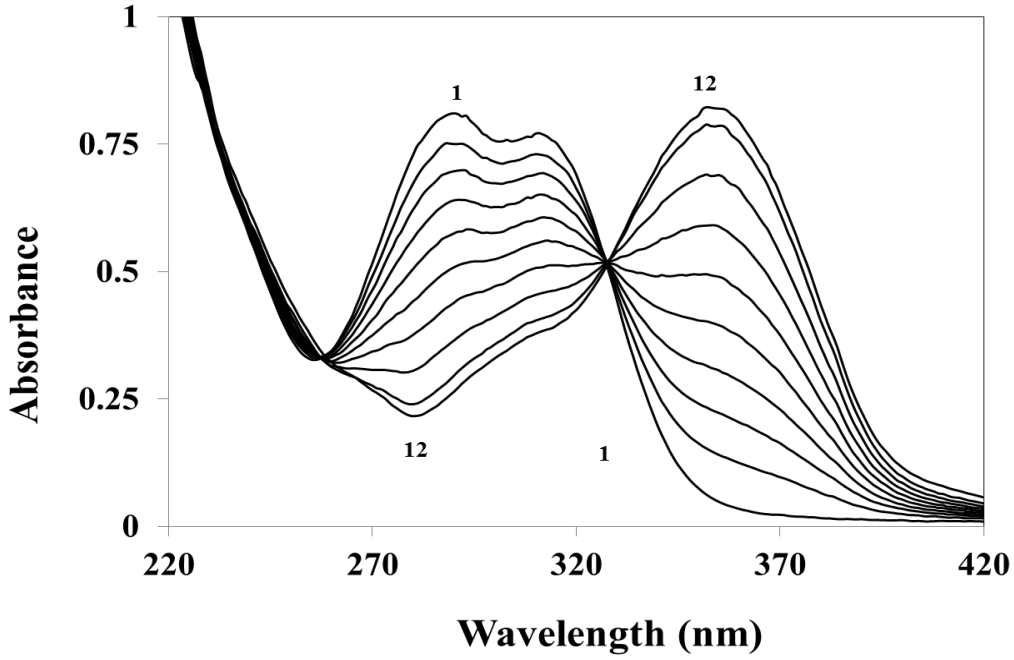

Figure 5.4: Ultraviolet spectral changes associated with the oxidation NAcDeDopa by mushroom tyrosinase at pH 8.0. A reaction mixture containing 0.1 mM NAcDeDopa and 5 µg mushroom tyrosinase in 50 mM sodium phosphate buffer pH 8.0 was incubated at room temperature and the spectral changes accompanying the enzymatic oxidation was monitored at 30 sec intervals (scan 1; 0 time reaction; scan 12: 330 sec reaction).

The same results were obtained at other pH values as well. Figure 5.4 for example shows the spectral changes associated with the oxidation of NAcDeDopa at pH 8.0. Again the visible absorbance maximum at 400 – 450 nm, indicative of quinone production, is missing under these conditions. Yet the rapid spectral changes indicated the production of a product that exhibits an absorbance maximum at about 370 nm. In the

case of a few catechols, it is known that the initial quinone is extremely unstable and decomposes rapidly. Thus 3, 4-mandeloquinone, which could not be seen during the normal time course of oxidation of 3, 4-dihydroxymandelic acid could be visualized under pre-steady state conditions (Sugumaran, 1986; Sugumaran et al., 1992). Similarly, dehydro NADA upon oxidation generates a very transient quinone methide imine amide rather than the conventional quinone that could only be visualized under pre-steady state conditions (Sugumaran et al., 1987; Sugumaran et al., 1988a; Sugumaran et al., 1990; Sugumaran et al., 1992a; Sugumaran, 2000). Since tyrosinase generates only catalytic amounts of the quinonoid product, it is likely that the small amount of quinonoid intermediate formed, coupled with the fact that it is also undergoing rapid transformation, is escaping the limits of the detection technique. Sodium periodate is known to oxidize catechols quantitatively and stoichiometrically and has been a valuable tool in monitoring transient quinonoid intermediates such as Dehydro NADA quinone methide (Sugumaran, 2000). Therefore, a molar ratio of sodium periodate was used to oxidize NAcDeDopa. Figure 5.5 shows the spectral changes accompanying the oxidation of NAcDeDopa during the first few seconds of periodate oxidation of NAcDeDopa. As is evident, a colored quinonoid product exhibiting absorbance maximum at 485 nm is instantaneously formed (within three sec) and is rapidly decomposed resulting in the production of colorless product. The transient compound with 485 nm absorbance maximum cannot be the conventional *o*-quinone product because most related *o*-quinone show absorbance maximum at 400 - 420 nm, which is nearly 60 nm lower than the observed result. The *o*-quinone of DeNAc Dopa methyl ester, the esterified product of NAcDeDopa itself shows

absorbance maximum at about 420 nm (Sugumaran et al, 1992). The *o*-quinone of Dehydro NADA generated under acidic conditions again shows an absorbance maximum at about 400 nm only (Sugumaran, 2000). However, this quinone rapidly undergoes isomerization to its quinone methide with an absorbance maximum of 485 nm as soon as the pH is brought to near neutral conditions (Sugumaran, 2000). Based on the close structural analogy, the initial colored product formed in the case of NAcDeDopa was also determined to be a QMIA. The major difference between these two QMIA is their further reactivity. In the case of Dehydro NADA, the QMIA formed, rapidly reacts with the parent catechol generating dimeric and trimeric benzodioxan type adducts. However, since NAcDeDopa QMIA possesses an internal carboxyl group suitably positioned to exhibit an intramolecular cyclization reaction, it seems to undergo cyclization than exhibiting external reaction. The UV spectrum of the product formed in Figures 5.3 and 5.4 are consistent with such a proposal and attest to the production of a colorless compound with dihydroxy coumarin skeleton.

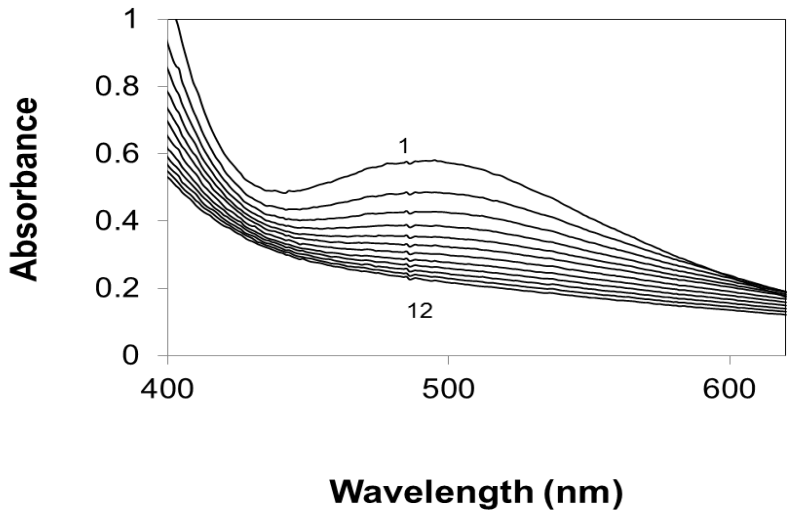

Figure 5.5: Evidence for the formation of quinone methide during sodium periodate - catalyzed oxidation of NAcDeDopa. A reaction mixture containing 0.2 mM of NAcDeDopa and 0.2 mM sodium periodate in 50 mM sodium phosphate buffer, pH 6.0 was incubated at room temperature and the spectral changes accompanying the oxidation for the first few minutes was monitored continuously at 400 to 600 nm (scan 1: 0 time reaction; scan 12: 330 sec reaction).

In order to characterize the reaction product(s), HPLC studies were carried out. Figure 5.6A shows the HPLC analysis of the reaction mixture containing NAcDeDopa and tyrosinase. Even as early as 3 min of the reaction, the production of a new product eluting at about 9 min is evident. As the incubation time is increased, an additional product is formed with an elution time of 6 min. The UV spectra of all three chromatographic peaks observed in the HPLC are shown in Figure 5.6B. The 4 min peak

was due to the starting compound, NAcDeDopa. The 9 min peak was ascribed to the colorless product exhibiting absorbance maximum at about 360 nm. The UV absorbance properties of this peak matched that of esculetin type compounds indicating that the transient NAcDeDopa QMIA has undergone rapid intramolecular cyclization generating 3-aminoacetylesculetin. Long-term incubations generated a new product eluting at 6 min range, which possessed a combination of absorbance spectrum of the substrate, NAcDeDopa and the product, 3-aminoacetylesculetin.

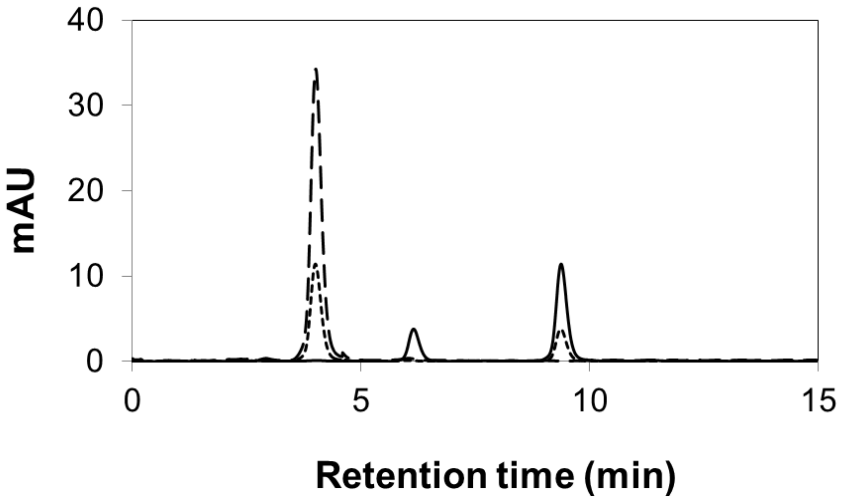

Figure 5.6A: HPLC analysis of oxidation products of NAcDeDopa mushroom tyrosinase reaction. A reaction mixture (1 ml) containing 0.1 mmoles of NAcDeDopa and 5 μg mushroom tyrosinase in 50 mM sodium phosphate, pH 6.0 was incubated at room temperature and an aliquot of the reaction mixture (5 μl) was subjected to HPLC analysis as outlined under material and methods. The long dashed broken line represents the zero min (control) reaction, the short dashed line represents 3.5 min reaction and the solid line represents 45 min reaction.

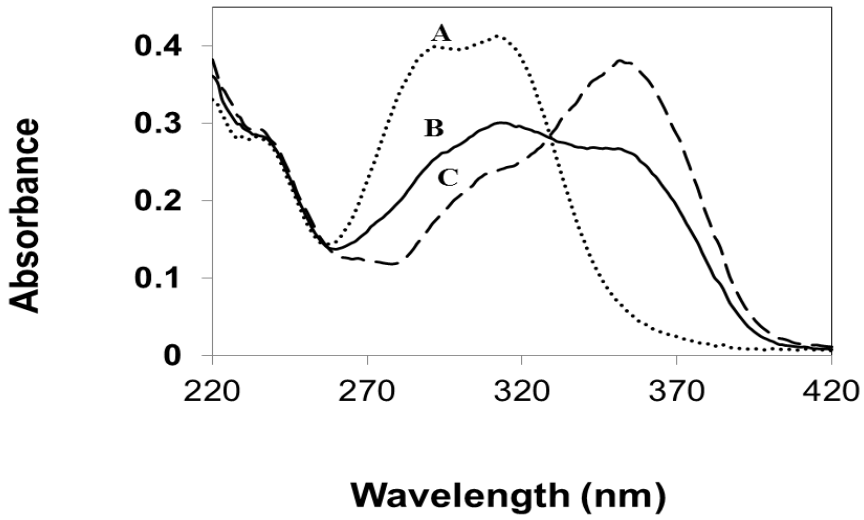

Figure 5.6B: The ultraviolet absorbance spectrum of the product peaks from figure 5.6A. Dotted line (A) represents the UV spectrum of substrate peak (retention time = 4.02 min), solid line (B) represents the UV spectrum of the product peak eluting with the retention time of 6.1 min and the broken line (C) represents the product eluting at 9.39 min.

To further analyze the nature of these products, samples from control and reaction products were subjected to RP-HPLC/ESI/MS-MS analysis. The base peak chromatogram of the product(s) of NAcDeDopa oxidation catalyzed by tyrosinase during the initial phase of the reaction (5 min reaction) as analyzed by RP-HPLC/ESI/MS-MS indicated the generation of a single product eluting at about 8.4 min with a molecular

mass of 235.05 units consistent with the production of 3-aminoacetylesculetin. The average ESI-mass spectrum of this peak is shown in Figure 5.7. It exhibits major ions at m/z 236 and 194. The ion at m/z 236 corresponds to the protonated 3-aminoacetylesculetin, the m/z 194 ion represents the protonated deacylated or decarboxylated product. The CID spectrum of the m/z 236 ion (Figure 5.7 bottom) shows an abundant product ion at m/z 194, corresponding to the protonated deacylated product.

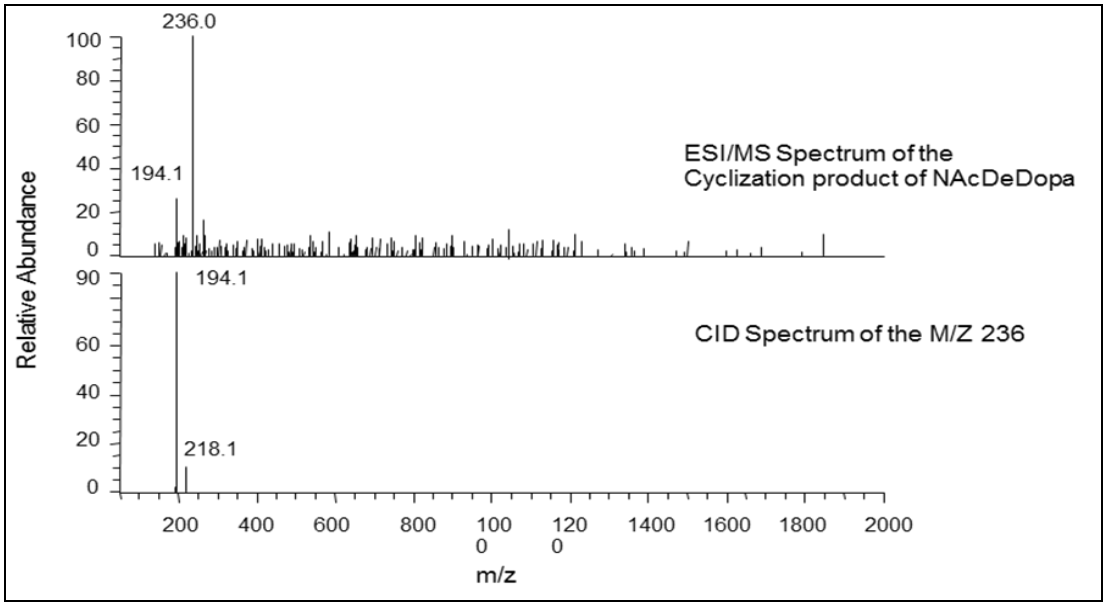

Figure 5.7: The average electrospray mass spectrum of the initial product of NAcDeDopa/ tyrosinase reaction (Top). The m/z 236 ion corresponds to the protonated 3-aminoacetylesculetin and the m/z 194 ion represents the protonated deacylated product. Bottom: The average CID mass spectrum of the m/z 236 parent ion shows an abundant product ion at m/z 194, corresponding to the protonated deacylated product.

The base peak chromatogram depicted in Figure 5.8 shows the products of NAcDeDopa oxidation catalyzed by tyrosinase generated during a long-term incubation of the reaction (30 min) as analyzed by RP-HPLC/ESI/MS-MS. The mass spectrum associated with the initial peak at 11 min shows a parent ion at m/z 469.0, which represents the dimer(s) of 3-aminoacetyl esculetin. The mass spectra associated with the next set of peaks observed between 18.0 min 19.7 min shows a parent ion at 702.0, which is indicative of the trimers. The mass spectra associated with the chromatographic peaks between 20 and 21 min shows a parent ion at m/z 935.0, which is indicative of the tetramers of 3-aminoacetylesculetin. The mass spectra associated with the minor chromatographic peak at 21.2 min shows a parent ion at m/z 1167.9, which is indicative of the pentamer(s). The multiple peaks observed for some of the oligomers arise because of the formation of different stereoisomeric addition products. For example, oxidation of dehydro NADA leads to the production of multiple isomeric oligomeric benzodioxan type products (Abebe et al., 2010). This multiple adduct formation is consistent with the nonenzymatic addition reaction of dehydro NADA with its oxidation product, QMIA and subsequent addition of QMIA to dimers and trimers. Since nonenzymatic reactions are generally nonstereospecific, it usually leads to multiple isomeric products; a fact that has been verified with the naturally occurring dimers of dehydro NADA in the cuticle of insects (Tada et al., 2002). These nonstereospecific chemical additions naturally result in the production of broad oligomeric peaks in the chromatogram. As a result, there is some degree of co-elution between oligomeric products.

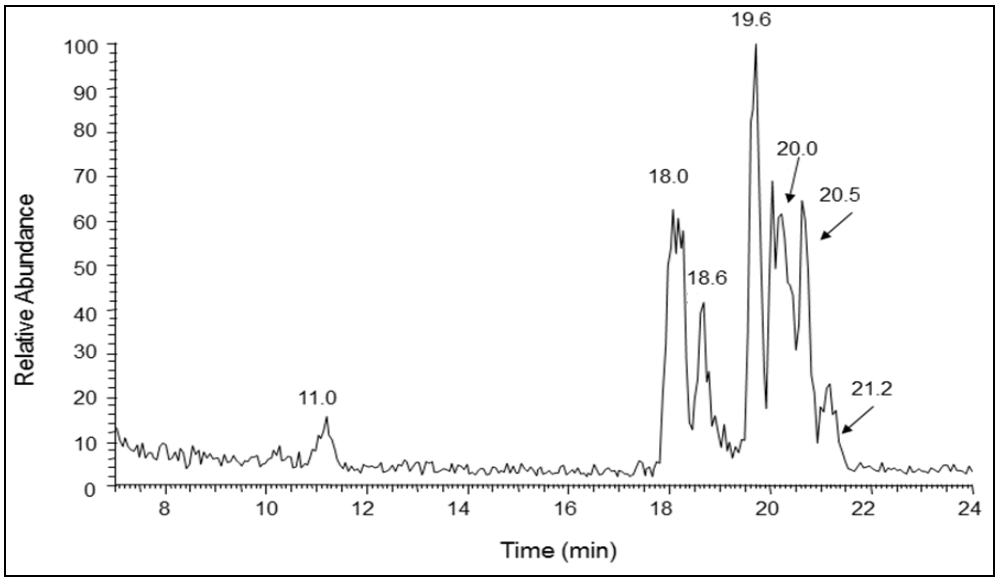

Figure 5.8: The Base Peak Chromatogram from the RP-HPLC/ESI/MS-MS analysis of NAcDeDopa /tyrosinase reaction mixture performed after long-term (30 min) incubation. The marked retention times indicate the location of the polymeric species identified. The first chromatographic peaks near 11 min are identified as isomers of the dimeric product (Figure 5.10). The peaks between 18.0 and 19.7 min are identified as isomers of the trimeric product (Figure 5.11). The peaks between 20.0 and 21.0 min are identified as isomers of the tetrameric product (Figure 5.12). The peaks at 21.2 min are identified as isomers of the pentameric product (Figure 5.13).

The base chromatogram and ion chromatograms corresponding to the dimers, trimers, tetramers, pentamers and hexamers obtained from the RP-HPLC/ESI/MS-MS analysis of NAcDeDopa tyrosinase long-term reaction is shown in Figure 5.9. The ion chromatograms of the m/z 469, 702, 935, 1168, and 1401 correspond to dimers, trimers, tetramers, pentamers and hexamers, respectively. Detailed structural analysis of the m/z

ions 469, 702, 935, and 1168 is described in the text associated with Figures 5.10, 5.11, 5.12, and 5.13.

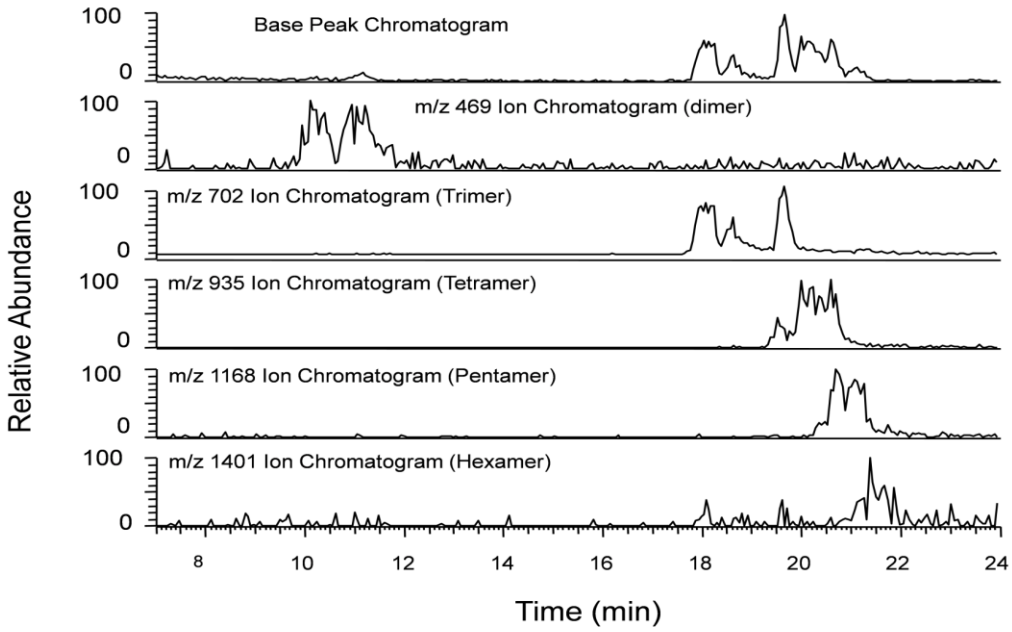

Figure 5.9: The base chromatogram and ion chromatograms corresponding to the oligomers obtained from the RP-HPLC/ESI/MS-MS analysis of NAcDeDopa tyrosinase long term reaction. The ion chromatograms of the m/z 469, 702, 935, 1168, and 1401 correspond to dimers, trimers, tetramers, pentamers and hexamers.

The average ESI-mass spectrum of the 11 min peak (from Figure 5.8) is shown in Figure 5.10. It exhibits major ions at m/z 469 and 385. The ion at m/z 469 corresponds to the dimer of 3-aminoacetylesculetin and the m/z 385 ion represents its deacetylated product. The CID mass spectrum (Figure 5.10 bottom) of the m/z 469 ion shows a

dominant product ion at m/z 427 (due to loss of C_2H_2O from the $NHCOCH_3$ moiety) and the minor peak at 385 is again the deacetylated product (the loss of two C_2H_2O groups one from each $NHCOCH_3$ moiety).

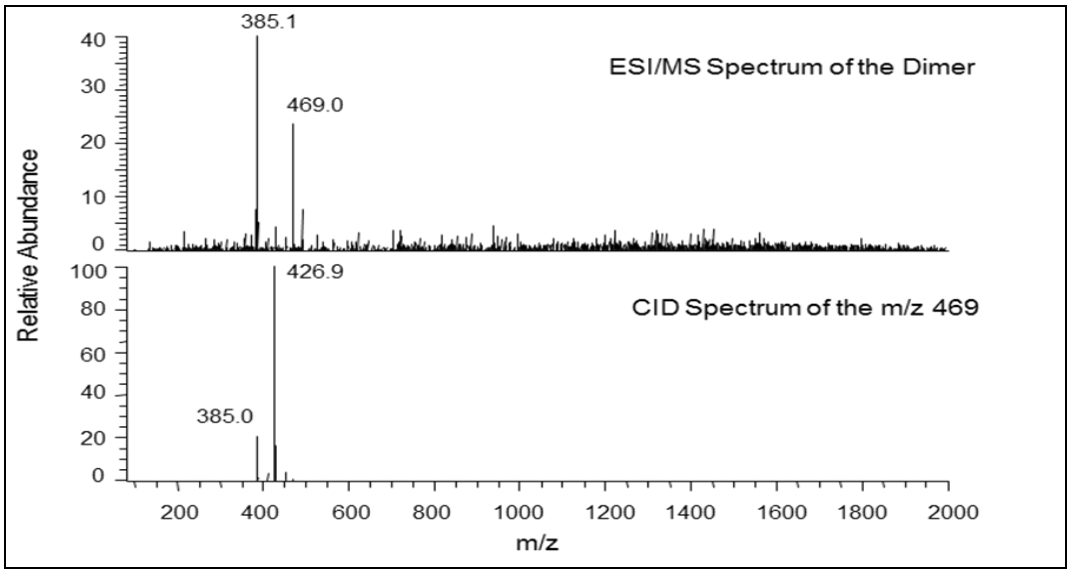

Figure 5.10: The average electrospray mass spectrum of dimeric product of 3-aminoacetylesculetin (Top). The m/z 469 ion corresponds to the protonated dimer ion, and m/z 385 ion represent its deacetylated products. Bottom: The average CID mass spectrum of the m/z 469 parent ion, the m/z 427 is the deacetylated product of m/z 469.

The average ESI-mass spectrum from 18.03 to 18.63 min peaks (from Figure 5.8) is shown in Figure 5.11. It exhibits major ion at m/z 702 which corresponds to the protonated trimer of 3-aminoacetylesculetin. The m/z 1402.6 ion represents its proton-bound dimeric form of this trimer ion, which is formed in the gas-phase during

electrospray ionization and the minor ions at m/z 660 and m/z 618 are deacetylated products of m/z 702. The CID mass spectrum of the 702 ion (Figure 5.11 bottom) shows a dominant product ion at m/z 660 ion due to loss of C_2H_2O from the $NHCOCH_3$ moiety and the minor peak at 618 due to the loss of C_2H_2O from two of the $NHCOCH_3$ moieties.

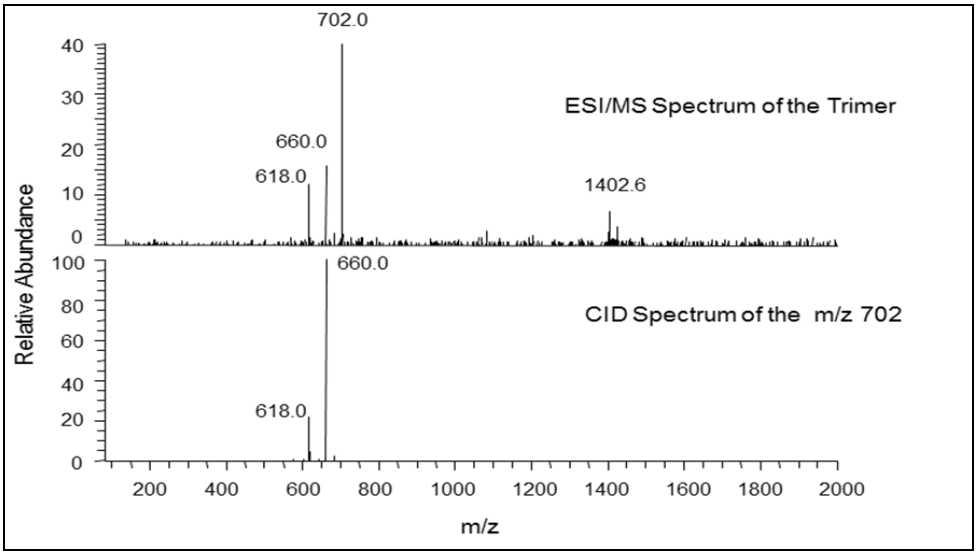

Figure 5.11: The average electrospray mass spectrum of trimeric product of 3-aminoacetylesculetin. The m/z 702 ion corresponds to the protonated trimer ion. The m/z 660 and 618 ions represent its deacetylated products. The m/z 1402.6 ion corresponds to the proton-bound dimer of the trimeric product and is formed in the gas-phase during electrospray ionization. Bottom: The average CID mass spectrum of the m/z 702 parent ion.

The average ESI-mass spectrum from 20 to 21 min peaks (from Figure 5.8) is shown in Figure 5.12. It exhibits major ions at m/z 935 and minor ion at 957. The ion at m/z 935 corresponds to the protonated tetramer of 3-aminoacetylesculetin, and the m/z 957 ion represents its sodiated tetramer of 3-aminoacetylesculetin. The CID mass spectrum (Figure 5.12 bottom) of the m/z 935 ion shows a dominant product ion at m/z 893 and two minor product ions at m/z 851 and 809. These product ions are formed from the loss of C_2H_2O ($[MH-42]^+$) from the $NHCOCH_3$ moieties.

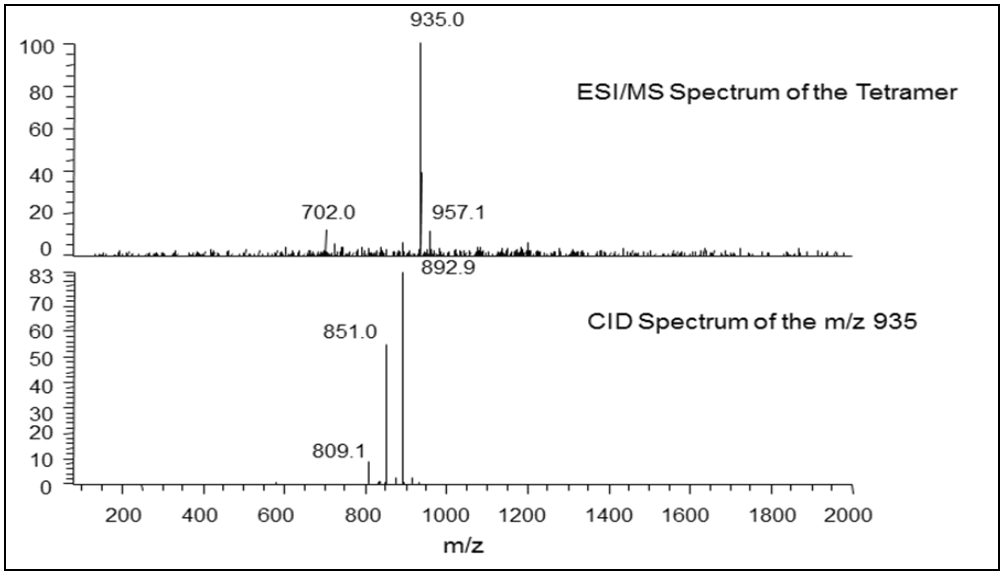

Figure 5.12: The average electrospray mass spectrum of tetrameric product of 3-aminoacetylesculetin. The m/z 957.1 ion corresponds to the sodiated tetramer ion (Top). Bottom: The average CID mass spectrum of the m/z 935 parent ion.

The average ESI-mass spectrum of the 21.25 min peak (from Figure 5.8) is shown in Figure 5.13. It exhibits a major ion at m/z 1168, which corresponds to the protonated pentamer of 3-aminoacetyl esculetin (the m/z 935 ion is co-eluting tetramer and m/z 742.7 is an unidentified ion). The CID mass spectrum (Figure 5.13 Bottom) of the m/z 1168 ion shows a dominant product ion at m/z 1126 and m/z 1084 and a minor product ion at m/z 1042. These product ions are formed from the loss of C_2H_2O ($[MH-42]^+$) from the $NHCOCH_3$ moieties.

These results confirm that the 3-aminoacetylesculetin that is formed initially is undergoing further oxidative polymerization generating oligomers, which differ by a molecular weight of 233 amu corresponding to the sequential addition of 3-aminoacetylesculetin QMIA to the starting material (viz., 3-aminoacetylesculetin) to form dimers, trimers, tetramers, pentamers and hexamers.

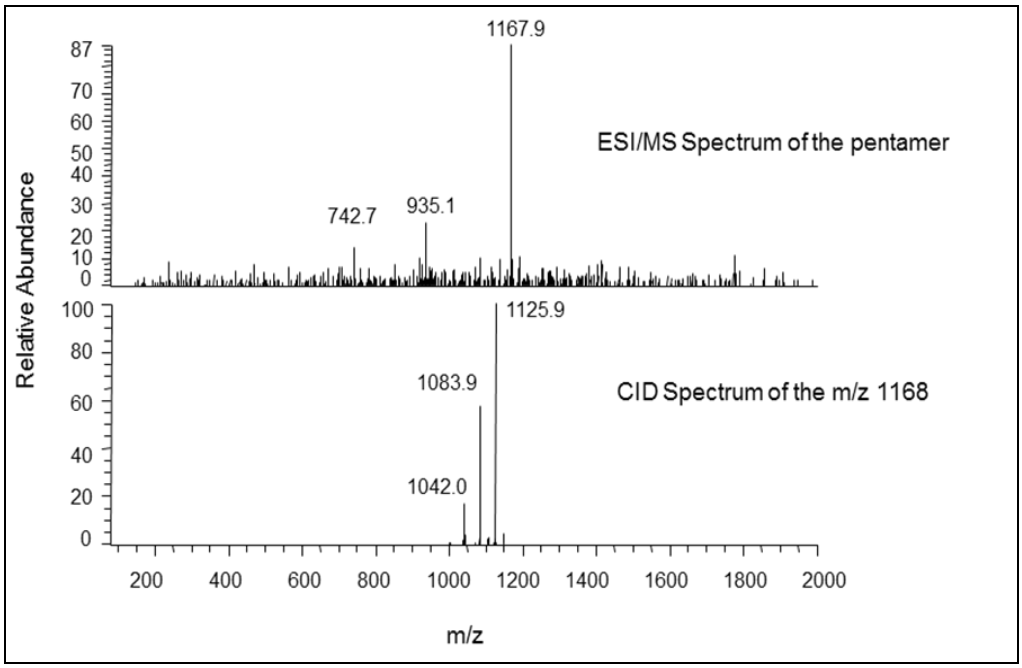

Figure 5.13: The average electrospray mass spectrum of pentameric product of 3-aminoacetylesculetin. The m/z 1168 ion corresponds to the protonated tetramer ion (Top). Bottom: The average CID mass spectrum of the m/z 1168 parent ion.

5.5 Discussion

The results presented in this section on the oxidative transformation of NAcDeDopa can be summarized as follows. Tyrosinase rapidly oxidizes NAcDeDopa to its corresponding QMIA similar to the reaction reported in the case of dehydro NADA, a close structural analog that lacks a carboxyl group. Thus both QMIA produced from NAcDeDopa (current work) and Dehydro NADA (Sugumaran et al., 1992; Abebe et al., 2010) show typical visible absorbance maximum at 485 nm. The normally generated quinone should have an absorbance maximum at about 400 - 420 nm range, as observed for the related DeNAcDopa methyl ester (Sugumaran et al., 1992). The QMIA formed, being extremely unstable, undergoes rapid and direct oligomerization in the case of dehydro NADA (Abebe et al., 2010). In the case of NAcDeDopa, however its QMIA, due to the presence of an internal carboxyl group that is suitably positioned to exhibit an intramolecular cyclization, instead produces a coumarin derivative as shown in Figure 5.14. 3-aminoacetylesculetin thus formed, subsequently undergoes further oxidative polymerization as shown in Figure 5.15. The QMIA thus formed will undergo an addition reaction with the remaining 3-aminoacetylesculetin forming benzodioxan-type dimer first. The dihydroxy group of this dimer adds on to another molecule of QMIA producing the trimer. The process continues to produce tetramers, pentamers and hexamers. This reaction is similar to the oligomerization of dehydro NADA that was reported recently from this laboratory (Abebe et al., 2010). It is important to note that the dehydro NADA structure is embedded in the skeleton of 3-aminoacetylesculetin. Based on this structural

feature, it is naturally expected that 3-aminoacetyl esculetin is also oxidized by tyrosinase to its QMIA and the resultant QMIA exhibits oligomerization reaction with the parent 3-aminoacetylesculetin.

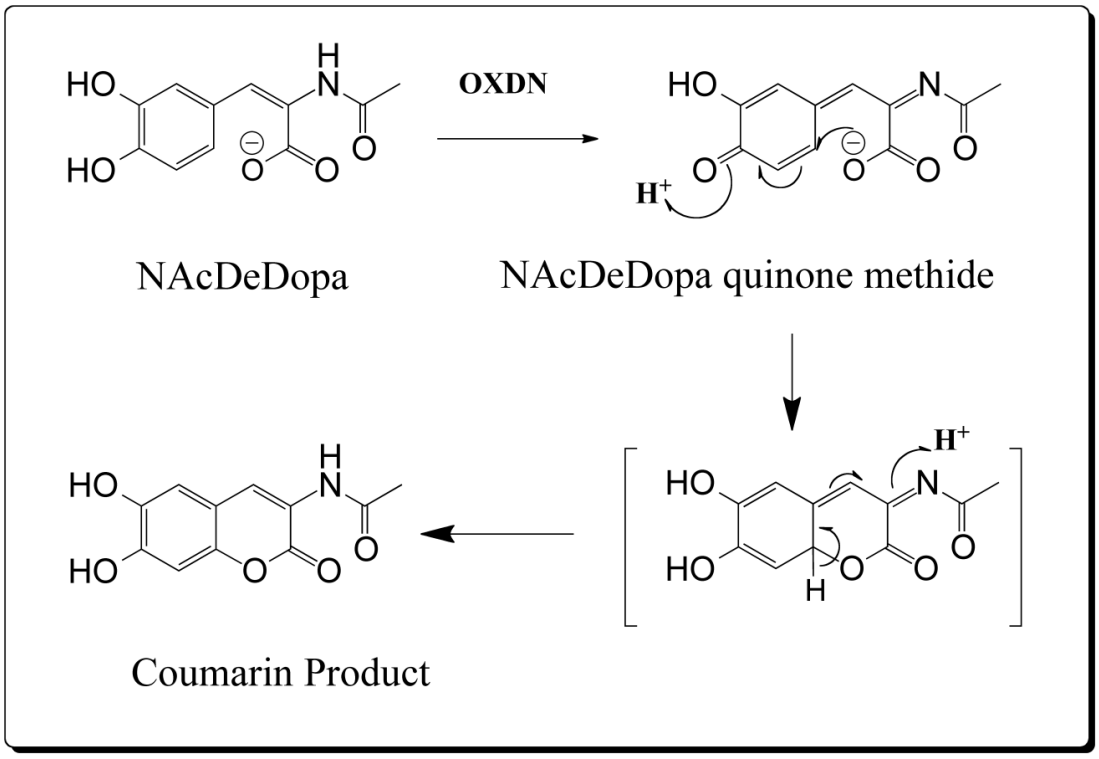

Figure 5.14: Proposed mechanism for the tyrosinase catalyzed oxidation of NAcDeDopa. Tyrosinase oxidizes NAcDeDopa to its corresponding p-quinone methide rather than the conventional o-quinone derivative. The resultant quinone methide is very unstable as it exhibits rapid intramolecular cyclization producing 3-aminoacetylesculetin via a transient dienone intermediate.

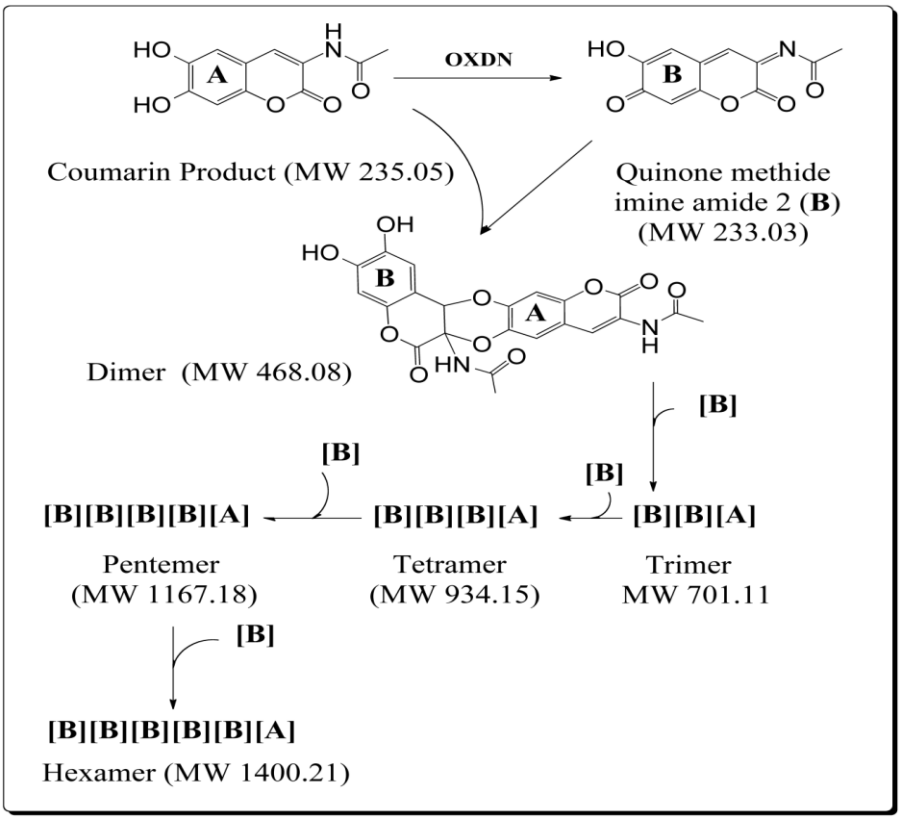

Figure 5.15: Proposed mechanism for the further transformation of NAcDeDopa – tyrosinase reaction product. 3-Aminoacetylesculetin produced during the oxidation of NAcDeDopa by tyrosinase, being a catechol conjugated with a double bond, is extremely labile and suffers further oxidation. The product formed in this case is a highly reactive QMIA rather than the simple quinone. QMIA due to the presence of quinone methide nucleus and Schiff's base undergoes rapid reaction with the parent 3-aminoacetylesculetin through the two phenolic hydroxyl groups resulting in the formation of a benzodioxan type dimer. The dimer adds onto another molecule of QMIA producing trimer. The oligomerization seems to generate as many as six polymeric products.

5.6 Conclusion

The above studies strongly support the proposal that lamellarin-type compounds could arise by oxidative coupling of dehydrodopyl derivatives. Dehydrodopyl and dehydrotyrosyl derivatives have been shown to be abundantly present in numerous marine invertebrates (Sugumaran and Robinson, 2010). Tyrosinase present in these invertebrates can definitely cause nonspecific oxidation of these compounds and generate their quinonoid products. Production of dihydroxycoumarin skeletons found in compounds such as lamellarins and ningalins is therefore, certainly possible by the oxidative cyclization of dehydrodopyl derivatives present in these marine invertebrates. It is interesting to note that the majority of the lamellarins are methylated at the catecholic group. The methylation reactions prevent the further oxidation of the esculetin type products formed by oxidative cyclization. This is certainly necessary and important to prevent the oxidative polymerization as observed in the present study with the model compound.

CHAPTER 6

ENZYMATIC OXIDATION OF 1, 2-DEHYDRO-N-ACETYL DOPA METHYL ESTER

6.1 Chapter summary

Some peptidyl tyrosine residues undergo post-translational modification to dopa and are used for a variety of purposes such as natural glues, metal chelators, antimicrobial agents etc. Previous studies have indicated that peptidyl dopa units are converted to dehydrodopa derivatives under oxidative conditions. In an effort to understand the further fate of peptidyl dehydrodopa units, a model oxidation studies with 1, 2-dehydro-N-acetyldopa methyl ester (DeNAcDopa methyl ester) was conducted. Ultraviolet and visible spectral studies associated with tyrosinase-catalyzed oxidation of DeNAcDopa methyl ester indicated the facile production of transient DeNAcDopaquinone methyl ester as the primary two-electron oxidation product. This unstable quinone rapidly reacted with the parent compound probably via a Diels-Alder type condensation generating benzodioxan adduct(s). Essentially the same result was obtained with chemical oxidation. Liquid chromatography studies of DeNAcDopa methyl

ester -tyrosinase reaction mixture indicated the production of more than one product(s). Mass spectrometry confirmed this contention and provided evidence for the production of dimeric and other oligomeric products. Based on these results, I propose that peptidyl dehydrodopa also can undergo similar transformations accounting for the adhesive and cementing properties of the dopyl proteins in nature.

6.2 Introduction

Tyrosine residues in peptides are frequently the targets of post-translational modification, one of which involves hydroxylation to peptidyl dopa. These modifications seem to be critical and associated with a number of biological processes such as biological glue and cement formation (Waite, 1990; Rubin et al., 2010). The marine bivalves for example, produce tyrosine rich peptides and the enzyme tyrosinase at the site of foot adhesion to substratum. The resultant mixture generates peptides heavily decorated with dopa units and these units upon further oxidative transformation, produce cross-links and adducts that are necessary for binding in water, allowing them to attach themselves in marine environments, in spite of adverse effects caused by salinity, humidity, tides, turbulence, and waves. These adhesive proteins are able to form not only permanent and strong but also flexible underwater bonds to substrates such as glass, Teflon, metal, and plastic. Moreover, the bivalve does not have to expend energy to maintain its position on substrate. The adhesion is rapid, strong, and tough, and prevents the organism from being dislodged and dashed to pieces by the next incoming wave. This

ability to produce a strong attachment in the form of byssus made them dominate in hard surfaces in temperate aquatic habitat. The same reactions are also used for the hardening of the periostracum in bivalves (Waite, 1990; Rubin et al., 2010). It was reported that mussel adhesive protein analogs without dopa showed greatly reduced ability for adhesion (Yu and Deming, 1998). The stickiness of mussel's foot, especially how it works in a wet environment could be mimicked to develop new kinds of biocompatible building materials, use as medical adhesives such as for bonding broken teeth and bones since they are nontoxic to human body and do not impose immunogenicity (Dove and Sheridan, 1986). Unlike the urea-formaldehyde wood adhesives, which are associated with health concerns and are based on expensive petroleum products, mussel adhesives biodegradable properties makes them environmentally friendly 'green" products with no apparent deleterious or toxic impact on the environment. Mainly with this reason, several groups of workers have been examining the oxidative fate of both naturally occurring and synthetic dopyl peptides.

Our laboratory first reported that dihydrocaffeate methyl ester (Figure 1.11 Compound 1 A = H; B = $COOCH_3$) and dihydrocaffeate methylamide (Figure 1.11, Compound 1 A = H; B = $CONHCH_3$) (the deaminated derivatives of dopa) undergo unique oxidative transformation yielding caffeate derivatives (Sugumaran et al., 1989a, b). This unusual side chain dehydrogenation was shown to occur through the intermediacy formation of the corresponding quinone and its isomeric quinone methide (Figure 1.11). These catechols once oxidized, produce their corresponding quinones,

which exhibit rapid nonenzymatic isomerization generating transient quinone methide analogs, which finally yielded caffeic acid derivatives through yet another isomerization reaction (Figure 1.11). Subsequently, it was demonstrated that even peptidyl model compounds such as N-acetyldopa esters (Figure 1.11, Compound 1; A = $NHCOCH_3$; B = $COOCH_3$or $COOC_2H_5$) could generate dehydro dopyl units through this mechanism (Sugumaran and Ricketts 1995; Rzepecki et al., 1991; Rzepecki and Waite 1991). It has also been established a similar transformation with the insect cuticular sclerotizing precursor, N-acetyldopamine (NADA; Figure 1.11 Compound 1; A = H B = $NHCOCH_3$) (the decarboxylated derivative of dopa). In this case, however, enzymatic intervention was absolutely essential to witness the side chain desaturation. Thus, isomerization of NADA quinone required the use of a new quinone isomerase and the subsequent conversion of NADA quinone methide to dehydro NADA required the use of yet another isomerase, quinone methide isomerase (Saul and Sugumaran 1988, 1989a, 1989b, 1990a). This is in sharp contrast with the oxidative transformations of dihydrocaffeates and N-acetyldopa esters where beyond tyrosinase action, the rest of the reactions seem to occur without the need for any enzymes. The driving force for the introduction of double bond in carbonyl containing compounds apparently is coming from the carboxyl group that seems to assist the isomerization reactions. Thus a number of dehydro dopa units can be easily produced by the oxidative transformation of dopyl units.

A careful survey of naturally occurring compounds reveals that a variety of dehydro dopa derivatives are found in marine organism especially tunicates. Some of the

dehydro compounds found in marine animals are listed in Table 1.1. The biological significances of these molecules are still not clear. Various workers have theorized that they could serve as metal chelators and trap vanadium in the center, or serve as hardening agent for the tunic. Some of them have been identified as antibiotic compounds and some are associated with cementing/adhering properties (Cai et al., 2008). With the exception of simple dehydro NADA, which is formed in insect cuticle in relation to cuticular hardening process, practically nothing is known about the fate of other dehydro compounds. In this chapter the reaction pathway of peptidyl tyrosine following its hydroxylation to peptidyl dopa was explored using a model compound DeNAcDopa methyl ester.

Extensive studies carried out on the oxidation chemistry of dehydro NADA reveal that upon enzymatic oxidation at physiological pH, generates a quinone methide imine amide as the immediate two-electron oxidation product and not the conventional quinone (Sugumaran 2000; Sugumaran et al., 1992a). The normally expected quinone is only produced under acidic conditions, which prevents the conversion of quinone-to-quinone methide tautomerization. The quinone methide thus formed is very unstable and highly reactive. The quinone methide nucleus undergoes facile Michael-1, 6-addition reaction and the Schiff's base amide undergoes rapid addition. As a result both the side chain carbon atoms form adduct with external nucleophiles generating adducts and crosslinks (Sugumaran, 1998). In the absence any external nucleophiles, the reactive intermediate forms adducts with parent catechols resulting in dimer formation. A similar reaction is

possible with other peptidyl dopa derivatives also but this realization has not been assessed. In order to assess this possibility, oxidation studies was conducted with the peptidyl dehydro dopa mimic, 1, 2-dehydro-N-acetyldopa methyl ester (DeNAcDopa methyl ester) and found similar reaction is possible although by a different mechanistic route.

6.3 Materials and methods

DeNAcDopa methyl ester was synthesized from N-acetyltyrosine through N-acetyltyrosine methyl ester in methanol and HCl gas with 87% yield and was further purified by Biogel P-2 column chromatography using 0.2 M acetic acid as the eluent. Dehydro NADA is prepared as outlined in chapter 2 materials and methods section. Mushroom tyrosinase and laccase were procured from Sigma Chemical Co., St. Louis, MO. All other chemicals were of analytical grade purchased from Fisher and/or VWR. HPLC grade methanol and ammonium formate (99%) were purchased from Acros, Morris Plains NJ. HPLC grade water was obtained from MilliQ synthesis A10 Water purification system purchased from Millipore, Milford, MA.

Enzyme assays: A reaction mixture containing different catechols (usually 0.2 mM), about 10 μg of tyrosinase in 50 mM sodium phosphate buffer at specific pH was incubated at room temperature and the spectral changes associated with the oxidation was followed. For non-enzymatic reactions the enzyme was omitted and the pH of the buffer used was 8.0.

RP-HPLC analysis of DeNAcDopa methyl ester: A reaction mixture (1 ml) containing 0.25 mM DeNAcDopa methyl ester and 10 μg mushroom tyrosinase in 50 mM sodium phosphate pH 6.0 was incubated at room temperature. An aliquot of the reaction mixture (5 μl) was subjected to HPLC analysis on Agilent 1100 HPLC series (Agilent Technologies, Santa Clara, CA) fitted with diode array detector and reversed phase C_8 Cartridge (IBM Instrument Inc. premium LC Columns) (250 x 4.0 mm, 5 μm size) using isocratic elution with 50 mM Citrate buffer pH 3.0 containing 7% acetonitrile at a flow rate of 1ml/min.

Mass Spectrometer Parameters-Direct injection: A Thermofinnigan LCQ Advantage ion trap mass spectrometer (Sunnyvale, CA) was used to detect and characterize the reaction products. The sample was directly injected to the LC-MS/MS and the operating parameters of the ion trap mass spectrometer were as follows: capillary temperature (280 °C), spray voltage (4.00 kV), sheath gas (30 cm^3/min). Collision-induced decomposition (CID) was performed at a relative collision energy of 28, an isolation mass window of 2.5 amu, and a default activation Q and activation time of 0.250 and 30 ms, respectively. The CID experiment was designed to obtain the product spectra of a specific parent oligomer by programming the mass spectrometric method to perform CID for the appropriate m/z ratio during the time window that corresponded to elution time of the oligomer.

6.4 Results

Tyrosinase is a non-specific enzyme readily attacking a number of *o*-diphenolic compounds and converting them to their corresponding quinones. Accordingly mushroom tyrosinase oxidized a number of dopa derivatives such as dopa, dopamine, dopa methyl ester, N-acetyldopa, N-acetyldopa methyl ester, dehydro-N-acetyldopa and a plethora of related catechol derivatives. Typically oxidation of catechols by tyrosinase generates the corresponding *o*-quinone as the initial observable product. Most *o*-benzoquinones exhibit visible absorbance maximum at 400 nm. However, spectral changes depicted in Figure 6.1, that is associated with the tyrosinase-catalyzed oxidation of DeNAcDopa methyl ester failed to support the generation and accumulation of its corresponding *o*-quinone having an absorbance maximum at around 400 nm range. Yet the rapid spectral changes occurring in the UV region clearly indicated the facile oxidative transformation of this compound. Essentially the same results were observed even if the reaction was conducted at different physiological pH values. Figure 6.2 for example shows the UV and visible spectral changes accompanying the oxidation of DeNAcDopa methyl ester by tyrosinase at pH 8.0. Again, the absence of the typical absorbance maximum at 400 nm due to quinone accumulation is quite evident.

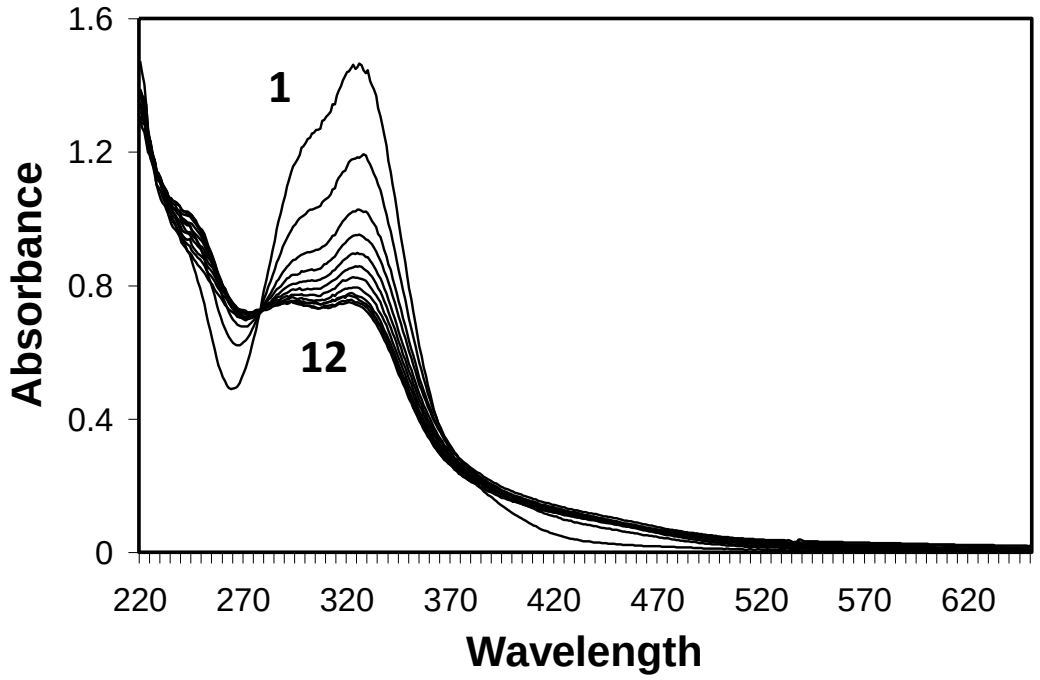

Figure 6.1: Ultraviolet spectral changes associated with the tyrosinase-catalyzed oxidation of DeNAcDopa methyl ester at pH 6.0. A reaction mixture containing 0.2 mM of DeNAcDopa methyl ester in 50 mM sodium phosphate, pH 6.0 and 10 μg of tyrosinase was incubated at room temperature and the spectral changes associated with oxidation of DeNAcDopa methyl ester was monitored at one minute interval (scan 1: zero time; scan 12: 11 minutes). The reaction was initiated by the addition of substrate.

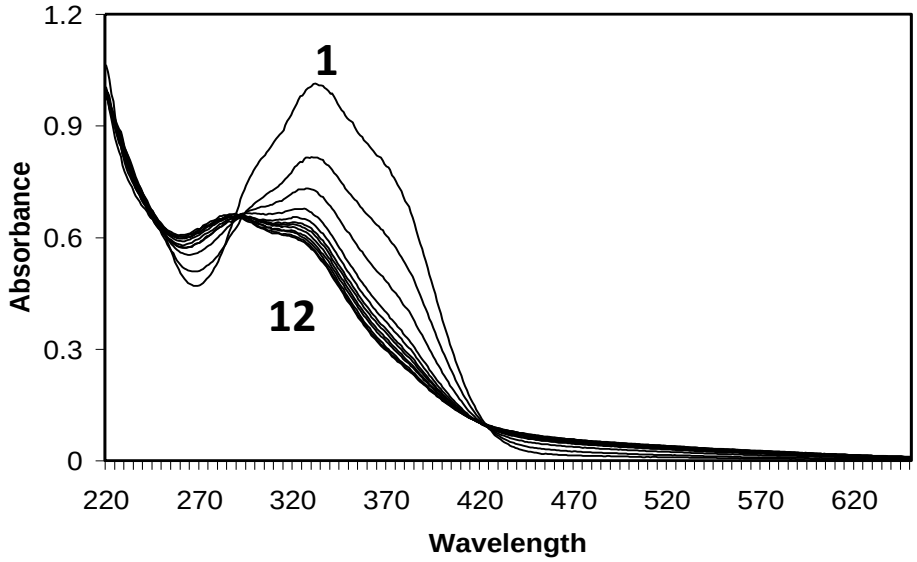

Figure 6.2: Ultraviolet spectral changes associated with tyrosinase-catalyzed oxidation of DeNAcDopa methyl ester at pH 8.0. The same conditions used for Figure 6.1 were employed except for replacing the pH of the sodium phosphate buffer with pH 8.0 (scan 1: zero time; scan 12: 11 minutes).

It is established earlier from this laboratory that the oxidation of dehydro NADA by tyrosinase produces a transient isomeric quinone methide imine amide (QMIA) with an absorbance maximum at 485 nm. To assess whether the quinone or the quinone methide formed during the initial phase of the oxidation of DeNAcDopa methyl ester fast reaction studies were conducted by monitoring the increase in absorbance at 400 nm (due to quinone) and 485 nm (due to quinone methide). Figure 6.3 shows the absorbance increase at these two wavelengths during the initial phase of enzymatic oxidation. Clearly absorbance increase at 400 nm is consistent with the conventional quinone production. Notably the transient isomeric QMIA that would exhibit absorbance maximum at 485 nm

was either absent or non-detectable. The detection of conventional quinone and not the QMIA in this case was quiet surprising. But internal hydrogen bonding considerations and energy calculations indicate that the conventional quinone is the most stable compound in this case and not the isomeric quinone methide.

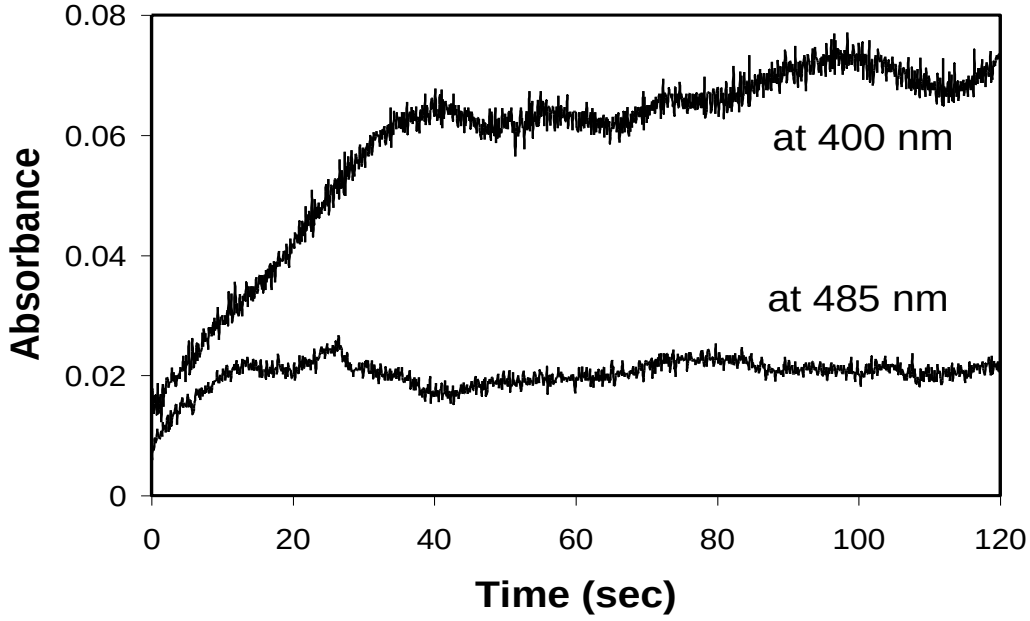

Figure 6.3: Visible spectral changes associated with the oxidation of DeNAcDopa methyl ester at 400 nm and 485 nm. A reaction mixture containing 0.2 mM of DeNAcDopa methyl ester in 50 mM sodium phosphate, pH 6.0 and 10 μg of tyrosinase was incubated at room temperature. The spectral changes associated with oxidation of DeNAcDopa methyl ester was monitored continuously at 400 nm (for quinone production) and at 485 nm (for quinone methide imine amide production).

To visualize the quinone more directly and to demonstrate its transient nature, chemical oxidation study with sodium periodate were conducted. Admixing mole to mole ratio of sodium periodate and any catechol instantaneously generates the corresponding quinone (Sugumaran, 2000). Figure 6.4 shows the UV and visible spectral changes accompanying the oxidation of DeNAcDopa methyl ester with sodium periodate. From the inset to Figure 6.4, it is clear that the DeNAcDopa methyl ester quinone formed is very unstable and is rapidly decomposing to colorless products. Again, during the chemical oxidation of DeNAcDopa methyl ester also, no quinone methide generation was observed.

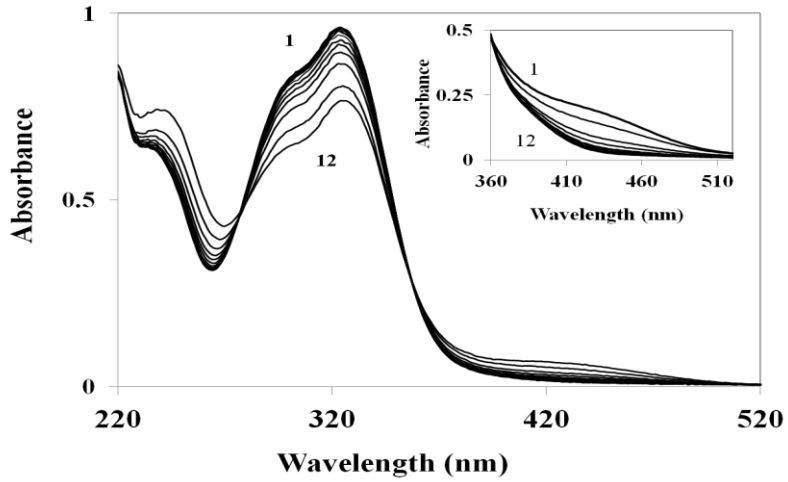

Figure 6.4: Evidence for the formation of quinone during the sodium periodate-catalyzed oxidation of DeNAcDopa methyl ester. A reaction mixture containing 0.2 mM DeNAcDopa methyl ester and 0.2 mM sodium periodate in 50 mM sodium phosphate buffer, pH 6.0 (scan 1: zero time; scan 12: 110 sec). Inset: Visible spectrum of the transient quinone produced during the reaction (scan 1: zero time; scan 12: 90 sec).

The spectral changes shown in Figures 6.1 and 6.2 were remarkably similar to those observed for dehydro NADA, where a dimerization reaction was shown to occur through a transient quinone methide intermediate. The quinone methide in this case undergoes facile addition reaction with the parent catechol forming benzodioxan dimers. Such a reaction may be unlikely in the present case, as the quinone methide was not observed even as the transient intermediate during the oxidation. Yet, the UV spectral changes given in Figure 6.1 and 6.2 indicated dimer formation and remarkably resembled the UV spectral changes accompanying the oxidative dimerization reaction of dehydro NADA.

RP-HPLC was carried out to characterize reaction products formed during tyrosinase catalyzed oxidation of DeNAcDopa methyl ester. As shown in Figure 6.5. HPLC analysis revealed the production of two new compounds eluting at about 8 min and 9.5 min respectively. The drastic decrease in the amount of the starting material and appearance of products with retention time at 8 and 9.5 min indicated the formation of oligomeric products. The UV-Vis spectrum of these compounds indicated that the 7.2 min peak is due to starting material, the 8 min peak is due to dimeric products and 9.5 min is due to trimeric products. The relative abundance of the products concomitant with the rapid disappearance of the substrate peak at 7.2 min is listed in table 6.1.

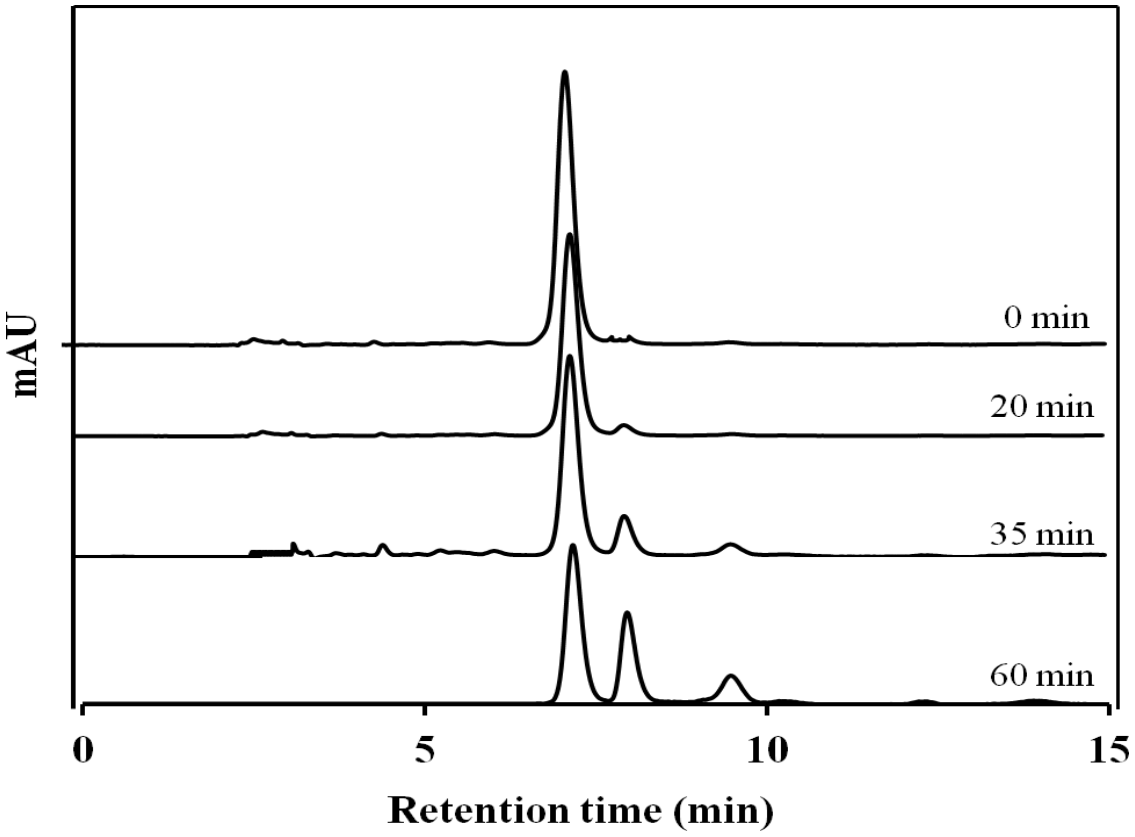

Figure 6.5: HPLC studies associated with the oxidation of DeNAcDopa methyl ester. A reaction mixture (1 ml) containing 0.25 mM of DeNAcDopa methyl ester and 10 µg mushroom tyrosinase in 50 mM sodium phosphate, pH 6.0 was incubated at room temperature and an aliquot of the reaction mixture (5 µl) was subjected to HPLC as outlined in materials and methods. Peak eluted at 7.2 min is due to the starting material, peak at 8 min may be due to dimer and peak at 9.5 min may be due to trimer.

Reaction time (min)	Retention time (min)	Area (mAU)	Product or Area (%)
0 (Control)	7.2	864.02	98.5
20	7.2	579	90
	8.0	29.47	3.5
35	7.2	246.5	70
	8.0	26.8	7.64
	9.51	13.12	3.7
60	7.2	92	45.4
	8.0	25.2	12.4
	9.5	13.08	6.4

Table 6.1: RP-HPLC analysis summary of the relative abundance of products formed during DeNAcDopa methyl ester oxidation by mushroom tyrosinase.

Dopa proteins are generally sticky, as a result attempts to analyze reaction mixture with LC-MS was unsuccessful. Direct injection mass spectral study of the reaction mixture from Figure 6.5 was conducted to confirm the oligomeric nature of the products. Figure 6.6 shows the average electrospray mass spectra of the control DeNAcDopa methyl ester with [M+ H^+] 252 prominent ion. The average electrospray mass spectrum of the half hour reaction mixture is shown in Figure 6.7. The peaks at 252 and 274 are M+1 ion and M+Na ion respectively. The peak at 523 is due to the sodiated dimer (500

plus 23). The peak at 525 may be the dimeric product of DeNAcdopa methyl ester that forms during the electrospray process. The peak at 748 is due to the oxidized trimer plus a proton. The peak at 770 is due to the sodiated trimeric product that is oxidized to its quinonoid product. The same happens with the tetrameric product also. Thus the peak at 997 is oxidized trimer plus a proton and the peak at 1019 is the sodiated tetrameric product that has been oxidized to its quinonoid product. These results certainly confirm the oxidative dimerization and oligomerization of DeNAcDopa methyl ester by tyrosinase.

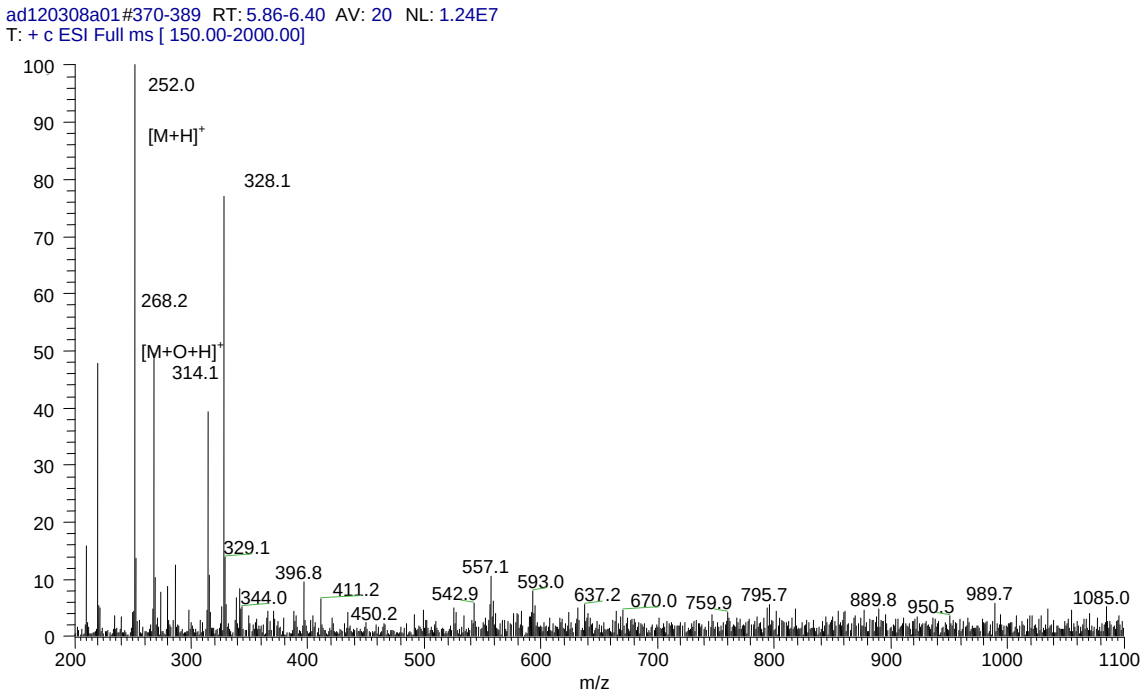

Figure 6.6: The average electrospray mass spectrum of the control DeNAcDopa methyl ester and tyrosinase reaction. The m/z 252 ion corresponds to the protonated DeNAcDopa methyl ester monomer ion.

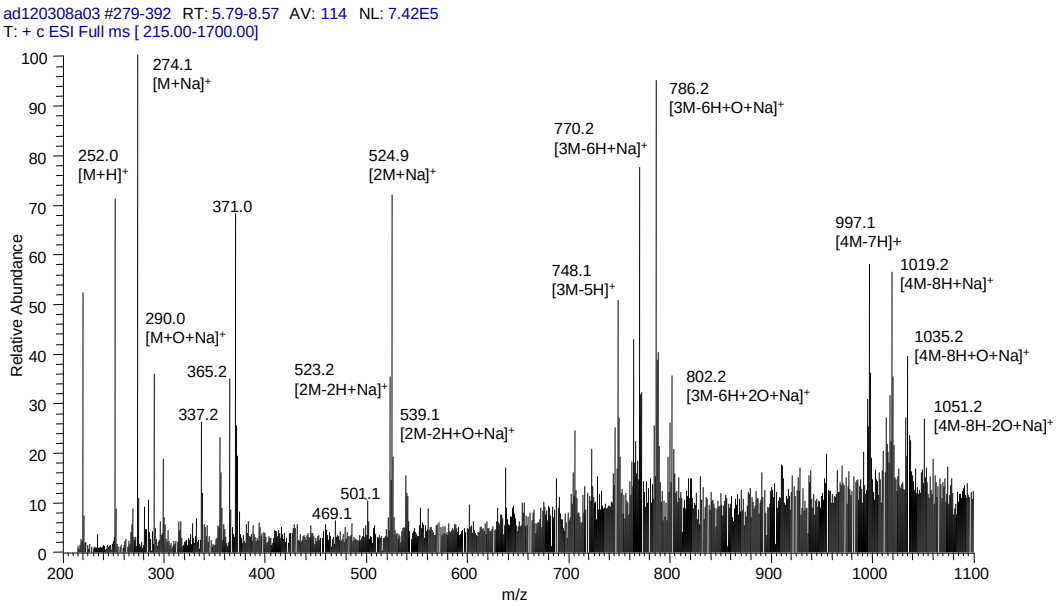

Figure 6.7: The average electrospray mass spectrum of DeNAcDopa methyl ester and tyrosinase 30 min reaction.

Detailed mass spectral studies of the reaction could not be conducted as outlined for dehydro NADA reaction. RP-HPLC-MS/MS analysis did not help us resolve and chromatograph different oligomers perhaps due to their sticky nature as witnessed in the case of tunichromes. Nevertheless, direct injection of reaction mixture into mass spectrometer did support the production of dimeric and oligomeric species of Dehydro NAc dopa methyl ester.

6.5 Discussion

The observed oxidative dimerization and oligomerization of DeNAcDopa methyl ester can occur by three different mechanistic routes. The first route calls for the intermediary formation of a two-electron oxidation product, QMIA similar to the one identified for the dehydro NADA (Sugumaran et al., 1992) (Figure 1.8). However, available experimental evidences indicate that such an intermediate is not likely to be formed during the initial phase of enzymatic oxidation of DeNAcDopa methyl ester. First of all we could not witness the transient production of quinone methide during the oxidation at about 480 nm. Second conventional quinone production could be observed both during the initial phase of enzymatic as well as chemical oxidation (Figures 6.3 and 6.4). Finally energy considerations indicate that the quinone is more stable than the quinone methide in this case as opposed to dehydro NADA, where quinone methide is more stable than the isomeric quinone. Therefore dimerization of DeNAcDopa methyl ester must proceed through the transiently formed quinone intermediate (Figure 6.8). The transient quinone could react with the parent compound by an ionic Diels Alder type reaction. Although Diels Alder type additions are rare in biological systems, a couple of addition reactions have been show to occur via Diels Alder type condensation in recent years (Takao et al., 2005). The biological Diels Alder additions could occur either by a retro Diels Alder type addition or more likely by an ionic Diels Alder reaction. In any case, the quinone production will require only a Diels Alder type addition for dimerization and other oligomerization reactions observed in the present case.

The last possibility calls for the transient production of semiquinone radicals. Radical coupling of the isomeric quinone methide radical with semiquinone radical and eventual ring closure can also produce the same dimeric and oligomeric products. However, semiquinone production at physiological pH employed for the current experiments is unlikely as they will rapidly undergo dismutation generating the two-electron oxidation product and the parent catechol. Hence free radical mediated coupling seems to be rather unlikely to occur at this pH value.

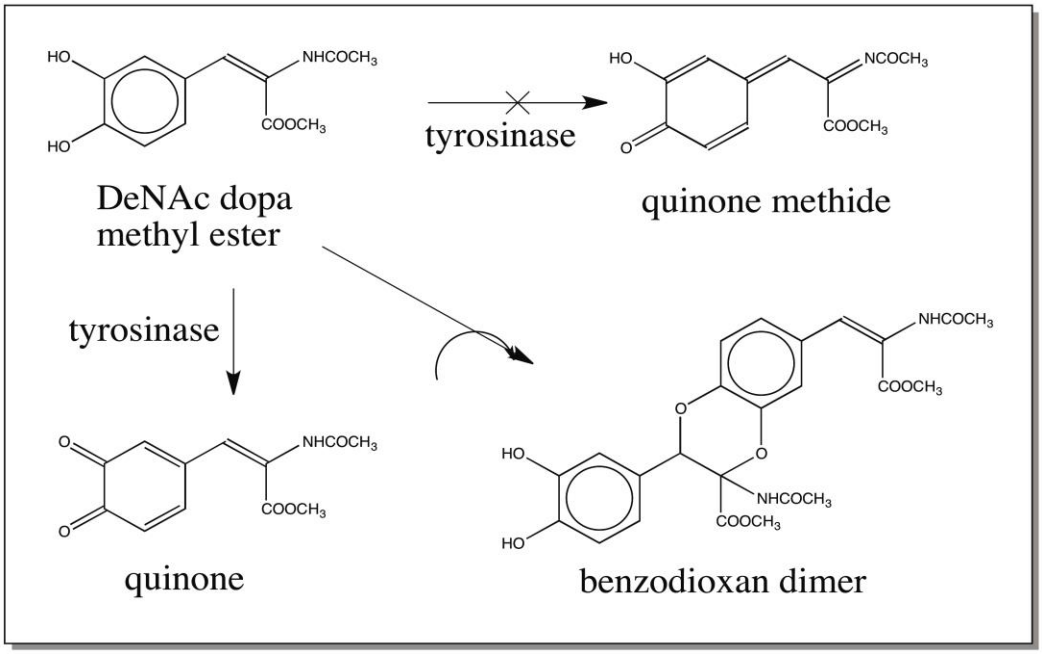

Figure 6.8: The proposed mechanism for the oxidative fate of DeNAcDopa methyl ester.

6.6 Conclusion

Tyrosinase catalyzed oxidation of tyrosine residues in various proteins has been known to produce dopyl peptides. However, what happens to the dopyl proteins has remained a mystery for a long time. Earlier studies from our lab indicated its possible oxidation transforms to dehydrodopyl peptides (Sugumaran and Ricketts, 1995). But the further fate of dehydrodopyl peptides has never been reported until now. My current studies are aimed to fill this void in dopyl protein chemistry and shed light on possible route for its further transformation. Oxidation of the model peptidyl dopa, DeNAcDopa methyl ester by tyrosinase generated its corresponding quinone as a transient product, which seemed to undergo a Diels-Alder type addition with the parent catechol, producing the benzodioxan adducts. This is quite contrary to the oxidation of dehydro NADA which has been shown to produce QMIA.

Although dehydro NADA and DeNAcDopa methyl ester differ simply by the presence of a single carboxy ester group, the oxidative transformation seems to be quite different. In the case of dehydro NADA, we could not observe the corresponding quinone at all during both enzymatic and nonenzymatic oxidation under physiological pH values. We witnessed the production of only quinone methide imine amide derivative as the primary two–electron oxidation product (Sugumaran et al., 1992). In the case of DeNAcDopa methyl ester, the reverse seems to be true, namely quinone is observed as the transient intermediate and not the quinone methide imine amide. Quinone thus formed seems to undergo a novel Diels Alder addition generating dimers. A similar

reaction with peptidyl dehydrodopa as shown in Figure 6.9 could lead to dimer production that will partly account for gluing reactions witnessed with peptidyl dopa derivatives.

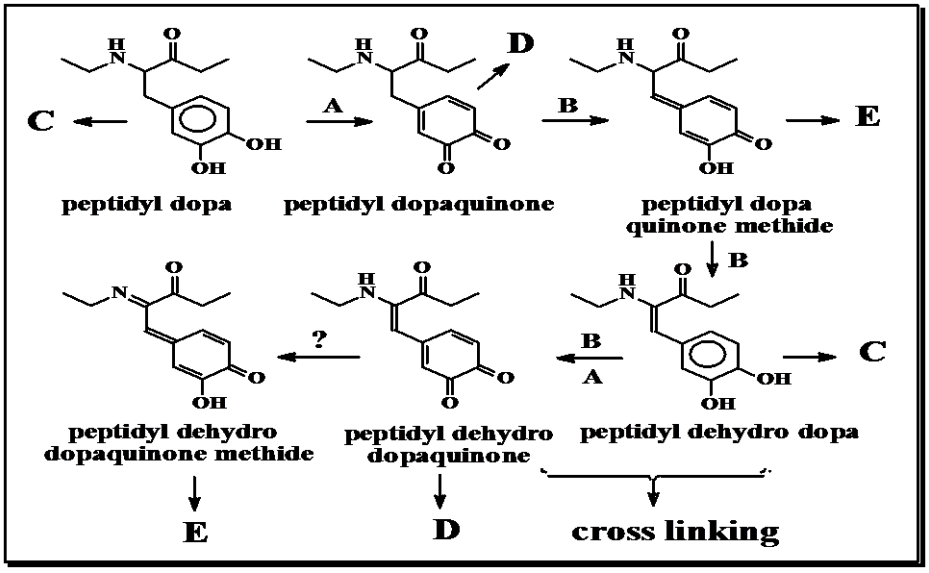

Figure 6.9: The proposed mechanism for the oxidative fate of dopa containing peptides. N-acyldopamines are oxidized by phenoloxidases (A) to their corresponding quinones that can participate in quinone tanning reactions. Quinone isomerase (B) converts the quinones to quinone methides and provides them for quinone methide tanning (type D and E) reaction. Quinone methides are also isomerized to 1, 2-dehydro-N-acyldopamines by quinone methide isomerase type reaction (C). Oxidation of the dehydro compounds yields the quinone methide imine amides and dehydro dopyl quinones that can react with their side chain forming adducts and cross links (E and D reaction).

CHAPTER 7

REACTIVITY OF 1,2-DEHYDRO-N-ACETYLDOPAMINE WITH N-ACETYLCYSTEINE

7.1 Chapter summary

1, 2-dehydro N-acetyldopamine (dehydro NADA) is an important major cuticular sclerotizing precursor for a vast majority of insect cuticle. It readily undergoes oxidative dimerization to form benzodioxan type dimers. Based on this reaction and other considerations, the side chain of dehydro NADA has been invoked in crosslinking and covalent binding to amino acid side chains of structural proteins and to the sugar residues of chitin fibers. This process has been named as α,β-sclerotization. However direct evidence for the presence of side chain adducts of dehydro NADA with proteins/chitin is still missing. Model sclerotization studies with dehydro NADA and N-acetylcysteine (NAcCys) was conducted to shed light on the formation of side chain adducts of dehydro NADA. NAcCys is specifically chosen to represent the reactions of protein bound cysteine residue with dehydro NADA. Ultraviolet and visible spectral studies of reaction mixtures containing dehydro NADA and NAcCys in different molar ratios indicated the production of side chain and ring adducts of NAcCys to dehydro NADA. Liquid chromatography and mass spectral studies supported this contention and confirmed the

production of several different products. Mass spectral analysis of these products do support the potentials of dehydro NADA to form side chain adducts that can lead to colorless, but sclerotized cuticle consistent with the predictions of α,β-sclerotization process.

7.2 Introduction

Sclerotization of cuticle, a process essential for the successful survival of most insects, is achieved by covalent crosslinking of catecholamine derivatives such as N-acetyldopamine (NADA) and N-β-alanyldopamine (NBAD) with structural proteins and chitin polymer (Andersen, 2010; Hopkins et al., 1982; Hopkins and Kramer 1992; Kerwin et al., 1999; Karlson and Sekaris, 1962, Sugumaran, 1998, 2010). As early as 1980, Andersen's group (Andersen and Roepstrorff, 1981, 1982; Andersen et al., 1980) isolated and characterized 1, 2-dehydro-N-acetyldopamine (dehydro NADA) and its dimeric products from the sclerotized cuticle of locusts. They proposed that the quinone of dehydro NADA is somehow involved in the adduct formation reaction with cuticular proteins and chitin resulting in the formation of colorless cuticle (Andersen, 1989; Andersen and Roepstroff, 1982). Our group, however advocated an alternate reactive species for the production of colorless cuticle (Sugumaran 1987; Sugumaran 1988, Sugumaran et al., 1989). We identified quinone methides as new reactive intermediates of sclerotization and argued that quinone methides are the causative agents of colorless cuticle (Saul and Sugumaran; 1988; 1989a, b, c; 1990; Sugumaran, 1987; 1988). Furthermore, we indicated that dehydro NADA could arise from NADA quinone methide

by a simple isomerization reaction (Sugumaran, 1987; 1988). Work conducted in our laboratory lead to the finding that 1, 2-dehydro-N-acyldopamines are biosynthesized from N-acyldopamines (NADA and NBAD) by the combined action of three enzymes namely, phenoloxidase (both *o*-diphenoloxidase and laccase), quinone isomerase and quinone methide isomerase (Saul and Sugumaran, 1988; 1989a, b, c; 1990; Ricketts and Sugumaran, 1994). Discovery of quinone isomerase and quinone methide isomerase interlinked enzymatically produced quinone methides with dehydro N-acyldopamines (Saul and Sugumaran, 1989 b, c; Sugumaran 1998; Ricketts and Sugumaran, 1994). This provided evidence to concretely establish that upon *o*-diphenoloxidase action, dehydro NADA generates a reactive quinone methide imine amide (QMIA) which is capable of reacting with nucleophiles forming side chain adducts (Sugumaran, 2000; Sugumaran et al., 1987; 1988; 1990; 1992; Abebe et al., 2010). The normally expected dehydro NADA quinone was not produced at physiological conditions. Under acidic conditions however, the production of dehydro NADA quinone could be witnessed; but as soon as the pH is raised to physiological level, rapid isomerization of dehydro NADA quinone occurred resulting in the production of more stable QMIA (Sugumaran, 2000). Even though QMIA is comparatively more stable than its quinone isomer, it is extremely reactive due to the presence of both quinone methide nucleus (that will exhibit rapid Michael-1,6-addition reaction) and a modified Schiff's base (which will also form an adduct with nucleophiles). As a result, QMIA rapidly reacts even with the phenolic groups of dehydro

NADA forming benzodioxan type adducts (Figure 1.8). Andersen and Roepstroff (1981) also isolated a number of mixed dimers of dehydro NADA from insect cuticle confirming the generality of this reaction. It has been demonstrated that even simple 1, 2-dihydroxybenzene can add on to QMIA forming benzodioxan adducts (Sugumaran et al., 1987; 1988; 1990, 1992). Since dimer formation is due to the covalent addition of two phenolic groups of the parent catechol to the QMIA nucleus, it is reasonable to expect that *in vivo* also QMIA can react with cuticular nucleophiles producing adducts and crosslinks (Figure 1.8). Additional support for this proposal comes from the trapping experiments performed with dehydro NADA and different quinoniod traps (Sugumaran et al., 1990). Ultraviolet spectral studies indicated that both simple catechol and *o*-amino phenol were able to form adducts on the side chain carbon atoms of dehydro NADA, under oxidative conditions. Moreover, enzymatically oxidized dehydro NADA readily incorporated into the cuticle and formed colorless cuticle with intact *o*-diphenolic group attached to them (Sugumaran et al., 1988). However, the exact nature of linkage of dehydro NADA to the cuticle remains to be established by structural analysis of adducts. In order to characterize dehydro NADA - side chain addition products and to lend support for the key role played by QMIA in crosslinking process, we conducted model sclerotization studies with dehydro NADA and different nucleophiles representing protein side chains. In this chapter, I outline the reactions of one simple model compound, NAcCys with oxidized dehydro NADA and confirms the production of side chain adducts of dehydro NADA with thiol nucleophiles.

7.3 Materials and methods

Mushroom tyrosinase, sodium periodate, sodium borate, NAcCys, acetic anhydride and general laboratory chemicals were obtained from Sigma Chemical Co., St. Louis. MO. All other chemicals were acquired from Fisher Scientific Co and/or VWR Scientific Co, NJ. HPLC grade solvents and ammonium formate and ammonium acetate were purchased from Acros, Morris Plains, NJ. HPLC grade water was purified using a Milli-Q A-10 water purification system from Millipore, Milford, MA. Dehydro NADA was synthesized as outlined in an earlier publication (Dali and Sugumaran, 1988).

Adduct formation between dehydro NADA and NAcCys was examined using a reaction mixture containing 0.1 mM of dehydro NADA, varying amounts of NAcCys and 10 µg tyrosinase in 50 mM of sodium phosphate buffer, pH 6.0. The reaction was incubated at room temperature and its progress was monitored using UV-Vis spectrophotometric studies. The reaction conditions for individual experiments are described under the legends to the figures. The reactions were conducted in 1 ml spectrophotometric cuvettes (10 mm path length). For non-enzymatic oxidation, the reactions were conducted in specified alkaline pH values without the use of enzyme.

RP-HPLC analysis of dhydro NADA reaction mixture: A reaction mixture containing 1 mM dehydro NADA, different amounts of NAcCys and 10 µg mushroom tyrosinase in 50 mM sodium phosphate, pH 6.0 was incubated at room temperature. An aliquot of the

reaction mixture (5 µl) was subjected to RP-HPLC analysis on an Agilent 1100 HPLC series (Agilent Technologies, Santa Clara, CA) fitted with a diode array detector and reversed phase C_{18} cartridge (5 µm, 4.6 x 150 mm) using isocratic elution with 50 mM acetic acid containing 0.2 mM sodium octyl sulfonate in 20 % methanol at a flow rate of 0.6 ml/min.

Liquid Chromatography –Mass spectrometry (LC-MS): A reaction mixture containing 100 µmole dehydro NADA, 10 µg mushroom tyrosinase and 100 µmole or 1 mM of NAcCys was incubated at room temperature. After each time interval 50 µl aliquot was withdrawn and the reaction was arrested by adding 3 volumes of 90% methanol containing 2% acetic acid. The entire content was subjected to LC-MS analysis.

RP-HPLC conditions for LC-MS: A low-flow rate Shimadzu (Kyoto, Japan) HPLC system fitted with a 10 cm x 1 mm ID, 3 µM particle size, C_{18} Betabasic column from Thermo Electron Corporation (Sunnyvale, CA) was used to separate products. The HPLC was operated at a flow rate of 35 µL/min using a linear gradient of 0 – 50% B in 40 min consisting of the mobile phase A = 10 mM formic acid in water and B = 10 mM formic acid in methanol.

Mass spectral analysis: A Thermo Finnigan LCQ Advantage ion trap mass spectrometer (Sunnyvale, CA) was used to detect and characterize the products. The operating conditions of the ion trap mass spectrometer are: Capillary temperature 280˚C; Spray voltage 4.00 kV; and sheath gas 30 cm^3/min. Collision induced decomposition (CID)

was performed at a relative collision energy of 28, an isolation mass window of 2.5 amu, and a default activation Q and activation time of 0.025 and 30 msec respectively.

7.4 Results

Oxidation of dehydro NADA alone by phenoloxidases produces dimeric materials that exhibit the same ultraviolet spectral pattern but reduced intensity (Abebe et al., 2010). Therefore, ultraviolet spectral analysis of such a reaction will exhibit spectral changes that simply get reduced in intensity over time to about half the original value. Contrary to this expectation, ultraviolet spectral changes accompanying the oxidation of dehydro NADA / NAcCys reaction mixture (mole ratio 1:10) exhibited a pattern that is consistent with the addition of the sulfur nucleophile to the aromatic ring as evidenced by the appearance of a new absorbance peak at about 250 nm (Figure 7.1). The reactions of NAcCys with *o*-benzoquinone, 4-methyl quinone and N-acetyldopamine quinone rapidly produce 3-S-(N-acetyl)-cysteinyl catechol , 5-S-(N-acetyl)-cysteinyl- 3,4-dihydroxy toluene and 5-S-(N-acetyl)-cysteinyl-N-acetyldopamine, respectively, as additional products (Sugumaran et al., 1989). All these compounds show absorbance maxima at 250 nm (due to the sulfur addition to the catecholic ring), in addition to the normal 280 nm aromatic absorption. Therefore, the 250 nm absorbing species produced during the reaction of dehydro NADA with NAcCys should also be a similar ring adduct. Thus the 250 nm absorbing compound witnessed in Figure 7.1 was tentatively identified as the quinone adduct of dehydro NADA to NAcCys.

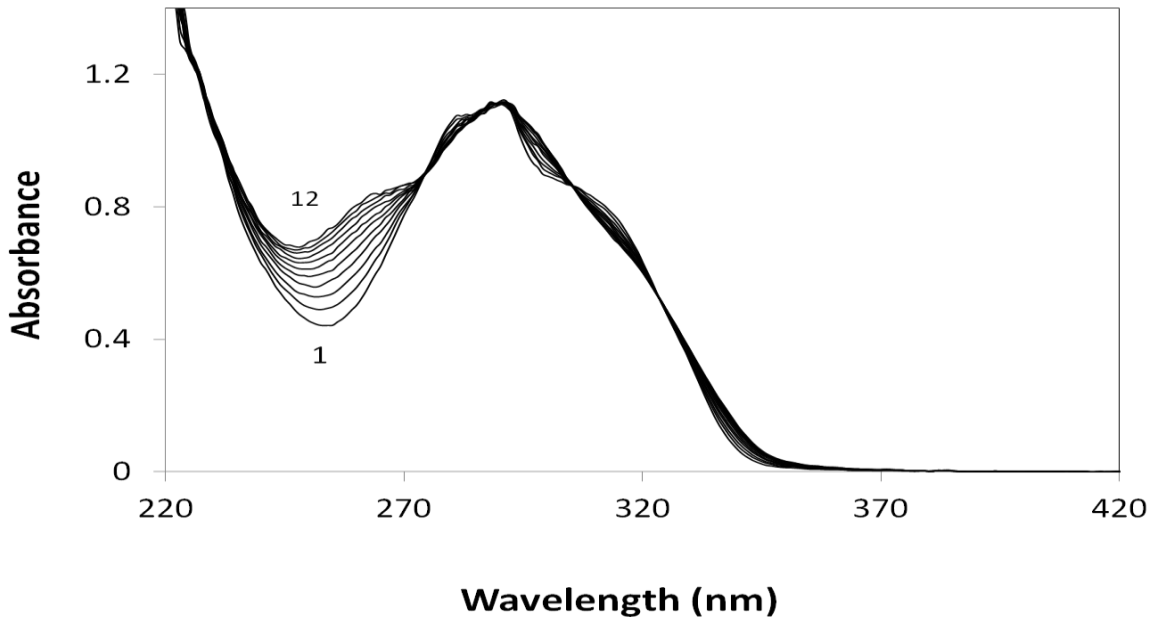

Fig 7.1: Ultraviolet spectral changes associated with the oxidation dehydro NADA in presence of NAcCys at 1:10 mole ratio. A reaction mixture (1 ml) containing 0.1 mM dehydro NADA, and 1.0 mM NAcCys and 10 µg mushroom tyrosinase in 50 mM sodium phosphate buffer, pH 6.0 was incubated at room temperature and the spectral changes accompanying the enzymatic oxidation was monitored at 60 sec intervals (scan 1: zero time and scan 12: 11 min). Note a steady production of 250 nm absorbing peak due to the ring adduct of NAcCys with dehydro NADA.

The base peak chromatogram depicted in Figure 7.2 shows the products of tyrosinase-catalyzed oxidation of dehydro NADA in the presence of NAcCys at a mole ratio of 1:10. The reaction was incubated for 45 min at room temperature and analyzed by

RP-HPLC/ ESI/MS-MS. The mass spectrum associated with the peak at 13.4 min shows a parent ion at m/z 355, which represents the addition of one NAcCys to the monomer of dehydro NADA. The CID mass spectrum of the 355 ion (Figure 7.3) shows a dominant product ion at m/z 313 ion due to loss of C_2H_2O from the $NHCOCH_3$ moiety and the minor peak at 250 due to the loss of the $NHCOCH_3$. Other major product ions include m/z 337 (loss of 18), m/z 277 (loss of 78), m/z and m/z 208 (loss of 147). The absence of a product ion at m/z 226, $[M-126]^+$ suggests that no significant addition to the side chain has occurred under these conditions.

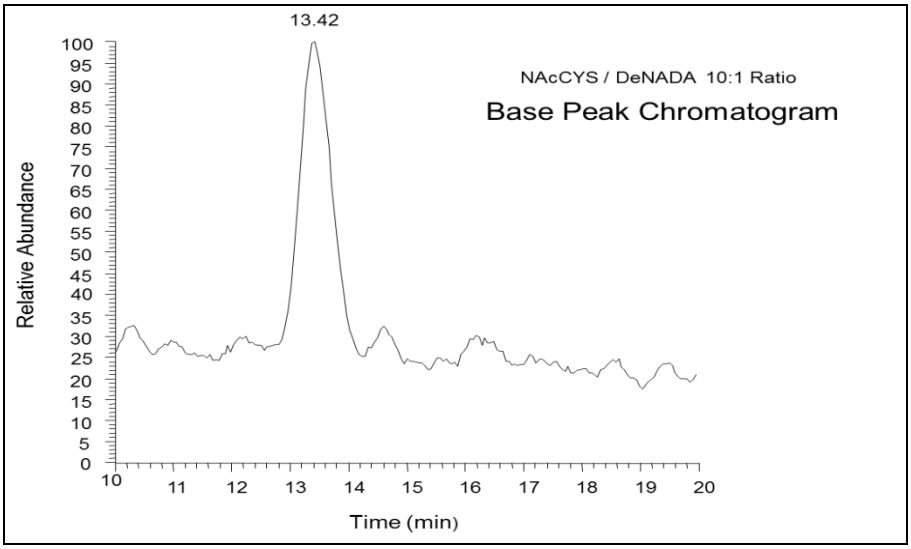

Figure 7.2: The base peak chromatogram from the RP-HPLC/ESI/MS-MS analysis of tyrosinase catalyzed oxidation of dehydro NADA in the presence of NAcCys at a 1:10 mole ratio. The marked retention time indicates the location of the product.

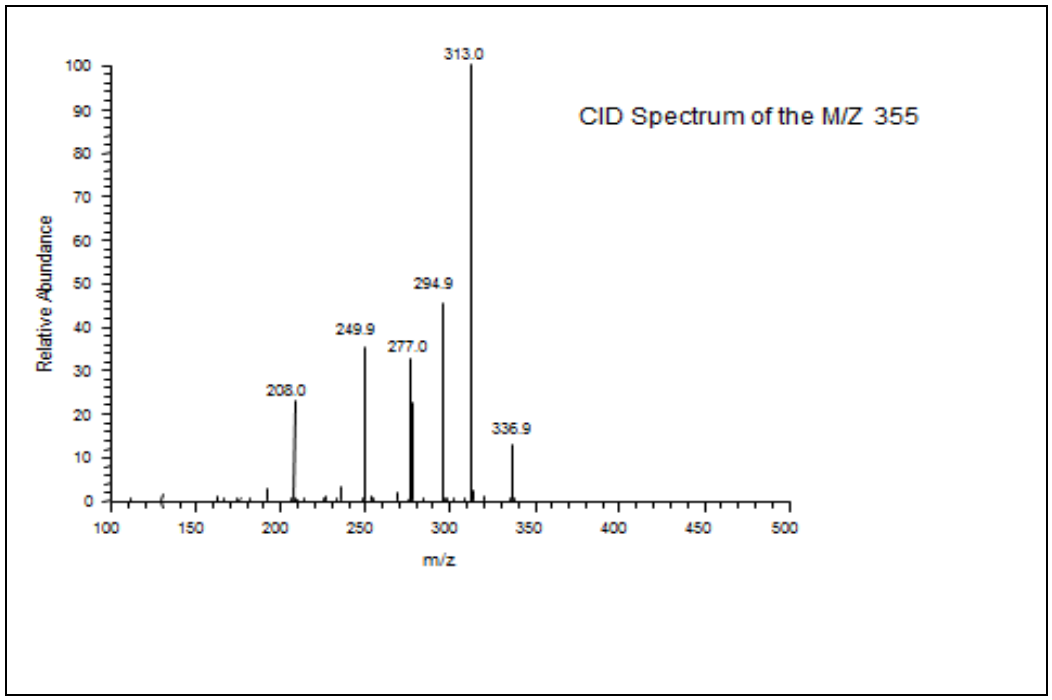

Figure 7.3: The CID mass spectrum of the product eluting at 13.4 min (see Figure 7.2 for details).

However, when the reaction stoichiometry was altered to 1: 1 level, an entirely different UV spectral pattern accompanied the oxidation of dehydro NADA and NAcCys mixture was obtained. Figure 7.4 shows the UV spectral changes associated with the oxidation of dehydro NADA in presence of equimolar amount of NAcCys. Initially there does appear a peak at 250 nm begins to develop but as the reaction progress the absorbance across the range of wavelengths 230-350 nm decrease steadily. This observation was puzzling at first and hence additional experiments were carried out with RP-HPLC coupled with a diode array spectrophotometer.

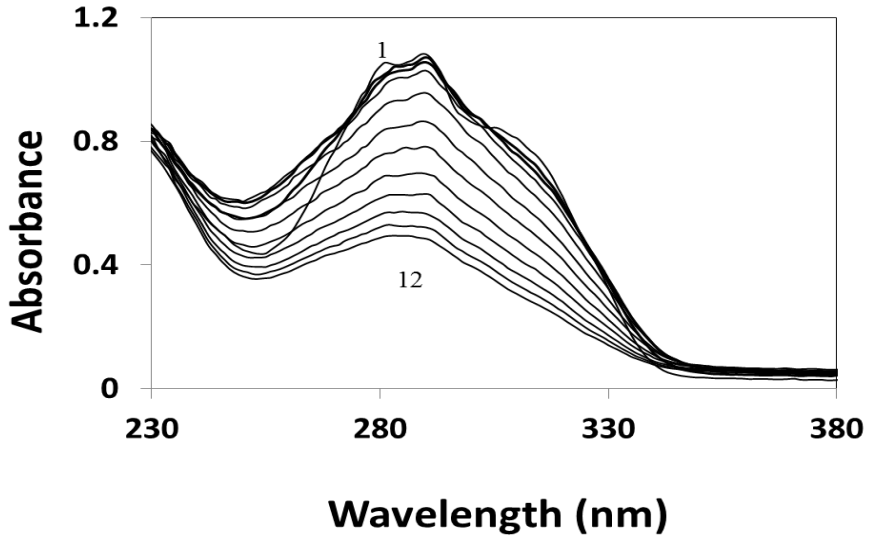

Figure 7.4: Ultraviolet spectral changes associated with the oxidation dehydro NADA in presence of NAcCys at 1:1 mole ratio. A reaction mixture (1 ml) containing 0.1 mM dehydro NADA, and 0.1 mM NAcCys and 10 µg mushroom tyrosinase in 50 mM sodium phosphate buffer, pH 6.0 was incubated at room temperature and the spectral changes accompanying the enzymatic oxidation were monitored at 60 sec intervals (scan 1: 0 time; scan 12: 11 min). Note absence of a 250 nm absorbing peak due to the ring adduct of NAcCys with dehydro NADA.

RP-HPLC analysis of a reaction mixture containing 1:1 mole ratio of dehydro NADA – NAcCys indicated the formation of three peaks eluting at 5.9 min, 6.7 min and 11.3 min (Figure 7.5). The ultraviolet absorbance spectra of these three peaks are shown in Figure 7.6. The ultraviolet absorbance spectrum of peaks marked B and C (eluting at

6.7 min and 11.3 min respectively) possessed absorbance maximum at both 250 nm and 280 nm consistent with the production of ring adduct of NAcCys. The product peak A eluting at 5.9 min on the other hand, exhibited only 280 nm absorbance suggesting that it might be a compound formed from the addition of NAcCys to the side chain of dehydro NADA.

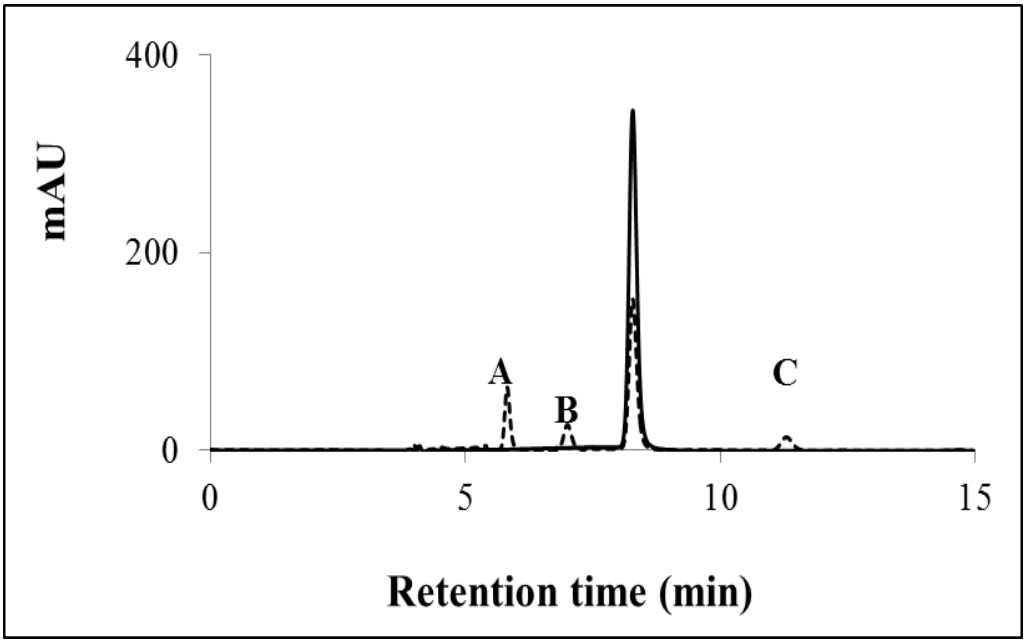

Figure 7.5: RP-HPLC analysis of dehydro NADA - NAcCys (1:1) reaction mixture. A reaction mixture (1 ml) containing 0.1 mM of dehydro NADA, 0.1 mM of NAcCys and 10 µg mushroom tyrosinase in 50 mM sodium phosphate, pH 6.0 was incubated at room temperature. An aliquot of the reaction mixture (5 µl) was subjected to HPLC analysis as outlined in materials and methods. The solid line represents the 0 min (control) reaction; the broken line represents the 45 min reaction. The peaks marked A, B and C represent products eluting at 5.9 min, 6.7 min and 11.3 min respectively.

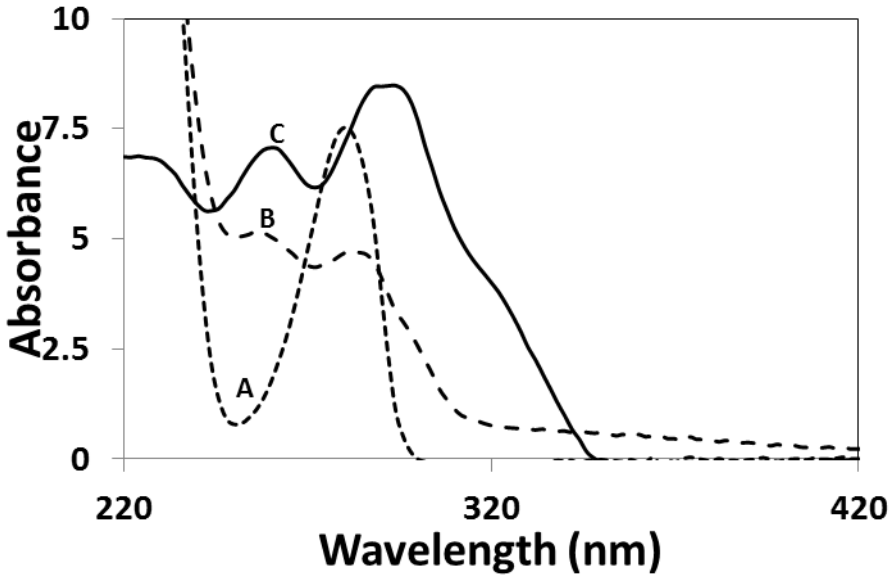

Figure 7.6: Ultraviolet absorbance spectrum of the three products isolated from dehydro NADA –NAcCys (1:1) reaction. A - UV spectrum of product eluting at 5.9 min (Figure 7.5), B s UV spectrum of product eluting at 6.7 min (Figure 7.5) and C - UV spectrum of product eluting at 11.3 min (Figure 7.5).

In an effort to gather more conclusive evidence, RP-HPLC analysis coupled with electrospray ionization tandem mass spectrometry (ESI/MS-MS) was conducted on the reaction mixture containing equimolar amounts of dehydro NADA and NAcCys (1:1) in the presence of tyrosinase. Figure 7.7 shows the base peak chromatogram of products formed. The average mass spectra associated with the initial three peaks between 20.4 and 22.4 min give a parent ion at m/z 546 (Figure 7.8 top), which corresponds to a set of

protonated dehydro NADA dimeric compounds with one NAcCys attached. As seen from Figure 7.7 the mono adduct is not the dominant product. The mass spectra associated with the next set of peaks at about 24.7 and 27.6 min give a parent ion at m/z 707 (Figure 7.8 middle) which corresponds to a set of protonated dimeric products with two NAcCys attached. The last peak intensly observed at 29.4 min (Figure 7.8 bottom) gives a parent ion at m/z 868 which corresponds to three NAcCys addition to one dehydro NADA dimer.

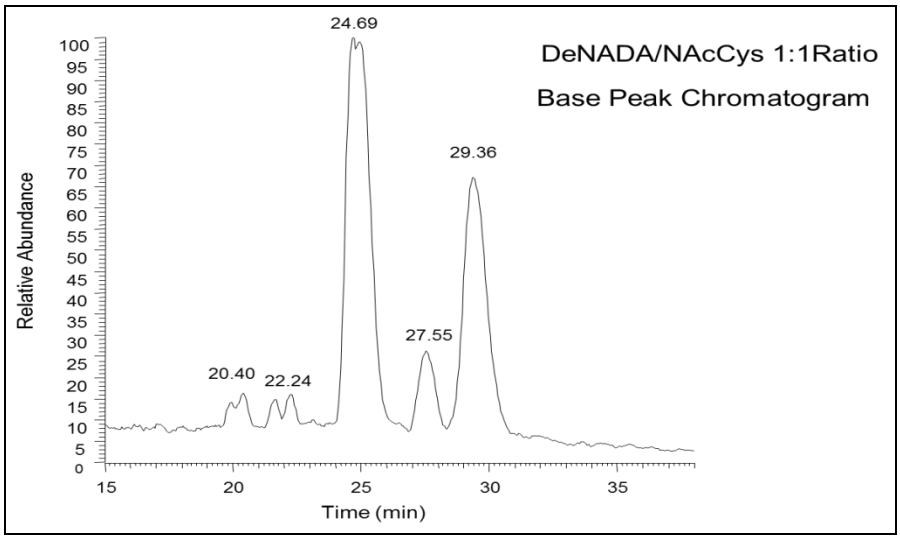

Figure 7.7: The Base Peak Chromatogram of the RP-HPLC/ESI/MS-MS analysis of Dehydro NADA and NAcCys 1:1 ratio. The mass spectra associated with the initial peaks 20.4 and 22.24 min are due to one NAcCys addition to dehydro NADA dimer. The mass spectra associated with the next sets of peaks at 24.69 min and 27.55 min are due to two NAcCys addition to dehydro NADA dimer. The mass spectra associated with 29.51 min is due to three NAcCys addition to the dehydro NADA dimer.

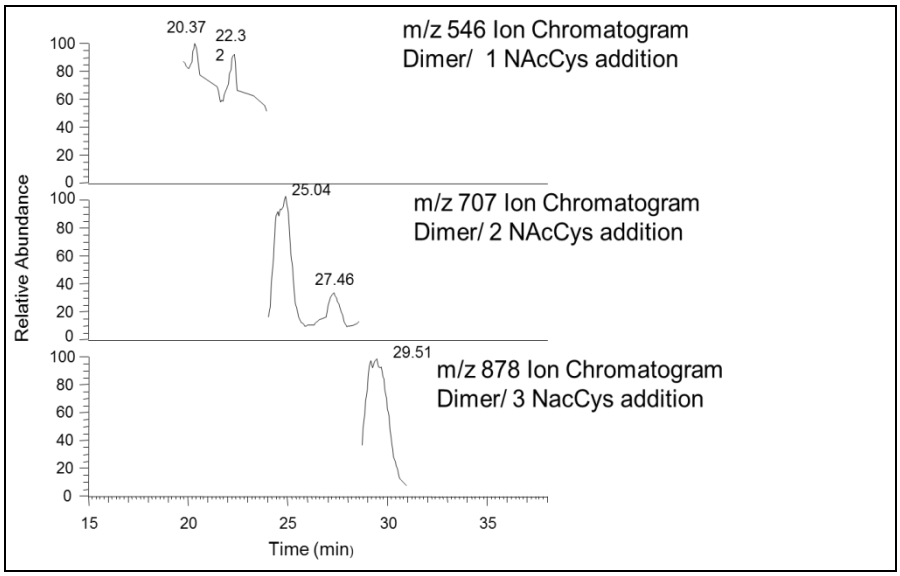

Fig 7.8: The ion chromatogram of the products produced during the reaction of dehydro NADA with NAcCys (1:1 mole ratio).

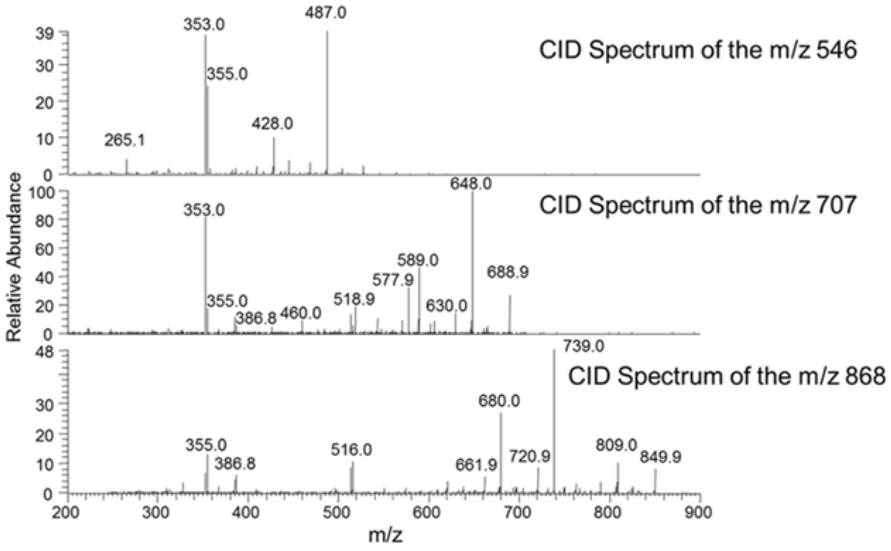

Fig 7.9: The CID mass spectrum of the products produced during the reaction of dehydro NADA with NAcCys (1:1 mole ratio).

Collision induced decomposition (CID) spectra were obtained for each of the three parent ions to shed some light on the structural features and to distinguish between side chain addition and ring addition on the basis of product ion formation. The top panel of Figure 7.9 shows the average CID mass spectrum of the m/z 546 parent ion, which again corresponds to the protonated dehydro NADA dimeric species with one NAcCys attached. It shows a dominant product ion at m/z 353, corresponding to the loss of the monomeric moiety (193, protonated QMIA ion), which is a logical decomposition product of the protonated dimer. The product ions at m/z 487 and 428 correspond to the loss of one and two $NHCOCH_3$ groups, respectively. The middle panel of Figure 7.9 shows the average CID spectrum of the m/z 707 parent ion, which corresponds to the proton-bound dimer of dehydro-NADA with two NAcCys attached. The CID spectra of the m/z 707 parent ion shows dominant product ions at m/z 648, corresponding to the loss of the monomeric moiety with an attached NAcCys adduct. There is a product ion of moderate intensity at m/z 578 $[M-129]^+$ that corresponds to the loss of NAcCys.

The bottom panel of Figure 7.9 shows average CID spectrum of the m/z 868 parent ion which corresponds to the proton-bound dimer of dehydro NADA with three NAcCys attached. The base peak is the m/z 739, which is [M-129] +, corresponding to the loss of NAcCys moiety from cleavage at the S ($-C_5H_7O_3N$). This provides very strong supporting evidence that one of the three NAcCys is adding to the side chain of dehydro NADA, as opposed to the ring. The m/z 355 ion correspond to the loss of the monomer moiety with an attached NAcCys adduct and m/z 516 ion corresponds to the loss of

monomer moiety with two attached NAcCys adduct. Other major product ions include m/z 850 (loss of 18), m/z 809 (loss of 59), m/z 680 (loss of 178), m/z 651 (loss of 210) and m/z 386 (loss of 482).

Careful inspection of the bottom two product ions in the CID spectra illustrated in Figure 7.9 shows certain similarities. These are a) the common loss of 129, b) the products ion at 353/355 and c) the mass difference between each molecular ion is 161. These similarities are consistent with the presence of both side chain and ring addition. Figure 7.10 shows the average CID spectrum of the m/z 707 product obtained for the minor isomeric species eluting between the two more abundant peaks in the chromatogram (26.0 to 27.0 min- top panel, Figure 7.10). The [M-129] + product ion is the base peak in this spectrum, where as it is only a minor peak in the CID spectra of the more abundant species eluting at 24.8 and 27.6 min. These results suggest that although the ring adduct appears to form more readily, the side chain adduct also occurs to a certain extent.

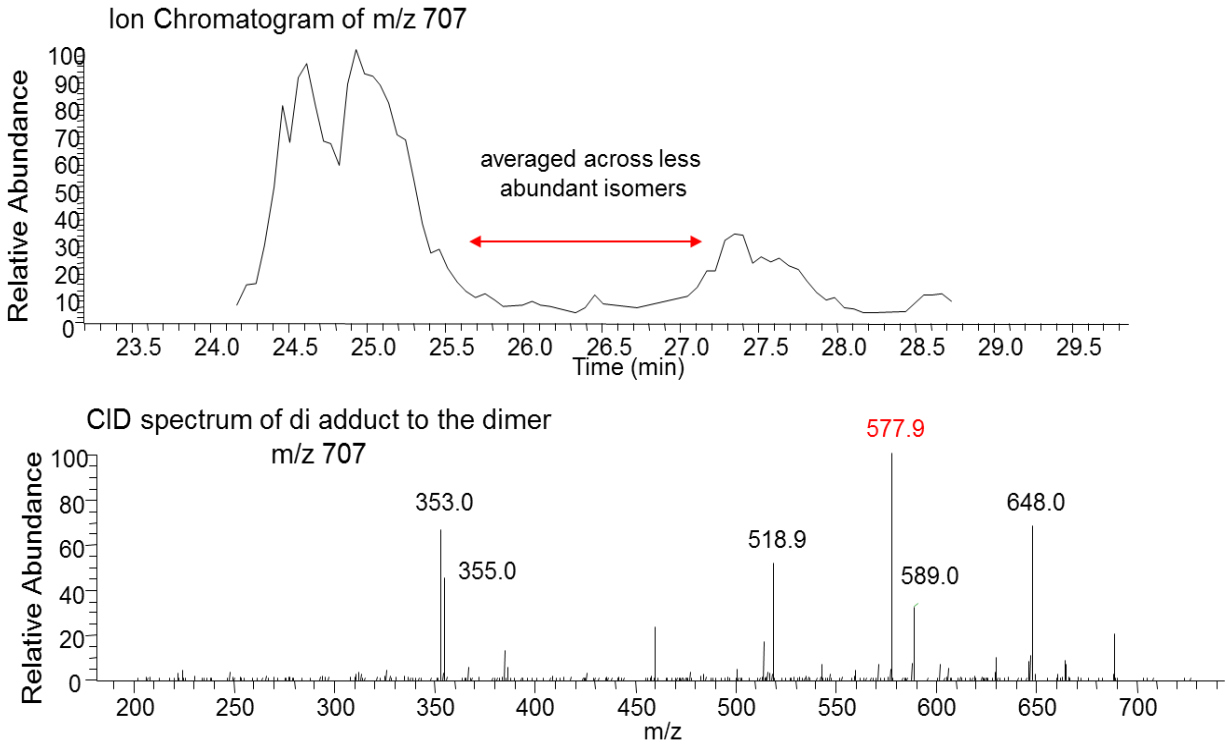

Figure 7.10: The average CID mass spectrum (bottom panel) of the m/z 707 product ion obtained from the isomeric species eluting between 25 min and 27 min (top panel).

Since dehydro NADA is also well known for its instability and sensitivity to oxidation even under mild alkaline conditions (Sugumaran et al., 1988), nonenzymatic oxidation of dehydro NADA in the presence of NAcCys was examined. The base peak chromatogram depicted in Figure 7.11 shows the products of the nonenzymatic oxidation of dehydro NADA in the presence of a 1:10 mole excess NAcCys after a long-term incubation as analyzed by RP-HPLC/ESI/MS-MS. The mass spectrum associated with the less abundant peak at 18.2 min shows a parent ion at m/z 377, which represents

products formed from the mono addition of NAcCys to the monomer of dehydro NADA. The m/z 377 peak is its sodiated parent. The peak at 18. 9 min shows a parent ion at m/z 538, which represents products formed from the addition of two NAcCys to the monomeric dehydro NADA.

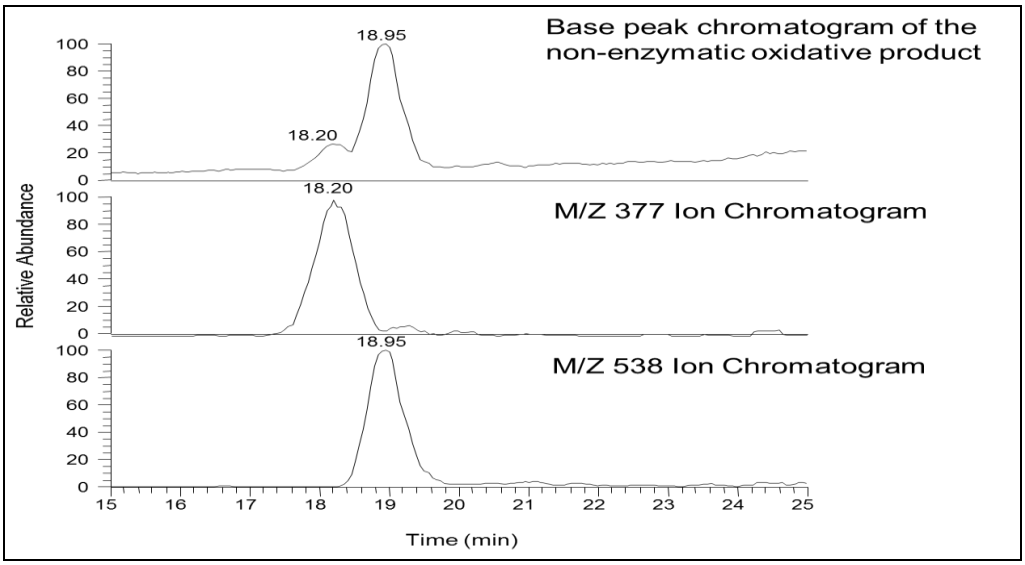

Figure 7.11: The base peak and ion chromatogram from the RP-HPLC/ESI/MS-MS analysis of dehydro NADA and NAcCys nonenzymatic reaction mixture. The marked retention times indicate the location of the products.

The CID spectrum of the m/z 377 ion shown in the top panel of Figure 7.12 contains a dominant peak at m/z 246, which may correspond to the dissociation of the S-C bond on the NAcCys moiety (loss of 131). The minor peak 317.7 corresponds to the loss of

$NHCOCH_3$. The major product ions include m/z 151.8 (loss of 225), m/z 289 (loss of 88), m/z 335 (loss of 42), m/z 359 (loss of 18) and m/z 386 (loss of 482). The CID spectrum of the m/z 538 ion is shown in the bottom panel of Figure 7.12. It contains a dominant peak at m/z 409 [M-129] +, which as described above, likely corresponds to the dissociation of the S-C bond on the NAcCys moiety. Other major product ions include m/z 478 (loss of 78), m/z 496 (loss of 43) and m/z 280 (loss of 258). This CID spectrum seems to suggest that side chain addition to the monomeric dehydro NADA species is occurring under non enzymatic oxidative conditions.

The products of the non-enzymatic oxidation of dehydro NADA in the presence of NAcCys at 1:1 mole ratio after long term incubation were investigated under the same condition as described above. The results were very similar to the results published earlier on the enzymatic oxidation of dehydro NADA (Abebe et al., 2010). Dimeric and trimeric species of dehydro NADA were evident in the chromatogram but there was no evidence of any NAcCys addition to either the dehydro NADA monomeric or polymeric species.

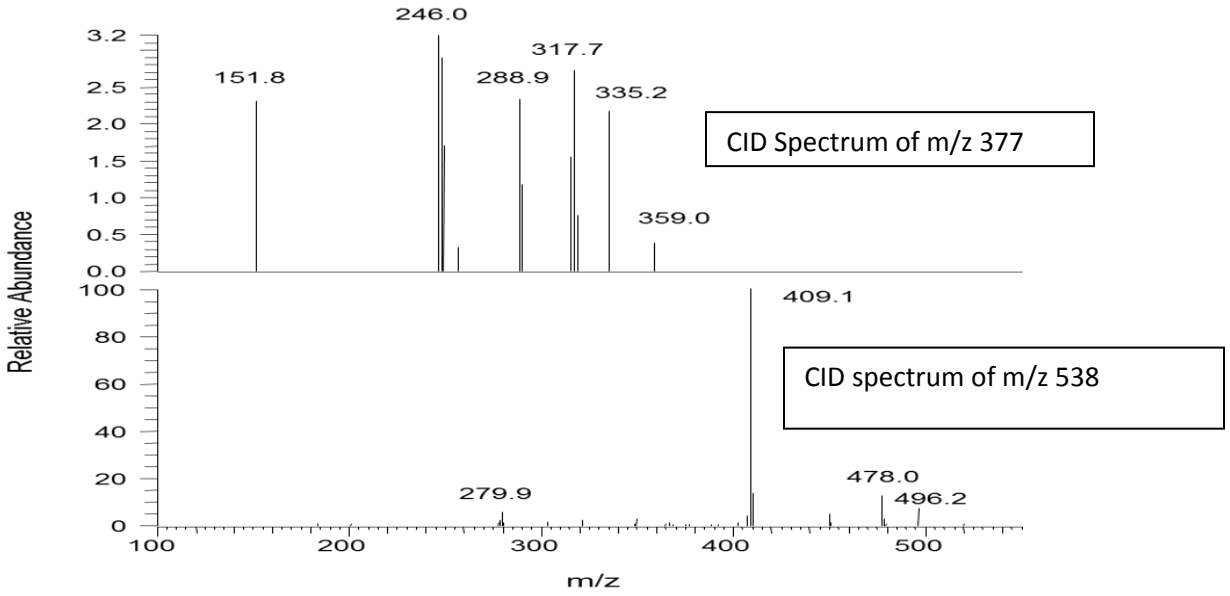

Figure 7.12: The CID mass spectrum of the products produced during the nonenzymatic reaction of dehydro NADA with NAcCys at alkaline pH.

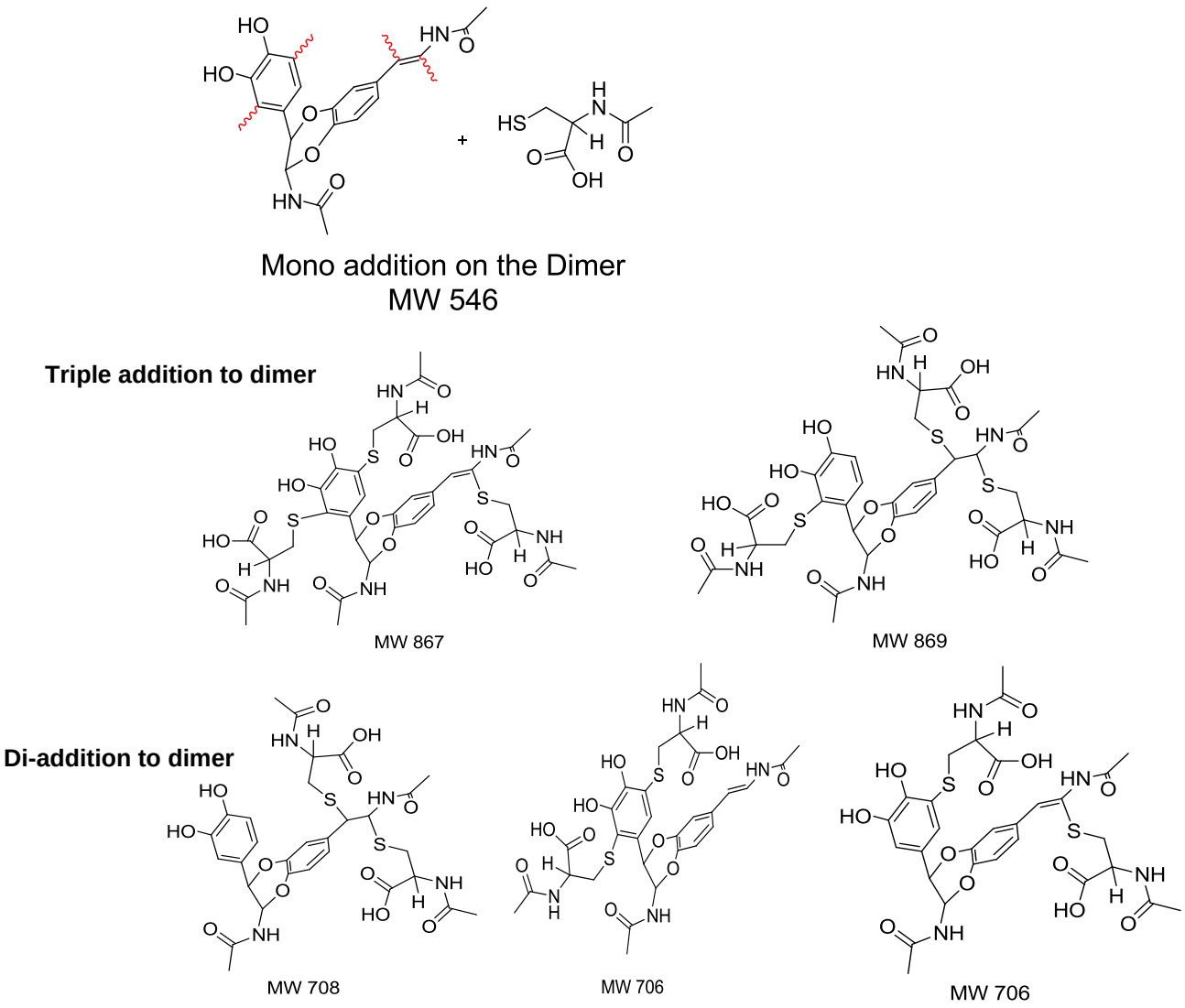

Figure 7.13: Structures of possible products of dehydro NADA: NAcCys (1:1 mole ratio) reaction.

7.5 Discussion

The results presented in this study can be summarized as follows. Under 1:10 stoichiometric conditions, tyrosinase catalyzed oxidation of dehydro NADA/NAcCys mixture, produces a ring adduct of NAcCys to dehydro NADA as the major product (marked ring adduct in Figures 7.14 and 7.15). This result is consistent with the preliminary studies reported earlier from our laboratory on the addition of NAcCys to dehydro NADA (Sugumaran et al., 1990). It is not clear why thiol is adding to the ring in preference to the side chain, while the phenolic OH group readily adds on to the side chain under the same conditions. Also at present the exact ring carbon atom to which the NAcCys is attached cannot be specified. The abnormal addition of thiol to the quinonoid nucleus is not surprising, as previous studies have shown that thiols addition to quinones do not follow typical nucleophilic Michael -1,4-addition. In relation to eumelanin production in animals, the reaction of cysteine with a number of catecholic compounds has been investigated by a number of workers. For instance, Ito and Prota (1977) witnessed that the reaction of cysteine with dopa under oxidative conditions generated 5-cysteinyldopa and 3-cysteinyldopa. This was contrary to the normal expectation of a nucleophilic addition to a quinone, which in general leads to the production of Michael-1,4-adducts as opposed to 1,3- or 1,5-adducts. Perhaps thiols interact with the quinonoid nucleus much differently than typical nucleophiles. The thiol addition also shows another difference. An external nucleophilic addition to quinone is naturally expected to be slower than any possible internal Michael-1, 4-addition reaction. Thus for example, the

internal reactivity of a suitably positioned amino group in dopaquinone is expected to be far greater than any external nucleophilic addition. On the other hand, cysteine addition to dopaquinone occurs in preference to the internal reactivity of dopaquinone (Ito and Prota, 1977). Thus sulfur addition to quinones seems to be operating by a different mechanism than the conventional Michael -1, 4-addition reaction. Although cysteinyl radical addition has been suggested as alternate reactive species associated with such reactions, the exact mechanism by which sulfur nucleophiles exhibit fast as well as abnormal reactivity still remains to be elucidated (Sugumaran 1998; 2010). Finally, at the pH values employed in enzymatic oxidation, the QMIA is the predominant species compared to dehydro NADA quinone (Sugumaran 2000). Yet, cysteine seems to trap the quinone far more efficiently than the QMIA thus accounting for the predominant quinone adduct.

At 1:1 stoichiometric conditions, tyrosinase catalyzed oxidation of dehydro NADA/NAcCys generated a number of products, all belong to the dehydro NADA dimer family. The monomeric thiol adduct observed under 1:10 stoichiometry could not be seen at all under 1:1 stoichiometric conditions. Nor one could see any unsubstituted dimer of dehydro NADA. Of the three products characterized by the mass spectrometry, the one with m/z 546, corresponds to the ring adduct of NAcCys to dehydro NADA dimer. This adduct is perhaps formed by the addition of NAcCys dehydro NADA ring adduct to QMIA. The majority of the second compound with parent ion at m/z 707 corresponds to a di-adduct of NAcCys to dehydro NADA dimer. Most likely, it is generated by the

addition of QMIA of mono NAcCys-dehydro NADA adduct to NAcCys-dehydro NADA ring adduct. While this is the major product, there is compelling evidence from the fragmentation pattern of other parent ions and their elution profile for the presence of other isomeric products that seem to have at least one (or even two) NAcCys attached to the side chain of dehydro NADA. Compared to the ring adduct, the side chain adduct formation seems to occur at a minimal level only. The last compound with parent ion at m/z 868 corresponds to a tri–adduct of NAcCys to dimeric dehydro NADA (one possible structure shown in Figure 7.14). This compound gives compelling arguments for the side chain participation in adduct formation with NAcCys. From the CID mass spectrum, it is clear that at least one NAcCys group is linked to the side chain of dehydro NADA dimer in this molecule thereby providing first concrete proof for the participation of dehydro NADA side chain in nucleophilic addition reactions with thiol.

Finally the results of nonenzymatic oxidation of dehydro NADA in presence of NAcCys provides further proof for the dehydro NADA side chain participation in adduct formation. Nonenzymatic oxidation of dehydro NADA even at mild alkaline condition will generate its corresponding semiquinone as the primary product (Figure. 7.16). If thiol traps this semiquinone radical at the side chain, one would predominantly get the side chain adduct. On the other hand, if it traps through the ring, one would get a ring adduct. However, semiquinones are notoriously unstable and they tend to undergo rapid dismutation to generate the parent catechol and quinonoid species (Nakamura 1960). Since quinone to quinone methide isomerization is a base catalyzed reaction (Bolton et

al., 1996, Sugumaran, 2000), and the reaction conditions are alkaline, it is expected that QMIA would be the most predominant oxidation species present under these conditions. Therefore, one would expect the efficient trapping of QMIA by the nucleophile, to generate the side chain adduct as the majority of the product. Accordingly, the nonenzymatic oxidation of dehydro NADA/NAcCys under mild alkaline conditions seems to give predominantly the side chain adduct. This is irrespective of the fact that the reaction involves one electron oxidation product or two-electron oxidation product. If semiquinone is the reactive species directly forming the adduct, it seems to generate predominantly the side chain adduct attesting that the side chain radical is the dominant reactive species. In any case, the results of nonenzymatic oxidation very strongly supports the major production of side chain adduct thus providing concrete evidence for the participation of dehydro NADA side chain in adduct formation with nucleophiles such as thiols that are available on proteins. Thus not only phenolic groups but also thiol groups can add to the side chain of dehydro NADA generating side chain adducts in insect cuticle and supporting the operation of α,β-sclerotization.

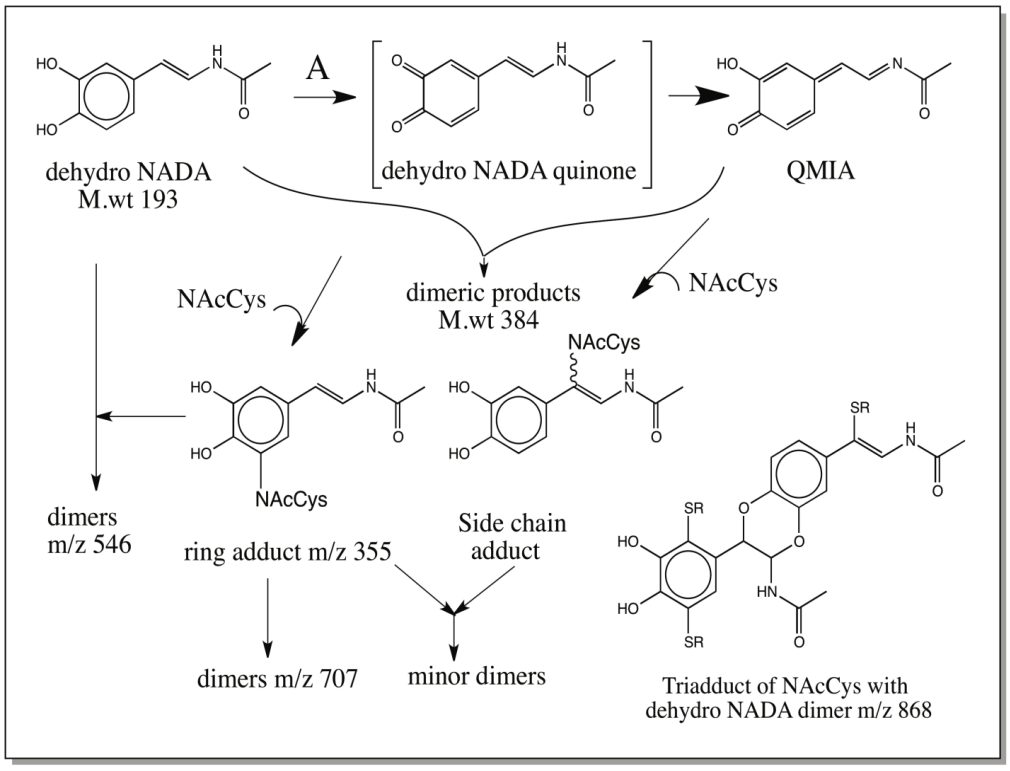

Figure 7.14: Proposed mechanism for tyrosinase catalyzed oxidation of dehydro NADA in the presence of NAcCys.

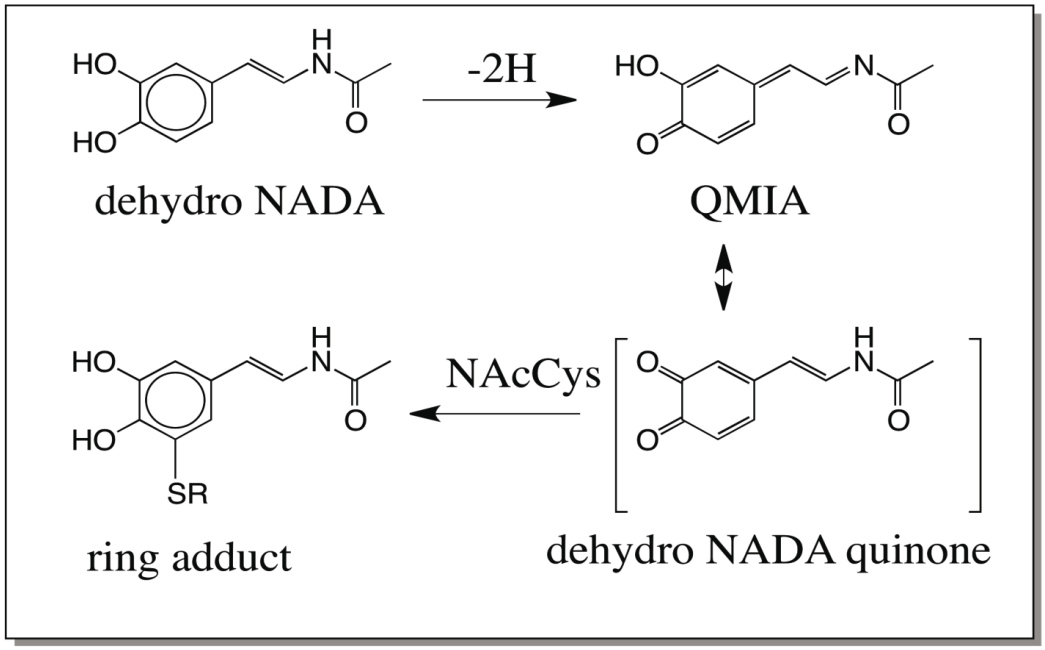

Figure 7.15: Proposed mechanism for ring adduct formation during tyrosinase catalyzed oxidation of dehydro NADA in the pressence of NAcCys (1: 10 mole ratio). Dehydro NADA upon enzymatic oxidation produces QMIA. The quinone may be formed as a transient intermediate. NAcCys traps the quinone as ring adduct.

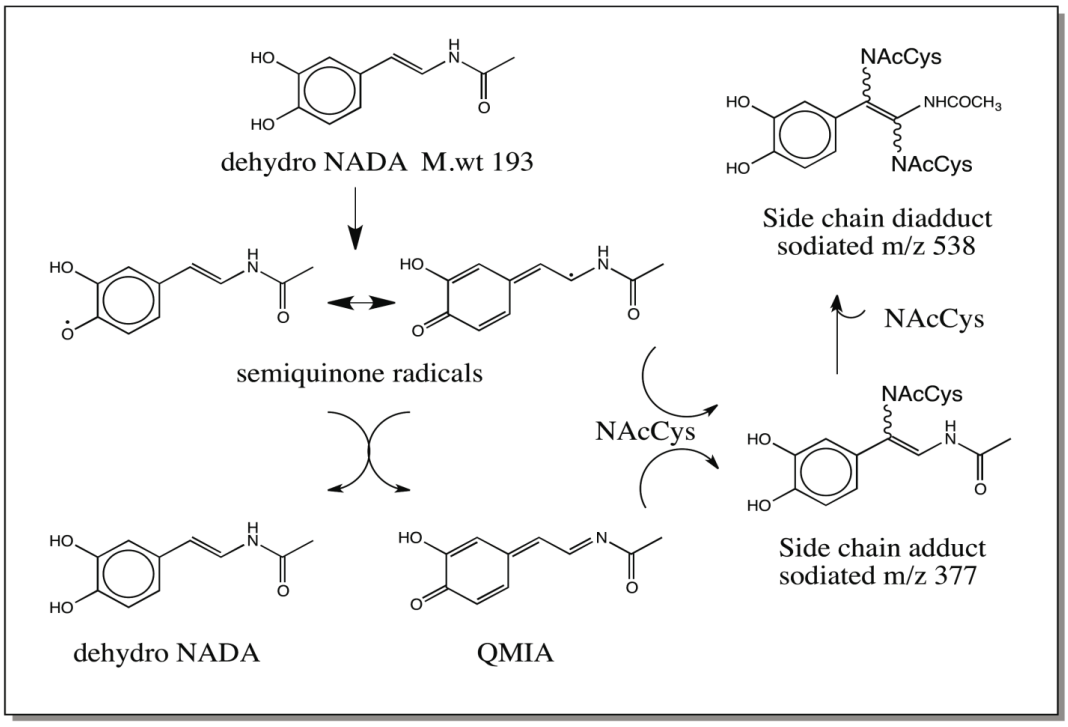

Figure 7.16: Proposed mechanism for nonenzymatic oxidation of dehydro NADA in the presence of NAcCys. Dehydro NADA upon n onenzymatic oxidation produces semiquinone radicals that can form adduct with NAcCys. Semiquinone can also undergo dismutation to produce parent dehydro NADA and QMIA. Addition of NAcCys to QMIA under this mild alkaline condition can produce the side chain adduct as the sole product.

7.6 Conclusion

Preliminary studies from our laboratory indicated that NAcCys is reacting rapidly and forming a ring adduct with dehydro NADA (Sugumaran et al., 1990). However, at that time, no detailed study was carried out and the product analysis was based on the similarity of the UV spectrum of dehydro NADA/ NAcCys adduct with those of cysteine adducts of a few well known quinones. In order to assess the production of side chain adduct, I conducted a detailed study on the reaction of dehydro NADA with NAcCys. My results indeed support the production of not only dehydro NADA ring adducts of NAcCys, but also the side chain adducts. The major products formed during the enzymatic oxidation dehydro NADA with NAcCys are the ring adducts. However, there is evidence from the mass spectral data presented in this chapter, that side chain adducts of dehydro NADA with NAcCys are also produced in the reaction albeit at a lower level. Interestingly the reaction of dehydro NADA with NAcCys at mild alkaline pH values provided convincing evidence for the production of side chain adducts of dehydro NADA with NAcCys. Therefore, such adduct formation in biological system is also highly likely. Another interesting observation about the side chain adduct is the regeneration of the dehydro NADA nucleus in the product. The retention of the double bond in the side chain is quite unexpected and could be explained by the mechanism shown in Figure 7. 17. As outlined in earlier chapters, dehydro NADA dimerization calls for the addition of two nucleophiles to the side chain of QMIA resulting in the production of a dimer with one saturated side chain (top line in Figure). Addition of NAcCys

described in this chapter on the other hand reveals the presence of an adduct which retains its side chain desaturation as shown in the figure. 7.17. Reoxidation of this adduct and coupling of another molecule of NAcCys at the α-carbon atom would again produce the di adduct with the retention of the double bond. Note that this reaction is different from the benzodioxan adduct formation that leads to solely the side chain saturation on the dehydro NADA nucleus where addition is taking place. Nevertheless, these new reactions will also lead to adduct and crosslink formation in cuticle.

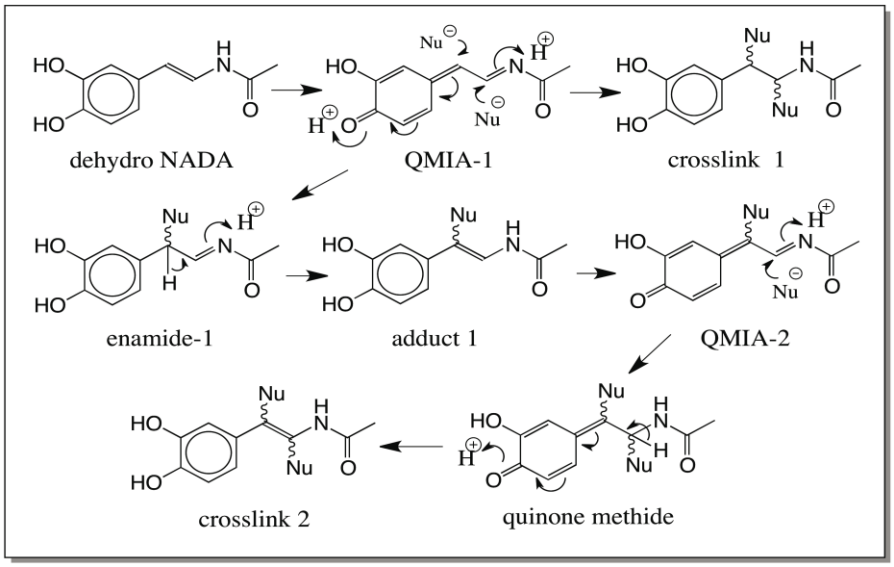

Figure. 7.17 Mechanism for the production of side chain adduct of dehydro NADA with NAcCys. The QMIA formed at alkaline pH, adds onto the NAcCys with the retention of double bond on its side chain. A similar mechanism can produce the same product from NAcCys and the semiquinone. Reoxidation and a second coupling will generate the bi-adduct. Note the difference between the crosslink 1 and crosslink 2 arising from these two different pathways.

CHAPTER 8

INCORPORATION OF 1, 2-DEHYDRO-N-ACETYL DOPAMINE INTO INSECT CUTICLE AND ITS FATE DURING HYDROLYSIS

8.1 Chapter summary

In this chapter the mode of incorporation of dehydro NADA into cuticle undergoing sclerotization and the mechanism by which arterenone is released from sclerotized cuticle is investigated using β-deuterated dehydro NADA. Incubation of unsclerotized *S. bullata* larval cuticle with dehydro NADA resulted in the incorporation of the bulk of dehydro NADA into the cuticular matrix. Whatever remained unbound, turned out to be dehydro NADA dimeric products that are formed by the coupling of dehydro NADA to QMIA in the reaction mixture. Acid hydrolysis of dehydro NADA treated cuticle released a mixture of ketocatecholic compounds mainly consisting of arterenone (and N-acetylarterenone). Arterenone (2-amino-3', 4'-dihydroxy acetophenone) has been shown to be an important hydrolytic product generated from lightly colored sclerotized cuticle that uses N-acyldopamine derivatives for crosslinking reactions. However, the

mechanism of generation of arterenone which has two protons on the α-carbon and no proton on the β-carbon atom from dehydro NADA cross links that have one proton each on these two side chain carbons remained elusive. Examination of the structure of hydrolyzed products suggests that a proton migration from β-carbon to α-carbon during hydrolysis is a likely route for arterenone production. Therefore β-deuterated dehydro NADA was synthesized and used to examine the mechanism of arterenone production. Analysis of the hydrolysis products obtained from β-deuterated dehydro NADA treated cuticle confirms the migration of deuterium from β-position to α-position. The results support the hypothesis that dehydro NADA, which is bound through its side chain carbon atoms, upon acid hydrolysis allows the migration of proton from β-carbon to the α-carbon by hydride shift generating arterenone and related products.

8.2 Introduction

Sclerotization of insect cuticle is achieved by covalent crosslinking of sclerotizing agents generated from sclerotizing precursors such as N-acetyldopamine (NADA) and N-β-alanyl dopamine (NBAD) to cuticular proteins and chitin (Andersen 2010, Kramer and Hopkins, 1987; Sugumaran, 1998, 2010). Acid hydrolysis of sclerotized cuticle produced a variety of catecholic compounds. Structural analyses of these compounds have paved ways to formulate different theories of cuticular hardening. Arterenone and ketocatechol are two important hydrolytic products generated from lightly colored sclerotized cuticle that use N-acyldopamine derivatives as sclerotizing precursors for crosslinking reactions.

The structures of these two related compounds are shown in Figure 8.1. Since un-sclerotized cuticle does not have any extractable amount of arterenone, it is generally agreed that arterenone and related compounds arise during the hydrolysis of crosslinks derived from the reaction of dehydro NADA with structural proteins and/or chitin. However, the mechanism of generation of arterenone which has two protons on the α-carbon and no proton on the β-carbon atom from dehydro NADA cross links that have one proton each on the two side chain carbons remained unclear. If the β-carbon of N-acyldopamines is linked to two nucleophile substituents, upon acid hydrolysis, they could produce arterenone. But this calls for two cycles of combined operation of phenoloxidase and quinone isomerase pair on N-acyldopamines. In the first cycle of operation, these two enzymes will produce N-acyldopamine quinone methide, which forms an adduct with a cuticular nucleophile. This cuticle bound adduct upon a second cycle of oxidation and isomerization by phenoloxidase and quinone methide pair, will produce another quinone methide that generates an adduct with cuticular nucleophile resulting in two nucleophilic substitution at the β-carbon. Although phenoloxidases are quite capable of acting on a variety of catecholamine derivatives, both free and peptide bound, currently there is no evidence for such wide substrate specificity of quinone isomerase there by ruling out the second cycle of operation. Alternatively, N-acetylarterenone can be produced in cuticle by a different mechanism without the involvement of cuticular cross links. The combined action of phenoloxidase quinone isomerase pair on N-acetyldopamine will initially produce N-acetyldopamine quinone methide. This quinone methide rather than undergoing addition reaction with cuticular nucleophiles, forms an adduct with water in

the surrounding resulting in the production of N-acetylnorepinephrine. Further action of phenoloxidase-quinone isomerase pair on N-acetylnorepinephrine will produce the N-acetylnorepinephrine quinone methide, which will undergo rapid intramolecular isomerization to produce N-acetylarterenone. This possibility has been shown to occur in the case of N-acetyldopamine as exemplified in Figure 8.2 (Saul and Sugumaran, 1990b). N-acetylarterenone thus formed may remain in the cuticle and upon acid hydrolysis of the cuticle may produce arterenone as the product. However, this route cannot explain the generation of ketocatechol from N-acetyldopamine that is covalently bound to the cuticle.

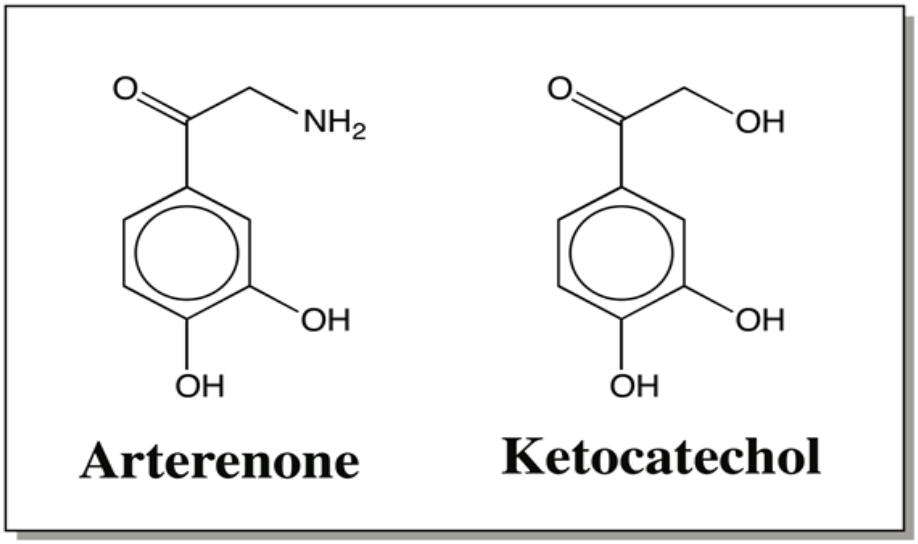

Figure 8.1: Structure of arterenone and ketocatechol.

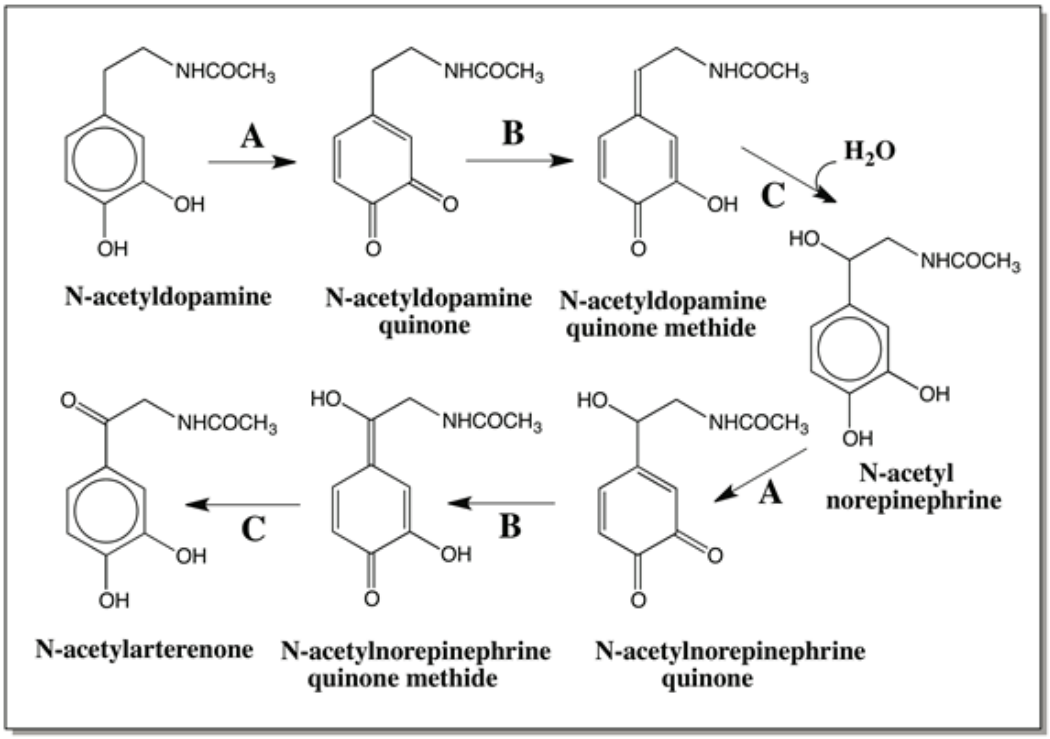

Figure 8.2: Route I for the formation of N-acetylarterenone. Phenoloxidase (A) will convert N-acetyldopamine to its corresponding quinone. Quinone isomerase (B) converts N-acetyldopamine quinone to its quinone methide isomer. Quinone methide isomer nonenzymatically (C) reacts with water forming N-acetylnorepinephrine. Further oxidation of N-acetylnorepinephrine to its quinone by phenoloxidases and conversion of this quinone by quinone isomerase produces a transient quinone methide, which undergoes intramolecular rearrangement generating N-acetylarterenone.

A more plausible route for the production of arterenone (and ketocatechol) is by the hydrolysis of dehydro NADA bound to cuticle as shown in Figure 8.3. This has been

shown to be the case with cuticle treated with dehydro NADA (Sugumaran et al., 1988a). But the question that remains is how dehydro NADA that is bound to cuticle with both its side chain carbons possessing one hydrogen atom each able to generate arterenone (and ketocatechol) which has two hydrogen atoms attached to the α-carbon and no hydrogen on the β-carbon atom in the product? A hydrolysis induced hydride shift from the β-carbon to the α-position would account for this result. However, this hypothesis has not been verified so far. The mechanism of this transformation was investigated using specifically labeled β-deuterated dehydro NADA and *Sarcophaga bullata* cuticle undergoing larval puparial transformation. Incubation of dehydro NADA with cuticle produced both dimeric products and cuticle bound dehydro NADA. Hydrolysis of dehydro NADA treated cuticle as well as soluble dehydro NADA dimer obtained from the reaction, generated arterenone as the major product. Liquid chromatography-mass spectrometric analysis of this arterenone revealed the retention of deuterium from β-position of dehydro NADA to the α-carbon atom of arterenone. Interestingly dehydro NADA also generated arterenone as a hydrolytic product more so under aerobic condition rather than the anaerobic condition used for protein hydrolysis. Analysis of the arterenone generated from dehydro NADA under aerobic hydrolysis also revealed the migration of proton from β-position to the α-position.

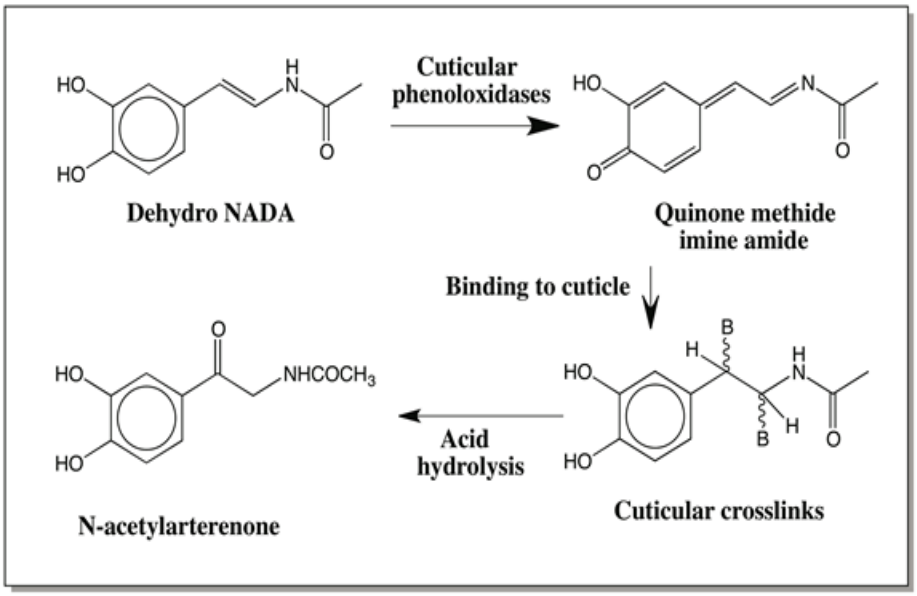

Figure 8.3: Route II for the formation of N-acetylarterenone. Enzymatic oxidation of dehydro NADA generates QMIA that reacts with the cuticle forming adducts/crosslinks. QMIA also reacts with the parent compound forming dimers. The crosslinks and/or dimer upon mild acid hydrolysis produce N-acetylarterenone.

8.3 Materials and methods

Sodium borodeuteride, dimethyl sulfoxide, deuterated water, and other chemicals were obtained from Sigma Chemical Co. St Louis MO. Dehydro NADA was synthesized as outlined earlier (Dali and Sugumaran, 1988). Synthesis of β-deuterated dehydro NADA was achieved by the reactions outlined in Figure 8.4. The following protocol

summarizes its synthesis. Sodium borodeuteride (0.9 gm) was slowly added to a solution of 3.2 gm of arterenone in 20 ml of D_2O over a period of half an hour with constant stirring. The contents were left for an additional 2 hr at room temperature. At the end of this period, the reaction mixture was acidified with acetic acid, filtered and lyophilized. The crude β-deuterated norepinephrine was dissolved in 10 ml of triethylamine and heated to 110 ºC for 1 hr with 40 ml of acetic anhydride. The reaction mixture was poured on ice and extracted with ethyl acetate. Work up of ethyl acetate layers gave β-deuterated tetraacetylnorepinephrine in 90% yield. A mixture of tetraacetylnorepinephrine (4.0 gm) and anhydrous potassium carbonate (2 gm) in 30 ml of dimethyl sulfoxide was heated under nitrogen at 110 ºC for 2 hr. At the end, the reaction mixture was poured over ice and β-deuterated dehydro NADA was purified as outlined in earlier publication (Dali and Sugumaran, 1988). The ^1H spectra of control dehydro NADA and deuterated dehydro NADA were obtained using a 300 MHz Varian NMR spectrometer in dimethyl sulfoxide-d_6. The residual solvent signals served as the internal standard. The temperature was set at 25 ºC (accuracy ± 1 ºC) and controlled by the Varian control unit.

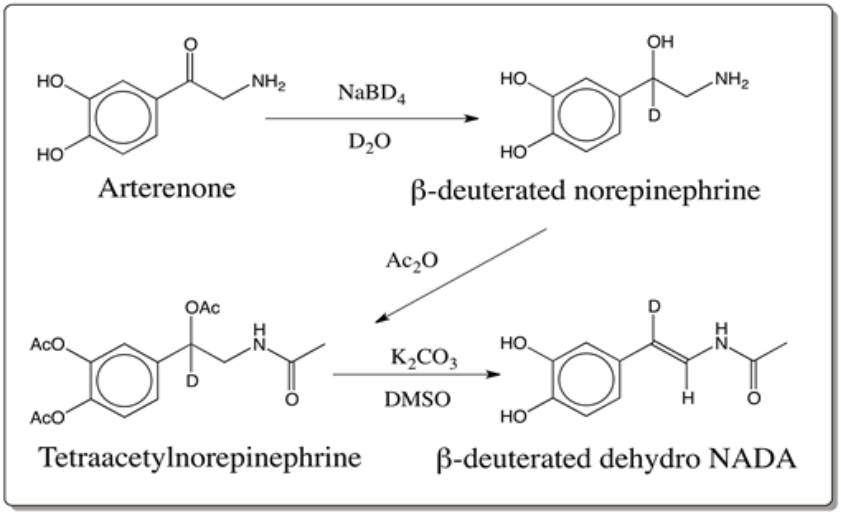

Figure 8.4: Scheme for the synthesis of β-deuterated dehydro NADA. Arterenone is reduced with sodium borodeuteride water. The resultant β-deuterated norepinephrine was acetylated with acetic anhydride to produce tetra acetyl norepinephrine. Treatment of tetra acetyl norepinephrine with potassium carbonate in dimethyl sulfoxide produced the required β-deuterated dehydro NADA.

S. bullata larvae were obtained from commercial supplier (Carolina Biological Supply Company, Burlington, North Carolina). Larvae of *S. bullata* were raised on a dog food diet. Last instar larval cuticle was homogenized in ice cold water with a blender at half maximum speed. The contents were passed through a 100 µm sieve and re-homogenized. The process was repeated until the cuticle became translucent at which point the cuticle sheaths were recovered by sieving the homogenate through cheesecloth. After washing with water, the cuticle was suspended in 50 mM sodium phosphate buffer,

pH 6.0 for 30 min and filtered. The cleaned cuticle was washed with water extensively and used for all biochemical studies.

Processing of dehydro NADA treated cuticle: The reaction of dehydro NADA with cuticle was monitored by following the disappearance of dehydro NADA in the solution using Arnow's reagent (Arnow, 1937). A typical reaction mixture containing 0.1-0.5 mM dehydro NADA, appropriate amounts of the cuticle in 50 mM sodium phosphate buffer, pH 6.0 was incubated at room temperature and at different time intervals the amounts of catechol remaining in the reaction was estimated by withdrawing aliquots from the reaction mixture and incubating it with Arnow's reagent (sodium nitrite-sodium molybdate). Arnow's reagent forms a bright red color upon reacting with catechols, which is used to quantify the catechols remaining in solution.

Processing of β-deuterated dehydro NADA treated cuticle: Washed, cleaned, and air dried wandering stage *S. bullata* larval cuticle (250 mg) was incubated with 2 mg of β-deuterated dehydro NADA for three hr in 3 ml of 50 mM sodium phosphate buffer, pH 6.0. Binding of the β-deuterated dehydro NADA to the cuticle was monitored every 15 min by Arnow's assay. At the end of the incubation period, cuticle was washed extensively with sodium phosphate buffer, pH 6.0 followed by water and methanol. The cuticle was air dried and hydrolyzed with 2 ml of 1 N HCl at 108 ºC for 24 hr. The hydrolyzed cuticle was lyophilized, and the fluffy powder was extracted with 1.5 ml of methanol. The methanol layer was subjected to RP-HPLC-MS analysis. The same procedure was used for the reaction of protium form of dehydro NADA with cuticle.

Processing of dimeric and monomeric dehydro NADA: The dimer formed during the oxidation of dehydro NADA with tyrosinase was chromatographed on Biogel P-2 column using 0.2 M acetic acid as the eluent. Fractions of two ml were collected and the fractions containing the dimeric compound were isolated, pooled and lyophilized. The dimer was also hydrolyzed with 1N HCl for 24 hr at 108 ºC. The hydrolyzate was concentrated by lyophilization. The soluble catechols from this mixture were isolated by extraction with methanol and subjected to RP-HPLC-MS analysis. Dehydro NADA, both the protium form and the deuterated form was also hydrolyzed the same way as the dimer and used for product analysis.

RP-HPLC conditions for hydrolysis product: An aliquot of lyophilized and methanol resuspended (5 µl) hydrolyzed product was analyzed using reversed phase-high performance liquid chromatography (RP-HPLC) with isocratic elution (50 mM acetic acid containing 0.2 mM sodium octyl sulfonate in 20% methanol) at a flow rate of 0.6 ml/min on a C_{18} cartridge column (Agilent Technologies, 5 µm, 4.6 x 150 mm). The instrument was equipped with diode array spectrophotometer to detect the UV spectrum of the eluting compounds.

RP-HPLC-MS: Reversed phase HPLC-MS was performed on an Agilent 6130 quadrupole mass spectrophotometer fitted with Agilent 1200 HPLC system. The operating conditions were: Atmospheric Pressure Chemical Ionization (APCI) positive mode, capillary voltage 3kV, corona current 15 µA, drying gas temperature 250 ºC, nitrogen gas flow 12 l/min, and nebulizer pressure was 35 psi. M/Z ratio of 50 to 500 was

recorded during HPLC/APCI/MS run. The RP-HPLC conditions were: Agilent 1200 fitted with Agilent G1329A auto sampler, Waters Symmetry C_{18} columns, 4.6 x 50 mm, 5 µm was used to separate products. The HPLC was operated at a flow rate of 0.7 ml/mi using mobile phase A (water) and mobile phase B (methanol) both with 0.01% trifluoroacetic acid with gradient elution 0 min 75% B, 4 min 100% B, 6 min 100% B, 6.01-7 min 75% B and 7 min stop, and the injection volume was 4 µl.

8.4 Results

Experiments carried out with protium form of dehydro NADA: Incubation of dehydro NADA with larval cuticle isolated at the wandering stages of *S. bullata*, resulted in the rapid covalent binding of dehydro NADA to the cuticle. As shown in Figure 8.5 this binding caused a rapid reduction in the amounts of Arnow's positive catechols in the reaction mixture. Part of dehydro NADA got bound to the cuticle and portion remained in solution. RP-HPLC analysis of the reaction indicated that even this small portion is due to the presence of dimeric dehydro NADA and not due to starting compound, dehydro NADA itself. Figure 8.6 for example shows the RP-HPLC analysis of a time course reaction. At the initial phase, bulk of dehydro NADA remained in the solution, as time passed, more and more dimeric compounds accumulated in the medium and at the end of about 45 min only dimeric compounds were present and almost no dehydro NADA could be observed in the supernatant.

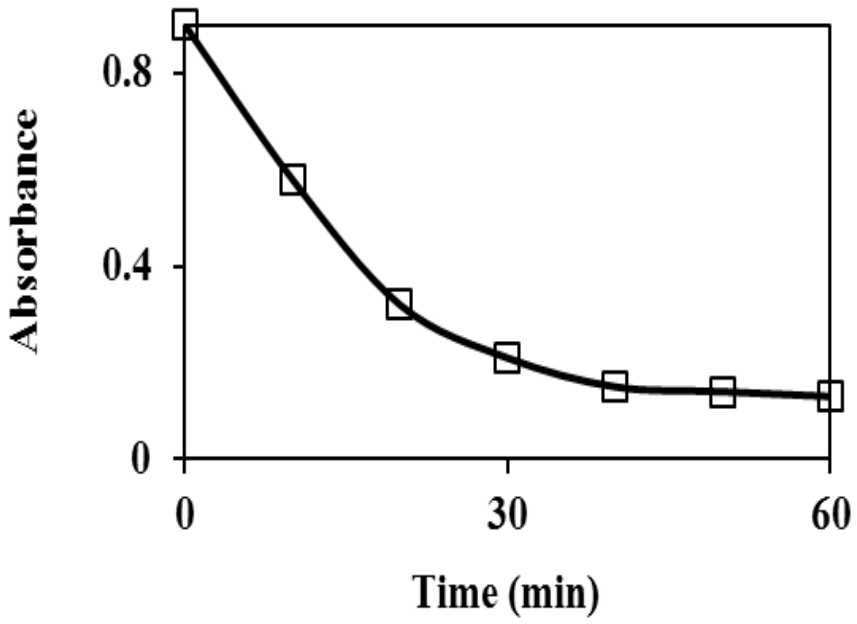

Figure 8.5: Time course of disappearance of dehydro NADA from solution during incubation of dehydro NADA with cuticle. The consumption of dehydro NADA from the reaction was monitored by Arnow's reaction for catechol. The dehydro NADA disappeared from the solution actually got bound to the cuticle.

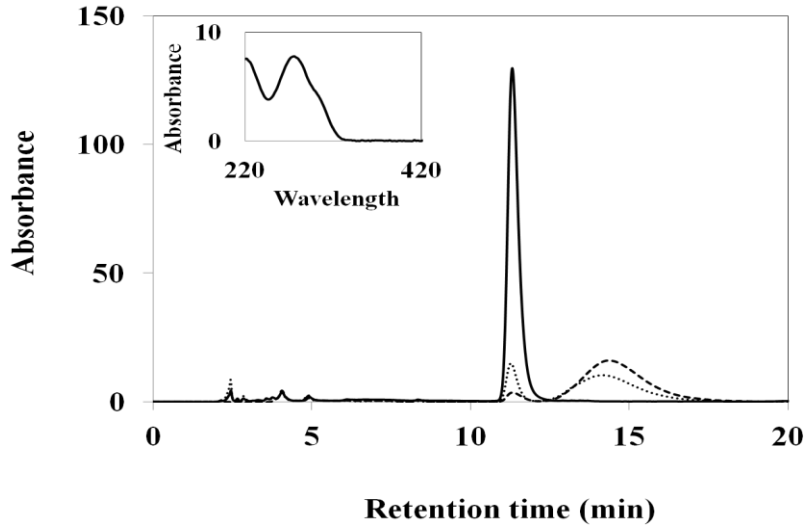

Figure 8.6: RP-HPLC analysis of dehydro NADA - cuticle reaction. Aliquots of the reaction mixture outlined in Figure-8.5 were subjected to RP-HPLC analysis at different time intervals. Note the rapid disappearance of dehydro NADA (11 min peak) and the production of dimeric peak at about 15 min. Solid line - zero time reaction, dotted line - 15 min reaction, and Dash line - 30 min reaction. Inset: Ultraviolet absorbance spectrum of the peak eluting at 14.3 min corresponding to dehydro NADA dimer.

To characterize the nature of dehydro NADA that is bound to the cuticle, cuticle treated with dehydro NADA was hydrolyzed with 1N HCl at 108 ºC for 24 hr and the cuticular hydrolyzate was analyzed on RP-HPLC (Figure 8.7). The peak eluting at 8.18 min (marked as B) was identified as arterenone based on the elution profile, retention time and its ultraviolet absorbance spectrum. Native cuticle that was not treated with dehydro NADA, did not produce this peak at all; there by confirming that arterenone is arising from the cuticle bound dehydro NADA during acid hydrolysis. Among the other

compounds chromatographed, ketocatechol could be identified as a minor product (marked peak A in Figure 8.7) by its characteristic elution profile and ultraviolet absorbance spectrum. Again, it was a minor product and no further attempt was made to study this compound.

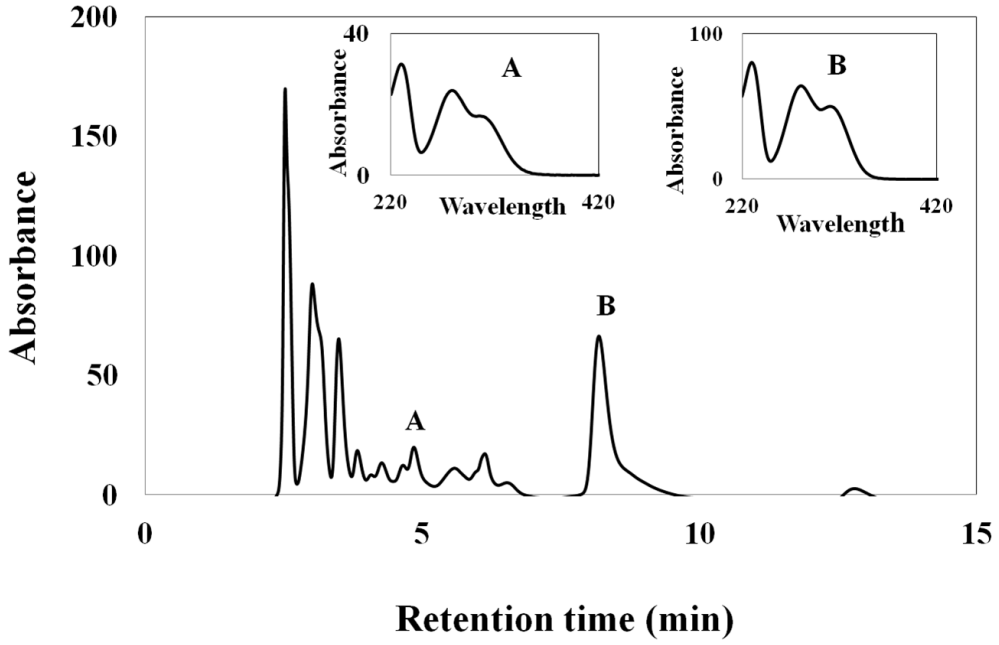

Figure 8.7: RP-HPLC analysis of cuticular hydrolyzates treated with dehydro NADA: The cuticular hydrolyzate was subjected to RP-HPLC analysis as outlined in materials and methods. Peak A with retention time of 4.8 min corresponds to ketocatechol and the peak eluting at 8.18 min marked B is due to arterenone. Inset: Ultraviolet absorbance spectrum of A: ketocatechol and B: arterenone.

Experiments carried out with deuterated dehydro NADA: To investigate the mechanism of arterenone production from cuticle, β-deuterated dehydro NADA was

synthesized as outlined in the materials and methods section. The NMR spectrum of the synthetic product obtained by this procedure is shown in Figure 8. 8 (bottom). For comparison, the NMR spectrum of the unlabeled dehydro NADA is shown in the same figure (Figure 8.8 top). The doublet at δ 5.95 and 5.90 is due to β-hydrogen atom and the multiplet at δ 7.1 is due to the α-hydrogen atom of dehydro NADA. The three aromatic ring protons are observed as the broad multiplet centered around δ 6.6. The two phenolic protons are observed at δ 8.9 as a broad singlet peak and the NH proton is observed as a doublet at about δ 10. In the β-deuterated compound the proton signal due to β-proton is nearly missing and the adjacent proton on the side chain is no longer exhibiting a multiple band. Rather it shows as a doublet confirming the replacement of protium form with deuterium at the β-position. The NMR spectrum also confirmed the presence of > 99% deuterium in the β-position of dehydro NADA. Thus, the NMR studies clearly confirmed the synthesis of β-deuterated dehydro NADA by the protocol outlined in Figure 8. 4.

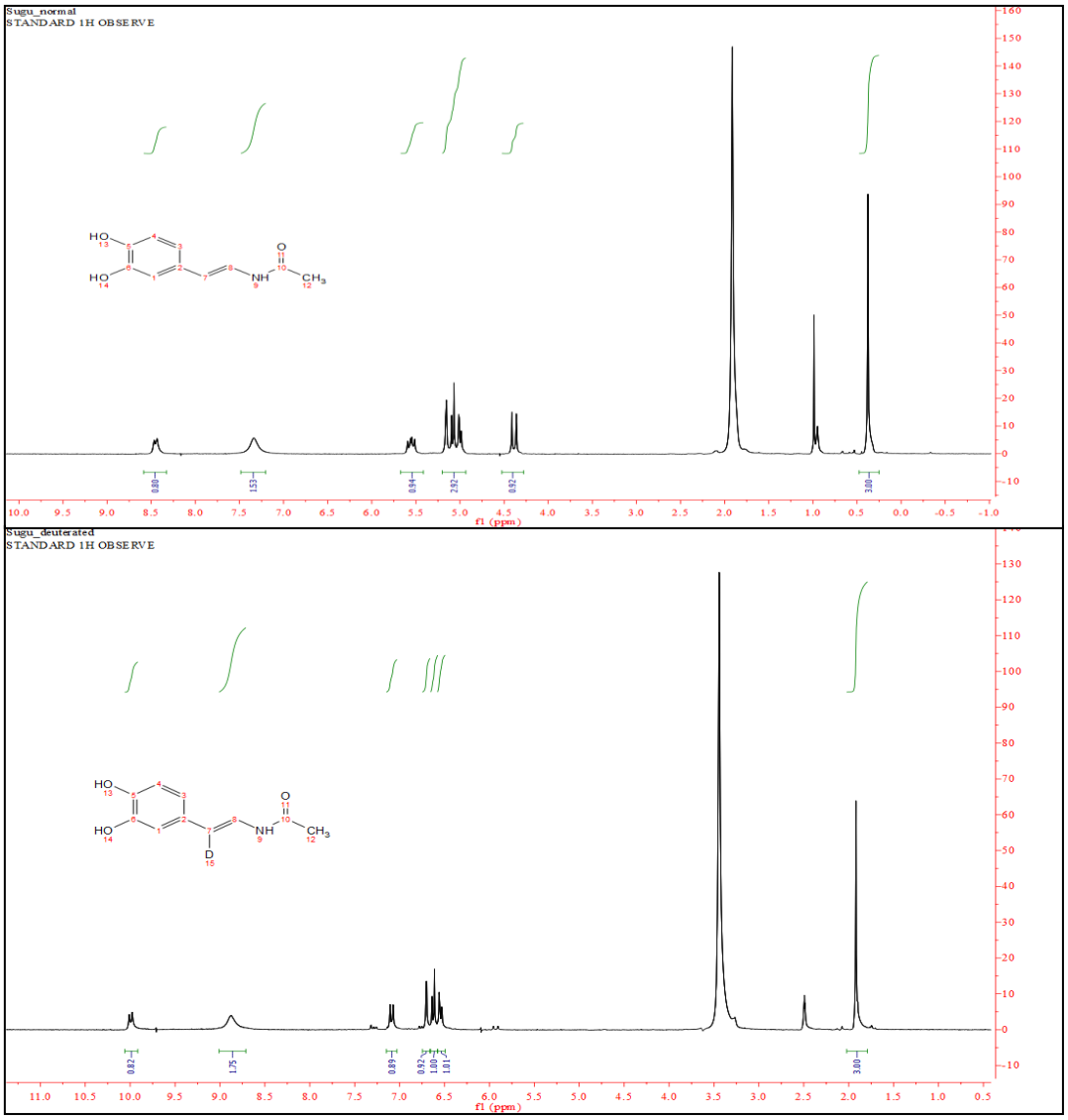

Figure 8.8: NMR spectrum of control dehydro NADA (Top panel) and β-deuterated dehydro NADA (bottom panel) in dimethyl sulfoxide-d_6.

Deuterated dehydro NADA readily served as the substrate for phenoloxidase and its oxidation resulted in the production of dimers. The dimeric product arising from the oxidation of both protium and deuterated dehydro NADA were isolated and hydrolyzed

with 1 N HCl for 24 hr at 108 ºC. The hydrolyzate was lyophilized and contents were analyzed by RP-HPLC-MS. Figure 8.9 shows HPLC-MS analysis of hydrolyzates of protium form of dehydro NADA dimer. A prominent peak observed at 0.77 min is due to arterenone. Its mass spectrum accordingly exhibited the M+1 ion at 168 mass unit (Figure 8.9 top panel). Analysis of the hydrolyzate of β-deuterated dehydro NADA dimer is shown in Figure 8.10. As expected, this compound also produced the 0.77 min peak corresponding to arterenone. However, the mass spectral analysis revealed that arterenone generated from β-deuterated dehydro NADA dimer had one mass unit higher than that of the control arterenone. It exhibited a M+1 ion at 169 mass unit rather than 168 (Figure 8.10 top panel).

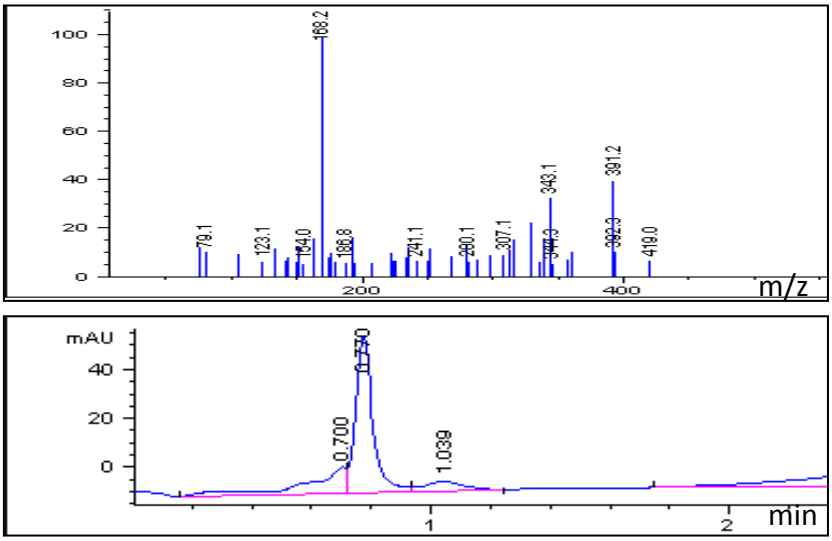

Figure 8.9: HPLC-MS analysis of dehydro NADA dimer hydrolyzate. Bottom: RP-HPLC analysis of dimer hydrolyzate; 0.77 min peak is due to arterenone. Top: Mass spectra of the above run. Note the prominent M+1 peak at 168 corresponds to the protonated arterenone.

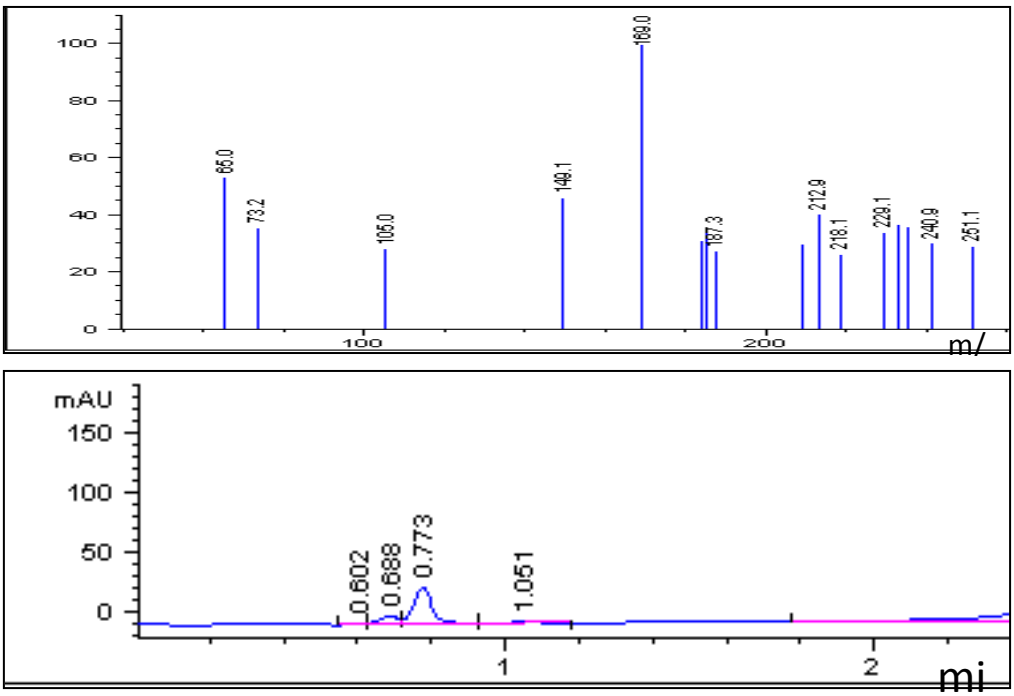

Figure 8.10: HPLC-MS analysis of β-deuterated dehydro NADA dimer hydrolyzates. Bottom: RP- HPLC analysis of labeled dimer hydrolyzate; 0.77 min peak is due to arterenone. Top: mass spectra of the above run. Note the prominent M+1 peak at 169 instead of 168 for the arterenone.

Similar results were obtained with cuticular reactions also. Figure 8.11 shows the HPLC-MS analysis of protium form of dehydro NADA treated cuticle hydrolyzate. The prominent peak eluting at 0.77 min is due to arterenone, which is exhibited typical M+1 ion at 168 mass unit. On the other hand, the cuticle treated with β-deuterated dehydro NADA upon acid hydrolysis released arterenone, which exhibited a M+1 ion at 169 mass unit (Figure 8.12). This is possible only if the deuterium has migrated from β-position to the α-position. Cuticular hydrolyzates also exhibited the presence of N-acetylarterenone

as one of the product (Figures 8.11 and 8.12). Mass analysis of this product revealed that the N-acetylarterenone (from the protium form of dehydro NADA treated cuticle) exhibiting a M+1 ion at 210.1 mass units while that from deuterated dehydro NADA treated cuticle exhibited an increase mass of one unit at 211.1. Thus the results clearly indicate that both dimer and the dehydro NADA that is bound to cuticle upon mild acid hydrolysis generate arterenone that retains the proton from the β-position by transferring to the α-position.

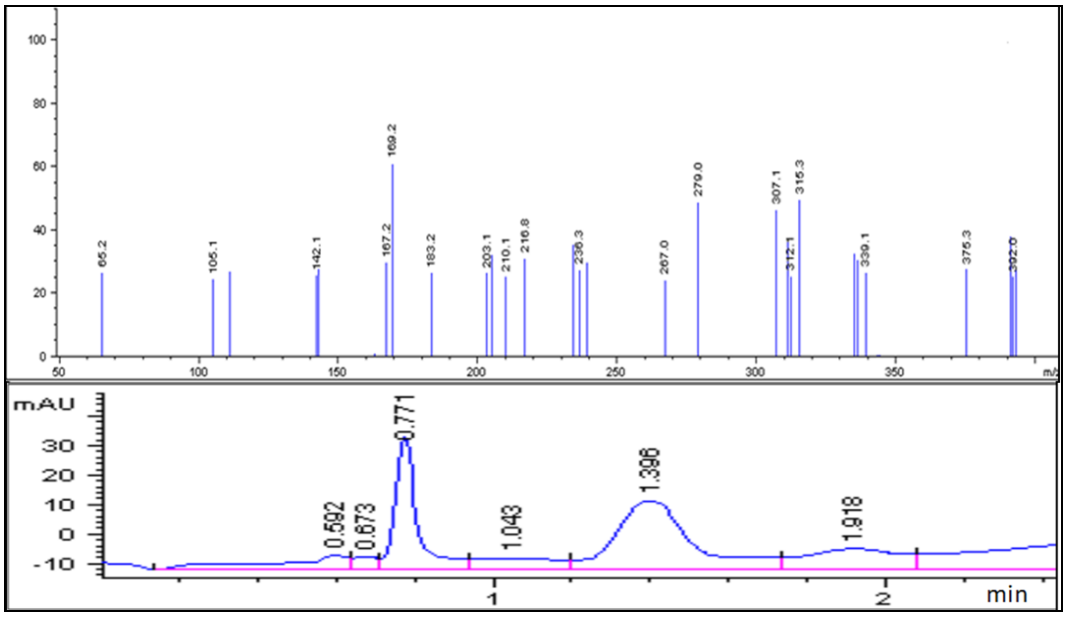

Figure 8.11: RP-HPLC-MS analysis of cuticular hydrolyzate treated with dehydro NADA. Bottom: HPLC analysis of cuticular hydrolyzate treated with dehydro NADA; 0.77 min peak is due to arterenone and 1.39 min peak is due to N-acetylarterenone. Top: Mass spectra of the above run. Note the prominent M+1 peak at 168 corresponding arterenone and the peak at 210.2 is due to N-acetylarterenone.

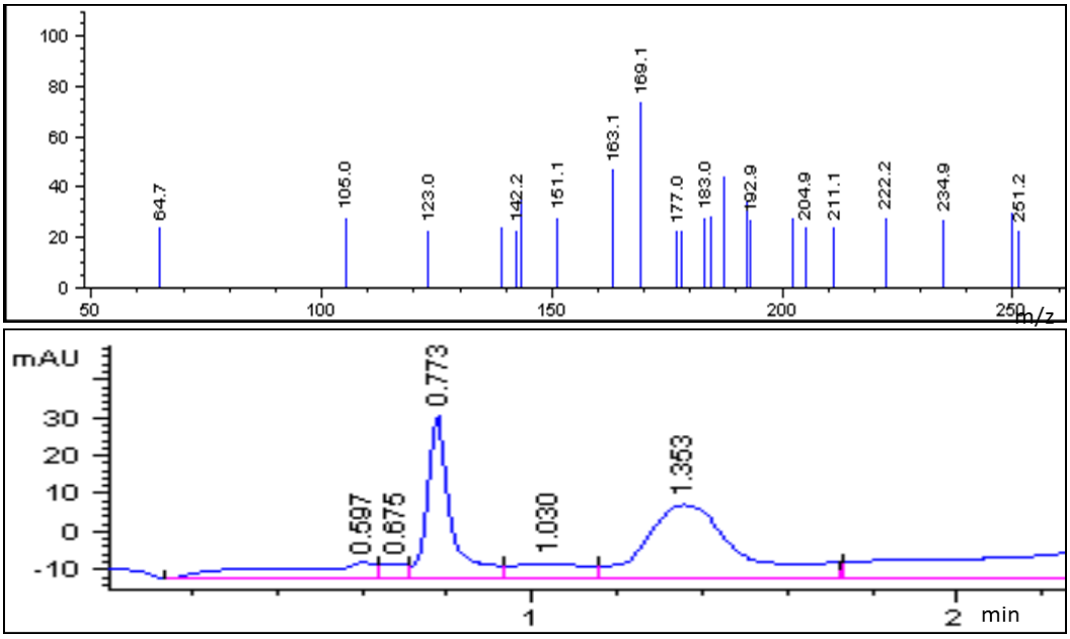

Figure 8.12: RP-HPLC-MS analysis of cuticular hydrolyzates treated with β-deuterated dehydro NADA. Bottom: RP-HPLC analysis of cuticular hydrolyzates treated with labeled dehydro NADA; 0.77 min peak due to arterenone and the peak at 1.35 min is due to N-acetylarterenone. Top: Mass spectra of the above run. Note the prominent M+1 peak at 169 instead of 168 for arterenone. Similarly note the peak at 211.1 mass units instead of 210 mass unit for N-acetylarterenone.

Hydrolysis of free dehydro NADA: I suspected that even dehydro NADA could generate arterenone upon acid hydrolysis. Therefore, I tested the ability of dehydro NADA to generate arterenone after acid hydrolysis. Based on its amide nature, one can predict that dehydro NADA will undergo simple hydrolytic fission at the amide bond

generating the enamine and acetic acid. The enamine being unstable would undergo rapid rearrangement and hydrolysis producing 3, 4-dihydroxyphenylacetaldehyde and ammonia (Sugumaran, 2010). Figure 8.13 shows the RP-HPLC analysis of hydrolytic products of dehydro NADA obtained under anaerobic conditions. The major peak was identified tentatively as 3, 4-dihydroxyphenylacetaldehyde based on its simple ultraviolet absorbance spectrum (280 nm peak). The minor peak was identified as arterenone based on its elution profile and ultraviolet absorbance spectrum. The above results were obtained when the hydrolysis was conducted under anaerobic condition that is routinely used for protein hydrolysis. Different results, however were obtained when the hydrolysis reaction was performed in the presence of oxygen. Figure 8.14 shows the RP-HPLC analysis of the hydrolytic products of dehydro NADA in the presence of oxygen. The major peak eluting at 8 min (peak marked B) was identified as arterenone based on its elution profile and ultraviolet absorbance spectrum. Two minor products seems to arise during the hydrolysis of dehydro NADA. The peak eluting at about 12 min marked peak C, exhibited a simple UV spectrum with absorbance maximum at about 280 nm with no shoulder at 320 nm compared to the previously obtained 3,4-dihydroxyphenyl acetaldehyde. The other peak was not identified. The production of arterenone as the major product in this case was puzzling. Therefore, the mechanism of arterenone production from β-deuterated dehydro NADA was studied. Figure 8.15 and 8.16 shows the RP-HPLC-MS analysis of hydrolytic products arising from the protium form of dehydro NADA and β-deuterated dehydro NADA respectively. The protium form

produced arterenone with its normally expected M+1 ion at 168 mass units (Figure 8.15 top panel). While β-deuterated dehydro NADA produced arterenone that exhibited the mass unit of 169 confirming the production of the labeled arterenone at the α-position (Figure 8.16 top panel). The strict requirement of oxygen for the production of arterenone indicates that most likely dehydro NADA is first oxidized to QMIA and is subsequently hydrolyzed to generate arterenone.

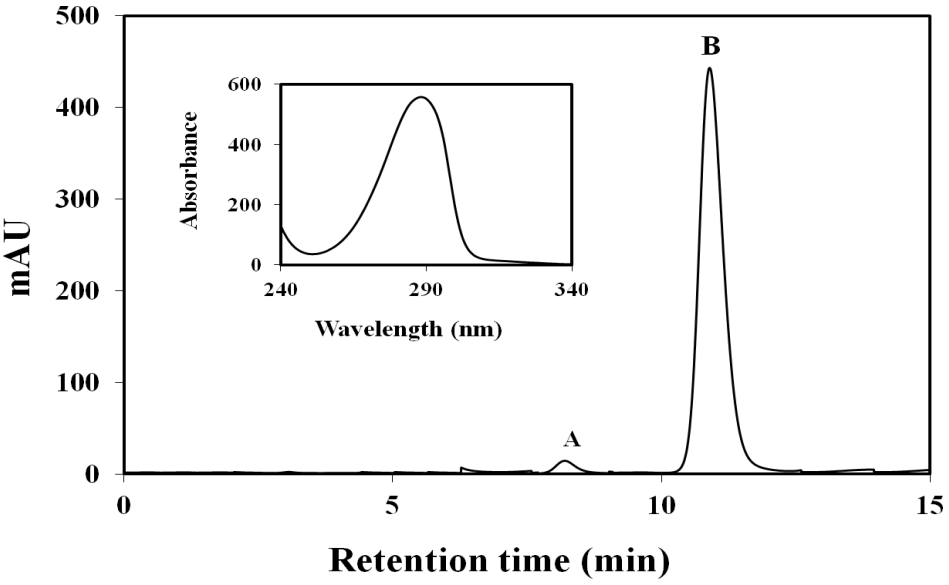

Figure 8.13: RP-HPLC analysis of hydrolysis products arising from dehydro NADA under anaerobic conditions. The hydrolysis of dehydro NADA was carried out as outlined in materials and methods section and the hydrolytic products were analyzed by RP-HPLC. The peak marked A is due to arterenone. The peak marked B exhibited a simple 280 nm absorbance (inset to figure) and may correspond to 3, 4-dihydroxyphenyl acetaldehyde.

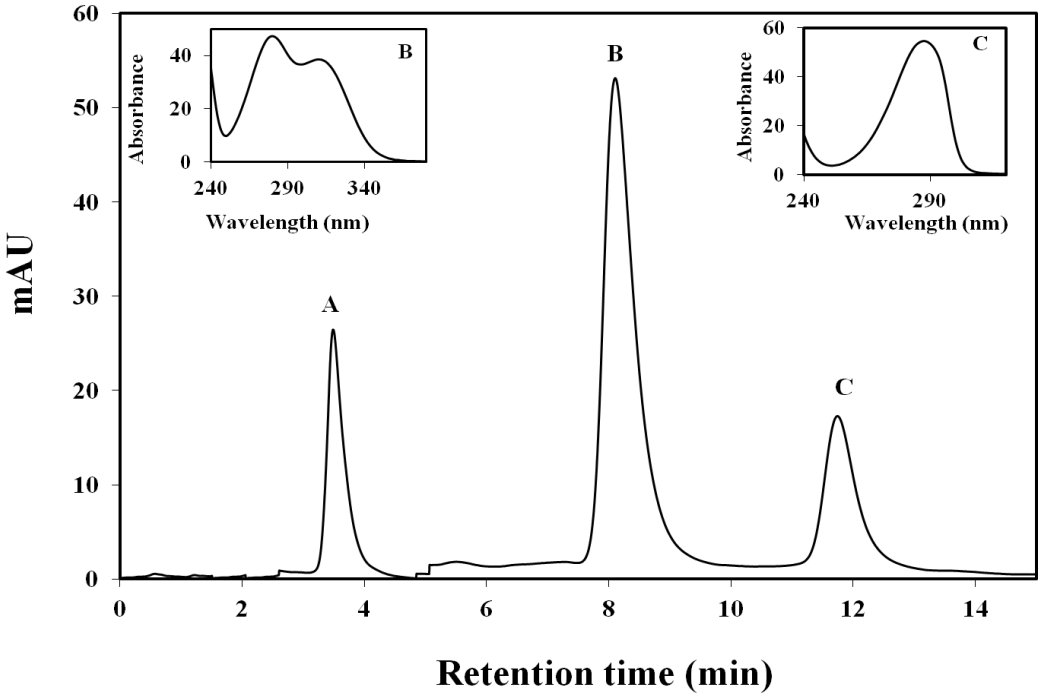

Figure 8.14: RP-HPLC analysis of hydrolysis products arising from dehydro NADA under aerobic conditions. The hydrolysis of dehydro NADA was carried out as outlined in materials and methods section and the hydrolytic products were analyzed by RP-HPLC. The peak marked B is due to arterenone. The peak marked C exhibited a simple 280 nm absorbance and may correspond to 3, 4-dihydroxyphenylacetaldehyde. Inset: Ultraviolet absorbance spectrum of arterenone (B); and the peak marked C.

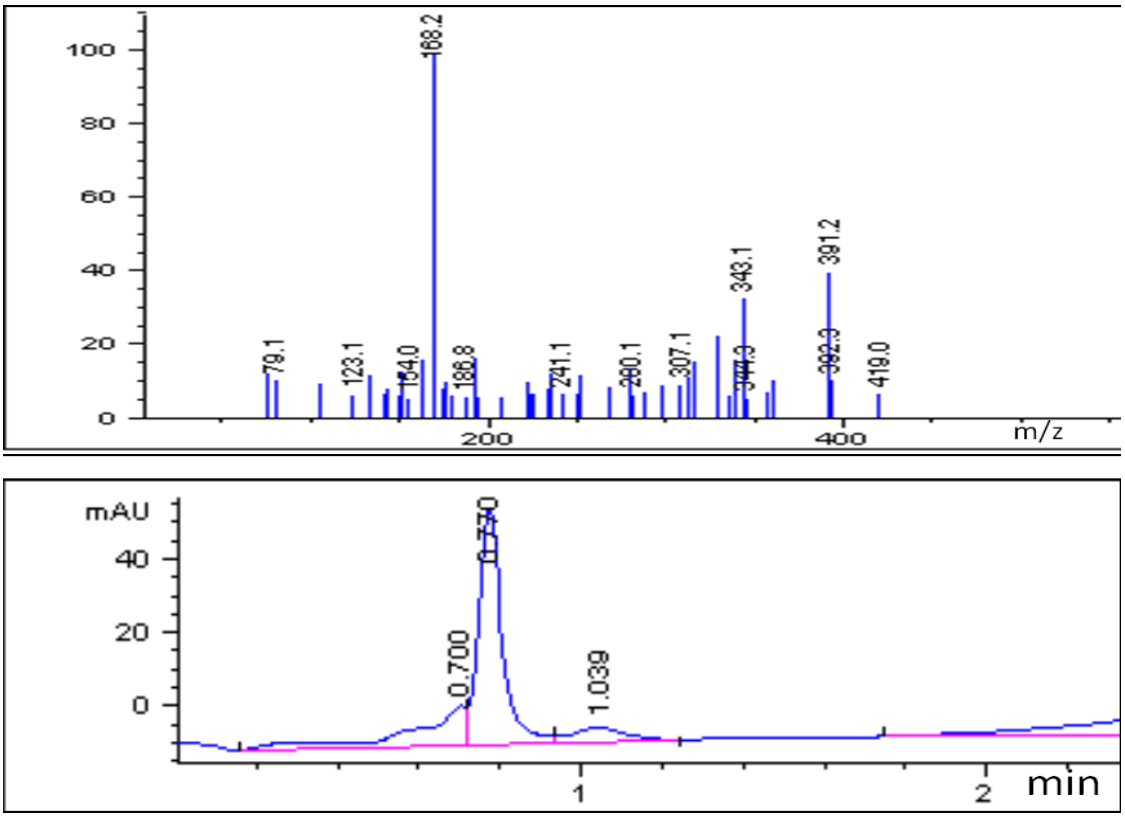

Figure 8.15: RP-HPLC-MS analysis of dehydro NADA hydrolyzate. Bottom: RP-HPLC analysis of dehydro NADA hydrolyzate; 0.77 min peak is due to arterenone. Top: Mass spectra of the above run. Note the prominent M+1 peak at 168 correspond to arterenone.

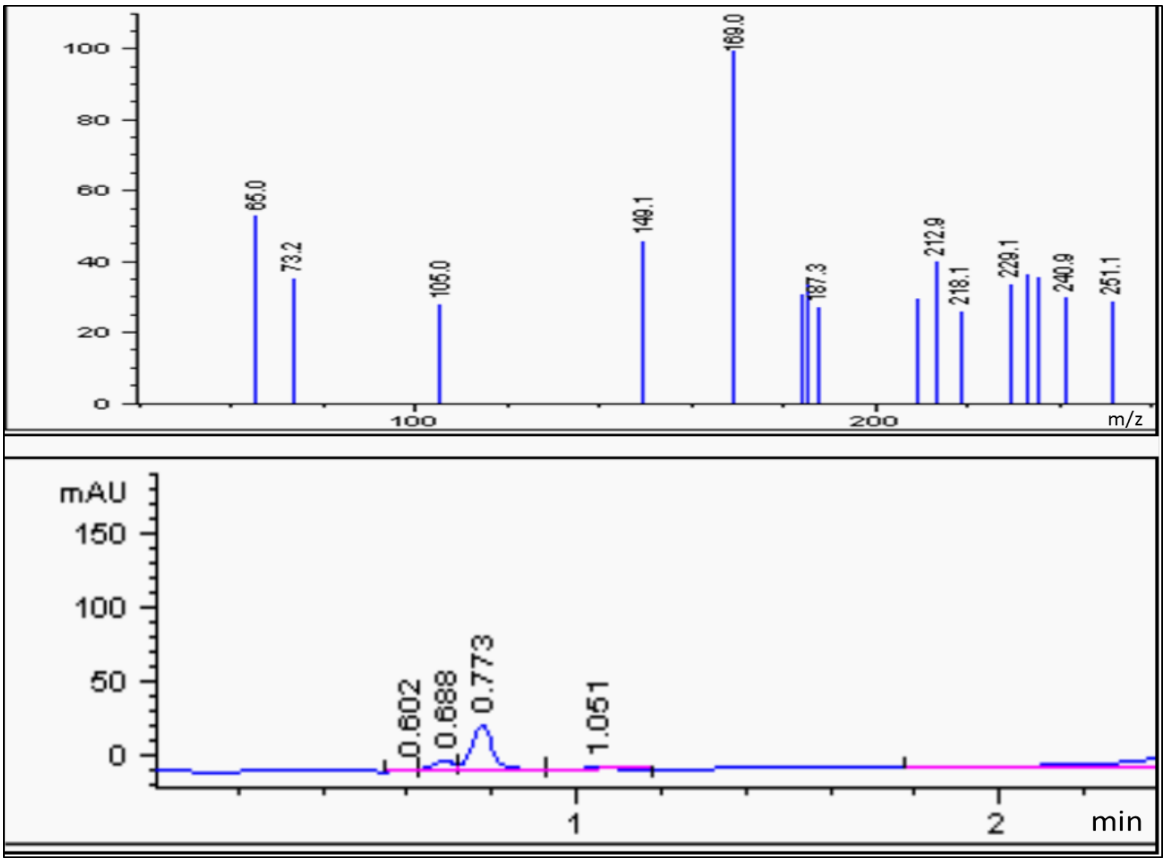

Figure 8.16: RP-HPLC-MS analysis β-deuterated dehydro NADA hydrolyzate. Bottom: HPLC analysis of labeled dehydro NADA hydrolyzate; 0.77 min peak is due to arterenone. Top: Mass spectra of the above run. Note the prominent M+1 peak at 169 instead of 168 for the arterenone.

8.5 Discussion

The results presented in this chapter confirm the occurrence of the second route for the production of arterenone in cuticular hydrolyzates (Figure 8.2). As stated in the introduction, arterenone could arise from N-acetylarterenone by two cycles of operation of phenoloxidase –quinone isomerase action on N-acetyldopamine. In the first cycle, N-acetylnorepinephrine is formed. When the phenoloxidase –quinone isomerase acts on this compound in the second cycle N-acetylarterenone is produced. In general compounds possessing carbonyl group attached to the catecholic ring serve as poor substrate for phenoloxidase (Saul and Sugumaran, 1990b). Hence N-acetylarterenone could accumulate in the cuticle as an end product. This is certainly the case with soluble reaction of N-acetyldopamine with phenoloxidase-quinone isomerase pair (Saul and Sugumaran, 1990a). Such reaction in cuticle will produce N-acetylarterenone that may not be accessible to nondestructive extraction agents. However, during acid hydrolysis, it could be hydrolyzed to produce arterenone as the end product.

The second and more plausible route for arterenone production is the liberation from dehydro NADA that is bound to cuticle by a hydrolytic mechanism involving hydride shift presented in this section. This mechanism is presented in Figure 8.17. Incubation of cuticle with β-deuterated dehydro NADA results in the oxidation of dehydro NADA to its QMIA and eventual binding of QMIA to the cuticle as shown in the Figure 8.17. QMIA will also bind to the parent compound, dehydro NADA forming

dimers and other oligomers (Abebe et al., 2010). During acid hydrolysis, both the dimer and the cuticle bound dehydro NADA could generate a transient positive charge on the α-position that assist the migration of proton from the β-position of bound dehydro NADA to the α-position. This will also be assisted by the conversion of secondary alcoholic group to keto group. Such a rearrangement eventually results in the production of N-acetylarterenone. It is important to note that mild acid hydrolysis of sclerotized cuticle releases N-acetylarterenone as one of the hydrolytic products. Further hydrolysis of N-acetylarterenone will generate arterenone that retains the proton from the β-position of dehydro NADA, now at the α-position. The liberation of arterenone during the hydrolysis of free dehydro NADA seems to be supported by oxygen. Initial oxidation of dehydro NADA to its QMIA and subsequent hydrolysis of the QMIA could produce the same positively charged ion that is depicted in Figure 8.17. The final migration of proton from β-position to the α-position would then generate N-acetylarterenone and eventually arterenone from dehydro NADA during its hydrolysis also.

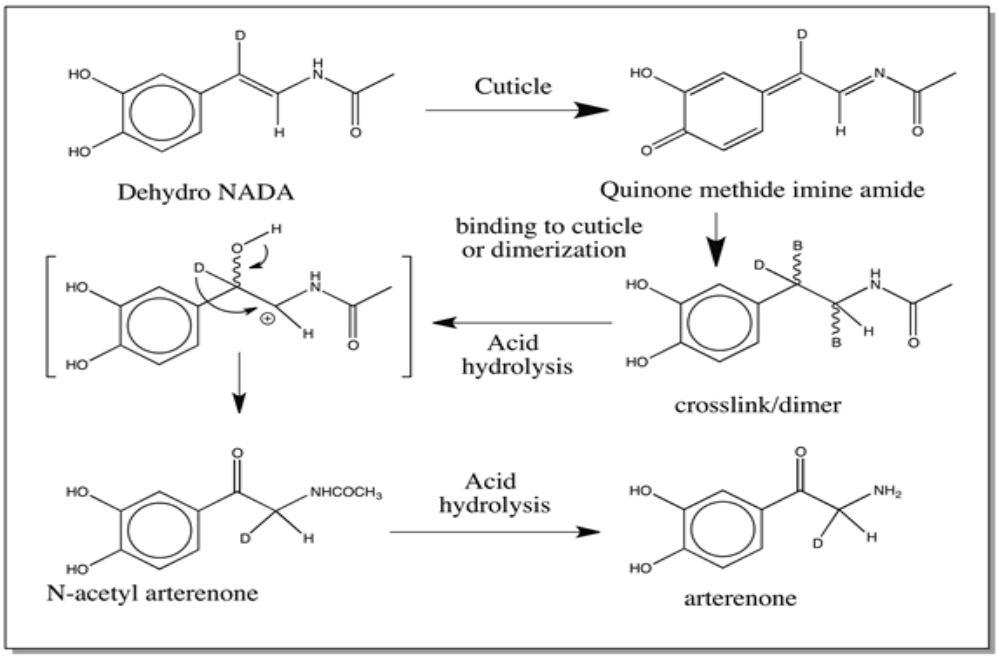

Figure 8.17: Proposed mechanism for hydrolysis of deuterated dehydro NADA. Cuticular enzymes oxidize dehydro NADA to its QMIA which binds to the cuticle or forms dimeric (and other oligomeric) products with dehydro NADA. These adducts and crosslinks upon acid hydrolysis produce a positively charged ion that generates N-acetylarterenone with the migration of the proton from the β-position to the α-position. Hydrolysis of N-acetylarterenone produces arterenone. Hydrolysis of dehydro NADA will also produce the same positively charged ion that generates N-acetylarterenone with the migration of the proton from the β-position to the α-position. Thus, dehydro NADA hydrolysis will also produce arterenone as the end product.

8.6 Conclusion

Arterenone is a major hydrolytic product of sclerotized insect cuticle. It is believed to originate from dehydro NADA bound covalently to cuticle through its side chain. However, the mechanism arterenone production in cuticular hydrolyzates remained a mystery for over three decades. Although its structure was useful in formulating theories of β-sclerotization, the actual mechanism by which it is produced from sclerotized cuticle remained elusive. Since the discovery of dehydro NADA, it has been proposed that the cuticle bound dehydro NADA could be the hydrolytic precursor for arterenone. Accordingly earlier studies revealed that cuticle treated with dehydro NADA, upon acid hydrolysis produced arterenone as the primary product (Sugumaran et al., 1988). To investigate the mechanistic origin of arterenone, β-deuterated dehydro NADA was synthesized and used to investigate its mode of binding to cuticle and the mechanism of liberation of arterenone. Results presented in this chapter confirm that arterenone is produced from dehydro NADA bound cuticle through an unusual migration of proton from the β-position to the α-position accounting for the generation of β-carbonyl group in the arterenone. A similar mechanism could explain the production of ketocatechol also. But due to the low amounts of ketocatechol produced in the reaction mixture, we could not test this hypothesis. Nevertheless, close structural similarity suggests that the same mechanism must be involved in ketocatechol production also. The results of this study have been published already (Sugumaran et al., 2013).

FUTURE PERSPECTIVE

The research described in the previous chapters is the outcome of my initial studies with the dehydrodopamine/dehydrodopa compounds. But numerous aspects related to the biochemistry of these novel compounds are yet to be unraveled. In the case of dehydro NADA itself, in spite of all the detailed reaction chemistry of this compound, the actual biosynthetic aspect in insects remains largely unexplored. Our laboratory first reported the purification and characterization of N-acetyldopamine quinone isomerase from the hemolymph of *Sarcophaga bullata* nearly 23 years ago (Saul and Sugumaran 1990). Even after the determination of the entire genome sequence of three insects (fruit flies, mosquitoes and silkworm), the molecular biological aspects of this important enzyme remain still in dark. I tried to varying degree unsuccessfully to characterize the genomic sequence of quinone isomerase from *Sarcophaga bullata*. Definitely future studies are needed on this enzyme to understand its role in sclerotization as well as immune response of insects. The next enzyme involved in the biosynthesis of dehydro NADA is N-acetyldopamine quinone methide isomerase. This enzyme uses transiently produced N-acetyldopamine quinone methide that has been difficult to make in test tube chemically. As a result characterization of this enzyme itself has been very difficult. Using coupled assays, it was discovered in 1989 by our group (Saul and Sugumaran 1989). But purification and characterization of this enzyme has been extremely difficult due to the unavailability of substrate. However, it appears that these two isomerases are found to be present as an enzyme complex with phenoloxidases in the cuticle of at least

in *Sarcophaga bullata*, so using modern proteomic approaches, it is possible to characterize the isomerases in future.

In relation to dehydro NADA biosynthesis, it is important to draw particular attention to the proposal made by Andersen and Roepstroff (1982). These authors proposed the presence of a specific NADA side chain desaturase that might work like succinate dehydrogenase complex and introduce a double bond in the side chain of NADA. To this date, no one has isolated such a complex to prove its existence. However, these authors also reported that inhibitors of phenoloxidase inhibit this putative desaturase. Our group has questioned the presence of this desaturase and explained the observed inhibition by phenoloxidase inhibitors, to the actual participation of phenoloxidase in initiating the sequence of reactions that lead to the biosynthesis of dehydro NADA by the three component enzyme system. Andersen's group, however without providing any proof for its existence, claims that it is present in locust cuticle. It would be interesting to settle this dispute once in for all by proving (or disproving) the presence of this enzyme.

Another unresolved aspect in the biosynthesis of dehydro NADA is the role of phenoloxidases in generating quinone methides in cuticle. Initially our group proposed that NADA quinone methide could arise by a phenoloxidase action. Phenoloxidases perform oxidation of catechols at 1,4-postion. The insect phenoloxidases could similarly perform oxidation of NADA at 1,6-position generating directly quinone methide. However, we abandoned this proposal in favor of the phenoloxidase- quinone isomerase

pair working together to generate quinone methides in insect cuticle after the discovery of quinone isomerase in 1990. However, both Kramer's group and Andersen's group insist on phenoloxidase-catalyzed production of quinone methides in insect cuticle (Andersen 2010). They specifically quote that *Manduca* laccase could convert as much as 44% of NBAD provided to the enzyme into N-β-alanylnorepinephrine, which is the water adduct of NBAD quinone methide (Thomas et al., 1989: Andersen 2010). However, we attributed such conversion to possible contamination by quinone isomerase. Since quinone isomerase readily forms complex with phenoloxidases, it is possible that their laccase preparation possessed quinone isomerase and that is why they were able to witness the production of high concentrations of N-β-alanylnorepinephrine. Since several laccase clones are now available, it would be possible to verify this and settle the role of oxidases and isomerases in generating quinone methides in cuticle. Finally, the molecular biological tools will be very valuable to establish the importance of the isomerases in cuticular hardening as well as other processes such as wound healing and immune responses in insects. Such studies could eventually lead to novel insecticides, which will be environmentally friendly with no or minimum side effects to humans and other animals.

As far as the chemistry of the sclerotization process, not all adducts and crosslinks present in the cuticle are characterized. Several adducts and crosslinks especially those involving dehydro NADA are yet to be discovered. Even with quinone and quinone methide adducts, only the reactions of histidine and to certain extent, lysine has been

characterized. The reactivities of other nucleophiles such as hydroxyl groups and carboxyl groups remain largely unexplored. Thus, it would be worthwhile to investigate the potential of oxygen nucleophiles in participation of sclerotization. Oxygen nucleophiles are present in excess of 30 % in cuticualr proteins, while both nitrogen and sulfur nucleohiles have combined average of less than 5 % of the cuticular proteins (Andersen et al., 1995). This suggests that amino acids other than histidine, lysine, methionine and cysteine may be playing a role in the crosslinking process. Because of the unique chemical reactivity, quinonoid compounds generated from dehydro NADA, could play a vital role in crosslinking oxygen nucleophiles in cuticle. Theoretically oxygen nucleophiles can form adducts and crosslinks (Sugumaran 1988, 1998), but it has not been demonstrated unequivocally.

The entire biochemistry of dehydrodopyl compounds of marine organisms remains to be investigated. Marine organisms provide a plethora of dehydrodopyl compounds with a vast array of biological activities (Sugumaran and Robinson, 2010). Biosynthetic and chemical synthetic studies of these compounds will provide new pharmaceuticals as well as biomaterials. For instance, the byssal thread protein in mussels is being investigated for potential use in gluing tooth, bones and other biomaterials under water. Unraveling the molecular mechanism of crosslinking process could lead to newer, simpler and more efficient crosslinkers for future use.

REFERENCES

Abebe, A., Zheng, D., Evans, J., Sugumaran, M. 2010. Reexamination of the mechanisms of the oxidative transformation of insect cuticular sclerotizing precursor, 1,2-dehydro-N- acetyldopamine. *Insect Biochem. Mol. Biol.* 40, 650-659.

Andersen, R. J., Faulker, D. J., He, C., Van Duyne, G. D., Clardy, J. 1985. Metabolites of the marine prosobranch mollusk *Lamellaria* sp. *J. Amer. Chem. Soc.* 107, 5492-5495.

Andersen, S.O. 1970. Isolation of arterenone (2-amino-3',4'-dihydroxyacetophenone) from hydrolysates of sclerotized insect cuticle. *J.Insect. Physiol.* 16(10), 1951-1959.

Andersen, S.O. 1985. Sclerotization and tanning of the cuticle. Comprehensive insect physiology, Biochemistry and pharmacology. Vols. 1-13. Oxford: Pergamon.

Andersen, S. O. 1989. Enzymatic activities involved in incorporation of N-acetyldopmaine into insect cuticle during sclerotization. *Insect Biochem.* 19, 375-382.

Andersen, S. O., 2010. Insect cuticular sclerotization: A review. *Insect Biochem. Mol. Biol*. 40, 166 -178.

Andersen, S.O., Roepstroff, P., 1981. Sclerotization of insect cuticle – II. Isolation and identification of phenolic dimers from sclerotized insect cuticle. *Insect Biochem.* 11, 25-31.

Andersen, S.O., Roepstroff, P., 1982. Sclerotization of insect cuticle – III. An unsaturated derivative of N- derivative of N-acetyldopamine and its role in sclerotization. *Insect Biochem*. 12, 269-276.

Andersen, S.O., Jacobsen, J. P., Roepstroff, P., 1980. Studies of the sclerotization of insect cuticle. The structure of a dimeric product formed by incubation of N-acetyldopamine with locust cuticle. *Tetrahedron.* 36, 3249-3252

Andersen, S.O., Peter, M.G., Roepstroff,P. 1996. Cuticular Sclerotization in Insects. *Comp.Biochem.Physiol*. 113B, 689-705.

Arakane, Y., Muthukrishnan, S., Beeman, R. W., Kanost, M. R. Kramer, K. J., 2005. Laccase 2 is the phenoloxidase gene required for beetle cuticle tanning. *Proc. Natl. Acad. Sci.(USA)* 102, 11337–11342.

Arizza, V., Cammarata, M., Tomasino, M. C., Parrinello, N., 1995. Phenoloxidase characterization in vacuolar hemocytes from the solitary ascidian *Styela plicata*. *J. Invert. Pathol.* 66, 297-302.

Arnow, L.E., 1937. Colorometric determination of the components of 3,4-dihydroxyphenylalanine-tyrosine mixtures. *J. Biol. Chem.* 111, 531-537.

Aso, Y., Kramer, K.J., Hopkins, T.L., Whetzel, S.Z., 1984. Properties of tyrosinase and DOPA quinone imine conversion factor from pharate pupal cuticle of *Manduca sexta* (L.). *Insect Biochem.* 14; 463-472.

Ballarin, L., 2008. Immunobiology of compound ascidians, with particular reference to *Botryllus schlosseri*: State of the art. *Invertebrate Survival Journal*. 5, 54-74.

Ballarin, L. 2012. Ascidian cytotoxic cells: State of the art and research perspectives. *Invertebrate survival Journal*. 9, 1-6.

Ballarin, L., Cima, F., Sabbadin, A., 1998. Phenoloxidase and cytotoxicity in the compound ascidian, *Botryllus schlosseri*. *Dev. Comp. Immunol*. 22, 479-492.

Barett, F.M. 1987. Phenoloxidase from larval cuticle of the sheep blow fly, *Lucilia cuprina*: Characterization, developmental changes, and inhibition by antiphenoloxidase antibodies. *Arch.Insect Biochem. Physiol.* 5; 99-118.

Barett, F.M., 1991. Phenoloxidase and the Integument. In: Binnington, K., Retnakaran, A. (Eds), Physiology of Insect epidermis. CSIRO, Australia, pp. 195-212.

Barett, F.M., Andersen, S.O., 1981. Phenoloxidase in the larval cuticle of blowfly, *Caliphora vicina*. *Insect Biochem*. 11; 17-23.

Bayer E., Schiefer G., Waidelich D., Scippa S., De Vincentiis M., 1992. Structure of the tunichrome of tunicates and its role in concentration of vanadium, Angew. Chem. Inter. Ed. Engl., 31: 52-54.

Bolton, J.L., Wu, H.M., Hu, Q.L. 1996. Mechanism of isomerization of 4-propyl-o-quinone to its tautomeric p-quinone methide. *Chem.Res.Toxicol*. 9; 109-113.

Bruening R. C., Oltz E. M., Furukawa J., Nakanishi K., Kustin K., 1986. Isolation of tunichrome B-1, a reducing blood pigment of the sea squirt, *Ascidia nigra, J. Nat. Prod*., 49: 193-204.

Bruening R. C., Oltz, E.M., Furukawa, J., Nakanishi, K., 1985. Isolation and structure of tunichrome B-1, a reducing blood pigment from the tunicate *Ascidia nigra* L.,

J.Am.Chem. Soc. 107, 5298-5300.

Brunet, P.C.J. 1980. The metabolism of aromatic aminoacids concerned in the cross-linking of insect cuticle. *Insect biochem*. 10; 467-500.

Burzio, L. A., Waite, H.J., 2001. Reactivity of peptidyl tyrosine to hydroxylation and crosslinking. *Protein Sci.* 10, 735- 740.

Cai, M., Sugumaran, M., Robinson, W., 2008. The crosslinking and antibacterial properties of tunichromes. *Comp. Biochem. Physiol*. 151B: 110-117.

Cammarata, M., Parrinello, N., 2009. The ascidian prophenoloxidase activating system. *Invertebrate survival Journal*. 6, S67-S76.

Cammarata, M., Arizza, V., Vazzana, A., Parrinello, N., 1996. Prophenoloxidase activating system in tunicate hemolymph. *Ital. J. Zool.* 63, 345-351.

Cerenius, L., Söderhäll, K., 2004. The prophenoloxidase-activating system in invertebrates. *Immunol.Rev.* 198, 116-126.

Claus, H. 2003. Lacasses and their occurrence in prokaryotes. *Arch. Microbiol*. 179; 145-150.

Dali, H., Sugumaran, M., 1988. An improved synthesis of 1,2-dehydro-N-acetyldopamine. *Org. Prep. Proc. Intl.* 20, 191-195.

Dittmer, N. T., Suderman, R. J., Haobo Jiang, H., Zhu, Y-C., Gorman, M. J., Kramer, K. J., Kanost, M. R., 2004. Characterization of cDNAs encoding putative laccase-like multicopper oxidases and developmental expression in the tobacco hornworm, *Manduca sexta*, and the malaria mosquito, *Anopheles gambiae*. *Insect Biochem. Mol. Biol*. 34, 29-41.

Dong, C., Wang, Y., Zhu, Y. Z., 2009. Asymmetric synthesis and biological evaluation of Danshensu derivatives as anti-myocardial ischemia drug candidates. *Bioorg. Med. Chem*. 17, 3499- 3507.

Dove, J., and Sheridan, P. 1986. Adhesive proteins from mussels: possibility for dentistry, medicine, and industry. *J. Am. Dent. Assoc*. 112, 879.

Facompe, M., Trady, C., Bal-Mahieu, C., Colson, P., Perez, C., Mazanares, C., Cuevas, C., Bailly, C., 2003. Lamellarin D: a novel potent inhibitor of topoisomerase I. *Cancer Res*. 63,7392-7399.

Fan, H., Peng, J., Hamann, M.T., Hu, J.F., 2008. Lamellarins and related pyrrole derived alkaloids from marine organisms. *Chem. Rev*. 108, 264-287.

Flurkey, W.H. 2003. Laccse, In: Whitaker, J.R., Voragen, A.G.J., Wong, D.W.S. (eds). Handbook of food enzymology. Marcel Dekker, Inc., New York. 525-537.

Gorman, M.J., Arakane, Y. 2010. Tyrosine hydroxylase is required for cuticle sclerotization and pigmentation in *Tribolium castaneum*. *Insect Biochem. Mol. Biol.* 40; 267-273.

Hasson, C., Sugumaran, M., 1987. Protein cross-linking by peroxidase: possible mechanism for sclerotization of insect cuticle. *Arch. Insect Biochem. Physiol.* 5, 13-28.

Hata, S., Azumi, K., Yokosawa, H., 1998. Ascidian phenoloxidase: its release from hemocytes, isolation, characterization and physiological roles. *Comp. Biochem. Physiol. B.* 119, 769-776.

Hopkins, T.L., Morgan, T.D., Aso,Y., Kramer, K.J., 1982. N-β-Alanyldopamine: Major role in insect cuticle tanning. *Science.* 217, 364-366.

Hopkins, T.L., Kramer,K.J., 1992. Insect cuticle sclerotization. *Annu.Rev.Entomol*. 37, 273-302.

Ishibashi, F., Tanabe, S., Oda, T., Iwao, M., 2002. Synthesis and structure-activity relationship study of lamellarin derivatives *J. Nat. Prod. 65*, 500-504.

Ito, S., Prota, G.A. 1977. A facile one step synthesis of cysteinyldopas using mushroom tyrosinase. *Experientia.* 33, 1118-1119.

Iwanaga, S., Lee, B.L., 2005. Recent advances in the innate immunity of invertebrate animals. *J. Biochem. Mol. Biol.* 38, 128-150.

Jackson, A. D., Smith, V. J., Peddie, C. M., 1993. *In vitro* phenoloxidase activity in the blood of *Ciona intestinalis* and other ascidians. *Dev. Comp. Immunol*. 17, 97-108.

Kai, K., Mizutani, M., Kawamura, N., Yamamoto, R., Tamai, M., Yamaguchi, H., Skata, K., Shimizu, B., 2008. Scopoletin is biosynthesized via ortho-hydroxylation of feruloyl CoA by a 2-oxolutarate-dependent dioxygenase in *Arabidopsis thaliana*. Plant J. 55, 989–999.

Kang, H., Fenical, W., 1997. Ningalins A-D: Novel aromatic alkaloids from a Western Australian ascidian of the Genus *Didemnum. J. Org. Chem. 62,* 3254-3262.

Karlson, P., Sekeris, C. E., 1962. N-acetyldopamine as sclerotizing agent of the insect cuticle. *Nature*. 195, 183-184.

Kanost, M.R., Gorman, M.J., 2008. Phenoloxidase in Insect imunity. In: beckage,N. (Ed.), insect immunology. Academic Press/ Elsevier, Sandiego, pp. 69-96.

Kehrer, J. P., 2000. The Haber-Weiss reaction and mechanism of toxicity. *Toxicology* 149, 43-50.

Kerwin, J.L., Turecek, F., Xu, R., Kramer,K.J., Hopkins, T.L., Gatlin, C.L., Yates III, J.R., 1999. Mass spectrometric analysis of catechol-histidine adducts from insect cuticle. *Anal.Biochem.* 268,229-237.

Kim D., Li Y., Horenstein B. A., Nakanishi K., 1990. Synthesis of the tunichromes Mm-1 and Mm-2, blood pigments of the iron-assimilating tunicate, *Molgula manhattensis*, *Tetrahedron letters*, 12: 7119-7122.

Koppenol, W. H., Van Buuren, K. J., Butler, J., Braams, R., 1976. The kinetics of the reduction of cytochrome c by the superoxide anion radical. *Biochim. Biophys. Acta.* 449, 157-168.

Kustin K., Robinson W. E., Smith M. J., 1990, Tunichromes, vanadium, and vacuolated blood cells in tunicates. *Invert. Reprod. and Develop*., 17: 129-139.

Kramer, K.J and Hopkins, T.L. 1987. Tyrosine metabolism for insect cuticle tanning. *Arch. Biochem. Physiol.* 6, 279-301

Lee S., Kustin K., Robinson W. E., Frankel R. B., Spartalian K., 1988, Magnetic properties of tunicate blood cells. I. *Ascidia nigra*, *J. Inorg. Biochem.*, 33: 183-192.

Lindquist, N., Fenical, W., Van Duyne, G. D., Clardy, J., 1988. New alkaloids of the lamellarin class from the marine ascidian, *Didemnum chartaceum* (Sluiter, 1909). *J. Org. Chem*. 53, 4570-4574.

Macara I. G., McLeod G. C., Kustin K., 1979a. Isolation, properties and structural studies on a compound from tunicate blood cells that may be involved in vanadium accumulation, *Biochem. J.*, 181, 457-465.

Macara I. G., McLeod G. C., Kustin K., 1979b. Vanadium in tunicates: Oxygen-binding studies, *Comp. Biochem. Physiol.*, 62, 821-826.

Menna, M., Fatturosso, E., Imperatore, C., 2011. Alkaloids from the Marine Ascidians. *Molecules*. 16, 8694-8732.

Merlini, L., Zanarotti, P., Pelter, A., Rockefort, M. Hansel, R.,1980. Benzodioxans by oxidative phenooxidative phenol coupling. Synthesis of silybin. *J. Chem. Soc. Perkins.Transactions I*, 775-778.

Morgan, T.D., Thomas, B.R., Yonekura, M., Czapla, T.H., Kramer, K.J., Hopkins, T.L. 1990. Soluble tyrosinase from pharate pupal integument of the tobacco horn worm, *Manduca sexta* (L.). *Insect Biochem*. 20; 251-260.

Nakamura, T., 1960. On the process of enzymatic oxidation of hydroquinone. *Biochem. Biophys. Res. Commun*. 2**,** 111–113.

Nette, G., Scipa, S., Vincentiis, M., 2000. Origin of the Henze solution/precipitate from morula cells of the blood of the ascidian *Phallusia mammillata*. *Naturwissenschaften.* 87, 220-224.

Niu, B.-L., Shen W.-F., Liu, Y., Weng, H.-B., He, L.-H., Mu, J.-J., Wu, Z.-L., Jiang, P., Tao,Y.-Z., Meng Z.-Q., 2008. Cloning and RNAi-mediated functional characterization of *MaLac2* of the pine sawyer, *Monochamus alternatus. Insect Mol. Biol.* 17, 303 -308.

Novellino, L., Napolitano, A., Prota, G., 1999. 5,6-Dihydroxyindoles in the Fenton reaction: a model study of the role of melanin precursors in oxidative stress and hyperpigmentary processes. *Chem. Res. Toxicol.* 12, 985-992.

Okot-Krotber, B.M., Morgan, T.D., Hopkins, T.L., and Kramer, K.J., 1994. Characterization of two high molecular weight containing glycoproteins from the pharate pupal cuticle of the tobacco horn worm, Manduca sexta. *Insect Biochem. Mol. Biol.* 24, 787-802.

Oltz E. M., Bruening R. C., Smith, M. J., Kustin K., Nakanishi K., 1988. The tunichromes. A class of reducing blood pigments from sea squirts: Isolation, structures and vanadium chemistry. *J. Amer. Chem. Soc.*, 110: 6162-6172.

Oltz E. M., Pollack S., Delohery T., Smith M. J., Ojika M., Lee S., Kustin K., Nakanishi K., 1989. Distribution of tunichrome and vanadium in sea squirt blood cells sorted by Flow cytometry, *Experientia*, 45, 186-190.

Pan,C., Zhou, Y., Mo, J. 2009. The clone of laccase gene and its potential function in cuticular penetration resistance of *Culex pipens pallens* to fenualerate. *Pestic. Biochem. Physiol.* 93; 105-111.

Pryor, M.G.M., 1940. On the hardening of the ootheca of *Blatta orientalis*. *Proceedings of the Royal Society B.* 128, 378-398.

Quesada, A.R., Garcia Gravalos, M.D., Fernandez Puentes, J.L., 1996. Polyaromatic alkaloids from marine invertebrates as cytotoxic compounds and inhibitors multidrug resistance caused by P-glycoproteins. *Br. J. Cancer.* 74 (5); 677-682.

Redd, M.V., Rao, M.R., Rhodes, D., Hansen, M.S., Rubin, K., Bushman, F.G., Venkateswarlu, Y., Faulkner, D.J., 1999. Lamellarin alpha 20-sulfate, an inhibitor of HIV-1 integrase active against HIV-1 virus in cell culture. *J. Med.Chem.* 42 (11); 1901-1907.

Ricketts, D., Sugumaran, M., 1994. 1,2-dehydro-N-β-alanyldopamine as a new intermediate in insect cuticular sclerotization. *J. Biol. Chem*. 269, 22217-22221.

Rosenzweig, A.C., Sazinsky, M.H., 2006. Structural insights into dioxygen-activating copper enzymes. *Curr. Opin. Struct. Biol*. 16; 729-735.

Rubin, D.J., Miserez, A., Waite, H.J., 2010. Diverse strategies of protein sclerotization in marine invertebrates: Structure-property relationships in natural biomaterials. *Adv.Insect Physiology*. 38, 75-133.

Rzepecki, L. M., Nagafuchi, T., Waite, J. H., 1991. α,β-dehydro-3,4-dihydroxyphenylalanine derivatives. Potential sclerotization intermediates in natural composite materials. *Arch. Biochem. Biophys.* 285, 17 – 26.

Rzepecki, L. M., Waite, J. H., 1991. α,β-dehydro-3,4-dihydroxyphenylalanine derivatives. Rate and mechanism of formation. *Arch. Biochem. Biophys*. 285, 27 – 36.

Saul, S. J., Sugumaran, M., 1988. A novel quinone: quinone methide isomerase generates quinone methides in insect cuticle. *F. E. B. S. Lett*. 237, 155-158.

Saul, S. J., Sugumaran, M., 1989a. *o*-Quinone: quinone methide isomerase - a novel enzyme which prevents the destruction of self-matter by phenoloxidase generated quinones during immune response in insects. *F. E. B. S. Lett.* 249, 155-158.

Saul, S. J., Sugumaran, M., 1989b. Characterization of a new enzyme system that desaturates the side chain of N-acetyldopamine. F. E. B. S. Lett. 251, 69-73.

Saul, S. J., Sugumaran, M., 1989c. N-Acetyldopamine quinone methide/1,2-dehydro-N-acetyldopamine tautomerase - A new enzyme involved in sclerotization of insect cuticle. *F. E. B. S. Lett.* 255, 340-344.

Saul, S. J., Sugumaran, M., 1990a. 4-Alkyl-*o*-quinone/2-hydroxy-*p*-quinone methide isomerase from the larvae hemolymph of *Sarcophaga bullata*. I. Purification and characterization of enzyme catalyzed reaction. *J. Biol. Chem.* 265, 16992-16999.

Saul, S. J., Sugumaran, M., 1990b. Biosynthesis of dehydro-N-acetyldopamine by a soluble enzyme preparation from the larval cuticle of *Sarcophaga bullata* involves intermediary formation of N-acetyldopamine quinone and N-acetyl dopamine quinone methide. *Arch. Insect Biochem. Physiol.* 15, 237-254.

Schafer, J., Kramer, K.J., Garbow, J.R., Jacobs,G.S., Stejskal, E.O., Hopkins, T.L., Spires, R.D., 1987. Aromatic cross-links in insect cuticle: detection by solid-state ^{13}C ^{15}N NMR. *Science*. 235, 1200-1204.

Smith M. J., Kim, D., Horenstein, B., Nakanishi, K., Kustin, K., 1991. Unraveling the chemistry of tunichrome. *Acc. Chem. Res.* 24, 117-124.

Smith, M.J., Ryan, D.E., Nakanishi, K., Frank, P, Hodgson, K.O., 1995. Vanadium in ascidians and the chemistry of tunichromes. In: Sigel, H. and Sigel, A. (eds). Metal Ions in Biological Systems. Volume 31. Vanadium and its Role in Life. Marcel Dekker, Inc., New York. pp.423-490.

Solomon, E.I., Sunddaram, U.M., Machonik, T.E., 1996. Multicopper oxidase and oxygenases. *Chem. Rev*. 96, 2563-2606.

Sterjiades, R., Ranocha, P., Boudet, A. M., Goffner, D., 1996. Identification of specific laccase isoforms capable of polymerizing monolignols by an "in-gel" procedure. *Anal. Biochem*. 242, 158 -161.

Suderman, R. J., Dittmer, N. T., Kanost, M. R., Kramer, K. J., 2006. Model reactions for insect cuticle sclerotization: Cross-linking of recombinant cuticular proteins upon their laccase-catalyzed oxidative conjugation with catechols. *Insect Biochem. Mol.Biol.* 36, 353–365.

Sugumaran, M., 1986. Tyrosinase catalyzes an unusual oxidative decarboxylation of 3,4-dihydroxymandelate. *Biochemistry.* 25, 4489-4492.

Sugumaran., M., 1987. Quinone methide sclerotization - A revised mechanism for β-sclerotization of insect cuticle. *Bioorg. Chem*. 15, 194-211.

Sugumaran, M., 1988a. Quinone methides – and not dehydrodopamine derivatives – as reactive intermediates of β-sclerotization in the puparia of flesh fly, *Sarcophaga bullata*. *Insect Biochem.Physiol.* 8, 73-88.

Sugumaran, M., 1998. Unified mechanism for sclerotization of insect cuticle. *Adv. Insect Physiol*. *27*, 229-334.

Sugumaran, M., 2000. Oxidation chemistry of 1,2-dehydro-N-acetyldopamines: Direct evidence for the formation of 1,2-dehydro-N-acetyldopamine quinone. *Arch. Biochem. Biophys.* 378, 404-419.

Sugumaran, M., 2002. Comparative biochemistry of eumelanogenesis and the protective roles of phenoloxidases and melanin in insects. *Pigment Cell Res. 15*, 2-9.

Sugumaran, M., 2010. Chemistry of cuticular sclerotization. *Adv. Insect physiol.* 39, 151 – 209.

Sugumaran, M., Lipke,H. 1982. Crosslinking precursor for the dipteran puparium. *Proc Natl. Acad. Sci. USA.* 79; 254-262.

Sugumaran, M., Lipke,H. 1983. Quinone methide formation from 4-alkyl-catechols, a novel reaction catalyzed by cuticular polyphenoloxidase. *FEBS let.* 155, 65-68.

Sugumaran, M., Dali, H. 1989. Chemical-and cuticular phenoloxidase-mediated synthesis of cysteinyl-catechol adduct. *Arch. Insect Biochem. Physiol.* 11(2); 127-137.

Sugumaran, M., Semensi, V. 1991. Quinone methide as a new intermediate in eumelanin biosynthesis. *J. Biol. Chem. 266*, 6073-6078.

Sugumaran, M., Ricketts, D., 1995. Model sclerotization studies. 3. Cuticular enzyme catalyzed oxidation of peptidyl model tyrosine and dopa derivatives. *Arch. Insect Biochem.Physiol. 28,* 17 - 32.

Sugumaran, M., Robinson, W. E., 2010. Bioactive dehydrotyrosyl and dehydrodopyl compounds of marine origin. *Marine Drugs.* 8, 2906– 2935.

Sugumaran, M., Hennigan, B., O'Brien, J., 1987b. Tyrosinase catalyzed protein polymerizationas an *in vitro* model for quinone tanning of insect cuticle. *Arch. Insect Biochem. Physiol. 6,* 9-25.

Sugumaran, M., Dali, H., Semensi, V., 1989. Chemical and cuticular phenoloxidase mediated synthesis of cysteinyl catechol adducts. *Arch. Insect Biochem. Physiol.* 11, 127-137.

Sugumaran, M., Dali, H., Semensi, V., 1992. Mechanistic studies on tyrosinase catalyzed oxidative decarboxylation of 3,4-dihydroxymandelic acid. *Biochem. J.* 281, 353-357.

Sugumaran, M., Dali, H., Semensi, V., Hennigan, B., 1987a. Tyrosinase catalyzed\ unusual oxidative dimerization of 1,2-dehydro-N-acetyldopamine. *J. Biol. Chem. 262*, 10546-10549.

Sugumaran, M., Hennigan, B., Semensi, V., Dali, H., 1988a. On the nature of nonenzymatic and Enzymatic oxidation of the putative sclerotizing precursor, 1,2-dehydro-N- acetyldopamine. *Arch. Insect Biochem. Physiol*. 8, 89-100.

Sugumaran, M., Dali, H., Kundzicz, H., Semensi, V., 1989. Unusual intramolecular cyclization and side chain desaturation of carboxyethyl-*o*-benzoquinone derivatives. *Bioorg. Chem. 17*, 443-453.

Sugumaran, M., Semensi, V., Dali, H., Saul, S.J., 1989b. Nonenzymatic transformations of enzymatically generated N-acetyl dopamine quinone and isomeric dihydrocaffeiyl methylamide quinone. *FEBS Lett. 255*, 345-349.

Sugumaran, M., Schinkmann, K., Bedell-Hogan, D., Dali, H. 1990. Mechanism of activation of 1,2-dehydro-N-acetyldopamine for cuticular sclerotization. *Arch. Insect Biochem. Physiol*. 14, 93-109.

Sugumaran, M., Semensi, V., Kalyanaraman, B., Bruce, J. M., Land, E. J., 1992a. Evidence for the formation of a quinone methide during the oxidation of the insect cuticular sclerotizing precursor, 1,2-dehydro-N-acetyldopamine. *J. Biol. Chem*. 267, 10355-10361.

Sugumaran, M., Giglio, L.B., Kundzicz, H., Saul, S., Semensi V., 1992b. Studies on the enzymes involved in puparial cuticle sclerotization in *Drosophila melanogaster*. *Arch. Insect Biochem. Physiol. 19*, 271-283.

Sugumaran, M., Abebe, A., Oboite, O., Zheng, D. 2013. On the mechanism of formation of arterenone in insect cuticular hydrolyzates. *Insect Biochem. Mol. Biol.* 43(2); 209-218.

Tada, T., Ohnishi, K., Suzuki, K., Tomita, H., Okamori, M., Katuzaki, H., Komiya, T., Imai, K., 2002. Potential cosmetic whitening agents from insect cuticle: Tyrosinase inhibitory activity of N-acetyldopamine dimers from exuviae of cicada, *Cryptotympana tustulata. Fabr. J. Oleo. Sci.*, 51, 355-358.

Takao, K-I., Munakata, R., Tadano, K-I., 2005. Recent advances in natural product synthesis by using intramolecular Diels-Alder reactions. *Chem. Rev*. 105, 4779-4807.

Taylor S. W., Ross M. M., Waite H. J., 1995. Novel 3,4-di- and 3,4,5-trihydroxyphenylalanine- containing polypeptides from the blood cells of the ascidians *Ascidia ceratodes* and *Molgula manhattensis, Arch. Biochem. Biophys.,* 324: 228-240.

Taylor, S., Kammerer, B., Bayer, E., 1997a. New perspectives in the chemistry and biochemistry of the tunichromes and related compounds. *Chem. Rev.* 97, 333 - 346.

Taylor S. W., Kammerer B., Nicholson G. J., Pusecker K., Walk T., Bayer E., Scippa S., De Vincentiis M., 1997b, Morulin Pm: A modified polypeptide containing TOPA and 6-bromotryptophan from the morula cells of the ascidian, *Phallusia mammillata, Arch. Biochem. Biophys.*, 348: 278-288

Thomas, B. R., Yonekura, M., Morgan, T.D., Czapla, T. H., Hopkins. H.L., Kramer. K. J., 1989. A trypsin-solubilized laccase from pharate pupal integument of the tobacco hornworm, *Manduca sexta*. *Insect Biochem*. 19, 611-622.

Tincu J. A., Taylor S. W., 2002. Tunichrome *Sp-1*: New pentapeptide tunichrome from the hemocytes of *Styela plicata, J. Nat. Prod*., 65: 377-378.

Tincu J. A., Craig A. G., Taylor S.W., 2000. Plicatamide: A lead to the biosynthetic origins of the tunichromes. *Biochem. Biophys. Res. Commun.* 270: 421-424.

Tincu, J.A., Menzel, L.P., Azimov, R., Sands, J., Hong, T., Waring, A.J., Taylor, S.W., Lehrer, R.I., 2003. Plicatamide, an antimicrobial octapeptide from *Styela plicat* hemocytes. *J. Biol.Chem.* 278: 13546-13553.

Urban, S., Hooper, J.N.N., Capon, R.J., 1995. Lamellarins Q and R: New aromatic metabolites from an Australian marine Sponge *Dendrilla cactos*. *Aust.J.Chem*. 48, 1491-1494.

Vanhuyse, M., Kluza, J., Trady, C., Otero, G., Cuevas, C., Bailly, C., Lansiaux, A., 2005. Lamellarin D: A novel proapoptotic agent from marin origin insensitive to P-Glycoprotein mediated drug efflux. *Cancer Lett.* 22, 1655-175.

Vogt, T., 2010. Phenylpropanoid biosynthesis. *Molecular Plant*. 3, 2-20.

Vincent, J.F., Hillerton, J.E., 1979. The tanning of insect cuticle-a critical view and a revised mechanism. *J. Insect Physiol.* 25, 653-658.

Waite, J.H., 1990. The phylogeny and chemical diversity of quinone-tanning: *A review. Comp. Biochem. Physiol. B.* 97, 19–29.

Yatsu, J., Asano, T. 2009. Cuticular laccase of the silk worm, *Bombyx mori*; purification, gene identification and presence of its inactive precursor in cuticle. *Insect Biochem. Mol. Bio.* 39(4); 254-262.

Yu, M., and Deming, T.J., 1998. Synthetic polypeptide mimics of marine adhesives. *Macromolecules.* 31(15), 4739-4745.